

In presenting this thesis in partial fulfillment of the requirements for an advanced degree at Idaho State University, I agree that the Library shall make it freely available for inspection. I further state that permission for extensive copying of my thesis for scholarly purposes may be granted by the Dean of the Graduate School, Dean of my academic division, or by the University Librarian. It is understood that any copying or publication of this thesis for financial gain shall not be allowed without my written permission.

Signature \_\_\_\_\_

Date \_\_\_\_\_

Stratigraphic control on the transition from thin- to thick-skinned thrusting  
in the Idaho-Montana fold-thrust belt

by

Stuart D. Parker

A dissertation

submitted in partial fulfillment

of the requirements for the degree of

Doctor of Philosophy in the Department of Geosciences

Idaho State University

Summer 2021

To the Graduate Faculty:

The members of the committee appointed to examine the thesis of Stuart Parker find it satisfactory and recommend that it be accepted.

---

David Pearson,  
Major Advisor

---

Paul Link,  
Committee Member

---

Tracy Payne,  
Graduate Faculty Representative

---

Leif Tapanila,  
Committee Member

---

Emily Finzel,  
Committee Member

## TABLE OF CONTENTS

List of Figures .....	v
List of Plates .....	vii
List of Tables .....	viii
Abstract .....	ix
Chapter I: Pre-thrusting stratigraphic control on the transition from a thin- to thick-skinned structural style: an example from the double-decker Idaho-Montana fold-thrust belt.....	1
Abstract .....	3
Introduction .....	4
Background .....	11
Methods .....	21
Results.....	25
Discussion .....	46
Conclusions .....	59
References .....	61
Chapter II: A thermal profile across the Idaho-Montana fold-thrust belt reveals early burial to late exhumation during progressive growth of an orogenic wedge: U.S. Cordillera.....	93
Abstract .....	94
Introduction .....	95
Geologic Background .....	101
Methods .....	107
Results.....	111
Discussion .....	117

Conclusions .....	126
References cited .....	128
Chapter III: Balanced and restored cross section.....	154
Abstract.....	155
Introduction.....	156
Geologic Background .....	163
Methods .....	173
Results.....	177
Discussion.....	189
Conclusions.....	201
References cited .....	203
Appendix 1: Geologic map of the northern part of the Leadore Quadrangle.....	235

## LIST OF FIGURES

### Chapter I

Figure 1 Geometric and kinematic overlap of structural styles .....	7
Figure 2 Regional Geologic map.....	10
Figure 3 Regional stratigraphy .....	17
Figure 4 Geologic map of study area.....	24
Figure 5 Deformation features of sedimentary rock dip panel domain .....	30
Figure 6 Deformation features of the carbonate mylonite domain .....	33
Figure 7 Outcrop photos of Thompson Gulch mylonite.....	37
Figure 8 Field relationships from the western side of Jakes Canyon .....	40
Figure 9 Field relationships from the eastern side of Jakes Canyon .....	44
Figure 10 Simplified block diagrams of deformation events.....	46
Figure 11 Double-decker model.....	59

### Chapter II

Figure 1 Maximum temperature profiles of orogenic wedges .....	97
Figure 2 Overview map of U.S. Cordillera.....	100
Figure 3 Geologic map of study area.....	103
Figure 4 Examples of RSCM spectra .....	109
Figure 5 Contour map of cumulative exhumation magnitude .....	112
Figure 6 Maximum temperatures along transect.....	113
Figure 7 Interpretations of temperature data.....	116
Figure 8 Contour map of maximum temperatures .....	118

### Chapter III

Figure 1 Overview map of North American Cordillera.....	161
Figure 2 Regional stratigraphy .....	165
Figure 3 Outcrop photos of folds .....	182
Figure 4 Forward kinematic model of the Idaho-Montana fold-thrust belt .....	190

## LIST OF PLATES

Plate 1 Geologic map of Idaho-Montana fold-thrust belt.....	176
Plate 2 Balanced and restored cross section of Idaho-Montana fold-thrust belt .....	178

## LIST OF TABLES

### Chapter II

Table 1 Compiled Conodont alteration index data.....	149
Table 2 Raman Spectroscopy of Carbonaceous Material samples.....	153

Stratigraphic control on the transition from thin- to thick-skinned thrusting  
in the Idaho-Montana fold-thrust belt

Dissertation Abstract –Idaho State University (2021)

The wide varieties of thrust geometries in contractional mountain belts are often assigned to one of two end-member structural styles: thin-skinned or thick-skinned. This approach has been used in the North American Cordillera to differentiate the thin-skinned Sevier orogenic belt, with a décollement in sedimentary rocks, from the thick-skinned Laramide orogenic belt, with a décollement in the middle crust; each assigned to a distinct tectonic cause. This genetic interpretation of structural style and the distinction between “Sevier” and “Laramide” has little utility in the Idaho-Montana fold-thrust belt, where a continuum of thin- to thick-skinned thrusts overlap in space and time. This dissertation tests an alternative hypothesis: that pre-thrusting stratigraphy determines structural style by limiting the distribution of weak sedimentary rocks that may serve as sub-horizontal décollements. To test this hypothesis, I document the relationship between thin stratigraphy over the Lemhi arch basement high and the geometry, or “style”, of thrust faults formed during progressive shortening in the Idaho-Montana fold-thrust belt. Chapter 1 uses field mapping results from the central Beaverhead Mountains and cross cutting relationships to propose a preliminary double-decker model; describing the transition from an upper thin- to a lower thick-skinned thrust system as the migrating décollement crossed the basement/cover contact of the Lemhi arch. Chapter 2 tests this model by using Raman Spectroscopy of Carbonaceous Material to constrain maximum temperatures along a profile just above the Lemhi arch. From this, burial estimates define an early orogenic wedge geometry that mimics the flat-lying Lemhi arch. Elevated temperatures of ~ 270°C suggest regional burial of the Lemhi arch to ~ 6.5 km depth during the construction of an early (~145-90 Ma) low-relief orogenic wedge, providing preliminary support for the double-decker model and the hypothesis.

Chapter 3 refines the double-decker model by presenting the first balanced and restored regional cross section; linking the Sevier and Laramide belts and predicting a minimum of 170 km of shortening. Finally, a kinematic model is presented, predicting how progressive thin- to thick-skinned shortening through thin and irregular stratigraphy results in a self-organized transition from thin- to thick-skinned thrusting.

Key Words: thin-skinned, thick-skinned, thrust, Idaho, Montana, Lemhi arch, Laramide, Sevier

## Chapter I:

Pre-thrusting stratigraphic control on the transition from a thin- to thick-skinned structural style:  
an example from the double-decker Idaho-Montana fold-thrust belt

**Pre-thrusting stratigraphic control on the transition from a thin- to thick-skinned structural style: an example from the double-decker Idaho-Montana fold-thrust belt**

**S. D. Parker and D. M. Pearson**

Department of Geosciences, Idaho State University, Pocatello, ID, USA.

Corresponding author: Stuart Parker ([parkstua@isu.edu](mailto:parkstua@isu.edu))

**Key Points:**

- Thin- and thick-skinned thrusts record a progressive downward shift in the basal detachment of the Idaho-Montana fold-thrust belt
- A transition from thin- to thick-skinned thrusting occurred as the basal detachment encountered the basement high of the Lemhi arch
- Thin-skinned thrusts in the overlying cover and thick-skinned thrusts below the basement/cover contact form a double-decker fold-thrust belt

This work has been previously published as:

Parker, S.D., and Pearson, D.M., 2021, Pre-thrusting stratigraphic control on the transition from a thin-to thick-skinned structural style: An example from the double-decker Idaho-Montana fold-thrust belt, *Tectonics*, vol. 40, no. 5, e2020TC006429, doi:10.1029/2020TC006429.

## Abstract

Continental fold-thrust belts display a variety of structural styles, ranging from thin-skinned thrusts following weak lithologic contacts to thick-skinned thrusts that deform mechanical basement. The common practice of splitting fold-thrust belts into thin- and thick-skinned map domains has not yielded a predictive model of the primary controls on structural style. Within the Mesozoic-Paleogene Idaho-Montana fold-thrust belt (44–45°N, 112–114°W), we identify crosscutting thin- and thick-skinned thrusts within an otherwise thin-skinned map domain. This transition occurs within a thin (~2.5 km) portion of the western Laurentian passive margin, where lower strata pinch out over a prominent basement high (Lemhi arch). Early fold-thrust belt shortening of sedimentary cover rocks was accommodated through detachment folding, followed by east-directed, thin-skinned thrusting along regional-scale faults (Thompson Gulch and Railroad Canyon thrusts). Later, basement and cover rocks were tilted toward the southeast and a basement-involved normal fault was reactivated during thick-skinned thrusting (Radio Tower-Baby Joe Gulch-Italian Gulch thrusts), which accommodated shortening at an oblique angle to and truncated the basal detachment of the older thin-skinned thrusts. This progression from thin- to thick-skinned thrusting occurred >50 km from the foreland, coincident with a regional basement high. Thus, the Idaho-Montana fold-thrust belt is a double-decker system, with upper thin- and lower thick-skinned domains. This double-decker model is applicable to other fold-thrust belts and predicts that the transition from thin- to thick-skinned thrusting occurs where the growing critically-tapered wedge can no longer fit within the sedimentary cover rocks and the basal detachment steps down into structurally lower mechanical basement.

## 1 Introduction

Continental fold-thrust belts are often modeled as wedges of deformed rock that structurally overlie and are detached from underlying basement rocks (e.g., Bally et al., 1966; Armstrong, 1968; Dahlstrom, 1970; Price & Mountjoy, 1970; Burchfiel & Davis, 1972; Royse et al., 1975; Boyer & Elliott, 1982; Davis et al., 1983). The depth of the basal detachment exerts a fundamental control on the geometry of the orogenic wedge and the magnitude of crustal shortening (e.g., Erslev, 1993; Cook & Varsek, 1994; Lacombe & Bellahsen, 2016; Pfiffner, 2017). However, the primary controls on activation of deep vs. shallow basal detachments remain elusive, due in part to the considerable differences among global orogenic belts, both in their geodynamic settings (e.g., peripheral or retroarc position, subduction angle, convergence rates), crustal architecture, and their protracted pre-thrusting geological histories (e.g., Armstrong, 1968; Burchfiel & Davis, 1975; Allmendinger et al., 1983; Kulik & Schmidt, 1988; Erslev, 1993; Allmendinger & Gubbels, 1996; Kley, 1996; Kley et al., 1999; Pfiffner, 2006; 2017; Pearson et al., 2013; Yonkee & Weil, 2015; Lacombe & Bellahsen, 2016).

The wide varieties of thrust geometries in contractional mountain belts are often assigned to one of two end-member structural styles: thin-skinned or thick-skinned (e.g., Kley, 1996; DeCelles, 2004; Molinaro et al., 2005; McGroder et al., 2015; Yonkee & Weil, 2015; Lacombe & Bellahsen, 2016; Pfiffner, 2017; Fitz-Díaz et al., 2018). Thin-skinned thrusts generally have flat to low-angle upper crustal detachment horizons within weak sedimentary rocks (e.g., Bally et al., 1966; Dahlstrom, 1970; Boyer & Elliott, 1982). Thrusts that cut mechanical basement may be called thin-skinned if they are low-angle and/or have detachment horizons that mostly exploit weak sedimentary rocks (e.g., Yonkee & Weil, 2015; Pfiffner, 2017). In contrast, thick-skinned thrusts deform mechanical basement rocks, cutting across primary lithologic contacts at a

moderate to high angle (e.g., Lacombe & Bellahsen, 2016; Pfiffner, 2017). Thick-skinned thrusts often utilize preexisting weaknesses such as foliations or faults, and are generally rooted at mid-crustal or deeper levels (e.g., Blackstone, 1940; Smithson et al., 1979; Allmendinger et al., 1987; Kulik & Schmidt, 1988; Erslev, 1993; Lacombe & Bellahsen, 2016; Pfiffner, 2017; Groshong & Porter, 2019).

Structural style in some fold-thrust belts occurs along a continuum between thin- and thick-skinned endmembers (Lacombe & Bellahsen, 2016; Pfiffner, 2017; Butler et al., 2018). Figure 1 shows examples of this variability, where thin- and thick-skinned styles may occur (a) along a single thrust, (b) at various depths, and/or (c) within distinct but overlapping map domains. Throughout this paper, we use the terms thin- and thick-skinned in reference to the two idealized end-members defined above, in order to highlight important differences in fault geometry. We emphasize that while the structures being discussed are closer to the end-member being referenced, they in fact fall along a continuum of structural style that is dependent on both substrate and fault geometry. Accurate and detailed descriptions of structural style are foundational for predicting where and when basal detachments initiate, which is a prerequisite for developing tectonic models that integrate horizontal shortening of the upper, middle, and lower crust with changes in plate boundary geodynamics.

Critical taper theory offers testable predictions regarding the geometry and kinematics of thin-skinned fold-thrust belts (Davis et al., 1983), but does not apply at depths below the brittle-plastic transition, which are rarely exposed and difficult to image geophysically. For these reasons, studies of orogenic wedges have focused on deformation of the upper crust, generally integrating brittle rheologies for competent and viscous rheologies for weak rocks (see review by Gravelleau et al., 2012). As a consequence, there is much more uncertainty regarding detachment

geometries in thick-skinned thrust domains (e.g., Zawislak & Smithson, 1981; Groshong & Porter, 2019; Witte & Oncken, 2020). With some exceptions (e.g., Kulik & Schmidt, 1988; Williams et al., 1994), the practical result of this problem has been to separate deformation belts into thin- and thick-skinned domains and treat them as separate entities, making it difficult to synthesize results into a single deformation wedge.

Many modern and ancient mountain belts have spatially overlapping regions that are characterized by a spectrum of thin- and thick-skinned structural styles or exhibit a transition in style through time (Fig. 1; e.g., Allmendinger & Gubbels, 1996; Kley et al., 1999; Pearson et al., 2013; McGroder et al., 2015; Yonkee & Weil, 2015; Lacombe & Bellahsen, 2016; Pfiffner, 2017; Fitz-Díaz et al., 2018; Martínez et al., 2020; Williams et al., 2020). In the southern Subandean fold-thrust belt of the central Andes, the thin-skinned fold-thrust belt was carried atop and transitions along-strike southward to a basement-involved, thick-skinned fold thrust belt (e.g., Kley, 1996). Farther south in the Andes of west-central Argentina, early thin-skinned structures formed at structurally shallow levels and were subsequently deformed during thick-skinned inversion of structural deeper, basement-involved faults (Fig. 1a; Giambiagi et al., 2008; Fuentes et al., 2016). A shallow thin-skinned and deeper thick-skinned fold-thrust belt has been documented in the Zagros (Fig. 1b; e.g., Molinaro et al., 2005; Mouthereau et al., 2007; Barnhart et al., 2018). In contrast to these “double-decker” fold-thrust belts, thin- and thick-skinned structures in the Sevier-Laramide fold-thrust belt of the North American Cordillera were often considered by earlier workers to occupy geographically separate regions, with limited spatial and temporal overlap between them (e.g., Armstrong, 1968; Burchfiel & Davis, 1975; Dickinson & Snyder, 1978). However, more recent work in the North American Cordillera has shown that thin-skinned thrusts overlapped in time with or were deformed by later, structurally deeper,

thick-skinned thrusts (e.g., Schmidt & Perry, 1988; O'Neill et al., 1990; Zhou et al., 2006; Yonkee & Weil, 2015; Ramírez-Peña & Chávez-Cabello, 2017; Fitz-Díaz et al., 2018; Williams et al., 2020). Overlap of structural styles has primarily been documented near the foreland, leading to the interpretation of distinct thin- and thick-skinned thrusts domains that converge toward one another, each with a unique basal detachment and possibly stress field (Fig. 1c; e.g., Jordan & Allmendinger, 1986; Erslev, 1993; Yonkee & Weil, 2015). Alternatively, the North American Cordillera may qualify as a “double-decker” fold-thrust belt, with a continuum of thin- to thick-skinned structural styles that not only vary across and along strike, but also with depth (cf., Lacombe & Bellahsen, 2016; Pfiffner, 2017).

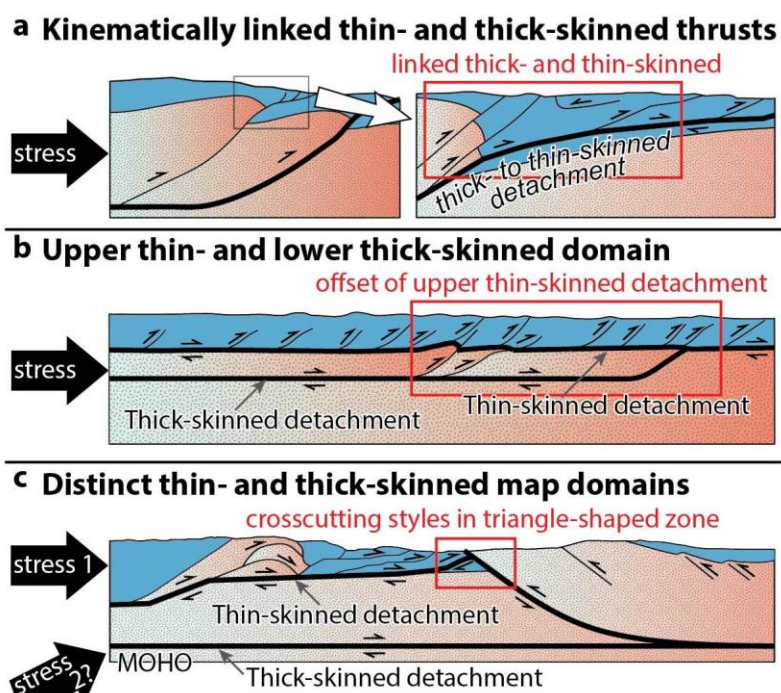


**Figure 1.** Simplified models showing possible geometric and kinematic overlap of thin- and thick-skinned structural styles. Red boxes call attention to specific areas of overlap. Sedimentary cover rocks (blue) overlie mechanical basement (pink patterns) in all models. **A)** Kinematically linked thin- and thick-skinned thrusts are attributed to mechanical properties of pre-thrusting rocks, preexisting weaknesses, and

a fixed basal detachment horizon (modified from Giambiagi et al., 2008, 2009; Fuentes et al., 2016). **B)** A double-decker system is attributed to mechanical properties and transient basal detachment horizons (modified from Molinaro et al., 2005; Mouthereau et al., 2007; Lacombe & Bellahsen, 2016). **C)** Distinct thin- and thick-skinned map domains are attributed to fixed basal detachment horizons and changes in plate boundary geodynamics and resultant changes in regional stresses (modified from Erslev, 1993; Yonkee & Weil, 2015).

To evaluate these models and investigate what controls the activation of deep vs. shallow basal detachments, the spatial relationship between structural domains must be well-constrained (e.g., Giambiagi et al., 2012). Where the interaction between basal detachments of thin-skinned thrusts and underlying thick-skinned structures is observable, we can begin to construct a more representative 3-dimensional view of the boundary separating structural domains and test whether the depth, relative strength, orientation, and/or continuity of the preexisting stratigraphy correlates with changes in structural style. Within the Idaho-Montana segment of the Sevier-Laramide fold-thrust belt (Fig. 2), both end-member structural styles have been documented and a wide range of structural levels are exposed in a relatively small, accessible area (e.g., Kulik & Schmidt, 1988; Perry et al., 1988, 1989; Schmidt et al., 1988; Skipp, 1988; Tysdal, 1988; O'Neill et al., 1990; McDowell, 1997; Tysdal, 2002). In the central part of the fold-thrust belt, erosion has fortuitously removed upper structural levels, creating a window into footwalls of thin-skinned thrusts. The study area is far from the foreland (Fig. 2), in a region that most previous workers have assumed is not thick-skinned despite the common outcrops of mechanical basement. Through mapping and structural analysis we constrain thrust geometries and interpret the series of deformation events that involve both thin- and thick-skinned thrusts near the contact between mechanical basement and overlying sedimentary rocks. Our results suggest that episodes of thin- and thick-skinned shortening overlapped in space and time and that the primary

control on structural style was pre-thrusting variations in thickness and lateral continuity of regional stratigraphic detachment horizons. These results provide a predictive framework for linking variable structural styles at various depths to a single deformation belt, suggesting that basal detachment horizons to continental fold-thrust belts are not fixed and instead migrate downward through the mechanically stratified crust with progressive shortening.

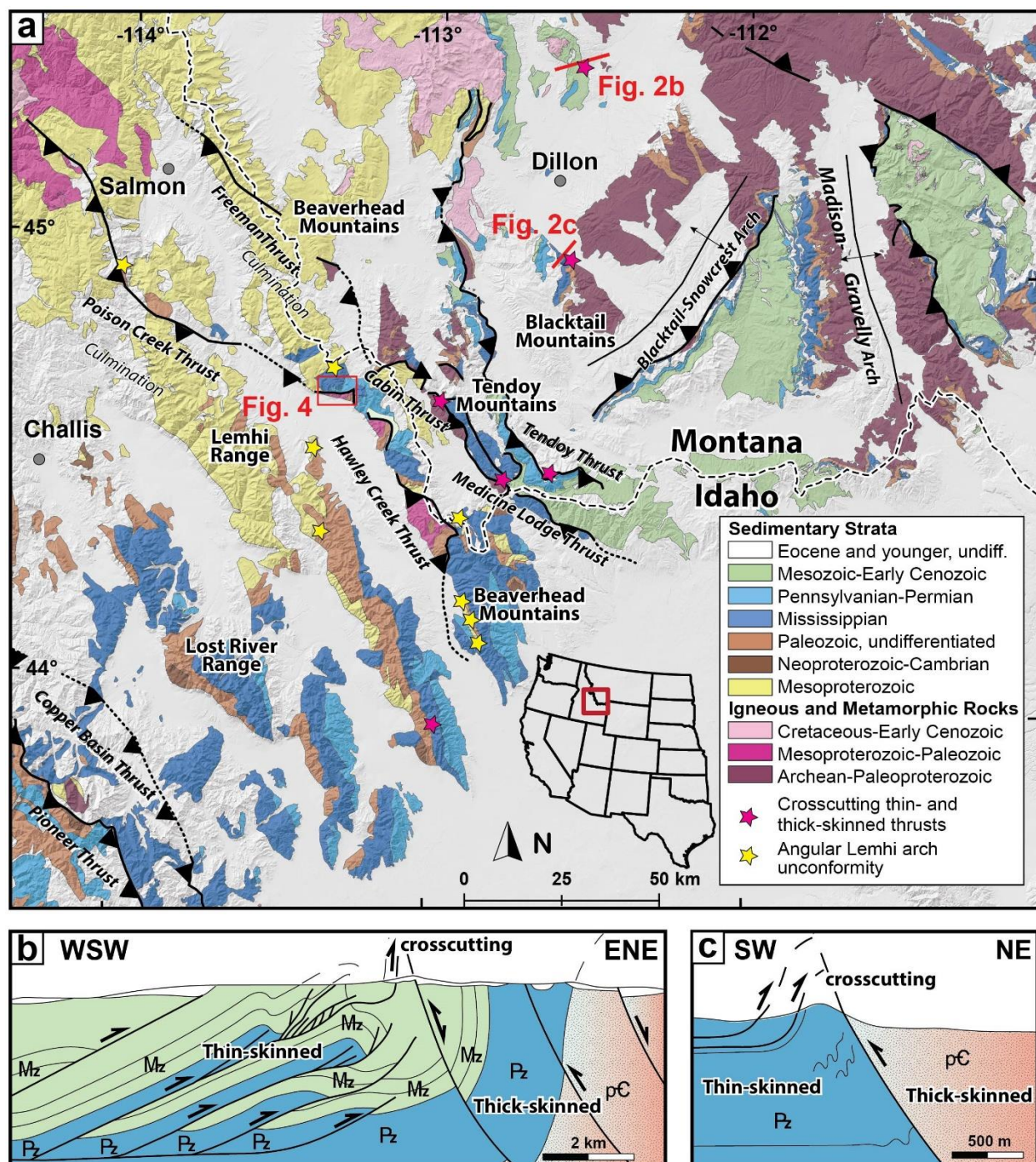


**Figure 2.** a) Simplified bedrock geologic map of the Idaho-Montana fold-thrust belt showing major thrusts (modified from Garber et al., 2020). Pink stars show where crosscutting thin- and thick-skinned thrusts have been previously documented (see text for discussion and citations). Yellow stars show where the Lemhi arch unconformities have a discordance of  $>10^\circ$  (Scholten, 1957; Scholten & Ramspott, 1968;

Ruppel, 1986; James & Oaks, 1977; Pearson & Link, 2017). Schematic cross sections showing crosscutting relationship between thin- and thick-skinned thrusts in the **b**) McCartney Mountain salient (redrafted from Schmidt et al., 1988) and **c**) Blacktail Mountains (redrafted from Tysdal, 1988).

## **2 Background**

### 2.1 Controls on structural style

In the shallow crust, the mechanical stratigraphy within a fold-thrust belt exerts a fundamental control on the geometries of its constitutive structures (Rich, 1934). Strength contrasts within sedimentary rocks promote ramps and flats, imbricate fans, and duplexes, which shorten cover rocks that are decoupled from the underlying mechanical basement (e.g., Rich, 1934; Boyer & Elliott, 1982; Stockmal et al., 2007). Classic localities exhibiting this thin-skinned structural style include the Canadian Rockies (Bally et al., 1966; Dahlstrom, 1970; Price, 1981; Fermor & Moffat, 1992; McMechan et al., 1993), Wyoming salient of the Sevier thrust belt (Armstrong, 1968; Burchfiel & Davis, 1972; Witschko & Dorr, 1983; Coogan, 1992; DeCelles, 1994; DeCelles & Mitra, 1995; DeCelles & Coogan, 2006; Yonkee & Weil, 2010; 2015), and the Subandean fold-thrust belt of the central Andes (Allmendinger et al., 1983; Baby et al., 1995; Dunn et al., 1995; Kley, 1996; Kley et al., 1999; McQuarrie, 2002; Echavarria et al., 2003; McGroder et al., 2015; Fuentes et al., 2016).

Deeper in the crust, we define mechanical basement as rocks that lack sub-horizontal, weak lithological layers that are exploited during thin-skinned thrusting. Rocks that we characterize as mechanical basement rocks are previously deformed, metamorphic, or plutonic rocks from prior tectonism. Whereas sedimentary cover rocks utilize pre-thrusting, weak lithologic layers as subhorizontal detachment horizons (e.g., Rich, 1934), mechanical basement

rocks do not break along primary lithologic contacts. Instead, mechanical basement often breaks along inherited weaknesses, leading to a wide range in orientations and dip angles of reverse faults. Our usage of terms highlights that while all rocks tend to exploit preexisting weaknesses, in the upper crust these weaknesses tend to be sub-horizontal for sedimentary cover rocks and in a variety of orientations for mechanical basement rocks, resulting in the observed range of thin- to thick-skinned structural styles.

In contrast to thin-skinned thrusts, thick-skinned thrusts generally carry thicker thrust sheets of mechanical basement rocks. These thrusts are often listric and merge into the middle to lower crust, where temperature-dependent strength contrasts likely separate regions that deform by frictional vs. plastic mechanisms and may therefore be utilized as sub-horizontal detachment horizons (Kulik & Schmidt, 1988; Erslev, 1993; Mouthereau et al., 2013; Lacombe & Bellahsen, 2016). Though thick-skinned systems may have detachments at various depths down to the lower crust (depending on the temperature and composition of the lithosphere), these faults do not cut the entire lithosphere (e.g., Smithson et al., 1979; McBride et al., 1992; Erslev, 1993; Richardson et al., 2013; Yeck et al., 2014; Lacombe & Bellahsen, 2016; Worthington et al., 2016). During thrusting, as basement rocks are translated from sub-horizontal detachment horizons over ramps in the upper crust (Fig. 1; e.g., Erslev, 1993), crowding at high structural levels may result in formation of synthetic and antithetic thick-skinned thrusts (e.g., Erslev, 1986; Gray et al., 2019; Groshong & Porter, 2019). Given that thin-skinned thrusts utilize weak lithologies within the upper crust and thick-skinned thrusts are thought to utilize sub-horizontal strength contrasts within the middle and lower crust, thin- and thick-skinned domains may occur in the same area but at different structural depths (Kulik & Schmidt, 1988; Betka et al., 2015; Lacombe & Bellahsen, 2016).

In some fold-thrust belts, including in a few localities within the Sevier fold-thrust belt, slivers of mechanical basement can be incorporated into structural culminations (Boyer & Elliot, 1982; Yonkee, 1992; DeCelles et al., 1995; O’Sullivan & Wallace, 2002; Pfiffner, 2006, 2017). In the North American Cordillera, formation of these anticlinoria was likely controlled by the basement step at the eastern limit of thick Neoproterozoic strata within the western Laurentian rift margin (Fig. 1c; Yonkee, 1992; DeCelles, 1994, 2004; Carney & Janecke, 2005; DeCelles & Coogan, 2006; Long, 2012). Regional-scale basement slivers can also be found in structurally deep portions of fold-thrust belts where the brittle-plastic transition occurs directly below the basement-cover contact (e.g., Lacombe & Bellahsen, 2016; Pfiffner, 2017). In our view, these basement-involved thrusts represent a transitional example in the continuum between thin- and thick-skinned structural styles, because basement is not fundamentally involved in shortening and basement deformation is facilitated by plastic—not frictional—deformation mechanisms (e.g., Yonkee, 1992).

Critical taper theory serves as a foundation for understanding how deformation propagates through a thin-skinned fold-thrust belt (Davis et al., 1983), but is less clearly applied to thick-skinned domains. In the critical taper model, horizontal shortening is accommodated by vertical thickening of the crust; during continued shortening, the locus of active deformation propagates away from the thickened region, creating a wedge-shaped fold-thrust belt. Thickening within the wedge increases the taper angle (dip of the basal detachment plus surface slope) beyond the critical value set by the compressive strength of the material within the wedge and the frictional resistance to sliding at the base of the wedge. In response, the thrust front propagates forward, surface slope decreases to sub-critical conditions, and internal thickening resumes. Deformation of the wedge alternates between forward propagation of “in-sequence”

thrusts and internal thickening during “out-of-sequence” thrusting. Crucially, critical taper models assume that a single, fixed basal detachment is utilized throughout deformation of the wedge.

In natural orogenic wedges, the basal detachment cuts up-section in the direction of transport and migrates forward through time (Dahlstrom, 1970; Boyer & Elliott, 1982), advancing when the wedge is in a supercritical state of taper (Davis et al., 1983). Slip is often transferred from the basal detachment to stratigraphically higher detachment horizons (including within foreland basin sedimentary rocks; Chapman & DeCelles, 2015) and eventually to the surface. As the orogenic wedge continues to propagate, slip along the frontal thrust wanes as the basal detachment begins to carry the former toe thrust in its hanging wall and feeds slip into a newly initiated frontal thrust. This results in sequential down-stepping of the frontal thrust to the basal detachment through time, which is widely documented globally, including in the Sevier fold-thrust belt (e.g., Royse et al., 1975), the Himalayan fold-thrust belt (e.g., DeCelles et al., 2001), and the central Andean fold-thrust belt (e.g., Echavarría et al., 2003).

Thick-skinned thrusts are generally not interpreted within the context of critical taper theory because their level of detachment (if any) is often unknown and is likely below the brittle-plastic transition, the large thrust spacing complicates approximations of the surface slope, and pre-existing weaknesses are often reactivated (e.g., Erslev, 1993; Pearson et al., 2013; Groshong & Porter, 2019). Models of thick-skinned thrust belts generally predict that the basal detachment utilizes strength contrasts, either becoming sub-horizontal near the brittle-plastic transition (e.g., Armstrong & Dick, 1974; Kulik & Schmidt, 1988), or continuing to deeper levels (Scheevel, 1983; McQueen & Beaumont, 1989; Erslev, 1993; Mazzotti & Hyndman, 2002), depending on the temperature-dependent strength profile of the lithosphere (Lacombe & Bellahsen, 2016).

Regardless of scale, modeling demonstrates that strength contrasts determine not only detachment horizons, but also the structural style (Stockmal et al., 2007; Simpson, 2010; Ruh et al., 2012; Bauville & Schmalholz, 2015). In the upper crust, thick-skinned thrust systems may also utilize pre-thrusting weaknesses such as basement foliations (e.g., Schmidt et al., 1995) or shear zones (Weil et al., 2014), dikes (e.g., Neely & Erslev, 2009), or older normal faults (e.g., Pearson et al., 2013).

## 2.2 Mechanical stratigraphy of the Idaho-Montana fold-thrust belt

Deformation within the thin-skinned Sevier fold-thrust belt coincides with the gradual westward thickening of sedimentary rocks of the Neoproterozoic and Paleozoic rift and passive margin succession (Burchfiel & Davis, 1975). A hinge line separates thinner stratigraphy overlying the craton in the east from stratigraphy of the carbonate shelf, which thickens toward the west (Kay, 1951; Huh, 1967). The basal detachment for much of the Sevier fold-thrust belt commonly exploited mechanically weak, fine-grained Neoproterozoic and Cambrian rocks that occur near the base of the sedimentary sequence, particularly west of the hinge line (Armstrong, 1968; Royse et al., 1975; Price, 1981; DeCelles & Coogan, 2006; Yonkee & Weil, 2015). Basement heterogeneities near the hinge line resulted in local involvement of mechanical basement, such as is documented in the Wasatch anticlinorium (Yonkee, 1992).

In its northward projection into east-central Idaho and Montana, the lower part of the sedimentary sequence is disrupted by significant along- and across-strike facies and thickness changes. Near the interior of the fold-thrust belt, in the Lemhi and Lost River ranges of east-central Idaho (Fig. 2), 5-6 km of predominantly pre-orogenic carbonate shelf strata overlie Mesoproterozoic quartzite (Shannon, 1961; Scholten & Hait, 1962; Skipp & Hait, 1977). Around

75 km to the northeast, near the frontal thin-skinned Tendoy thrust and adjacent thick-skinned thrusts of the foreland (Fig. 2), a 2-3 km thick Cambrian to Triassic, pre-orogenic section of mixed siliciclastic and carbonate strata (Fig. 3) overlies crystalline basement rocks of the craton (Skipp, 1988; Lonn et al., 2000). The study area is within the central Beaverhead Mountains (Figs. 2, 3) between the western carbonate shelf and eastern craton sections (Huh, 1967; Rose, 1976), where a ~2.5 km thick section of Devonian to Pennsylvanian carbonate and mixed siliciclastic strata (Ruppel, 1968; Lund, 2018; Lonn et al., 2019) unconformably overlies a thick, previously-tilted succession of fine-grained Mesoproterozoic quartzite (Lonn et al., 2019).

West of the study area, the thickness of Ordovician to Devonian carbonate rocks increases from <200 m in the Lemhi Range to >1 km in the Lost River Range (Figs. 2, 3) (Ross, 1947; Sloss, 1954). The area of thinner stratigraphy was termed the Lemhi arch by Sloss (1954) and interpreted as a positive topographic element during early to mid Paleozoic time. Two main unconformities define the basement high: (1) the sub-Ordovician Lemhi arch unconformity, defined below the Middle Ordovician Kinnikinic Quartzite and (2) the intra-Devonian Lemhi arch unconformity, defined below the upper part of the Late Devonian Jefferson Formation (Fig. 3). The sub-Ordovician Lemhi arch unconformity is observable throughout much of the Lemhi and Beaverhead ranges, where Kinnikinic Quartzite overlies Mesoproterozoic quartzite and hypabyssal ~500 Ma Beaverhead plutons (Lund et al., 2010; Link et al., 2017) often with an angularity of 20-30° (Scholten, 1957; Hansen & Pearson, 2016; Pearson & Link, 2017). The intra-Devonian Lemhi arch unconformity is exposed in the central and southern Beaverhead Mountains, where a thin (<50 m) upper Jefferson Formation rests on Mesoproterozoic quartzite (Scholten & Hait, 1962; Grader et al., 2017; Lonn et al., 2019). The thinning and pinching out of

pre-thrusting stratigraphy near the Lemhi arch basement high restricted the distribution of weak layers available for thin-skinned thrusting during Mesozoic time.

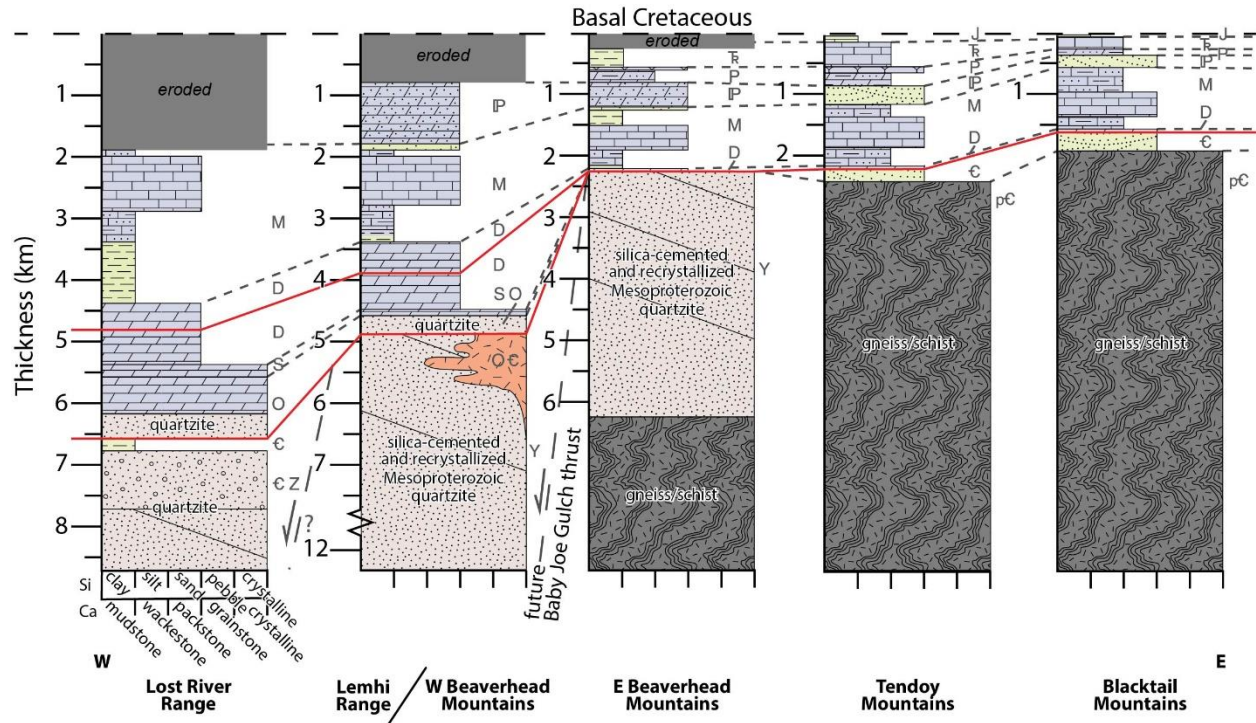


**Figure 3.** Generalized lithostratigraphic columns across the Idaho-Montana fold-thrust belt (see Fig. 2 for locations). Red lines show sub-Ordovician and intra-Devonian Lemhi arch unconformities (Grader et al., 2017), with angular unconformities shown where appropriate. Lithologies and grain sizes for siliciclastic (Si) and carbonate (Ca) units are shown on x-axis. Blue represents carbonate units; green represents poorly cemented siliciclastic units; tan represents quartzites. Approximate thicknesses are shown below a datum at the base of Cretaceous strata (or younger rocks, depending on erosion level). Generalized correlations of time periods and inferred normal faults are shown as dashed lines.

### 2.3 Structural styles of the Idaho-Montana fold-thrust belt

The fold-thrust belt of east-central Idaho and southwestern Montana (44°–45°N) forms a prominent reentrant between the Helena salient of central Montana and the Wyoming salient of

southeastern Idaho, Wyoming and northern Utah. In central Idaho (Fig. 2), the Pioneer and Copper Basin thrusts form the orogenic interior of an east- to northeast-verging, leading imbricate fan (Skipp & Hait, 1977; Dover, 1981; Rodgers & Janecke, 1992). Recent work (Brennan et al., 2020) demonstrates that these thrusts deformed a relatively thick succession of Neoproterozoic and Paleozoic rift and passive margin rocks southwest of the Lemhi arch basement high.

Northeast of the Pioneer and Copper Basin thrusts (Fig. 2) is a broad region where no major thrust faults are mapped; instead, large (>15 km wavelength) folds affected Mesoproterozoic quartzites at deeper structural levels (Tysdal, 2002; Hansen & Pearson, 2016; Lonn et al., 2016), structurally below a more tightly folded passive margin succession (Hait, 1965; Beutner, 1968). Northeast of this folded domain, major thrusts include (from west to east) the Hawley Creek, Cabin, Medicine Lodge, and Tendoy thrusts (Scholten et al., 1955; Lucchitta, 1966; Skipp & Hait, 1977; Skipp, 1988). The Cabin and Hawley Creek thrusts are interpreted as along-strike equivalents or footwall imbricates of the Freeman and Poison Creek thrusts, respectively (Fig. 2; Skipp, 1988; Evans & Green, 2003; Lonn et al., 2016). In most exposures, these moderately-dipping thrusts cut indiscriminately across lithologic contacts within the Mesoproterozoic quartzites and older gneisses and schists that defines the Lemhi arch basement high (Skipp, 1988; Hansen & Pearson, 2016; Lonn et al., 2016). Northeast of these mechanical basement-involved thrusts, the Medicine Lodge, Tendoy, and minor related thrusts form an imbricate fan that involves mostly Paleozoic to Mesozoic rocks, including syntectonic wedge-top conglomerates of the foreland basin (Perry & Sando, 1982).

The foreland of southwestern Montana marks the northwesternmost extent of the structurally defined Laramide province, where variably oriented thick-skinned thrusts involve

crystalline basement of the craton (Eardley, 1963; Dickinson & Snyder, 1978; Yonkee & Weil, 2015). At upper structural levels throughout the Idaho-Montana fold-thrust belt, including the foreland, middle Paleozoic and younger carbonate rocks accommodated shortening primarily by folding and bedding-parallel detachment (Ruppel & Lopez, 1988; Tysdal, 1988; Anastasio et al., 1997). Despite the regional continuity of folds and thrusts at these upper structural levels, most prior workers define the Tendoy thrust as the leading edge of the Sevier belt (Scholten et al., 1955; Skipp & Hait, 1977; Skipp, 1988; DeCelles, 2004) and the inferred boundary between thin- and thick-skinned thrust domains.

In the Idaho-Montana fold-thrust belt, interactions among thin- and thick-skinned thrusts can be directly observed. We highlight key areas (pink stars on Fig. 2) that illustrate a regional trend of overlapping thin- and thick-skinned thrusts. On the flank of the Blacktail-Snowcrest uplift, thin-skinned thrusts detached in Mississippian rocks are truncated by the thick-skinned Jake Canyon thrust (Fig. 2c: Schmidt et al., 1988; Tysdal, 1988). Similarly, the thin-skinned, east-vergent McCartney Mountain salient (McCarthy Mountain salient of Brumbaugh & Hendrix, 1981; O'Neill et al., 1990) is cut by or buttressed against the thick-skinned Biltmore anticline (Fig. 2b; Lopez & Schmidt, 1985; Schmidt et al., 1988). Folding related to blind thick-skinned thrusts beneath the thin-skinned Tendoy thrust occurred both before and after slip along the Tendoy thrust (Perry et al., 1988; McDowell, 1997). These examples highlight a regional trend of contemporaneous thin- and thick-skinned thrusts, one on top of the other (Kulik & Schmidt, 1988).

Observations of crosscutting and overlapping structural styles are not confined to the foreland of the Idaho-Montana fold-thrust belt. Most notably, the basement-involved Cabin thrust truncates the thin-skinned Medicine Lodge thrust in the Tendoy and Beaverhead

Mountains (Fig. 2a; Skipp, 1988). Farther west in the Lemhi and Lost River ranges, structural style changes noticeably with depth (e.g., Kuntz et al., 1994). An upper folded package defines an east-verging fold belt in the Lemhi Range, which is detached within anhydrite-bearing dolostones and shales at the intra-Devonian Lemhi arch unconformity (Beutner, 1968; Hait, 1965). This fold belt is offset and folded by thrusts that cut quartzites and massive dolostones below the intra-Devonian Lemhi arch unconformity. A regional anticline (Patterson culmination of Janecke et al., 2000) exposes Mesoproterozoic quartzites of the Lemhi arch in its broken core, with the tilted fold belt visible on its flank. Across the region, thrusts that cut quartzite, gneiss, and schist generally have short fault segments that vary from ~NW-SE to ~ E-W striking, with moderate to steep dips (Lucchitta, 1966; Beutner, 1968; Hait, 1965, Scholten & Ramspott, 1968; Skipp, 1988; M'Gonigle 1993; 1994), similar to the thick-skinned thrusts of the Montana foreland (e.g., Schmidt & Garihan, 1983; Schmidt et al., 1988). In summary, throughout the Idaho-Montana fold-thrust belt, thin-skinned thrusts with basal detachments in weak Paleozoic units are overprinted by deeper structures within the mechanical basement of the Lemhi arch.

The absolute age of deformation within these two packages is less constrained. A basal angular unconformity, isopach maps, and reconstructed paleocurrent data from the Lower to mid Cretaceous Kootenai Formation in the southwestern Montana foreland may suggest early, low-magnitude exhumation related to thick-skinned thrusting (Scholten, 1982; Schwartz, 1982; DeCelles, 1986), but within a regional continuous foreland basin setting with extrabasinal sources (Rosenblume et al., 2021). Provenance studies of the Late Cretaceous to Paleocene Beaverhead Group (Ryder & Scholten, 1973; Perry & Sando, 1982; Haley et al., 1991; Garber et al., 2020) and low-temperature thermochronologic data (Carrapa et al., 2019) suggest mid to Late Cretaceous exhumation of the Blacktail-Snowcrest arch, followed by in-sequence slip along

the thin-skinned Medicine Lodge and Tendoy thrusts. Similar observations and interpretations were made for the Hawley Creek and neighboring thrusts, which truncate an open, SW-plunging syncline (Lucchitta, 1966). These observations show a common relationship: thin-skinned thrusts and related folds are mutually crosscutting with deeper thick-skinned structures within the Idaho-Montana fold-thrust belt. Direct exposure of cross cutting thin- and thick-skinned thrusts thus makes the Idaho-Montana fold-thrust belt a suitable locality for investigating the influence of preexisting stratigraphy on progressive deformation and how a wide variety of structural styles can arise from one protracted shortening event.

### **3 Methods**

In this study, we evaluate the hypothesis that an upper thin-skinned and lower thick-skinned thrust domain are separated by a low-angle basement/cover contact that defines the Lemhi arch (Fig. 1b). To test this hypothesis we mapped the northern portion of the Leadore quadrangle (Fig. 4) at the 1:24,000-scale (Parker & Pearson, 2020), in the process documenting the range of structural styles present, their spatial and temporal relationships, and the stratigraphy involved. As a starting point, we used the stratigraphic framework established in the neighboring Bannock Pass quadrangle (Lonn et al., 2019) to the north and placed Devonian rocks in the regional context established by Grader et al. (2017). By comparing local and regional stratigraphy (Fig. 3), we constrain the position of the Lemhi arch basement high. We then interpret the deformation features of the study area in a Lemhi arch reference frame.

Field measurements of bedding, foliations, and cleavage planes, stretching lineations, and fold hinges were plotted on equal-area, lower hemisphere stereographic projections using the program Stereonet (v. 10.1.6 of Allmendinger et al., 2013); Kamb contouring at  $2\sigma$ -uncertainty

levels was performed to identify patterns (Mardia, 1972). We quantified patterns as clustered (P) or girdled (G), following methods of Vollmer (1990). After calculating eigenvectors ( $\lambda_1, \lambda_2, \lambda_3$ ) in Stereonet, we calculated the proportions that are classified as clustered ( $P=\lambda_1-\lambda_2$ ) and girdled ( $G=2(\lambda_2-\lambda_3)$ ). The remaining proportion (R) assesses the part of the distribution that is random ( $R=3(\lambda_3)$ ). All P, G, and R values are reported as percentages. For girdled distributions, Bingham statistics were used to calculate the cylindrical best fits of plotted points. For clustered distributions, mean vectors and associated  $\pm 2\sigma$  confidence cones were calculated using Fisher vector distributions. When clustered trends overlapped the margin of the plot, we manually rotated the data to fit in one frame of view before calculating the mean vector. The azimuths of fold hinges were plotted using rose diagrams and a mean vector and the associated  $\pm 2\sigma$  confidence interval was calculated using Krumbein's mean vector (Krumbein, 1939).

We documented kinematic indicators of faults and shear zones in the field and in oriented thin sections. Where observed, we measured lengths and heights of rugose corals as viewed in cross section and lengths and widths of crinoid ossicles as viewed along a common plane of view. In general, cross sections of strained corals have long axes parallel to cleavage and short axes approximately perpendicular to cleavage. Deformed crinoid ossicles were observed within shear zones and generally exhibited long axes that are approximately parallel to stretching lineations when viewed on the shear foliation surface. We calculated aspect ratios for each measured coral and crinoid, and mean values for all. Uncertainty values reflect standard deviation ( $2\sigma$ ) of all calculated aspect ratios (length/height) used to calculate the mean. These aspect ratios only approximate the amount of strain within the plane of view. Uncertainty regarding the initial lengths and orientations of strain markers in the field precluded a quantitative determination of the shape of the strain ellipsoid.

We established relative timing constraints from crosscutting relationships observed in the field and inferred from map relationships. Using this relative timeline, we constructed a series of deformation events that relate the preexisting stratigraphy to the resultant structural style by synthesizing our mapping results, measurements of deformation features, and kinematic constraints.

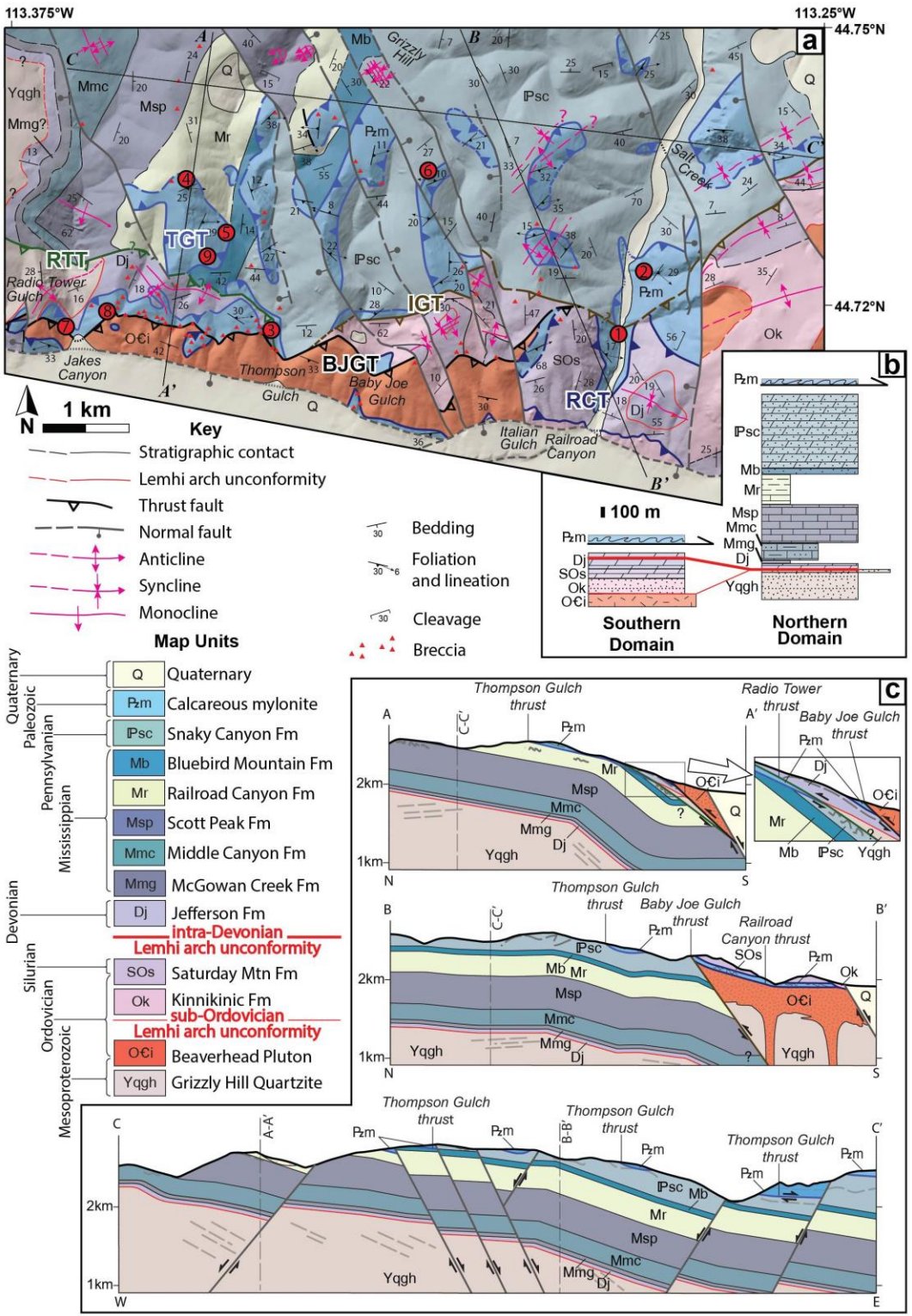


**Figure 4.** a) Simplified bedrock geologic map of the study area (see Fig. 2 for location; modified from Parker & Pearson, 2020). Thrust faults: RTT = Radio Tower thrust, TGT = Thompson Gulch thrust,

BJGT = Baby Joe Gulch thrust, IGT = Italian Gulch thrust, RCT = Railroad Canyon thrust. Numbers in red circles denote specific outcrops referenced in the text. **b)** Stratigraphic columns of the southern and northern domains. Red lines denote sub-Ordovician and intra-Devonian Lemhi arch unconformities. **c)** Simplified cross sections.

## 4 Results

### 4.1 Pre-thrusting stratigraphy

Our mapping results corroborate previous interpretations (Ruppel, 1968; Lund, 2018) that two unique stratigraphic packages are exposed in the northern and southern portions of the map area (Fig. 4b). We identify previously unrecognized calcareous mylonites overlying both stratigraphic packages.

Approximately 1.8 km of Devonian to Pennsylvanian shelf strata are exposed in the northern portion of the map area (Fig. 4; thicknesses walked in the field and measured from geologic map). The Mesoproterozoic Quartzite of Grizzly Hill is the lowest exposed unit. We interpret the age of this unit as Mesoproterozoic and not Cambrian to Mesoproterozoic (Lonn et al., 2019; Parker & Pearson, 2020) because all available detrital zircon dates are Mesoproterozoic in age and we were unable to find conclusive evidence of trace fossils in the field. Above the Quartzite of Grizzly Hill, <50 m of unfossiliferous laminated dolostone of the Devonian upper Jefferson Formation marks the intra-Devonian Lemhi arch unconformity. The overlying Mississippian section consists of (from bottom to top) 28 m of clay- to siltstone and silty lime mudstone of the McGowan Creek Formation, ~600 m of thin-bedded to massive limestone and chert of the Middle Canyon and Scott Peak formations, and ~250 m of lime mudstone, siltstone, and shale of the Railroad Canyon Formation. Above is >850 m of thinly-

bedded chert and limestone interbedded with calcareous-cemented quartz arenite of the Mississippian to Pennsylvanian Bluebird Mountain and overlying Snaky Canyon formations.

Distinct stratigraphy of the southern portion of the map area is exposed in the hanging walls of thrusts (Figs. 4a, 4b). In this stratigraphic package, the Cambro-Ordovician Beaverhead pluton is the lowest exposed unit and is overlain in inferred nonconformity (sub-Ordovician Lemhi arch unconformity) by the cliff-forming Ordovician Kinnikinic Quartzite. Above lies ~250 m of fossiliferous dolostones that are assigned to the Middle Ordovician-Silurian Saturday Mountain and the Late Devonian Jefferson formations on the basis of the fossils *Halysites* and *Amphipora* (Ross, 1934; Stock, 1990; Stearn, 1997).

Map relationships and detailed stratigraphy (Grader et al., 2017) require that prior to Mesozoic shortening, Devonian and younger strata were laterally continuous across the study area above the intra-Devonian Lemhi arch unconformity, but Ordovician to Devonian strata above the sub-Ordovician Lemhi arch unconformity are confined to the southern part of the map area. The spatial overlap of both unconformities in the study area constrains the specific locations of the Lemhi arch basement high, which is locally composed of the Quartzite of Grizzly Hill and the Beaverhead pluton.

#### 4.2 Structural domains

The stratigraphic section exposed in the northern part of the study area is part of a >20 km long SE-dipping homocline (Lonn et al., 2019), structurally beneath the stratigraphically different southern area (Fig. 4). To simplify the discussion, we separate the study area into three structural domains: (1) the sedimentary rock dip panel, (2) the carbonate mylonite, and (3) the basement-rooted domains. The sedimentary rock dip panel domain includes strata that is both

north of the Radio Tower, Baby Joe Gulch, and Italian Gulch thrusts and in the footwall of the Thompson Gulch Thrust. The sedimentary rock dip panel domain is visible on the map (Fig. 4) as the SE-dipping homocline that exposes the full Mesoproterozoic to Pennsylvanian section. The carbonate mylonite domain includes rocks in the hanging walls of the Thompson Gulch and Railroad Canyon thrusts. The carbonate mylonite domain is visible on the map as a series of low-angle klippe that overlies both the sedimentary rock dip panel and basement-rooted domains. The basement-rooted domain includes the non-mylonitized strata in the hanging walls of the basement-involved Radio Tower, Baby Joe Gulch, and Italian Gulch thrusts. The stratigraphy of the basement-rooted domain mostly defines the southern domain shown in Fig. 4b.

Normal faults overprint all domains. Rarely observed brecciation within fault zones constrains fault dips of  $\sim 60\text{-}70^\circ$  toward the WSW and ENE. Offset of thrust faults across these normal faults constrains normal fault throw to  $<100$  m. NNW-SSE striking normal faults apparently did not reactivate older deformation features resulting from horizontal shortening. These observations suggest that NNW-SSE striking normal faults post-date and are unrelated to deformation features accommodating horizontal shortening and will therefore not be discussed further.

#### 4.2.1 Sedimentary rock dip panel domain

Within the gently southeasterly dipping section of the sedimentary rock dip panel domain, carbonate rocks of the Mississippian Scott Peak and Pennsylvanian Snaky Canyon formations are folded into tight folds with locally overturned limbs, northeast vergence, wavelengths of meters to tens of meters, and occasional small-offset thrusts in fold hinge zones (Figs. 4, 5). The observed folds lack continuity into adjacent units, indicating bedding-parallel

detachment folding and some fault-propagation folding. Small, high-angle faults define angular, domino-style blocks with mm-scale down-to-the-SW normal offset (e.g., Goscombe et al., 2004) (Fig. 5g), consistent with top-to-the-NE, bedding-parallel slip within the fine-grained Railroad Canyon Formation.

Poles to bedding within 1 km of the Radio Tower thrust (N=107) define an east-southeast trending fold, with a calculated fold hinge plunging toward  $109^\circ$  at  $2^\circ (\pm 6^\circ)$  (Fig. 5b). This distribution is 40% clustered and 30% girdled, suggesting complexities in addition to the mapped fold. Otherwise, poles to bedding planes (N=150) are clustered (P=62%; G=2%) and define an average dip toward  $155^\circ$  at  $12^\circ (\pm 5^\circ)$  (Fig. 5a).

At some localities, a pervasive, low-angle pressure solution cleavage was observed with poles to cleavage planes (N=64) defining a clustered distribution (P=73%; G=8%) with a mean plane dipping toward  $229^\circ$  at  $11^\circ (\pm 6^\circ)$  (Fig. 5c); this orientation is clearly not axial planar to upright detachment folds. Near Grizzly Hill, strained rugose corals (N=22) have long axes that are parallel to cleavage, with a mean aspect ratio of  $2.2 \pm 0.5$  (Fig. 5e).

Cross-cutting relationships demonstrate that folding during bedding-parallel slip occurred prior to southeastward tilting within the sedimentary rock dip panel domain. The documented shallowly W-dipping pressure solution cleavage and associated sub-vertical shortening crosscuts folded bedding and is not associated with the hinge zones of folds, suggesting that cleavage formed after NE-directed folding. Tilting toward the southeast occurred after NE-directed folding. The tilted section continues ~10 km northwest of the study area, potentially related to the Peterson Creek thrust (Staatz et al., 1979).

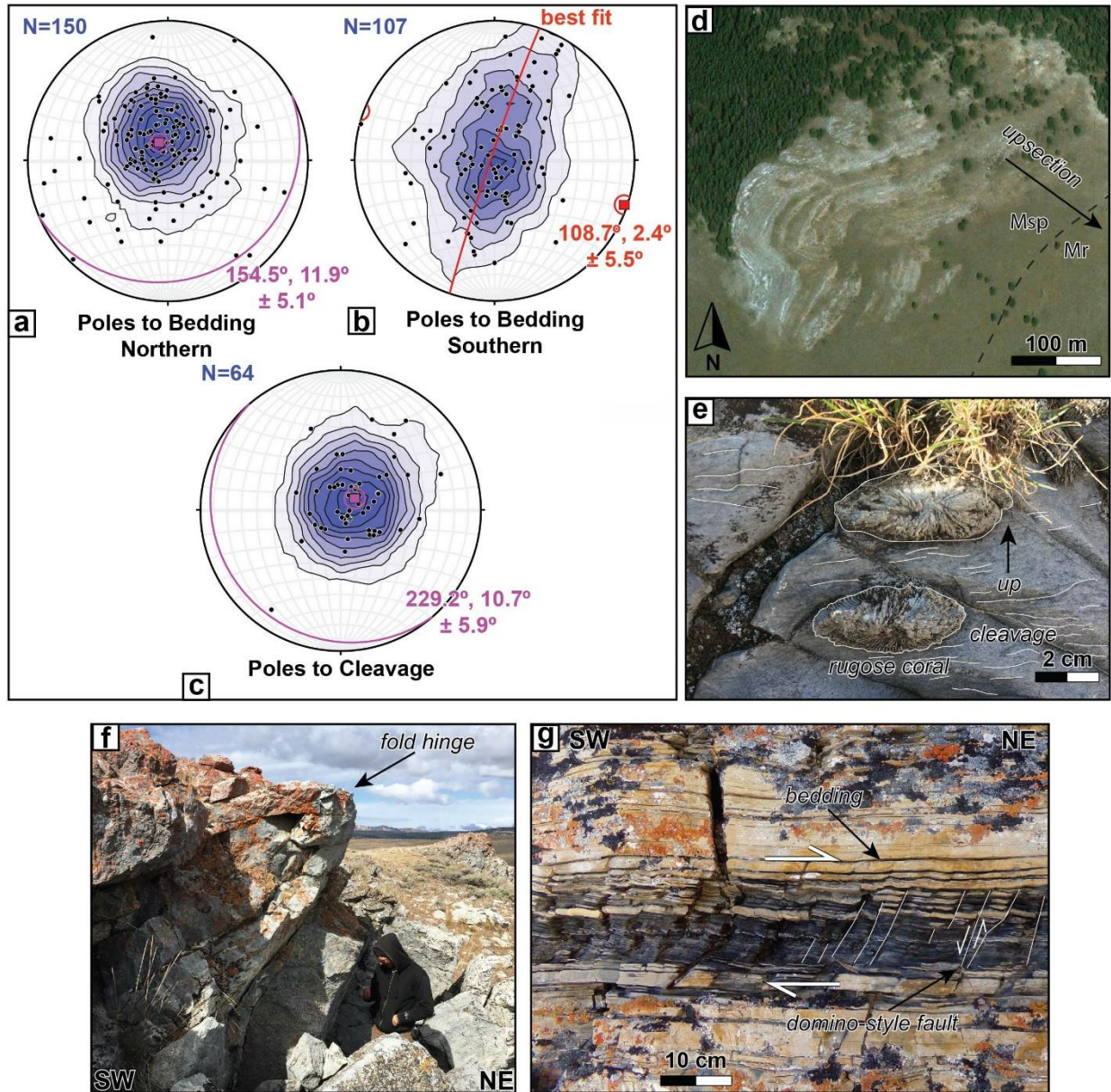


**Figure 5.** Deformation features of the sedimentary rock dip panel domain. Lower hemisphere stereographic projections showing: **a)** Poles to bedding >1 km away from moderately-dipping thrust faults. Mean vector and corresponding plane labeled. **b)** Pi-plot of poles to bedding within 1 km of moderately-dipping thrust faults. Cylindrical best fit and calculated fold hinge labeled. **c)** Poles to cleavage. Mean vector and corresponding plane labeled. **d)** Satellite photo showing folds in map view. **e)**

Outcrop photos of strained rugose coral in cross section, **f**) folded limestones near Grizzly Hill, and **g**) bed-parallel shear in the Railroad Canyon Formation.

## 4.2.2 Carbonate mylonite domain

### 4.2.2.1 General description

Prior mapping by Lund (2018) and Lucchitta (1966) recognized fine-grained foliated carbonate rocks of inferred Mississippian age thrust over lesser deformed upper Paleozoic sedimentary rocks. These foliated carbonated rocks have a striking banded appearance, with calcite with siliceous interlayers on the mm- to cm-scale (Fig. 6f). Segregation of dynamically recrystallized matrix grains ( $<20\ \mu\text{m}$ ) and deformed porphyroclasts define the foliation in thin section. In addition to mm-scale foliations, we document a previously unrecognized penetrative stretching lineation within these predominantly calcitic rocks (Figs. 4, 6f, 5f). The penetrative stretching lineation is defined by elongated aggregates of dynamically recrystallized grains, giving it a diffuse and streaky appearance on foliation surfaces (Fig. 6f). Based on the pervasive foliation and abundant evidence of dynamic recrystallization, we interpret the foliated carbonates that define the Thompson Gulch (Lund, 2018) as carbonate mylonites (Bell & Etheridge, 1973; White et al., 1980; Fossen, 2016). Mylonite outcrops form klippen, with thicknesses ranging from 40-80 m based on good exposures in Thompson Gulch and Railroad Canyon (Fig. 4). Exposures on ridges and in Railroad Canyon show a low-angle fault contact, at a low angle to bedding, leading us to classify both the Thompson Gulch and Railroad Canyon thrusts as thin-skinned.

Within the low-angle shear zones of both thrusts, particularly near Railroad Canyon, some siliceous interlayers have diffuse terminations parallel to the layering, suggesting that

silicification of mm- to cm-scale interlayers was secondary and occurred during mylonitization. Tabular beds of matrix-supported calcareous breccia with sub-rounded clasts are often observed in fault contact with carbonate mylonite. In the immediate footwall of the Baby Joe Gulch thrust, between Thompson Gulch and Jakes Canyon (Fig. 4), there is a recognizable tectonostratigraphy of calcareous breccia overlying tightly-folded silicified black shales, which, in turn, overlie the carbonate mylonite. Elsewhere, calcareous breccia and silicified black shales are associated with the carbonate mylonite, but are not preserved in a consistent structural succession. Cliff-forming rocks in Jakes Canyon, previously mapped as chert of the Phosphoria Formation (Evans & Green, 2003; Lund, 2018), are completely silicified, matrix-supported breccias with banded clasts (Fig. 8d) that we interpret as jasperoid (Lovering, 1962) overprinting carbonate mylonite.

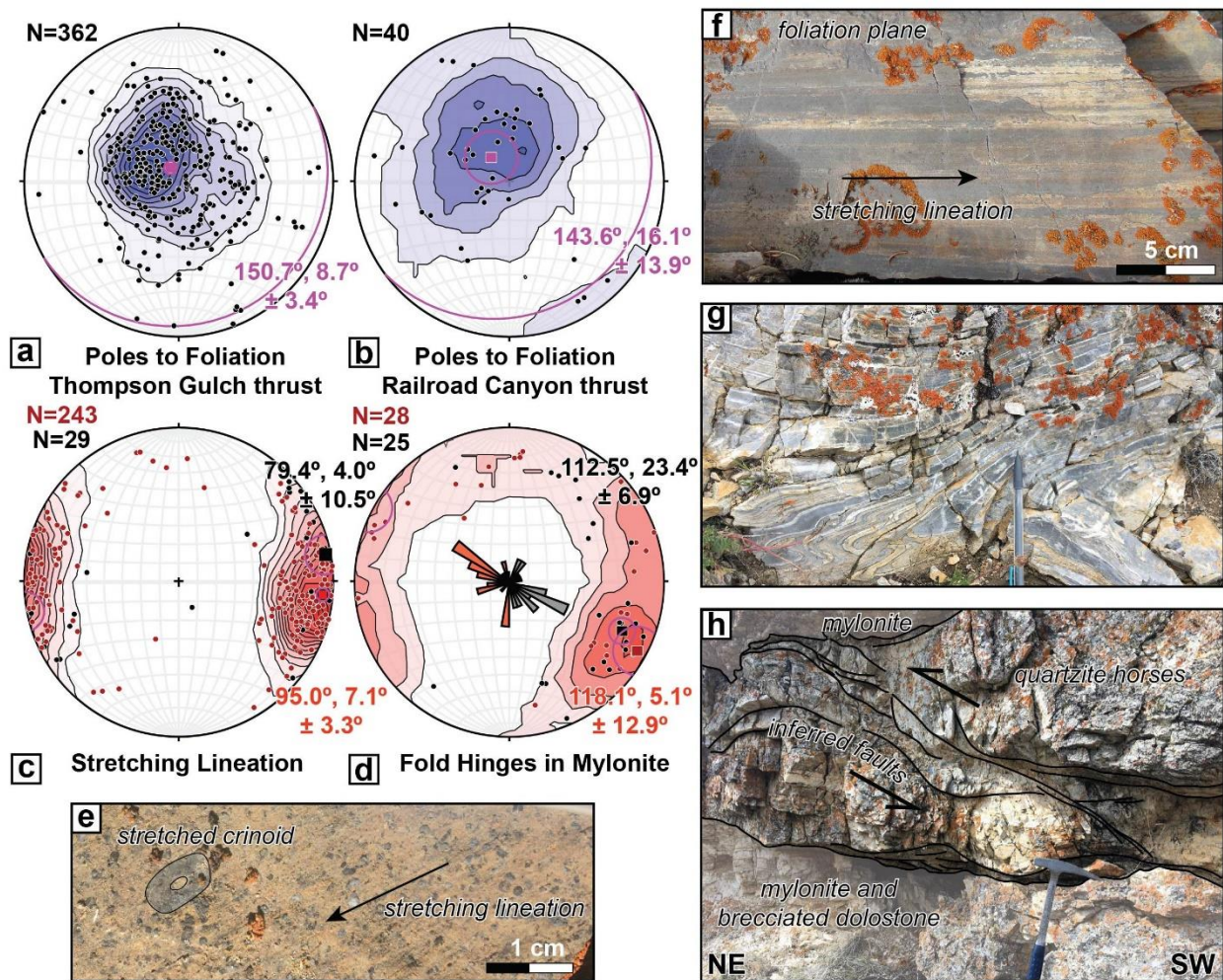


**Figure 6.** Deformation features of the carbonate mylonite domain. Lower hemisphere stereographic projections showing: poles to foliation of the **a**) Thompson Gulch and **b**) Railroad Canyon thrusts. Mean vector and corresponding plane labeled. **c**) Stretching lineations with mean vectors of Thompson Gulch thrust data (black) and Railroad Canyon thrust data (red) labeled. **d**) Fold hinges within mylonite with mean vectors labeled for post-mylonite (black) and syn-mylonite (red) folds. Inset rose diagram with  $10^\circ$  bins shows distribution of trends. Outcrop photos of **e**) stretched crinoid ossicle as viewed in plan view, **f**) typical carbonate mylonite as viewed in plan view, **g**) recumbent similar folds within otherwise parallel foliation as viewed in cross section, and **h**) quartzite horses between mylonite and brecciated dolostone as viewed in cross section.

#### 4.2.2.2 Thompson Gulch thrust

We refine the definition of the Thompson Gulch thrust by Lund (2018). Outcrops of carbonate mylonite define the shear zone, structurally above the sedimentary rock dip panel domain (Fig. 4). The thrust cuts up-section in its footwall toward the east (Fig. 4): in the western part of the map area near Jakes Canyon, the thrust occurs a few meters above the Devonian Jefferson Formation, within 10s of meters of the underlying Quartzite of Grizzly Hill; toward the west near Railroad Canyon, the thrust footwall consists of the Pennsylvanian Snaky Canyon Formation. Below the lowest exposure of the mylonite in the western part of the map area, 1-2 m thick horses of quartzite are thrust-bounded and merge upward into the superjacent mylonite (Fig. 6h); slickenline orientations on faults that bound the margins of the horses within the quartzite are indistinguishable from the orientations of stretching lineations in the overlying carbonate mylonite.

Plotted poles to foliation planes for the mylonite of the Thompson Gulch thrust (N=362) show a clustered distribution (P=56%; G=8%), with a mean plane dipping toward  $151^\circ$  at  $9^\circ$  ( $\pm 3^\circ$ ) (Fig. 6a). The mylonite contains tight, recumbent folds in close proximity to planar foliations (Fig. 6g). Rare shear bands are interpreted as C-C' fabrics. Boudins, minor brittle normal faults, and veins are uncommon (labeled red localities 1, 2 on Fig. 4) and overprint earlier mylonites. Stretching lineations (N=243) show a clustered distribution (P=72%; G=4%) and define a mean vector of  $095^\circ$ ,  $7^\circ$  ( $\pm 3^\circ$ ) (red dots, Fig. 6c). Crinoid ossicles on foliation planes are elongate parallel to the stretching lineation (Fig. 6g), with a mean aspect ratio of  $1.7 \pm 0.4$  (N=11).

In thin section, the mylonite of the Thompson Gulch thrust is mostly fine-grained (<20  $\mu\text{m}$  grain diameters in matrix grains) with a sub-horizontal shape-preferred orientation, and only rare asymmetric clasts indicative of non-coaxial strain. Coarse (>100  $\mu\text{m}$ ) calcite grains are characteristically twinned with tabular and sometimes curved morphologies (Fig. 7d). Oriented thin sections (5, 6, 7, 9 on Fig. 4) display  $\sigma$ -clasts, strain fringes, offset veins, and C-C' shears that give a consistent top-to-the-E sense of slip (Fig. 7c, d, e). An outcrop along the western side of Thompson Gulch (Fig. 7) clearly shows C-C' shear structures with an apparent top-to-the-ESE sense of shear within the shear zone of the Thompson Gulch thrust. At this location the mylonite of the Thompson Gulch thrust is in sharp contact with an overlying ~1 m thick, planar, matrix-supported breccia that defines a brittle fault zone interpreted as the Radio Tower thrust.

Folds within the mylonite are split into two categories: syn-mylonitic and post-mylonitic. Syn-mylonitic folds are commonly non-cylindrical, tight to isoclinal, similar folds with wavelengths from ~10-20 cm (Fig. 6f); sheath folds were also observed. Post-mylonitic folds are commonly cylindrical, tight to open, parallel folds with m-scale wavelengths; tight fold hinges are often brecciated. The orientations of both fold sets are very scattered, with a mean fold hinge of  $118^\circ, 5^\circ (\pm 13^\circ)$  for syn-mylonitic folds and  $113^\circ, 23^\circ (\pm 7^\circ)$  for post-mylonitic folds (Fig. 6d). Both sets of folds have gently-plunging hinges, resulting in an overall girdled distribution of plotted lines (P=28%; G=47%). Post-mylonitic folds are more often highly oblique to the stretching lineation. Near Railroad Canyon, post-mylonitic folds of the outcrop- to km-scale are NE-SW-trending, in the footwall of the Italian Gulch thrust (red localities 1, 2 on Fig. 4).

The interlayered carbonate, silicified shales, and local dolostone associated with the mylonite, as well as stretched crinoids in the shear zone, are consistent with a protolith within the lower half of the Paleozoic stratigraphy of the sedimentary rock dip panel (northern domain in

Fig. 4b). Results from mapping and structural analysis suggest overall eastward thrusting of the Thompson Gulch thrust hanging wall. Shallowly W-dipping pressure solution cleavage and sub-vertical flattening of rugose corals in the footwall of the Thompson Gulch thrust (sedimentary rock dip panel domain) are interpreted to have accommodated shear zone-normal flattening during thrusting, or alternatively may have been rotated during progressive non-coaxial shear as a result of diffuse deformation in the footwall of the Thompson Gulch thrust. The section was tilted toward the southeast either before or after thrusting. The shear zone of the Thompson Gulch thrust is a low-angle feature that spans more than 10 km (in the direction of transport) but involves only the thin-portion of the stratigraphic section (< 800 m) that contains silty and shaley intervals, demonstrating a correspondence with weak lithologic units. We therefore classify the Thompson Gulch thrust as thin-skinned. The Thompson Gulch thrust is truncated and folded by—and therefore older than—thrusts of the basement-rooted domain.

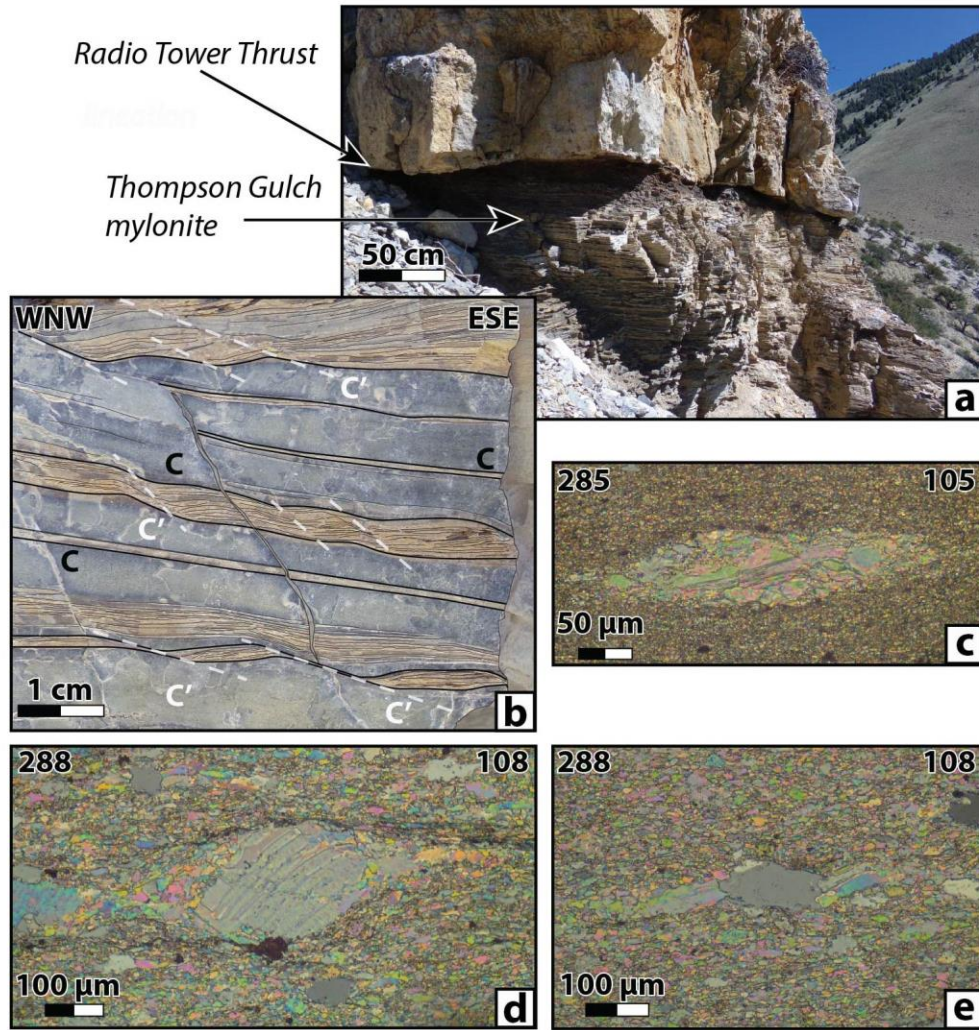


**Figure 7.** a) Outcrop photos showing fault contact of Radio Tower thrust and underlying Thompson Gulch mylonite (labeled red locality 3 on Fig. 4), and b) top-to-the-ESE C and C' shear fabrics within the Thompson Gulch mylonite. Oriented thin section photomicrographs showing c)  $\sigma$ -clast (location 3 on Fig.

4), **d**), **e**)  $\sigma$ -clast and calcite fibers in strain fringes around quartz grain (labeled red locality 4 on Fig. 4) all with a top-to-the-ESE sense of shear.

#### 4.2.2.3 Railroad Canyon thrust

In the southern part of the map area, carbonate mylonite indistinguishable from that of the Thompson Gulch thrust crops out in a different structural position in the hanging walls of the Italian Gulch, and Baby Joe Gulch thrusts. Between Jakes Canyon and Railroad Canyon, carbonate mylonite overlies the Beaverhead pluton and Kinnikinic Quartzite (red locality 8 on Fig. 4; 9d). Exposures in Railroad Canyon show a hanging-wall flat of the Saturday Mountain Formation above the mylonite (red locality 1 on Fig. 4). We assign the new name Railroad Canyon thrust to mylonites at this position.

Stretching lineations of the Railroad Canyon thrust (N=29) have a clustered distribution (P=64%; G=14%) and define a mean vector of  $79^\circ, 4^\circ (\pm 11^\circ)$  (solid dots, Fig. 6c). Plotted poles to foliation planes (N=40) show a loosely clustered distribution (P=42%; G=10%), with a mean vector defining a pole to a plane that dips towards  $144^\circ$  at  $16^\circ (\pm 14^\circ)$  (Fig. 6b).

The overall similarities in lithology, geometry, and kinematics of the Railroad Canyon and Thompson Gulch thrust mylonites suggests they formed as part of the same sequence of deformation. We make a distinction between the two on the basis of differing footwall stratigraphy. Unlike the Thompson Gulch thrust, the hanging wall geometry is well constrained near Railroad Canyon, where a hanging wall flat overlies the shear zone. We therefore classify the Railroad Canyon thrust as thin-skinned. Like the Thompson Gulch thrust, the Railroad Canyon thrust was offset by—and therefore older than—thrusts of the basement-rooted domain.

### 4.2.3 Basement-rooted domain

#### 4.2.3.1 General description

The hanging walls of the moderately to steeply dipping Baby Joe Gulch (Lund, 2018), Radio Tower, and Italian Gulch thrusts define the basement-rooted domain (Figs. 4, 8). These thrusts cut across bedded quartzites and plutonic rocks with no apparent relation to primary layering, suggesting that these rocks behaved as mechanical basement. We therefore categorize the Radio Tower, Baby Joe Gulch, and Italian Gulch thrusts as thick-skinned thrusts.

#### 4.2.3.2 Radio Tower Gulch thrust

A steeply (50-70°) S-dipping fault in Jakes Canyon, named here the Radio Tower Gulch thrust, juxtaposed the Mesoproterozoic Quartzite of Grizzly Hill over partly mylonitized and silicified younger footwall rocks that we tentatively assign to the Devonian Jefferson through Mississippian Middle Canyon formations (Fig. 8a, d). The intra-Devonian Lemhi arch unconformity shows ~1 km of apparent sinistral separation across the E-W Radio Tower thrust (Fig. 4). Hanging wall and footwall strata are folded by ESE-WNW-trending folds. East of Jakes Canyon, apparent stratigraphic separations were used to continue the uncertain trace of the fault to Thompson Gulch, where a moderately W-dipping thrust is well-exposed (Fig. 7a). The difference in dip along the fault plane requires folding or a complex fault geometry. The Radio Tower thrust clearly cuts the Thompson Gulch thrust in several locations and is therefore younger.

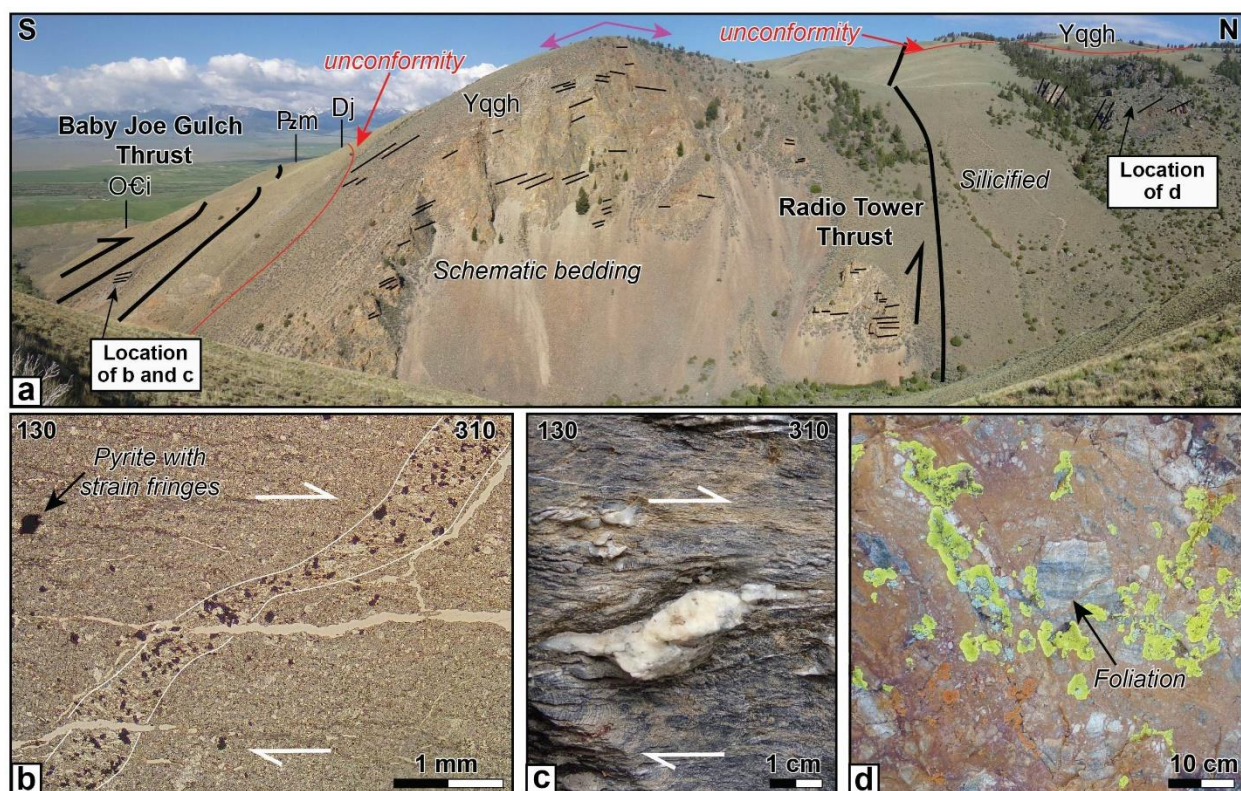


**Figure 8.** Field relationships and kinematics from the western side of Jakes Canyon (red locality 7 on Fig. 4). **a)** Thrust fault contacts marked in bold black lines, with fine black lines defining bedding orientation and an overall anticlinal structure (purple arrows). Red lines show the intra-Devonian Lemhi arch unconformity. Note that the Baby Joe Gulch thrust does truncate bedding at a low angle. **b)** Oriented thin section from the immediate footwall of the Baby Joe Gulch thrust showing vein with a top-to-the-NW sense of offset. Outcrop photos of **c)**  $\sigma$ -clast with a top-to-the-NW sense of shear and **d)** silicified breccia with relict foliation in clasts.

#### 4.2.3.3 Italian Gulch thrust

East of Thompson Gulch, the Ordovician Kinnikinic Quartzite and the structurally overlying mylonite of the Railroad Canyon thrust were thrust upon a footwall of mylonite of the Thompson Gulch thrust; we name this fault the Italian Gulch thrust. Unlike its footwall, the hanging wall of the Italian Gulch thrust carried the sub-Ordovician Lemhi arch unconformity and

Ordovician to Devonian strata. Where best constrained, west of Italian Gulch, the fault dips toward the south or southeast at 30-50°. Both ENE-WSW-trending and ESE-WNW-trending folds occur within the hanging wall and footwall of the Italian Gulch thrust. The Italian Gulch thrust clearly cuts the Thompson Gulch and likely the Railroad Canyon thrusts and is therefore younger. The presence of the sub-Ordovician Lemhi arch unconformity and overlying Ordovician and Silurian rocks in the hanging wall of the Italian Gulch thrust indicates a striking difference in pre-thrusting stratigraphy.

#### 4.2.3.4 Baby Joe Gulch thrust

The structurally highest thrust in the study area is the Baby Joe Gulch thrust, named by Lund (2018). Its trace is well-constrained from Jakes Canyon to Italian Gulch, where it cuts all other thrusts (Fig. 4). Unlike other mapped thrust faults that are either inferred with poorly constrained orientations (Italian Gulch thrust) or vary in orientation, possibly due to folding (Thompson Gulch, Railroad Canyon, and Radio Tower thrust) the Baby Joe Gulch is remarkably planar along most of its trace. The precisely mapped contact allows us to tightly constrain the orientation of the fault plane. Three-point problems define the fault that dips toward 198° at 38° ( $\pm 9^\circ$ ), roughly parallel to a weakly developed solid-state foliation within the Beaverhead pluton (Fig. 4). Across Italian Gulch, the trace of the Baby Joe Gulch thrust and foliation within the Beaverhead pluton transition from SSW-dipping to the west to SE-dipping toward the east. The trace of the Baby Joe Gulch thrust either intersects or merges with the trace of the Italian Gulch thrust east of Italian Gulch. The apparent dip of the Baby Joe Gulch thrust becomes less similar to that of the Italian Gulch thrust as you near their intersection, making it more likely that the Baby Joe Gulch thrust is truncated by the Italian Gulch thrust.

In the immediate footwall of the Baby Joe Gulch thrust on the eastern side of Jakes Canyon, post-mylonitic asymmetric kink bands (N=5) define a mean shear plane dipping toward  $207^\circ$  at  $57^\circ$  ( $\pm 7^\circ$ ) (Fig. 9b), with sigmoidal calcite veins suggesting a thrust sense of slip toward  $7^\circ$ . On the western side of Jakes Canyon (7 on Fig. 4), post-mylonitic shear zones have ~10 cm spacing and define a mean plane (N=4) dipping toward  $140^\circ$  at  $30^\circ$  ( $\pm 11^\circ$ ), with a top-to-the-NW sense of shear at the outcrop- and thin-section scale (Fig. 8b, c). Shear zones cut a low-angle crenulation cleavage, and both the crenulation cleavage and veins within the shear zones are folded. We are not confident that these kinematics are representative of the shortening direction of the Baby Joe Gulch thrust. We include these observations because they suggest different shortening directions for the Thompson Gulch and Baby Joe Gulch thrusts.

The Baby Joe Gulch thrust is apparently the youngest thrust in the study area: it cut the approximately flat-lying mylonites of the Thompson Gulch and Railroad Canyon thrusts as well as the steeply-dipping Radio Tower and Italian Gulch thrusts. Its approximately northeast- or northwestward displacement direction is highly oblique to that of the older Thompson Gulch thrust. Like the Italian Gulch thrust, the Baby Joe Gulch thrust carried a substantially different stack of rocks in its hanging wall. In the hanging walls of these thrusts, ~250 m of fossiliferous Ordovician to Devonian dolostones and an additional ~150 m of Ordovician sandstone rest unconformably on the Cambro-Ordovician Beaverhead pluton. These rocks are completely absent in the corresponding footwalls, where the exceptionally thin (~50 m) laminated dolostone of the Devonian Jefferson Formation (upper) rests directly on Mesoproterozoic quartzite. Restoration of the Italian Gulch and Baby Joe Gulch thrusts therefore requires pre-Devonian normal faults. These results suggest that “late-stage,” out-of-sequence thrusting associated with

the Baby Joe Gulch thrust cut the mechanical basement of the Lemhi arch in a thick-skinned style, and likely reactivated older normal faults.

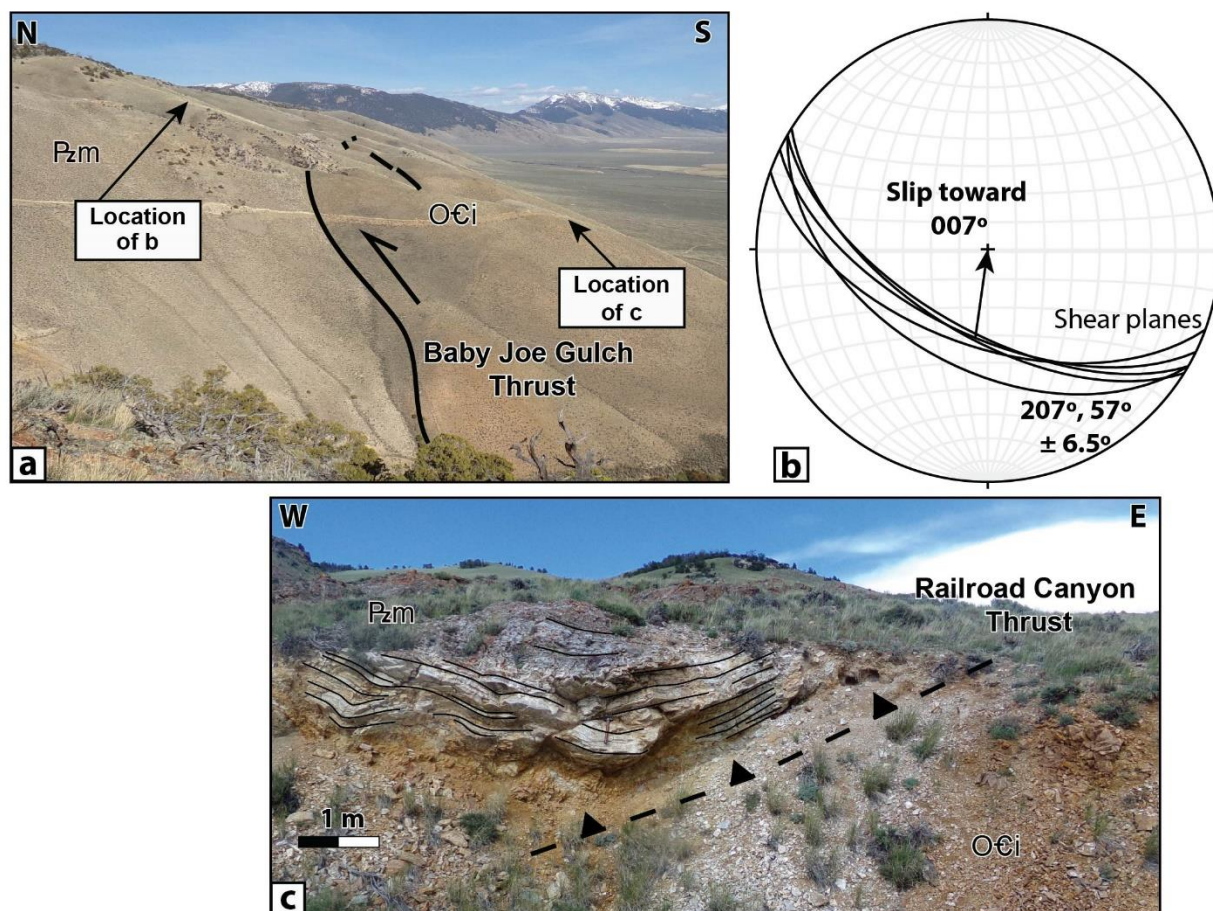


**Figure 9.** Field relationships from the eastern side of Jakes Canyon (red locality 8 on Fig. 4). **a)** along-strike view of the Baby Joe Gulch thrust, fault contact shown in black line and arrow on hanging wall. **b)** Lower hemisphere stereographic projection of shear planes (black lines) with arrow showing slip direction of the hanging wall. **c)** Outcrop photo showing low-angle fault contact of the Railroad Canyon thrust. Black lines highlight foliation of the hanging wall.

#### 4.3 Summary of deformation events

Progressive thin- to thick-skinned thrusting of the study area is summarized in three deformation events (Fig. 10). In the sedimentary dip panel domain, a low-angle pressure solution cleavage overprints NE-verging detachment folds. The cleavage parallels foliation within the neighboring shear zone of the Thompson Gulch thrust. This relationship constrains the early

phases of deformation. First, laterally continuous sedimentary cover rocks above the intra-Devonian Lemhi arch unconformity underwent NE-SW layer-parallel shortening (Fig. 10a). Second, sedimentary cover rocks were transported toward the east along a sub-horizontal thin-skinned Thompson Gulch thrust (Fig. 10b). Like the Thompson Gulch thrust, the Railroad Canyon thrust also contains calcareous mylonites and has a parallel, penetrative stretching lineation, suggesting similar deformation conditions and kinematics, but involving rocks at a different stratigraphic level between the sub-Ordovician and intra-Devonian Lemhi arch unconformities that pinch out to the north and east. A lateral ramp across the intra-Devonian Lemhi arch unconformity (Fig. 10b) may directly link the Thompson Gulch and Railroad Canyon thrusts, or they may be separate faults that were both active before thick-skinned thrusting. The Thompson Gulch and Railroad Canyon thrusts are truncated by the Radio Tower, Italian Gulch, and Baby Joe Thrusts, constraining the relative timing of deformation. Finally, the basement and cover rocks were tilted to the southeast by 5-15° (Fig. 10c) during activation of a deeper basal detachment horizon below the basement-cover contact, which must be linked to a thick-skinned thrust fault northwest of the current study area. Basement and cover rocks of the tilted sections were shortened, oblique to the previous shortening direction, along the thick-skinned Radio Tower, Italian Gulch, and Baby Joe Gulch thrusts (Fig. 10). The restored stratigraphic relationships of the Lemhi arch unconformities and the striking differences in pre-thrusting stratigraphy suggest thrust reactivation of a pre-Devonian normal fault, which was oblique to the regional shortening direction. These deformation events explain the apparent offsets and crosscutting relationships observed in the map relations (Fig. 10d).

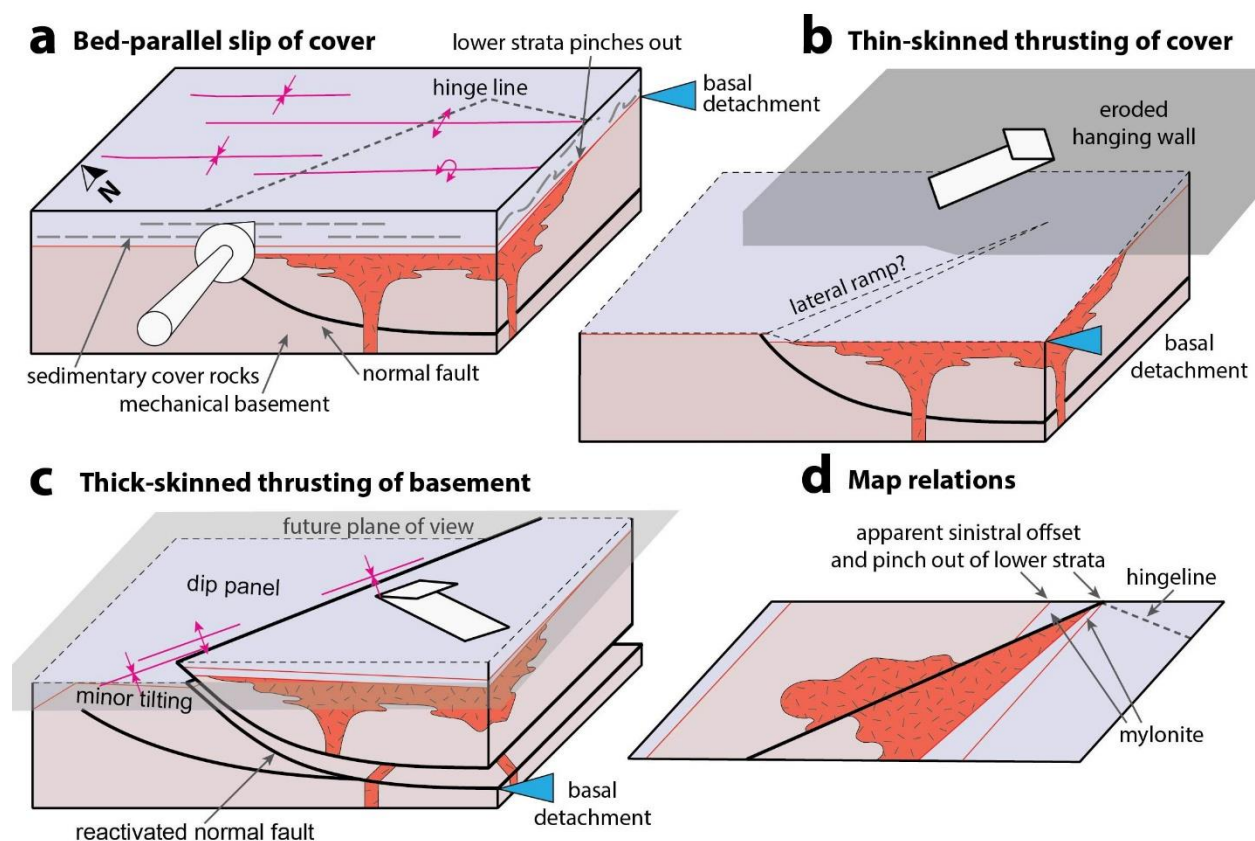


**Figure 10.** Simplified block diagrams showing the hypothesized series of deformation events and inferred basal detachment (**a-c**) used to explain the observed map relations (**d**). Lemhi arch unconformities shown in red. Pink fold symbols show orientation of active folds.

## 5 Discussion

### 5.1. Transition in structural style over a basement high

The study area exposes not only contrasting structural styles near the base of a thin-skinned thrust belt, but also major stratigraphic changes that define a regional basement high in the western North American passive margin. The transition from thin- to thick-skinned thrusting documented here coincides with an exceptionally thin stratigraphic section overlying the basement high (Fig. 3). The Jefferson and McGowan Creek formations mark the basement/cover

contact and dramatically thicken toward the interior of the fold-thrust belt (Fig. 3), from a local thickness of ~80 m to >2 km in the Lost River Range ~ 75 km toward the southwest (Grader & Dehler, 1999; Grader et al., 2017). The total preserved thickness of the stratigraphic section is locally 1.8 km, comparable in thickness to correlative sections throughout the Beaverhead and Tendoy mountains toward the foreland (Scholten, 1957; Rose, 1976; Peterson, 1981), but much thinner than the ~3-3.5 km in the Lemhi Range, and ~4 km in the Lost River Range (Ruppel & Lopez, 1988). Upper units (above the intra-Devonian Lemhi arch unconformity) are conformable and laterally continuous over the ~250 km width of the Idaho-Montana fold-thrust belt. Lower units (between the young and old unconformities) completely pinch out over the Lemhi arch basement high, becoming absent in the northern part of the study area and toward the front of the fold-thrust belt. The study area therefore marks a pronounced hinge line, where lower stratigraphic units thin drastically and/or pinch out near the regional basement high. As a result, regional stratigraphic weak layers are thinner, shallower, or absent altogether where the transition from thin- to thick-skinned thrusting occurs.

From the range of rheologies documented by deformation features, we can constrain approximate deformation temperatures and depths, thereby refining the relationship between the preexisting stratigraphy and the resulting fold-thrust belt. Deformation features in quartzose and dolomitic rocks of the study area are entirely brittle, whereas calcitic rocks record plastic deformation. Widespread dynamic recrystallization was observed, where significant grain size reduction resulted in grain sizes generally <20  $\mu\text{m}$ , as is expected for a carbonate rock undergoing deformation at low temperatures (~ 150-300°C; e.g., Burkhard, 1990; DeBresser et al., 2002). The observed tabular, thick, and sometimes curved calcite twins (Fig. 7d) are characteristic of Type II and Type III twins (Burkhard, 1993; Ferrill et al., 2004), suggesting a

rough temperature range of 200-250°C. This is in agreement with an independent maximum temperature estimate of 190-300°C (Dembicki, 2016) obtained from a conodont color alteration index of “4” for a sample of Mississippian rocks (Perry et al., 1983) collected along Railroad Canyon ~5 km north of the study area. Assuming a 20°C surface temperature and geothermal gradient of 25-30°C/km, temperatures of 200-250°C suggest a depth of deformation of 6-9 km. The study area offers the unique opportunity to directly observe the underlying mechanical basement, within the lower structural levels of a classic thin-skinned thrust belt nearly 50 km from the frontal thrust. This fortuitous view allows for us to discuss how structural style varies across-, along-strike, and with depth.

Given that the inferred range of protoliths of the carbonate mylonite is Ordovician (Saturday Mountain Formation) to Mississippian (Middle Canyon Formation) in age, we reconstructed the stratigraphic burial depths of these rocks using results from the current study area (for Ordovician to Pennsylvanian rocks) coupled with regional constraints (Skipp, 1988) where the overlying rocks were removed in the study area due to erosion (Triassic to Cretaceous rocks). The reconstructed overlying thickness of rocks ranges from ~3.2-3.5 km. Assuming a 25°C/km geothermal gradient, 2.5-6 km of additional strata must have been present above the basal detachment of the study area, in order to achieve temperatures between 200 and 250°C. Thickening related to distributed horizontal shortening may simply account for most of the missing overburden. Assuming plane strain, a rough area-balanced shortening estimate requires ~42-65% horizontal shortening above the carbonate mylonite in order to achieve 2.5-6 km of vertical thickening above the basal detachment. This shortening magnitude is comparable with estimates for other thin-skinned portions of the Cordillera (e.g., Mitra, 1994; DeCelles & Coogan, 2006). In the neighboring Lemhi Range, km-scale recumbent folds accommodate

similar magnitudes of shortening at comparable stratigraphic levels (Hait, 1965; Beutner, 1968). Burial prior to slip along the Thompson Gulch thrust was most likely due to distributed folding and not an overlying thrust sheet, given the widespread folding in the region (Hait, 1965; Beutner, 1968; Messina, 1993) and general absence of major thrusts to the west of the study area (Fig. 2). We emphasize that the substantial sub-vertical shortening associated with the shear zones of the thin-skinned thrusts of the study area likely reflects local flattening in the shear zone, and not distributed ductile thinning related to large-scale thickening of the crust (cf. Long & Kohn, 2020). Regional-scale horizontal shortening was accommodated by a combination of folding, thrusting, and localized ductile shearing, all of which involved only the sedimentary cover rocks above the basement high of the Lemhi arch.

Structurally below the sedimentary rock cover succession, the quartzose mechanical basement was horizontally shortened by later thick-skinned thrusting under brittle conditions. The apparent sinistral separation across the S-dipping Radio Tower and Baby Joe Gulch thrusts (Fig. 4) can be explained simply by ~N-directed thrusting across a dip panel with an apparent dip toward the east (Fig. 10c, d). Following this model and using the intra-Devonian Lemhi arch unconformity as a piercing point, we estimate that ~2 km of total horizontal shortening of the mechanical basement occurred on the Radio Tower and Baby Joe Gulch thrusts. Sinistral slip along these faults is also possible, but would require >7 km of E-W slip, which is less likely given the observed kinematics of the Baby Joe Gulch thrust. Estimated shortening magnitudes for the Hawley Creek thrust range from a minimum ~1 km (Skipp, 1988) to upwards of ~3 km of horizontal shortening as suggested by the juxtaposition of Ordovician and Triassic strata (ex. Lucchitta, 1966). Late-stage thick-skinned thrusting was therefore relatively minor and likely oblique compared to earlier thin-skinned thrusting. Given our small sample size, the kinematic

indicators we report for the Baby Joe Gulch thrust may not be representative of the overall slip direction. Though the shortening direction is poorly constrained, reactivation of a pre-Devonian normal fault is suggested by the juxtaposition of drastically different Ordovician to Devonian stratigraphy across the fault. Detailed sequence stratigraphic studies of the Devonian Jefferson Formation support this interpretation (Grader et al., 2017). The oblique orientation of the inherited normal fault to the regional shortening direction may have controlled the apparent change in the local shortening direction. This interpretation is consistent with previous studies that document local strain refractions near thick-skinned structures that are oblique to the regional shortening direction, consistent with reactivation of pre-existing basement weaknesses (e.g., Marshak et al., 2000; Kley & Monaldi, 2002; Erslev & Koenig, 2009; Neely & Erslev, 2009; Weil & Yonkee, 2012; Weil et al., 2016).

## 5.2. Age of deformation

The documented transition in structural style from early thin-skinned to late thick-skinned deformation is well-constrained by the mapped crosscutting relationships. However, assigning absolute ages to these phases of deformation is more difficult due to the lack of dateable syn-deformational rocks. In neighboring quadrangles, folded and cleaved rocks in the deformed footwall of the Thompson Gulch thrust include rocks as young as Triassic (e.g., Lucchitta, 1966) and are overlapped by unfolded volcanic and sedimentary rocks of lower to middle Eocene age (Vandenburg, 1997; Lonn et al., 2019). Additional age constraints come from recent detrital zircon provenance studies within synorogenic Beaverhead Group foreland basin rocks of southwestern Montana (Garber et al., 2020), which record arrival of distinctive ~500 Ma Beaverhead pluton (Evans & Zartman, 1988; Lund et al., 2010; Link et al., 2017) detrital zircons. Given that outcrops of the Beaverhead pluton are confined almost entirely to the hanging walls

of the Poison Creek-Baby Joe Gulch-Hawley Creek thrust system (e.g., Link et al., 2017), the ~500 Ma zircons are a unique population that are present only in sediment derived from the late phase of thick-skinned deformation. The first occurrence of ~500 Ma zircons derived from the Beaverhead pluton occurs within strata with a maximum depositional age of ~67 Ma (Garber et al., 2020), which is very similar to zircon (U-Th)/He ages from the hanging wall of the Poison Creek thrust, which give weighted mean cooling ages of  $68.4 \pm 0.9$  Ma (N=6) and  $56.8 \pm 0.7$  Ma (N=5) (Hansen & Pearson, 2016). We therefore interpret that the early phase of thin-skinned deformation predates the ~68 Ma phase of thick-skinned deformation.

### 5.3 Double-decker thin- to thick-skinned fold-thrust belt

The deformation events of the study area (Fig. 10) highlight slip along increasingly deeper basal detachments with progressive deformation, resulting in a shift from thin- to thick-skinned deformation, more than 50 km behind the leading edge of the thin-skinned wedge. This interpretation is consistent with the regional trend (Fig. 2) of an upper thin-skinned system that is deformed by a lower thick-skinned system. Thus, as described by some prior workers, the Sevier belt and Laramide province of the Idaho-Montana fold-thrust belt cannot be divided by a single line on the map (Kulik & Schmidt, 1988; O'Neill et al., 1990). Instead, the boundary between thin- and thick-skinned domains is low-angle: early, thin-skinned thrusting at high structural levels overlapped in timing with and was later overprinted by thick-skinned thrusting at lower levels. Taiwan and the Zagros are other notable examples that were originally interpreted as thin-skinned belts (Suppe & Namson, 1979; Namson, 1981; Davis & Engelder, 1985; McQuarrie, 2004), but are now interpreted to have deeper thick-skinned thrusts that disrupt the overlying thin-skinned detachment horizons (Hung et al., 1999; Yang et al., 2001; Molinaro et al., 2005; Lacombe & Mouthereau, 2002; Mouthereau et al., 2006; Sherkati et al., 2006; Mouthereau et al.,

2007; Mouthereau et al., 2012; Allen et al., 2013; Lacombe & Bellahsen, 2016; Le Garzic et al., 2019).

In spite of the clear value of critical taper theory, the shift toward more hybrid thin- and thick-skinned models challenges one significant assumption of the model: that a pre-thrusting throughgoing basal detachment horizon is utilized throughout deformation (e.g., Davis et al., 1983; Buitter, 2012). It has long been recognized that thick-skinned belts often occur within thin packages of sedimentary cover rocks (Allmendinger et al., 1983; Kley et al., 1999; Pearson et al., 2013; McGroder et al., 2015; Fitz-Díaz et al., 2018; Williams et al., 2020) and that thin-skinned belts are wider where sedimentary cover rocks are thicker (Marshak, 2004; Yonkee & Weil, 2010). Because the critical taper angle depends on intrinsic mechanical properties, the width and height of a thin-skinned wedge is limited by the thickness of sedimentary cover rocks (e.g., Boyer, 1995). If sedimentary cover rocks are very thin, such as demonstrated for the Lemhi arch (Fig. 3), activation of a deeper basal detachment horizon within the mechanical basement may be required to thicken the wedge and balance the stress state before more horizontal shortening can be accommodated. If the basement-cover unconformity is very steep, as inferred for the Lemhi arch (Fig. 3), it may be easier to reactivate preexisting weaknesses at deeper crustal levels than to short-cut the basement high and create a basement-involved duplex (e.g., Boyer & Elliot, 1982; Yonkee, 1992). Furthermore, if weak, viscous detachments deep in the crust are activated, then the wedge taper angle may be significantly reduced, promoting propagation of the wedge after minimal internal shortening (Williams et al., 1994; Ruh et al., 2012). Regardless, when a thin-skinned wedge is too thin and/or the basal detachment is too strong to achieve critical taper by shortening internally and increasing the surface slope, then activation of a deeper detachment

horizon provides a way to achieve critical taper by increasing the basal slope. In thin stratigraphic wedges, this may result in a transition from thin-to thick-skinned structural style.

The results of this study add to the growing list of observations that suggest a regionally continuous thin-skinned fold-thrust belt within the Idaho-Montana fold-thrust belt that was later dissected by a deeper thick-skinned thrust system. Our preferred interpretation—that the Thompson Gulch thrust is the transient basal detachment of a former thin-skinned fold-thrust belt—is consistent with the examples shown in Fig. 2 and described earlier in the text, which suggest regional continuity of deformation above the Lemhi arch when slip is restored on deeper crosscutting structures.

Based on the results of this study and the documented variations in structural style with depth across the Idaho-Montana fold-thrust belt, we propose a double-decker model (Fig. 11) that more accurately describes the geometry of structural style domains and offers testable predictions for continental fold-thrust belts elsewhere (e.g., Taiwan and Zagros, Lacombe & Bellahsen, 2016). Thin stratigraphy, such as over a basement high (Fig. 11a), promotes thick-skinned thrusting when the stratigraphy is too thin to fit the required critically tapered wedge. Initial thin-skinned thrusting is widespread when the growing orogenic wedge fits entirely above the basement/cover contact (Fig. 11b). In the Idaho-Montana fold-thrust belt, early thin-skinned thrusting from the Lost River Range to the Blacktail Mountains is evident from widely distributed NE-verging detachment folds that are ubiquitous above the intra-Devonian Lemhi arch unconformity (e.g., Perry & Sando, 1982; Anastasio et al., 1997; Lonn et al., 2000).

With continued horizontal shortening, the thin-skinned wedge grows, requiring activation of a deeper basal detachment near the front of the orogenic wedge. When a basement high is

present, the basal detachment must advance into the underlying basement high, promoting a transition from thin- to thick-skinned thrusting (Fig. 11c). The widespread occurrence of mechanical basement and the presence of both thin- and thick-skinned structures in the interior of the Idaho-Montana fold-thrust belt (Fig. 1) suggests a regional basal detachment within the deeper crust (Fig. 11c), most likely rooted near the brittle-plastic transition. We schematically show this detachment between the middle and upper crust (Fig. 11c), which is consistent with depth-to-detachment estimates for the Blacktail-Snowcrest uplift in southwestern Montana (McBride et al., 1992) as well as better-constrained structures in Wyoming (e.g., Smithson et al., 1979; Yeck et al., 2014; Groshong & Porter, 2019). Note that we expect the former ( $T_1$ ) and later ( $T_2$ ) basal detachment horizons to be closer together in the hinterland and farther from one another in the foreland (red boxes in Fig. 11c). This is expected for two reasons. First, in retroarc fold-thrust belts, the hinterland usually contains a relatively thick pre-thrusting stratigraphic section with the mechanical basement-cover contact occurring near or below the brittle-plastic transition. Second, increased temperatures due to crustal thickening in the internal part of the orogenic wedge generally increase hinterland geothermal gradients, resulting in a decrease in the depth of the brittle-plastic transition with progressive orogenesis. Both of these reasons mean that the foreland has more mechanical basement and fewer weak stratigraphic units, making the progressive down-stepping and change in structural style more pronounced in the foreland as compared to the hinterland (Fig. 11c). This integrated double-decker system is supported by available kinematic data for thick-skinned thrusts in southwestern Montana that constrain regional E-W shortening and demonstrate strain compatibility with thin-skinned thrusts in the region (Schmidt & Garihan, 1983; Schmidt et al., 1988; O'Neill et al., 1990).

While a general transition from thin- to thick-skinned thrusting is well documented, observations of mutually cross cutting thin- and thick-skinned structures in the Idaho-Montana fold-thrust belt suggest that in detail this transition in structural style was not sharp in time or space. For instance, the basal detachment of the Tendoy thrust truncated older folds that were inferred to be related to the Blacktail-Snowcrest arch, a major thick-skinned thrust of the region (McDowell, 1997). Studies within the foreland basin of southwestern Montana suggest that activity along similar low-magnitude, thick-skinned thrusts preceded the peak of thin-skinned thrusting (DeCelles, 1986; Perry et al., 1988; Garber et al., 2020). These examples of early, minor thick-skinned thrusts may signify that stress is more efficiently transferred along viscous detachment horizons within the middle crust as compared to frictional detachment horizons of the upper crust (Ruh et al., 2012; Borderie et al., 2018; Tavani et al., 2021). Strain may also be transferred gradually or shared between the upper thin-skinned and lower thick-skinned basal detachments as has been documented in the Zagros fold-thrust belt (e.g., Mouthereau et al., 2012). With more shortening, strain is completely transferred from the upper to the lower basal detachment as out-of-sequence thick-skinned thrusts completely crosscut older and higher thin-skinned thrusts (Fig. 11c). A similar progressive shift from early thin- to late thick-skinned deformation has been documented in the fold-thrust belts of the Zagros, Appennines, Oman, and Taiwan, where the inherited rift architecture limits the availability of brittle and plastic detachment horizons (Tavani et al., 2021). Like the Idaho-Montana fold-thrust belt, these examples also suggest that activation of a viscous detachment within the middle crust resulted in rapid propagation of early thick-skinned deformation and that ultimately the former upper thin-skinned belt was overprinted by the lower thick-skinned system as it became dominant (Tavani et al., 2021).

The double-decker model applies to fold-thrust belts in which a critically tapered wedge cannot be contained within only sedimentary cover rocks. Thick-skinned thrusts beneath overlying older thin-skinned thrusts provide a way to thicken the wedge with minimal horizontal shortening. The initial geometry of the basement-cover contact, which in the current study is a result of heterogeneities during prior rifting (Brennan et al., 2020), determines where structural style will transition from thin- to thick-skinned. Thick-skinned thrusting initiates as a more effective way to build structural relief, without large-magnitude horizontal shortening. With enough horizontal shortening, a self-organized transition from thin- to thick-skinned thrusting occurs near thin, shallow, and laterally discontinuous stratigraphy. This double-decker model suggests that the preexisting distribution of weak stratigraphic layers may determine structural style. Further, this depth-dependent model not only more accurately represents the 3-dimensional geometry of structural domains, it may also be a more predictive way to integrate a bewildering range of structural styles into a coherent set of deformation events independent of assumptions about plate boundary geodynamics.

#### 5.4 Implications of the double-decker model

Several different models may explain the occurrence of both thin- and thick-skinned thrusts within a given area (Fig. 1). Each model makes unique predictions about shortening magnitude and strain compatibility, both of which greatly impact our understanding of plate dynamics in orogenic belts. In the North and South American Cordilleras, many workers have described fold-thrust belts with discrete thin- and thick-skinned thrust domains in map and cross section view (Fig. 1c; e.g., Armstrong, 1968; Jordan & Allmendinger, 1986). In the thin-skinned domain, structural relief is achieved by major horizontal shortening (e.g., DeCelles, 2004), whereas in the thick-skinned domain, low magnitudes of horizontal shortening on steep

basement ramps more efficiently produce structural relief (e.g., Erslev, 1986). In this view, each thin- or thick-skinned domain has distinctive basal detachment horizons with different strain fields (Fig. 1c), which are often interpreted to reflect changes in plate boundary geodynamics (e.g., Hamilton, 1988; Erslev, 1993; Yonkee & Weil, 2015). This model works well for the classic Laramide province in the North American Cordillera and in central Argentina, where there is abundant independent evidence of flat-slab subduction that matches the timing and distribution of thick-skinned deformation (e.g., Coney & Reynolds, 1977; Dickinson & Snyder, 1978; Jordan et al., 1983; Jordan and Allmendinger, 1986; Kay et al., 1987; Bird, 1988; Saleeby, 2003; DeCelles, 2004; Anderson et al., 2007; Liu et al., 2010; Yonkee & Weil, 2015). But this model, which suggests a direct link between a shallowly subducting oceanic plate and thick-skinned deformation in the upper plate, is not sufficient in other localities. For example, in the Idaho-Montana fold-thrust belt, thick-skinned thrusts are 10s of m.y. older than predicted (e.g., Perry et al., 1988; Carrapa et al., 2019; Garber et al., 2020), and magmatism apparently remained active in the hinterland (e.g., Gaschnig et al., 2010, 2011). Similarly, in northwestern Argentina, active basement-involved, thick-skinned deformation occurs nearly 500 km north (e.g., Allmendinger et al., 1983; Kley et al., 1999; Pearson et al., 2013) of the modern region of shallow subduction (Anderson et al., 2007).

If thick- and thin-skinned thrusts are kinematically linked (Fig. 1a, b), then spatial heterogeneities in the mechanical properties of the deforming lithosphere offer a more appealing control on structural style than a change in plate boundary geodynamics. At the scale of a single major thrust, one example of how this may occur is where slip along thick-skinned thrusts is transferred to bedding-parallel thrusts (Fig. 1a; e.g., uncoupled basement-cover bonding model of Giambiagi et al., 2009). This model is similar to the synclinal crowding case of trishear fault-

propagation folding (Erslev, 1991; Von Hagke & Malz, 2018), a basement-involved wedge structure (Mount et al., 2011), or fault-bend fold (Suppe, 1983). In these examples, a continuum of thin- and thick-skinned structures results from slip along a single basal detachment horizon that passes through a heterogeneous mechanical stratigraphy and strain is transferred into thin-skinned thrusts with comparable slip but less structural relief.

At broader, regional and orogenic scales, our double-decker model predicts a continuum of structural styles that do not clearly delineate thin- and thick-skinned map domains, suggesting that plate boundary geodynamics cannot be inferred from structural style alone. Structural style is instead time- and depth-dependent, and ultimately determined by the pre-thrusting mechanical stratigraphy and a basal detachment horizon that steps to deeper structural levels with progressive deformation. As a result, younger and more deeply-detached structures of one style may crosscut older and more shallowly-detached structures of another style while forming in response to the same evolving stress field. Shortening directions may be refracted around preexisting structures, but highlight an overall regional trend (e.g., Schmidt & Garihan, 1983; Erslev & Koenig, 2009; Weil & Yonkee, 2012; Weil et al., 2014). In this way, local mechanical stratigraphy determines structural style, but regional trends in the pre-thrusting stratigraphy determine how the host of resulting structural styles may be linked across the orogenic wedge at a given time. These factors, in addition to the natural tendency of basal detachment horizons—particularly near the front of the orogenic wedge—to get deeper with time, may result in changes in the orogenic wedge's ability to shorten. A likely scenario is that early thin-skinned deformation may easily accommodate large magnitudes of horizontal shortening, but give way to later thick-skinned deformation that more effectively builds structural relief as higher-angle thrust ramps cut mechanical basement and uplift portions of the former overlying thin-skinned

belt. The double-decker model also predicts that the pre-thrusting mechanical stratigraphy has a stronger control on the geometry, kinematics, and magnitude of shortening in continental fold-thrust belts than previously appreciated: the mechanical properties of the upper plate may not only explain the continuum of structural styles observed in Cordilleran systems, but they may also effectively modulate an orogenic wedge's ability to shorten and thicken in a self-organized way.

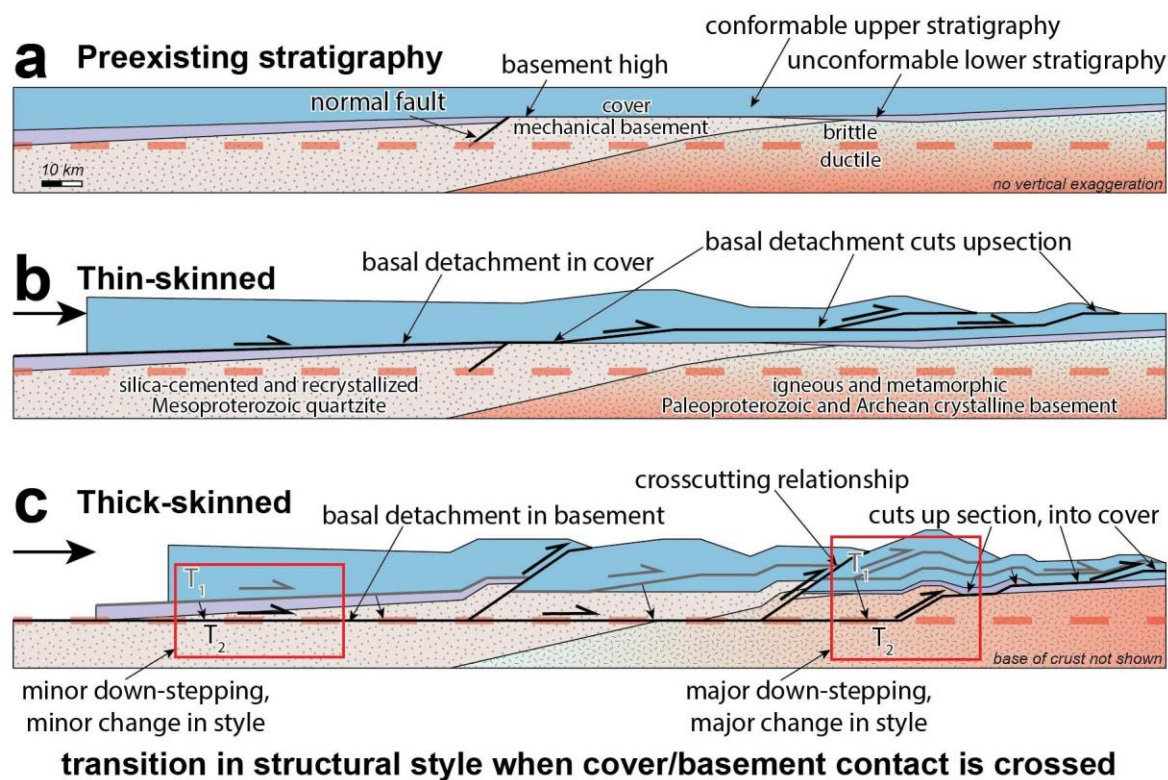


**Figure 11.** Schematic cross sections illustrating the double-decker model: **a)** initial undeformed state, **b)** early thin-skinned thrusting, and **c)** later thick-skinned thrusting.

## 6 Conclusions

Mapping and structural analysis in the Beaverhead Mountains of east-central Idaho define an early, thin-skinned thrust system in sedimentary cover rocks and a late, out-of-

sequence thick-skinned thrust system in the underlying mechanical basement of the Lemhi arch. Early detachment folding accommodated NE-SW shortening of the ~3.5 km-thick sedimentary cover rocks. Basement and deformed cover rocks were then tilted 5-15° toward the southeast as a basal detachment in the mechanical basement was activated. Thin-skinned top-to-the-east thrusting accommodated by the Thompson Gulch and Railroad Canyon thrusts cut across the sedimentary cover rocks, producing carbonate mylonite. Finally, reactivation of an inherited, pre-thrusting normal fault resulted in thick-skinned thrusting of the Baby Joe Gulch, Radio Tower, and Italian Gulch thrusts, which shortened the underlying mechanical basement and cover by at least ~2 km, crosscutting earlier thin-skinned thrusts in the tilted section. Progressive down-stepping of the basal detachment crossed the basement/cover contact near the thin, shallow, and discontinuous stratigraphy overlying the basement high, thereby shifting the structural style from thin- to thick-skinned. This stratigraphically-controlled transition to thick-skinned thrusting occurred at depths of 6-9 km, greater than 50 km inboard from thick-skinned thrusts of the southwestern Montana foreland. We propose a double-decker model that predicts a shift from an upper thin-skinned to a lower thick-skinned domain where and when the height of the critically tapered wedge exceeds the thickness of sedimentary cover rocks. This predictive depth-dependent model may aid in integrating thin- and thick-skinned domains of continental fold-thrust belts into a single deformation history where the thickness and lateral continuity of weak sedimentary rocks determine the structural style.

### **Acknowledgments**

This study represents a portion of SP's PhD dissertation. We thank Leif Tapanila for assistance with fossil identification and Paul Link for feedback on early map and manuscript drafts. DP thanks Tom Becker for discussions about structural style. Funding for this research

was provided by NSF-Tectonics EAR-1728563 to DP. Data supporting the conclusions is available in the accompanying text and figures and can be accessed in the Dryad data repository (<https://doi.org/10.5061/dryad.3bk3j9kjsx>). Additional data was not used, nor created for this research. We appreciate critical and constructive reviews by Dr. John Singleton, Dr. Arlo Weil, and an anonymous reviewer, as well as suggestions from the Associate Editor Dr. Elisa Fitz-Díaz and Editor Dr. Margaret Rusmore.

## References

- Allen, B., Saville, C., Blanc, E., Talebian, M., & Nissen, E. (2013). Orogenic plateau growth: expansion of the Turkish–Iranian Plateau across the Zagros fold-and-thrust belt. *Tectonics*, *32*, 171–90. <https://doi.org/10.1002/tect.20025>
- Allmendinger, R. W., Ramos, V. A., Jordan, T. E., Palma, M., & Isacks, B. L. (1983). Paleogeography and Andean structural geometry, northwest Argentina. *Tectonics*, *2*(1), 1-16. <https://doi.org/10.1029/TC002i001p00001>
- Allmendinger, R. W., Hauge, T. A., Hauser, E. C., Potter, C. J., Klemperer, S. L., Nelson, K. D., Knuepfer, P., & Oliver, J. (1987). Overview of the COCORP 40° N transect, western United States: The fabric of an orogenic belt. *Geological Society of America Bulletin*, *98*(3), 308-319. [https://doi.org/10.1130/0016-7606\(1987\)98<308:OOTCNT>2.0.CO;2](https://doi.org/10.1130/0016-7606(1987)98<308:OOTCNT>2.0.CO;2)
- Allmendinger, R. W., & Gubbels, T. (1996). Pure and simple shear plateau uplift, Altiplano-Puna, Argentina and Bolivia. *Tectonophysics*, *259*(1-3), 1-13. [https://doi.org/10.1016/0040-1951\(96\)00024-8](https://doi.org/10.1016/0040-1951(96)00024-8)
- Allmendinger, R. W., Cardozo, N. C., & Fisher, D. (2013). *Structural Geology Algorithms: Vectors & Tensors* (2). Cambridge, UK: Cambridge University Press.

Anastasio, D. J., Fisher, D. M., Messina, T. A., & Holl, J. E. (1997). Kinematics of décollement folding in the Lost River Range, Idaho. *Journal of Structural Geology*, 19(3-4), 355-368.

[https://doi.org/10.1016/S0191-8141\(97\)83028-3](https://doi.org/10.1016/S0191-8141(97)83028-3)

Anderson, M., Alvarado, P., Zandt, G., and Beck, S. (2007). Geometry and brittle deformation of the subducting Nazca Plate, Central Chile and Argentina, *Geophys J Int*, 171(1), 419–434.

<https://doi:10.1111/j.1365-246X.2007.03483.x>

Armstrong, R. L., & Dick, H. J. (1974). A model for the development of thin overthrust sheets of crystalline rock. *Geology*, 2(1), 35-40. [https://doi.org/10.1130/0091-](https://doi.org/10.1130/0091-7613(1974)2%3C35:AMFTDO%3E2.0.CO;2)

[7613\(1974\)2%3C35:AMFTDO%3E2.0.CO;2](https://doi.org/10.1130/0091-7613(1974)2%3C35:AMFTDO%3E2.0.CO;2)

Armstrong, R. L. (1968). Sevier orogenic belt in Nevada and Utah. *Geological Society of America Bulletin*, 79(4), 429-458. [https://doi.org/10.1130/0016-](https://doi.org/10.1130/0016-7606(1968)79[429:SOBINA]2.0.CO;2)

[7606\(1968\)79\[429:SOBINA\]2.0.CO;2](https://doi.org/10.1130/0016-7606(1968)79[429:SOBINA]2.0.CO;2)

Baby, P., Moretti, I., Guillier, B., Limachi, R., Mendez, E., Oller, J., & Specht, M. (1995).

Petroleum system of the northern and central Bolivian sub-Andean zone. In Tankard, A.J.,

Suarez Soruco, R., & Welsink, H.J., *Petroleum Basins of South America* (Vol. 62). Tulsa, OK:

American Association of Petroleum Geologists Memoir.

Bally, A. W., Gordy, P. L., & Stewart, G. A. (1966). Structure, seismic data, and orogenic

evolution of southern Canadian Rocky Mountains. *Bulletin of Canadian Petroleum Geology*,

14(3), 337-381. <https://doi.org/10.35767/gscpgbull.14.3.337>

Barnhart, W. D., Brengman, C. M., Li, S., & Peterson, K. E. (2018). Ramp-flat basement

structures of the Zagros Mountains inferred from co-seismic slip and afterslip of the 2017 Mw7.

3 Darbandikhan, Iran/Iraq earthquake. *Earth and Planetary Science Letters*, 496, 96-107.

<https://doi.org/10.1016/j.epsl.2018.05.036>

Bauville, A., & Schmalholz, S. M. (2015). Transition from thin-to thick-skinned tectonics and consequences for nappe formation: Numerical simulations and applications to the Helvetic nappe system, Switzerland. *Tectonophysics*, 665, 101-117. <https://doi.org/10.1016/j.tecto.2015.09.030>

Bell, T. H., & Etheridge, M. A. (1973). Microstructure of mylonites and their descriptive terminology. *Lithos*, 6(4), 337-348. [https://doi.org/10.1016/0024-4937\(73\)90052-2](https://doi.org/10.1016/0024-4937(73)90052-2)

Betka, P., Klepeis, K., & Mosher, S. (2015). Along-strike variation in crustal shortening and kinematic evolution of the base of a retroarc fold-and-thrust belt: Magallanes, Chile 53° S–54° S. *Geological Society of America Bulletin*, 127(7-8), 1108-1134. <https://doi.org/10.1130/B31130.1>

Beutner, E. C. (1968). *Structure and tectonics of the southern Lemhi Range, Idaho* (doctoral dissertation). State College, PA: Pennsylvania State University.

Bird, P. (1988). Formation of the Rocky Mountains, western United States: A continuum computer model. *Science*, 239(4847), 1501-1507. <https://doi.org/10.1126/science.239.4847.1501>

Blackstone Jr, D. L. (1940). Structure of the Pryor Mountains Montana. *The Journal of Geology*, 48(6), 590-618. <https://doi.org/10.1086/624917>

Borderie, S., Graveleau, F., Witt, C., & Vendeville, B. C. (2018). Impact of an interbedded viscous décollement on the structural and kinematic coupling in fold-and-thrust belts: Insights from analogue modeling. *Tectonophysics*, 722, 118-137.

<https://doi.org/10.1016/j.tecto.2017.10.019>

- Boyer, S. E., & Elliott, D. (1982). Thrust systems. *The American Association of Petroleum Geologists Bulletin*, 66(9), 1196-1230. <https://doi.org/10.1306/03B5A77D-16D1-11D7-8645000102C1865D>
- Boyer, S. E. (1995). Sedimentary basin taper as a factor controlling the geometry and advance of thrust belts. *American Journal of Science*, 295(10), 1220-1254. <https://doi.org/10.2475/ajs.295.10.1220>
- Brennan, D. T., M. Pearson, D. M., Link, P. K., & Chamberlain K. R. (2020), Neoproterozoic Windermere Supergroup near Bayhorse, Idaho: late-stage Rodinian rifting was deflected west around the Belt basin. *Tectonics*, 39 (8), 1-27. <https://doi.org/10.1029/2020TC006145>
- Brumbaugh, D. S., & Hendrix, T. E. (1981). The McCarthy Mountain structural salient southwestern Montana. In *Montana Geological Society field conference & symposium guidebook to southwest Montana* (pp. 201-210). Billings, MT: Montana Geological Society.
- Buiter, S. J. (2012). A review of brittle compressional wedge models. *Tectonophysics*, 530, 1-17. <https://doi.org/10.1016/j.tecto.2011.12.018>
- Burchfiel, B., & Davis, G. A. (1972). Structural framework and evolution of the southern part of the Cordilleran orogen, western United States. *American Journal of Science*, 272(2), 97-118. <https://doi.org/10.2475/ajs.272.2.97>
- Burchfiel, B. C., & Davis, G. A. (1975). Nature and controls of Cordilleran orogenesis, western United States: Extensions of an earlier synthesis. *American Journal of Science*, 275(A), 363-396.
- Burkhard, M. (1990). Ductile deformation mechanisms in micritic limestones naturally deformed at low temperatures (150–350 C). *Geological Society, London, Special Publications*, 54(1), 241-257. <https://doi.org/10.1144/GSL.SP.1990.054.01.23>

Burkhard, M. (1993). Calcite twins, their geometry, appearance and significance as stress-strain markers and indicators of tectonic regime: a review. *Journal of Structural Geology*, 15(3-5), 351-368. [https://doi.org/10.1016/0191-8141\(93\)90132-T](https://doi.org/10.1016/0191-8141(93)90132-T)

Butler, R. W., Bond, C. E., Cooper, M. A., & Watkins, H. (2018). Interpreting structural geometry in fold-thrust belts: Why style matters. *Journal of Structural Geology*, 114, 251-273. <https://doi.org/10.1016/j.jsg.2018.06.019>

Carney, S. M., & Janecke, S. U. (2005). Excision and the original low dip of the Miocene-Pliocene Bannock detachment system, SE Idaho: Northern cousin of the Sevier Desert detachment? *Geological Society of America Bulletin*, 117(3-4), 334-353. <https://doi.org/10.1130/B25428.1>

Carrapa, B., DeCelles, P. G., & Romero, M. (2019). Early inception of the Laramide orogeny in southwestern Montana and northern Wyoming: Implications for models of flat-slab subduction. *Journal of Geophysical Research: Solid Earth*, 124(2), 2102-2123. <https://doi.org/10.1029/2018JB016888>

Chapman, J. B., & DeCelles, P. G. (2015). Foreland basin stratigraphic control on thrust belt evolution. *Geology*, 43(7), 579-582. <https://doi.org/10.1130/G36597.1>

Coney, P. J., & Reynolds, S. J. (1977). Cordilleran benioff zones. *Nature*, 270(5636), 403-406. <https://doi.org/10.1038/270403a0>

Coogan, J. C. (1992). Structural evolution of piggyback basins in the Wyoming-Idaho-Utah thrust belt. In P.K. Link, M. A. Kuntz, & L. B. Piatt (Eds.), *Regional geology of eastern Idaho and western Wyoming* (Vol. 179, pp. 55–81). Boulder, CO: Geological Society of America Memoir. <https://doi.org/10.1130/MEM179-p55>

Cook, F. A., & Varsek, J. L. (1994). Orogen-scale decollements. *Reviews of Geophysics*, 32(1), 37-60. <https://doi.org/10.1029/93rg02515>

Dahlstrom, C. D. (1970). Structural geology in the eastern margin of the Canadian Rocky Mountains. *Bulletin of Canadian Petroleum Geology*, 18(3), 332-406.

Davis, D., & Engelder, T. (1985). Role of salt in fold-and-thrust belts. *Tectonophysics*, 119, 67–88. [https://doi.org/10.1016/0040-1951\(85\)90033-2](https://doi.org/10.1016/0040-1951(85)90033-2)

Davis, D., Suppe, J., & Dahlen, F. A. (1983). Mechanics of fold-and-thrust belts and accretionary wedges. *Journal of Geophysical Research: Solid Earth*, 88(B2), 1153-1172. <https://doi.org/10.1029/JB088iB02p01153>

De Bresser, J. H. P., Evans, B., & Renner, J. (2002). On estimating the strength of calcite rocks under natural conditions. *Geological Society, London, Special Publications*, 200(1), 309-329. <https://doi.org/10.1144/GSL.SP.2001.200.01.18>

Decelles, P. G. (1986). Sedimentation in a tectonically partitioned, nonmarine foreland basin: The Lower Cretaceous Kootenai Formation, southwestern Montana. *Geological Society of America Bulletin*, 97(8), 911-931. [https://doi.org/10.1130/0016-7606\(1986\)97<911:SIATPN>2.0.CO;2](https://doi.org/10.1130/0016-7606(1986)97<911:SIATPN>2.0.CO;2)

DeCelles, P. G. (1994). Late Cretaceous-Paleocene synorogenic sedimentation and kinematic history of the Sevier thrust belt, northeast Utah and southwest Wyoming. *Geological Society of America Bulletin*, 106(1), 32-56. [https://doi.org/10.1130/0016-7606\(1994\)106<0032:LCPSSA>2.3.CO;2](https://doi.org/10.1130/0016-7606(1994)106<0032:LCPSSA>2.3.CO;2)

DeCelles, P. G., & Mitra, G. (1995). History of the Sevier orogenic wedge in terms of critical taper models, northeast Utah and southwest Wyoming. *Geological Society of America Bulletin*, 107(4), 454-462. [https://doi.org/10.1130/0016-7606\(1995\)107<0454:HOTSOW>2.3.CO;2](https://doi.org/10.1130/0016-7606(1995)107<0454:HOTSOW>2.3.CO;2)

DeCelles, P. G., Lawton, T. F., & Mitra, G. (1995). Thrust timing, growth of structural culminations, and synorogenic sedimentation in the type Sevier orogenic belt, western United States. *Geology*, 23(8), 699-702. [https://doi.org/10.1130/0091-7613\(1995\)023<0699:TTGOSC>2.3.CO;2](https://doi.org/10.1130/0091-7613(1995)023<0699:TTGOSC>2.3.CO;2)

DeCelles, P. G., Robinson, D. M., Quade, J., Ojha, T. P., Garzione, C. N., Copeland, P., & Upreti, B. N. (2001). Stratigraphy, structure, and tectonic evolution of the Himalayan fold-thrust belt in western Nepal. *Tectonics*, 20(4), 487-509. <https://doi.org/10.1029/2000TC001226>

DeCelles, P. G. (2004). Late Jurassic to Eocene evolution of the Cordilleran thrust belt and foreland basin system, western USA. *American Journal of Science*, 304(2), 105-168. <https://doi.org/10.2475/ajs.304.2.105>

DeCelles, P. G., & Coogan, J. C. (2006). Regional structure and kinematic history of the Sevier fold-and-thrust belt, central Utah. *Geological Society of America Bulletin*, 118(7-8), 841-864. <https://doi.org/10.1130/B25759.1>

Dembicki, H. (2016). *Practical Petroleum Geochemistry for Exploration and Production*. Cambridge, MA: Elsevier.

Dickinson, W. R., & Snyder, W. S. (1978). Plate tectonics of the Laramide orogeny. In V. Matthews, (Ed.), *Laramide folding associated with basement block faulting in the western United States* (Vol. 151, pp. 355-366). Boulder, CO: Geological Society of America Memoir. <https://doi.org/10.1130/MEM151-p355>

Dover, J. H. (1981). Geology of the Boulder-Pioneer wilderness study area. Blaine and Custer Counties, Idaho: *US Geological Survey Bulletin*, 1497, 15-75.

Dunn, J. F., Hartshorn, K. G., & Hartshorn, P. W. (1995). Structural styles and hydrocarbon potential of the sub-Andean thrust belt of southern Bolivia. In Tankard, A.J., Suarez Soruco, R., & Welsink, H.J., *Petroleum Basins of South America* (Vol. 62). Tulsa, OK: American Association of Petroleum Geologists Memoir.

Eardley, A. J. (1963). Relation of uplifts to thrusts in Rocky Mountains. In O. E. Childs, B. W., Beebe (Ed.), *Backbone of the Americas: Tectonic History from Pole to Pole* (Vol. 2, pp. 209-219). Denver, CO: Rocky Mountain Association of Geologists.

Echavarría, L., Hernández, R., Allmendinger, R., & Reynolds, J. (2003). Subandean thrust and fold belt of northwestern Argentina: Geometry and timing of the Andean evolution. *The American Association of Petroleum Geologists Bulletin*, 87(6), 965-985.

<https://doi.org/10.1306/01200300196>

Erslev, E. A. (1986). Basement balancing of Rocky Mountain foreland uplifts. *Geology*, 14(3), 259-262. [https://doi.org/10.1130/0091-7613\(1986\)14<259:BBORMF>2.0.CO;2](https://doi.org/10.1130/0091-7613(1986)14<259:BBORMF>2.0.CO;2)

Erslev, E. A. (1991). Trishear fault-propagation folding. *Geology*, 19(6), 617-620.

[https://doi.org/10.1130/0091-7613\(1991\)019<0617:TFPF>2.3.CO;2](https://doi.org/10.1130/0091-7613(1991)019<0617:TFPF>2.3.CO;2)

Erslev, E. A. (1993). Thrusts, Back-Thrusts and Detachments of Rocky Mountain Foreland Arches. In C. J. Schmidt, R. B. Chase, E. A. Erslev (Eds.), *Laramide basement deformation in the Rocky Mountain foreland of the western United States* (Vol. 280, pp. 339-358). Boulder, CO: Geological Society of America Special Paper. <https://doi.org/10.1130/SPE280-p339>

Erslev, E. A., & Koenig, N. V. (2009). Three-dimensional kinematics of Laramide, basement-involved Rocky Mountain deformation, USA: Insights from minor faults and GIS-enhanced structure maps. In S. M. Kay, V. A. Ramos, & W. R. Dickinson (Eds.), *Backbone of the Americas: Shallow Subduction, Plateau Uplift, and Ridge and Terrane Collision* (Vol. 204, pp. 125-150). Boulder, CO: Geological Society of America Memoirs.

[https://doi.org/10.1130/2009.1204\(06\)](https://doi.org/10.1130/2009.1204(06))

Evans, K. V., & Green, G. N. (2003). *Geologic map of the Salmon National Forest and vicinity, east-central Idaho* (Geological Investigation Series Map I-2765, scale 1:100,000). Denver, CO: U.S. Geological Survey.

Evans, K. V., & Zartman, R. E. (1988). Early Paleozoic alkalic plutonism in east-central Idaho. *Geological Society of America Bulletin*, 100(12), 1981-1987. [https://doi.org/10.1130/0016-7606\(1988\)100<1981:EPAPIE>2.3.CO;2](https://doi.org/10.1130/0016-7606(1988)100<1981:EPAPIE>2.3.CO;2)

Fermor, P. R., & Moffat, I. W. (1992). The Cordilleran collage and the foreland fold and thrust belt. In R. W., MacQueen, & D. A. Leckie (Eds.), *Foreland basins and fold belts* (55, pp. 81-105). Denver, CO: American Association of Petroleum Geologists.

Ferrill, D. A., Morris, A. P., Evans, M. A., Burkhard, M., Groshong Jr, R. H., & Onasch, C. M. (2004). Calcite twin morphology: a low-temperature deformation geothermometer. *Journal of Structural Geology*, 26(8), 1521-1529. <https://doi.org/10.1016/j.jsg.2003.11.028>

Fitz-Díaz, E., Lawton, T.F., Juárez-Arriaga, E., & Chávez-Cabello, G. (2018). The Cretaceous-Paleogene Mexican orogen: Structure, basin development, magmatism and tectonics. *Earth-Science Reviews*, 183, 56–84. <https://doi.org/10.1016/j.earscirev.2017.03.002>

Fossen, H. (2016). *Structural Geology* (Vol. 2). Cambridge, UK: Cambridge University Press.

Fuentes, F., Horton, B. K., Starck, D., & Boll, A. (2016). Structure and tectonic evolution of hybrid thick-and thin-skinned systems in the Malargüe fold–thrust belt, Neuquén basin, Argentina. *Geological Magazine*, *153*(5-6), 1066-1084.

<https://doi.org/10.1017/S0016756816000583>

Garber, K. L., Finzel, E. S., & Pearson, D. M. (2020). Provenance of Synorogenic Foreland Basin Strata in Southwestern Montana Requires Revision of Existing Models for Laramide Tectonism: North American Cordillera. *Tectonics*, *39*(2), 1-26.

<https://doi.org/10.1029/2019TC005944>

Gaschnig, R. M., Vervoort, J. D., Lewis, R. S., & McClelland, W. C. (2010). Migrating magmatism in the northern US Cordillera: in situ U–Pb geochronology of the Idaho batholith. *Contributions to Mineralogy and Petrology*, *159*(6), 863-883.

Gaschnig, R. M., Vervoort, J. D., Lewis, R. S., & Tikoff, B. (2011). Isotopic evolution of the Idaho batholith and Challis intrusive province, northern US Cordillera. *Journal of Petrology*, *52*(12), 2397-2429. <https://doi.org/10.1093/petrology/egr050>

Giambiagi, L., Bechis, F., García, V., & Clark, A. H. (2008). Temporal and spatial relationships of thick-and thin-skinned deformation: A case study from the Malargüe fold-and-thrust belt, southern Central Andes. *Tectonophysics*, *459*(1-4), 123-139.

<https://doi.org/10.1016/j.tecto.2007.11.069>

Giambiagi, L., Ghiglione, M., Cristallini, E., & Bottesi, G. (2009). Kinematic models of basement/cover interaction: Insights from the Malargüe fold and thrust belt, Mendoza, Argentina. *Journal of Structural Geology*, *31*(12), 1443-1457.

<https://doi.org/10.1016/j.jsg.2009.10.006>

Giambiagi, L., Mescua, J., Bechis, F., Tassara, A., & Hoke, G. (2012). Thrust belts of the southern Central Andes: Along-strike variations in shortening, topography, crustal geometry, and denudation. *Geological Society of America Bulletin*, 124(7-8), 1339-1351.

<https://doi.org/10.1130/B30609.1>

Goscombe, B. D., Passchier, C. W., & Hand, M. (2004). Boudinage classification: end-member boudin types and modified boudin structures. *Journal of Structural Geology*, 26(4), 739-763.

<https://doi.org/10.1016/j.jsg.2003.08.015>

Grader, G. W., & Dehler, C. M. (1999). Devonian stratigraphy in east-central Idaho: New perspectives from the Lemhi Range and Bayhorse area. In S. S. Hughes, & G. D. Thackray (Eds.), *Guidebook to the Geology of Eastern Idaho* (pp. 31-56). Pocatello, ID: Idaho Museum of Natural History, & Idaho State University Press.

Grader, G. W., Isaacson, P. E., Doughty, P. T., Pope, M. C., & Desantis, M. K. (2017). Idaho Lost River shelf to Montana craton: North American Late Devonian stratigraphy, surfaces, and intrashelf basin. In T.E. Playton, C. Kerans, & A.W., Weissenberger (Eds.), *New advances in Devonian Carbonates: Outcrop analogs, reservoirs, and chronostratigraphy* (Vol. 107, pp 347-379). Tulsa, OK: Society for Sedimentary Geology Special Publication.

<https://doi.org/10.2110/sepmsp.107.12>

Graveleau, F., Malavieille, J., & Dominguez, S. (2012). Experimental modelling of orogenic wedges: A review. *Tectonophysics*, 538, 1-66. <https://doi.org/10.1016/j.tecto.2012.01.027>

Gray, G., Zhang, Z., & Barrios, A. (2019). Basement-involved, shallow detachment faulting in the Bighorn Basin, Wyoming and Montana. *Journal of Structural Geology*, 120, 80-86.

<https://doi.org/10.1016/j.jsg.2018.10.015>

- Groshong, R. H., & Porter, R. (2019). Predictive models for the deep geometry of a thick-skinned thrust matched to crustal structure: Wind River Range, western USA. *Lithosphere*, *11*(4), 448-464. <https://doi.org/10.1130/L1031.1>
- Hait Jr, M. H. (1965). *Structure of the Gilmore area, Lemhi Range, Idaho* (doctoral dissertation). State College, PA: Pennsylvania State University.
- Haley, J. C., Bonilla, M. G., Meyer, R. F., Yeend, W. E., Lienkaemper, J. J., & Perry, W. J. (1991). The Red Butte Conglomerate: A Thrust-belt-derived Conglomerate of the Beaverhead Group, Southwestern Montana. *U.S. Geological Survey Bulletin*, *1945*, 1-19. Denver, CO: US Department of the Interior, US Geological Survey.
- Hamilton, W. B. (1988). Laramide crustal shortening. Interaction of the Rocky Mountain foreland and the Cordilleran thrust belt: *Geological Society of America Memoir*, *171*, 27-39. <https://doi.org/10.1130/MEM171-p27>
- Hansen, C. M., & Pearson, D. M. (2016). *Geologic Map of the Poison Creek Thrust Fault and Vicinity near Poison Peak and Twin Peaks, Lemhi County, Idaho*. (Technical Report T-16-1, scale 1:24,000). Moscow, ID: Idaho Geological Survey.
- Huh, O. K. (1967). The Mississippian system across the Wasatch line east central Idaho, extreme southwestern Montana. In *Montana Geological Society 18th Annual Field Conference 1967* (pp. 31-62). Billings, MT: Montana Geological Society.
- Hung, J. H., Wiltschko, D. V., Lin, H. C., Hickman, J. B., Fang, P., & Bock, Y. (1999). Structure and motion of the southwestern Taiwan fold and thrust belt. *Terrestrial, Atmospheric and Oceanic Sciences*, *10*, 543–68. [https://doi.org/10.3319/TAO.1999.10.3.543\(T\)](https://doi.org/10.3319/TAO.1999.10.3.543(T))

James, W. C., & Oaks, R. Q. (1977). Petrology of the Kinnikinic Quartzite (Middle Ordovician), east-central Idaho. *Journal of Sedimentary Research*, 47(4), 1491-1511.

<https://doi.org/10.1306/212F73A1-2B24-11D7-8648000102C1865D>

Janecke, S. U., VanDenburg, C. J., Blankenau, J. J., & M'Gonigle, J. W. (2000). Long-distance longitudinal transport of gravel across the Cordilleran thrust belt of Montana and Idaho.

*Geology*, 28(5), 439-442. [https://doi.org/10.1130/0091-7613\(2000\)28<439:LLTOGA>2.0.CO;2](https://doi.org/10.1130/0091-7613(2000)28<439:LLTOGA>2.0.CO;2)

Jordan, T. E., Isacks, B. L., Allmendinger, R. W., Brewer, J. A., Ramos, V. A., and Ando, C. J. (1983). Andean tectonics related to geometry of subducted Nazca plate, Geological Society of

America Bulletin, 94(3), 341–361. [https://doi.org/10.1130/0016-](https://doi.org/10.1130/0016-7606(1983)94<341:ATRTGO>2.0.CO;2)

[7606\(1983\)94<341:ATRTGO>2.0.CO;2](https://doi.org/10.1130/0016-7606(1983)94<341:ATRTGO>2.0.CO;2)

Jordan, T. E., & Allmendinger, R. W. (1986). The Sierras Pampeanas of Argentina; a modern analogue of Rocky Mountain foreland deformation. *American Journal of Science*, 286(10), 737-

764. <https://doi.org/10.2475/ajs.286.10.737>

Kay, M. (1951). *North American geosynclines* (Vol. 48). Boulder, CO: Geological Society of America Memoir. <https://doi.org/10.1130/MEM48>

Kay, S. M., MaksaeV, V., Moscoso, R., Mpodozis, C., and Nasi, C. (1987). Probing the evolving Andean Lithosphere: Mid-Late Tertiary magmatism in Chile (29°–30°30'S) over the modern zone of subhorizontal subduction, *J Geophys Res*, 92(B7), 6173–6189.

<https://doi.org/10.1029/JB092iB07p06173>

Kley, J. (1996). Transition from basement-involved to thin-skinned thrusting in the Cordillera Oriental of southern Bolivia. *Tectonics*, 15(4), 763-775. <https://doi.org/10.1029/95TC03868>

Kley, J., Monaldi, C. R., & Salfity, J. A. (1999). Along-strike segmentation of the Andean foreland: causes and consequences. *Tectonophysics*, 301(1-2), 75-94.

[https://doi.org/10.1016/S0040-1951\(98\)90223-2](https://doi.org/10.1016/S0040-1951(98)90223-2)

Kley, J., & Monaldi, C. R. (2002). Tectonic inversion in the Santa Barbara System of the central Andean foreland thrust belt, northwestern Argentina. *Tectonics*, 21(6), 11-1.

<https://doi.org/10.1029/2002TC902003>

Krumbein, W. C. (1939). Preferred orientation of pebbles in sedimentary deposits. *The Journal of Geology*, 47(7), 673-706. <https://doi.org/10.1086/624827>

Kulik, D. M., & Schmidt, C. J. (1988). Region of overlap and styles of interaction of Cordilleran thrust belt and Rocky Mountain foreland. In J. Schmidt, & W. J. Perry (Eds.), *Interaction of the Rocky Mountain Foreland and the Cordilleran Thrust Belt* (Vol. 171, pp 75-98). Boulder, CO:

Geological Society of America Memoir. <https://doi.org/10.1130/MEM171-p75>

Kuntz, M.A., Skipp, Betty, Lanphere, M.A., Scott, W.E., Pierce, K.L., Dalrymple, G.B.,

Champion, D.E., Embree, G.F., Page, W.R., Morgan, L.A., Smith, R.P., & Rodgers, D.W.

(1994). *Geologic map of the Idaho National Engineering Laboratory and adjoining areas,*

*eastern Idaho* (Miscellaneous Investigations Series Map I-2330, scale 1:100,000). Denver, CO:

U.S. Geological Survey.

Lacombe, O., & Mouthereau, F. (2002). Basement-involved shortening and deep detachment tectonics in forelands of orogens: insights from recent collision belts (Taiwan, western Alps,

Pyrenees). *Tectonics*, 21, 1030. <https://doi.org/10.1029/2001TC901018>

Lacombe, O., & Bellahsen, N. (2016). Thick-skinned tectonics and basement-involved fold–thrust belts: insights from selected Cenozoic orogens. *Geological Magazine*, *153*(5-6), 763-810.

<https://doi.org/10.1017/S0016756816000078>

Le Garzic, E., Vergés, J., Sapin, F., Saura, E., Meresse, F., & Ringenbach, J. C. (2019).

Evolution of the NW Zagros Fold-and-Thrust Belt in Kurdistan Region of Iraq from balanced and restored crustal-scale sections and forward modeling. *Journal of Structural Geology*, *124*,

51-69. <https://doi.org/10.1016/j.jsg.2019.04.006>

Link, P. K., Todt, M. K., Pearson, D. M., & Thomas, R. C. (2017). 500–490 Ma detrital zircons in Upper Cambrian Worm Creek and correlative sandstones, Idaho, Montana, and Wyoming:

Magmatism and tectonism within the passive margin. *Lithosphere*, *9*(6), 910-926.

<https://doi.org/10.1130/L671.1>

Liu, L., Gurnis, M., Seton, M., Saleeby, J., Müller, R. D., & Jackson, J. M. (2010). The role of oceanic plateau subduction in the Laramide orogeny. *Nature Geoscience*, *3*(5), 353-357.

<https://doi.org/10.1038/ngeo829>

Long, S. P. (2012). Magnitudes and spatial patterns of erosional exhumation in the Sevier hinterland, eastern Nevada and western Utah, USA: Insights from a Paleogene paleogeologic map. *Geosphere*, *8*(4), 881-901. <https://doi.org/10.1130/GES00783.1>

Long, S. P., & Kohn, M. J. (2020). Distributed ductile thinning during thrust emplacement: A commonly overlooked exhumation mechanism. *Geology*, *48*(4), 368-373.

<https://doi.org/10.1130/G47022.1>

Lonn, J. D., Skipp, B., Ruppel, E. T., Perry Jr, W. J., Sears, J. W., Janecke, S. U., Bartholomew, M. J., Stickney, M. C., Fritz, W. J., Hurlow, H. A., & Thomas, R. C. (2000). *Geologic map of the*

*Lima 30' x 60' quadrangle, southwest Montana* (Open-File Reports 408, scale 1:100,000). Butte, MT: Montana Bureau of Mines and Geology.

Lonn, J. D., Burmester, R. F., Lewis, R. S., & McFaddan, M. D. (2016). Giant folds and complex faults in Mesoproterozoic Lemhi strata of the Belt Supergroup, northern Beaverhead Mountains, Montana and Idaho. In J. W. Sears, & J. S. MacLean, (Eds.), *Belt Basin: Window to Mesoproterozoic Earth* (Vol. 522, pp. 139-162). Boulder, CO: Geological Society of America Special Paper. [https://doi.org/10.1130/2016.2522\(06\)](https://doi.org/10.1130/2016.2522(06))

Lonn, J. D., Elliott, C. G., Stewart, D. E., Mosolf, J. G., Burmester, R. F., Lewis, R. S., & Pearson, D. M. (2019). *Geologic map of the Bannock Pass 7.5' quadrangle, Beaverhead County, Montana, and Lemhi County, Idaho* (76, scale 1:24,000). Butte, MT: Montana Bureau of Mines and Geology.

Lopez, D. A., & Schmidt, C. (1985). Seismic profile across the leading edge of the fold and thrust belt of southwest Montana. In R. R., Gries (Ed.), *Seismic exploration of the Rocky Mountain region* (Vol. 1, pp. 45-50). Denver, CO: Rocky Mountain Association of Geologists.

Lovering, T. G. (1962). The origin of jasperoid in limestone. *Economic Geology*, 57(6), 861-889. <https://doi.org/10.2113/gsecongeo.57.6.861>

Lucchitta, B. K. (1966). *Structure of the Hawley Creek area, Idaho-Montana* (Doctoral dissertation). Retrieved from University Microfilms. no. 67-5941. University Park, PA, Pennsylvania State University.

Lund, K., Aleinikoff, J. N., Evans, K. V., DuBray, E. A., Dewitt, E. H., & Unruh, D. M. (2010). SHRIMP U-Pb dating of recurrent Cryogenian and Late Cambrian–Early Ordovician alkalic

magmatism in central Idaho: Implications for Rodinian rift tectonics. *Geological Society of America Bulletin*, 122(3-4), 430-453. <https://doi.org/10.1130/B26565.1>

Lund, K. (2018). *Geologic map of the central Beaverhead Mountains, Lemhi County, Idaho, and Beaverhead County, Montana* (Scientific Investigations Map 3413, scale 1:50,000). Denver, CO: U.S. Geological Survey.

Mardia, K. V. (1972). *Statistics of Directional Data*. London, UK: Academic Press.

Marshak, S., Karlstrom, K., & Timmons, J. M. (2000). Inversion of Proterozoic extensional faults: An explanation for the pattern of Laramide and Ancestral Rockies intracratonic deformation, United States. *Geology*, 28(8), 735-738. [https://doi.org/10.1130/0091-7613\(2000\)28<735:IOPEFA>2.0.CO;2](https://doi.org/10.1130/0091-7613(2000)28<735:IOPEFA>2.0.CO;2)

Marshak, S. (2004). Salients, recesses, arcs, oroclines, and syntaxes - A review of ideas concerning the formation of map-view curves in fold-thrust belts. In K. McClay (Ed.), *Thrust tectonics and hydrocarbon systems* (Vol. 82, pp. 131-156). Denver, CO: American Association of Petroleum Geologists.

Martínez, F., Giambiagi, L., Audemard, M., F. A., & Parra, M. (2020). Thrust and fold belts of South America. *Journal of South American Earth Sciences*, 104, 1-3. <https://doi.org/10.1016/j.jsames.2020.102822>

Mazzotti, S., & Hyndman, R. D. (2002). Yakutat collision and strain transfer across the northern Canadian Cordillera. *Geology*, 30(6), 495-498. [https://doi.org/10.1130/0091-7613\(2002\)030<0495:YCASTA>2.0.CO;2](https://doi.org/10.1130/0091-7613(2002)030<0495:YCASTA>2.0.CO;2)

McBride, B. C., Schmidt, C. J., Guthrie, G. E., & Sheedlo, M. K. (1992). Multiple reactivation of a collisional boundary: An example from southwestern Montana. In M.J. Bartholomew, D.W.

Hyndman, D. Mogk, R. Mason, (Eds.) *Basement Tectonics* (Vol. 8, pp. 341-357). Dordrecht, NL. Springer.

McDowell, R. J. (1997). Evidence for synchronous thin-skinned and basement deformation in the Cordilleran fold-thrust belt: the Tendoy Mountains, southwestern Montana. *Journal of Structural Geology*, 19(1), 77-87. [https://doi.org/10.1016/S0191-8141\(96\)00044-2](https://doi.org/10.1016/S0191-8141(96)00044-2)

McGroder, M. F., Lease, R. O., & Pearson, D. M. (2015). Along-strike variation in structural styles and hydrocarbon occurrences, Subandean fold-and-thrust belt and inner foreland, Colombia to Argentina. In P.G. DeCelles, M.N. Ducea, B. Carrapa, and P.A. Kapp, (Eds.), *Geodynamics of a Cordilleran Orogenic System: The Central Andes of Argentina and Northern Chile*: (Vol. 212, pp. 79–113). Boulder, CO: Geological Society of America Memoir. [https://doi.org/10.1130/2015.1212\(05\)](https://doi.org/10.1130/2015.1212(05))

McMechan, M. E., Thompson, R. I., Caldwell, W. G. E., & Kauffman, E. G. (1993). The Canadian Cordilleran fold and thrust belt south of 66 N and its influence on the Western Interior Basin. In W. G. E. Caldwell & E. G. Kauffman (Eds.), *Evolution of the Western Interior Basin*, (Vol. 39, p. 73-90). St. John's, NL: Geological Association of Canada.

McQuarrie, N. (2002). The kinematic history of the central Andean fold-thrust belt, Bolivia: Implications for building a high plateau. *Geological Society of America Bulletin*, 114(8), 950-963. [https://doi.org/10.1130/0016-7606\(2002\)114<0950:TKHOTC>2.0.CO;2](https://doi.org/10.1130/0016-7606(2002)114<0950:TKHOTC>2.0.CO;2)

McQuarrie, N. (2004). Crustal scale geometry of the Zagros fold–thrust belt, Iran. *Journal of Structural Geology*, 26(3), 519-535. <https://doi.org/10.1016/j.jsg.2003.08.009>

- McQueen, H. W. S., & Beaumont, C. (1989). Mechanical models of tilted block basins. Origin and Evolution of Sedimentary Basins and Their Mineral Resources (Ed. by R.A. Price), *AGU/IUGG Monograph*, 48, 65-71. <https://doi.org/10.1029/GM048p0065>
- Messina, T. A. (1993). *The geometry and kinematics of intra-thrust sheet decollement folding: Lost River Range, Idaho* (MS thesis). Bethlehem, Pennsylvania, Lehigh University.
- M'Gonigle, J. W. (1993). *Geologic map of the Medicine Lodge Peak quadrangle, Beaverhead County, southwest Montana* (Geologic Quadrangle Map GQ-1724, scale 1:24,000). Denver, CO: U.S. Geological Survey.
- M'Gonigle, J. W. (1994). *Geologic map of the Deadman Pass quadrangle, Beaverhead County, Montana, and Lemhi County, Idaho* (Geologic Quadrangle Map GQ-1753, scale 1:24,000). Denver, CO: U.S. Geological Survey.
- Mitra, G. (1994). Strain variation in thrust sheets across the Sevier fold-and-thrust belt (Idaho-Utah-Wyoming): Implications for section restoration and wedge taper evolution. *Journal of Structural Geology*, 16(4), 585-602. [https://doi.org/10.1016/0191-8141\(94\)90099-X](https://doi.org/10.1016/0191-8141(94)90099-X)
- Molinaro, M., Leturmy, P., Guezou, J. C., Frizon de Lamotte, D., & Eshraghi, S. A. (2005). The structure and kinematics of the southeastern Zagros fold-thrust belt, Iran: From thin-skinned to thick-skinned tectonics. *Tectonics*, 24(3). <https://doi.org/10.1029/2004TC001633>
- Mount, V. S., Martindale, K. W., Griffith, T. W., & Byrd, J. O. (2011). Basement-involved contractional wedge structural styles: Examples from the Hanna basin, Wyoming. In K. McClay, J. Shaw, and J. Suppe, (Eds.), *Thrust fault-related folding*: (Vol. 94, pp. 271-281). Denver, CO: American Association of Petroleum Geologists. <https://doi.org/10.1306/13251341M941003>

- Mouthereau, F., Lacombe, O., & Meyer, B. (2006). The Zagros Folded Belt (Fars, Iran): constraints from topography and critical wedge modelling. *Geophysical Journal International*, *165*, 336–56. <https://doi.org/10.1111/j.1365-246X.2006.02855.x>
- Mouthereau, F., Tensi, J., Bellahsen, N., Lacombe, O., De Boisgrollier, T., & Kargar, S. (2007). Tertiary sequence of deformation in a thin-skinned/thick-skinned collision belt: The Zagros Folded Belt (Fars, Iran). *Tectonics*, *26*(5). <https://doi.org/10.1029/2007TC002098>
- Mouthereau, F., Lacombe, O., & Verges, J. (2012). Building the Zagros collisional orogen: timing, strain distribution and the dynamics of Arabia/Eurasia plate convergence. *Tectonophysics*, *532–535*, 27–60. <https://doi.org/10.1016/j.tecto.2012.01.022>
- Mouthereau, F., Watts, A. B., & Burov, E. (2013). Structure of orogenic belts controlled by lithosphere age. *Nature Geoscience*, *6*(9), 785–789. <https://doi.org/10.1038/ngeo1902>
- Namson, J. (1981). Structure of the Western Foothills Belt, Miaoli-Hsinchu area, Taiwan: (I) Southern part. *Petroleum Geology of Taiwan*, *18*, 31–51.
- Neely, T. G., & Erslev, E. A. (2009). The interplay of fold mechanisms and basement weaknesses at the transition between Laramide basement-involved arches, north-central Wyoming, USA. *Journal of Structural Geology*, *31*(9), 1012–1027. <https://doi.org/10.1016/j.jsg.2009.03.008>
- O'Neill, J. M., Schmidt, C. J., & Genovese, P. W. (1990). Dillon cutoff-Basement-involved tectonic link between the disturbed belt of west-central Montana and the overthrust belt of extreme southwestern Montana. *Geology*, *18*(11), 1107–1110. [https://doi.org/10.1130/0091-7613\(1990\)018<1107:DCBITL>2.3.CO;2](https://doi.org/10.1130/0091-7613(1990)018<1107:DCBITL>2.3.CO;2)

O'Sullivan, P. B., & Wallace, W. K. (2002). Out-of-sequence, basement-involved structures in the Sadlerochit Mountains region of the Arctic National Wildlife Refuge, Alaska: Evidence and implications from fission-track thermochronology. *Geological Society of America Bulletin*, 114(11), 1356-1378. [https://doi.org/10.1130/0016-7606\(2002\)114<1356:OOSBIS>2.0.CO;2](https://doi.org/10.1130/0016-7606(2002)114<1356:OOSBIS>2.0.CO;2)

Parker, S. D., & Pearson, D. M. (2020). *Geologic map of the northern part of the Leadore quadrangle, Lemhi County, Idaho* (Technical Report T-20-03, scale 1:24,000). Moscow, ID: Idaho Geological Survey.

Pearson, D. M., Kapp, P., DeCelles, P. G., Reiners, P. W., Gehrels, G. E., Ducea, M. N., & Pullen, A. (2013). Influence of pre-Andean crustal structure on Cenozoic thrust belt kinematics and shortening magnitude: Northwestern Argentina. *Geosphere*, 9(6), 1766-1782. <https://doi.org/10.1130/GES00923.1>

Pearson, D. M., & Link, P. K. (2017). Field guide to the Lemhi arch and Mesozoic-early Cenozoic faults and folds in east-central Idaho: Beaverhead Mountains. *Northwest Geology*, 46, 101-112.

Perry Jr, W. J., & Sando, W. J. (1982). Sequence of deformation of Cordilleran thrust belt in Lima, Montana region. In R. B., Powers (Ed.), *Geologic studies of the Cordilleran thrust belt* (Vol. 1, pp. 137-144). Denver, CO: Rocky Mountain Association of Geologists.

Perry Jr, W. J., Wardlaw, B. R., Bostick, N. H., & Maughan, E. K. (1983). Structure, burial history, and petroleum potential of frontal thrust belt and adjacent foreland, southwest Montana. *The American Association of Petroleum Geologists Bulletin*, 67(5), 725-743. <https://doi.org/10.1306/03B5B6A0-16D1-11D7-8645000102C1865D>

Perry Jr, W. J., Haley, J. C., Nichols, D. J., Hammons, P. M., & Ponton, J. D. (1988) Interactions of Rocky Mountain foreland and Cordilleran thrust belt in Lima region, southwest Montana. In J. Schmidt, & W. J. Perry (Eds.), *Interaction of the Rocky Mountain Foreland and the Cordilleran Thrust Belt* (Vol. 171, pp 267-290). Boulder, CO: Geological Society of America Memoir.

<https://doi.org/10.1130/MEM171-p267>

Perry Jr, W. J., Dyman, T. S., & Sando, W. J. (1989). Southwestern Montana recess of Cordilleran thrust belt. In *Montana Geological Society: 1989 Field Conference Guidebook: Montana Centennial Edition: Geologic Resources of Montana: Volume 1* (pp. 261-270). Billings, MT: Montana Geological Society.

Peterson, J. A. (1981). General stratigraphy and regional paleostructure of the western Montana overthrust belt. In *Montana Geological Society field conference & symposium guidebook to southwest Montana* (pp. 5-35). Billings, MT: Montana Geological Society.

Pfiffner, O. A. (2006). Thick-skinned and thin-skinned styles of continental contraction. In S. Mazzoli, & W. H. Butler (Eds.), *Styles of Continental Contraction* (Vol. 414, pp. 153-177).

Boulder, CO: Geological Society of America Special Paper.

[https://doi.org/10.1130/2006.2414\(09\)](https://doi.org/10.1130/2006.2414(09)).

Pfiffner, O. A. (2017). Thick-skinned and thin-skinned tectonics: a global perspective.

*Geosciences*, 7(3), 71. <https://doi.org/10.3390/geosciences7030071>

Price, R. A., & Mountjoy, E. W. (1970). Geologic structure of the Canadian Rocky Mountains between Bow and Athabasca Rivers—a progress report. *Structure of the southern Canadian Cordillera* (Vol. 6, pp. 7-25). St. John's, NL: Geological Association of Canada Special Paper.

Price, R. (1981). The Cordilleran foreland thrust and fold belt in the southern Canadian Rocky Mountains. *Geological Society, London, Special Publications*, 9(1), 427-448.

<https://doi.org/10.1144/GSL.SP.1981.009.01.39>

Ramírez-Peña, C. F., & Chávez-Cabello, G. (2017). Age and evolution of thin-skinned deformation in Zacatecas, Mexico: Sevier orogeny evidence in the Mexican Fold-Thrust Belt.

*Journal of South American Earth Sciences*, 76, 101-114.

<https://doi.org/10.1016/j.jsames.2017.01.007>

Rich, J. L., (1934). Mechanics of Low-Angle Overthrust Faulting as Illustrated by Cumberland Thrust Block, Virginia, Kentucky, and Tennessee. *The American Association of Petroleum*

*Geologists Bulletin*; 18 (12): 1584–1596. [https://doi.org/10.1306/3D932C94-16B1-11D7-](https://doi.org/10.1306/3D932C94-16B1-11D7-8645000102C1865D)

[8645000102C1865D](https://doi.org/10.1306/3D932C94-16B1-11D7-8645000102C1865D)

Richardson, T., Ridgway, K. D., Gilbert, H., Martino, R., Enkelmann, E., Anderson, M., & Alvarado, P. (2013). Neogene and Quaternary tectonics of the Eastern Sierras Pampeanas, Argentina: active intraplate deformation inboard of flat-slab subduction. *Tectonics*, 32(3), 780-796. <https://doi.org/10.1002/tect.20054>

Rodgers, D. W., & Janecke, S. U., (1992). Tertiary paleogeologic maps of the western Idaho-Wyoming-Montana thrust belt. In P. K. Link, M. A. Kuntz, & L. B. Piatt (Eds.), *Regional Geology of Eastern Idaho and Western Wyoming* (Vol. 179, pp 83-94). Boulder, CO: Geological Society of America Memoir. <https://doi.org/10.1130/MEM179-p83>

Rose, P. R. (1976). Mississippian carbonate shelf margins, western United States. *Journal of Research, U.S. Geological Survey*, 4(4), 449-466.

- Rosenblume, J. A., Finzel, E. S., & Pearson, D. M. (2021). Early Cretaceous provenance, sediment dispersal, and foreland basin development in southwestern Montana, North American Cordillera, *Tectonics*, *40*, 1–31, <https://doi.org/10.1029/2020TC006561>
- Ross, C. P. (1934). Correlation and interpretation of Paleozoic stratigraphy in south-central Idaho. *Bulletin of the Geological Society of America*, *45*(5), 937-1000.  
<https://doi.org/10.1130/GSAB-45-937>
- Ross, C. P. (1947). Geology of the Borah Peak quadrangle, Idaho. *Geological Society of America Bulletin*, *58*(12), 1085-1160. [https://doi.org/10.1130/0016-7606\(1947\)58\[1085:GOTBPQ\]2.0.CO;2](https://doi.org/10.1130/0016-7606(1947)58[1085:GOTBPQ]2.0.CO;2)
- Royse Jr, F., Warner, M. T., & Reese, D. L. (1975). Thrust Belt Structural Geometry and Related Stratigraphic Problems Wyoming-Idaho-Northern Utah. Denver, CO: Rocky Mountain Association of Geologists.
- Ruh, J. B., Kaus, B. J., & Burg, J. P. (2012). Numerical investigation of deformation mechanics in fold-and-thrust belts: Influence of rheology of single and multiple décollements. *Tectonics*, *31*(3). <https://doi.org/10.1029/2011TC003047>
- Ruppel, E. T. (1968). *Geologic map of the Leadore quadrangle, Lemhi County, Idaho* (GQ-733, scale 1:62,500). Denver, CO: U.S. Geological Survey.
- Ruppel, E. T. (1986). The Lemhi Arch: A Late Proterozoic and Early Paleozoic Landmass in Central Idaho. In J. A. Peterson (Ed.), *Paleotectonics and sedimentation in the Rocky Mountain Region, United States* (41, pp. 119-130). Denver, CO: American Association of Petroleum Geologists. <https://doi.org/10.1306/M41456C6>

Ruppel, E. T., & Lopez, D. A. (1988). Regional geology and mineral deposits in and near the central part of the Lemhi Range, Lemhi County, Idaho. *US Geological Survey Bulletin, 1480*. Denver, CO: US Geological Survey.

Ryder, R. T., & Scholten, R. (1973). Syntectonic conglomerates in southwestern Montana: Their nature, origin, and tectonic significance. *Geological Society of America Bulletin, 84*(3), 773-796. [https://doi.org/10.1130/0016-7606\(1973\)84<773:SCISMT>2.0.CO;2](https://doi.org/10.1130/0016-7606(1973)84<773:SCISMT>2.0.CO;2)

Saleeby, J. (2003). Segmentation of the Laramide slab—Evidence from the southern Sierra Nevada region. *Geological Society of America Bulletin, 115*(6), 655-668. [https://doi.org/10.1130/0016-7606\(2003\)115<0655:SOTLSF>2.0.CO;2](https://doi.org/10.1130/0016-7606(2003)115<0655:SOTLSF>2.0.CO;2)

Scheevel, J. R. (1983). Horizontal compression and a mechanical interpretation of Rocky Mountain Foreland Deformation. In W. W. Boberg (Ed.), *Geology of the Bighorn Basin* (pp. 53-62). Casper, WY: Wyoming Geological Association.

Schmidt, C. J., & Garihan, J. M. (1983). Laramide tectonic development of the Rocky Mountain foreland of southwestern Montana. In J. D., Lowell (Ed.), *Rocky Mountain foreland basins and uplifts* (pp. 271-294). Denver, CO: Rocky Mountain Association of Geologists.

Schmidt, C. J., & Perry, W. J. (1988). *Interaction of the Rocky Mountain Foreland and the Cordilleran Thrust Belt* (Vol. 171). Boulder, CO: Geological Society of America Memoir. <https://doi.org/10.1130/MEM171>

Schmidt, C. J., O'Neill, J. M., & Brandon, W. C. (1988). Influence of Rocky Mountain foreland uplifts on the development of the frontal fold and thrust belt, southwestern Montana. In C. J. Schmidt, & W. J. Perry, *Interaction of the Rocky Mountain Foreland and the Cordilleran Thrust*

*Belt* (Vol. 17, pp. 171-201). Boulder, CO: Geological Society of America Memoir.

<https://doi.org/10.1130/MEM171>

Schmidt, C. J., R. A. Astini, C. H. Costa, C. E. Gardini, P. E. Kraemer, A. J. Tankard, R. Suárez, and H. J. Welsink (1995). Cretaceous rifting, alluvial fan sedimentation, and Neogene inversion, southern Sierras Pampeanas, Argentina. *AAPG Memoir* 62, 341–341.

<https://doi.org/10.1306/M62593C16>

Scholten, R., Keenmon, K. A., & Kupsch, W. O. (1955). Geology of the Lima region, southwestern Montana and adjacent Idaho. *Geological Society of America Bulletin*, 66(4), 345-404. [https://doi.org/10.1130/0016-7606\(1955\)66\[345:GOTLRS\]2.0.CO;2](https://doi.org/10.1130/0016-7606(1955)66[345:GOTLRS]2.0.CO;2)

Scholten, R. (1957). Paleozoic evolution of the geosynclinal margin north of the Snake River Plain, Idaho-Montana. *Geological Society of America Bulletin*, 68(2), 151-170.

[https://doi.org/10.1130/0016-7606\(1957\)68\[151:PEOTGM\]2.0.CO;2](https://doi.org/10.1130/0016-7606(1957)68[151:PEOTGM]2.0.CO;2)

Scholten, R., & Hait Jr, M. H. (1962). Devonian System from shelf edge to geosyncline, southwestern Montana-central Idaho. In *Thirteenth annual field conference, Three Forks - Belt Mountains area, and Symposium: The Devonian system of Montana and adjacent areas. September 5-8, 1962*, (pp. 13-22). Billings, MT: Billings Geological Society.

Scholten, R., & Ramspott, L. D. (1968). *Tectonic Mechanisms Indicated by Structural Framework of Central Beaverhead Range, Idaho Montana* (Vol. 105). Boulder, CO: Geological Society of America Special Paper.

Scholten, R. (1982). Continental subduction in the northern US Rockies-a model for back-arc thrusting in the western cordillera. In R. B., Powers (Ed.), *Geologic studies of the Cordilleran thrust belt* (Vol. 1, pp. 123-136). Denver, CO: Rocky Mountain Association of Geologists.

- Schwartz, R. K. (1982). Broken Early Cretaceous foreland basin in southwestern Montana: sedimentation related to tectonism, In R. B., Powers (Ed.), *Geologic studies of the Cordilleran thrust belt* (Vol. 1, pp. 159-183). Denver, CO: Rocky Mountain Association of Geologists.
- Shannon Jr, J. P. (1961). Upper Paleozoic stratigraphy of east-central Idaho. *Geological Society of America Bulletin*, 72(12), 1829-1836. [https://doi.org/10.1130/0016-7606\(1961\)72\[1829:UPSOEI\]2.0.CO;2](https://doi.org/10.1130/0016-7606(1961)72[1829:UPSOEI]2.0.CO;2)
- Sherkati, S., Letouzey, J., & Frizon De Lamotte, D. (2006). Central Zagros fold-thrust belt (Iran): new insights from seismic data, field observation, and sandbox modeling. *Tectonics*, 25, <https://doi.org/10.1029/2004TC001766>
- Simpson, G. D. (2010). Influence of the mechanical behaviour of brittle–ductile fold–thrust belts on the development of foreland basins. *Basin Research*, 22(2), 139-156. <https://doi.org/10.1111/j.1365-2117.2009.00406.x>
- Skipp, B., & Hait Jr, M. H. (1977). Allochthons along the northeast margin of the Snake River Plain, Idaho. In E. L. Heisey, D. E. Lawson, E. R. Norwood, P. H. Wach, & L. A. Hale (Eds.), *Rocky Mountain Thrust Belt Geology and Resources; 29th Annual Field Conference Guidebook* (pp. 499-515). Casper, WY: Wyoming Geological Association.
- Skipp, B. (1988). Cordilleran thrust belt and faulted foreland in the Beaverhead Mountains, Idaho and Montana. In J. Schmidt, & W. J. Perry (Eds.), *Interaction of the Rocky Mountain Foreland and the Cordilleran Thrust Belt* (Vol. 171, pp 237-266). Boulder, CO: Geological Society of America Memoir. <https://doi.org/10.1130/MEM171-p237>

Sloss, L. L. (1954). Lemhi Arch, a mid-Paleozoic positive element in south-central Idaho.

*Geological Society of America Bulletin*, 65(4), 365-368. [https://doi.org/10.1130/0016-7606\(1954\)65\[365:LAAMPE\]2.0.CO;2](https://doi.org/10.1130/0016-7606(1954)65[365:LAAMPE]2.0.CO;2)

Smithson, S. B., Brewer, J. A., Kaufman, S., Oliver, J. E., & Hurich, C. A. (1979). Structure of the Laramide Wind River uplift, Wyoming, from COCORP deep reflection data and from gravity data. *Journal of Geophysical Research: Solid Earth*, 84(B11), 5955-5972.

<https://doi.org/10.1029/JB084iB11p05955>

Staatz, M. H., Sharp, B. J., & Hetland, D. L. (1979). Geology and Mineral Resources of the Lemhi Pass Thorium District, Idaho and Montana: A Description of the Distribution, Geologic Setting, Mineralogy, and Chemistry of the Thorium Veins in the Lemhi Pass District. *U.S. Geological Survey Professional Paper* (Vol. 1049-A, pp.1-98). Denver, CO: US Department of the Interior, US Geological Survey.

Stearn, C. W. (1997). Intraspecific variation, diversity, revised systematics and type of the Devonian stromatoporoid, *Amphipora*. *Palaeontology*, 40, 833-854.

Stock, C. W. (1990). Biogeography of the Devonian stromatoporoids. *Geological Society, London, Memoirs*, 12(1), 257–265. <https://doi.org/10.1144/gsl.mem.1990.012.01.24>

Stockmal, G. S., Beaumont, C., Nguyen, M., & Lee, B. (2007). Mechanics of thin-skinned fold-and-thrust belts: Insights from numerical models. In J. W. Sears, T. A. Harms, & C. A.

Evenchick (Eds.), *Whence the Mountains? Inquiries into the Evolution of Orogenic Systems: A Volume in Honor of Raymond A. Price* (Vol. 433, pp 63-98). Boulder, CO: Geological Society of America Special Paper. [https://doi.org/10.1130/2007.2433\(04\)](https://doi.org/10.1130/2007.2433(04))

Suppe, J., & Namson, J. (1979). Fault-bend origin of frontal folds of the western Taiwan fold-and-thrust belt. *Petroleum Geology of Taiwan*, 16, 1-18.

Suppe, J. (1983). Geometry and kinematics of fault-bend folding. *American Journal of science*, 283(7), 684-721. <https://doi.org/10.2475/ajs.283.7.684>

Tavani, S., Granado, P., Corradetti, A., Camanni, G., Vignaroli, G., Manatschal, G., Mazzoli, S., Muñoz, J. A., & Parente, M. (2021). Rift inheritance controls the switch from thin-to thick-skinned thrusting and basal décollement re-localization at the subduction-to-collision transition. *GSA Bulletin*, 1-14. <https://doi.org/10.1130/B35800.1>

Tysdal, R. G. (1988). Deformation along the northeast side of Blacktail Mountains. In J. Schmidt, & W. J. Perry (Eds.), *Interaction of the Rocky Mountain Foreland and the Cordilleran Thrust Belt* (Vol. 171, pp 203-215). Boulder, CO: Geological Society of America Memoir. <https://doi.org/10.1130/MEM171-p203>

Tysdal, R. G. (2002). Structural geology of western part of Lemhi Range, east-central Idaho. *U.S. Geological Survey Professional Paper* (Vol. 1659, pp.1-33). Denver, CO: US Department of the Interior, US Geological Survey.

VanDenburg, C. J. (1997). *Cenozoic tectonic and paleogeographic evolution of the Horse Prairie half graben, southwest Montana* (MS thesis). Logan, UT, Utah State University.

Vollmer, F. W. (1990). An application of eigenvalue methods to structural domain analysis. *Geological Society of America Bulletin*, 102(6), 786-791. [https://doi.org/10.1130/0016-7606\(1990\)102<0786:AAOEMT>2.3.CO;2](https://doi.org/10.1130/0016-7606(1990)102<0786:AAOEMT>2.3.CO;2)

Von Hagke, C., & Malz, A. (2018). Triangle zones—Geometry, kinematics, mechanics, and the need for appreciation of uncertainties. *Earth-Science Reviews*, 177, 24-42.

<https://doi.org/10.1016/j.earscirev.2017.11.003>

Weil, A. B., & Yonkee, W. A. (2012). Layer-parallel shortening across the Sevier fold-thrust belt and Laramide foreland of Wyoming: spatial and temporal evolution of a complex geodynamic system. *Earth and Planetary Science Letters*, 357, 405-420.

<https://doi.org/10.1016/j.epsl.2012.09.021>

Weil, A. B., Yonkee, A., & Kendall, J. (2014). Towards a better understanding of the influence of basement heterogeneities and lithospheric coupling on foreland deformation: A structural and paleomagnetic study of Laramide deformation in the southern Bighorn Arch, Wyoming. *Bulletin*, 126(3-4), 415-437. <https://doi.org/10.1130/B30872.1>

Weil, A. B., Yonkee, A., & Schultz, M. (2016). Tectonic evolution of a Laramide transverse structural zone: Sweetwater Arch, south central Wyoming. *Tectonics*, 35(5), 1090-1120.

<https://doi.org/10.1002/2016TC004122>

White, S. H., Burrows, S. E., Carreras, J., Shaw, N. D., & Humphreys, F. J. (1980). On mylonites in ductile shear zones. *Journal of structural geology*, 2(1-2), 175-187.

[https://doi.org/10.1016/0191-8141\(80\)90048-6](https://doi.org/10.1016/0191-8141(80)90048-6)

Williams, C. A., Connors, C., Dahlen, F. A., Price, E. J., & Suppe, J. (1994). Effect of the brittle-ductile transition on the topography of compressive mountain belts on Earth and Venus. *Journal of Geophysical Research: Solid Earth*, 99(B10), 19947-19974.

<https://doi.org/10.1029/94JB01407>

- Williams, S. A., Singleton, J. S., Prior, M. G., Mavor, S. P., Cross, G. E., & Stockli, D. F. (2020). The early Palaeogene transition from thin-skinned to thick-skinned shortening in the Potosí uplift, Sierra Madre Oriental, northeastern Mexico. *International Geology Review*, 1-21. <https://doi.org/10.1080/00206814.2020.1805802>
- Wiltschko, D. V., & Dorr, J. A. (1983). Timing of deformation in overthrust belt and foreland of Idaho, Wyoming, and Utah. *American Association of Petroleum Geologists Bulletin*, 67(8), 1304-1322. <https://doi.org/10.1306/03B5B740-16D1-11D7-8645000102C1865D>
- Witte, J., & Oncken, O. (2020). Uncertainty quantification in section-balancing using Pseudo-3D forward modeling—Example of the Malargüe Anticline, Argentina. *Journal of Structural Geology*, 104189. <https://doi.org/10.1016/j.jsg.2020.104189>
- Worthington, L. L., Miller, K. C., Erslev, E. A., Anderson, M. L., Chamberlain, K. R., Sheehan, A. F., Yeck, W. L., Harder, S. H., & Siddoway, C. S. (2016). Crustal structure of the Bighorn Mountains region: Precambrian influence on Laramide shortening and uplift in north-central Wyoming. *Tectonics*, 35(1), 208-236. <https://doi.org/10.1002/2015TC003840>
- Yang, K. M., Huang, S. T., Wu, J. C., Lee, M., Ting, H. H. & Mei, W. W. (2001). The characteristics of sub-surface structure and evolution of the Tachianshan-Chukou thrust system. *Annual Meeting of the Geological Society of China*, pp. 82–4.
- Yeck, W. L., Sheehan, A. F., Anderson, M. L., Erslev, E. A., Miller, K. C., & Siddoway, C. S. (2014). Structure of the Bighorn Mountain region, Wyoming, from teleseismic receiver function analysis: Implications for the kinematics of Laramide shortening. *Journal of Geophysical Research: Solid Earth*, 119(9), 7028-7042. <https://doi.org/10.1002/2013JB010769>

Yonkee, W. A. (1992). Basement-cover relations, Sevier orogenic belt, northern Utah. *Geological Society of America Bulletin*, 104(3), 280-302. [https://doi.org/10.1130/0016-7606\(1992\)104<0280:BCRSOB>2.3.CO;2](https://doi.org/10.1130/0016-7606(1992)104<0280:BCRSOB>2.3.CO;2)

Yonkee, A., & Weil, A. B. (2010). Reconstructing the kinematic evolution of curved mountain belts: Internal strain patterns in the Wyoming salient, Sevier thrust belt, USA. *Geological Society of America Bulletin*, 122(1-2), 24-49. <https://doi.org/10.1130/B26484.1>

Yonkee, W. A., & Weil, A. B. (2015). Tectonic evolution of the Sevier and Laramide belts within the North American Cordillera orogenic system. *Earth-Science Reviews*, 150, 531-593. <https://doi.org/10.1016/j.earscirev.2015.08.001>

Zawislak, R. L., & Smithson, S. B. (1981). Problems and interpretation of COCORP deep seismic reflection data, Wind River Range, Wyoming. *Geophysics*, 46(12), 1684-1701. <https://doi.org/10.1190/1.1441176>

Zhou, Y., Murphy, M. A., & Hamade, A. (2006). Structural development of the Peregrina–Huizachal anticlinorium, Mexico. *Journal of Structural Geology*, 28(3), 494-507. <https://doi.org/10.1016/j.jsg.2005.11.005>

## Chapter II:

A thermal profile across the Idaho-Montana fold-thrust belt reveals early burial to late exhumation during progressive growth of an orogenic wedge: U.S. Cordillera

# A thermal profile across the Idaho-Montana fold-thrust belt reveals early burial to late exhumation during progressive growth of an orogenic wedge: U.S. Cordillera

*Manuscript for submission to Geosphere*

**Stuart D. Parker<sup>1</sup> and David M. Pearson<sup>1</sup>**

*<sup>1</sup>Department of Geosciences, Idaho State University, Pocatello, Idaho 83209, USA*

## **ABSTRACT**

Growing orogenic wedges alter the thermal structure of rocks by cooling them during exhumation of hanging walls and heating them during burial of footwalls, leaving behind an indirect but resilient thermal record of earlier deformation in fold-thrust belts. In order to investigate early burial of deformed strata within the retroarc orogenic wedge, we use Raman Spectroscopy of Carbonaceous Material (RSCM) to construct a maximum temperature profile across the Idaho-Montana fold-thrust belt, thereby constraining the thickness of eroded rocks structurally above the Lemhi arch, pre-thrusting basement high. In the eastern portion of the study area, a sharp maximum temperature increase of  $121^{\circ}\text{C} (\pm 57)$  occurs across the Johnson thrust, signifying that regional burial and heating predated late-stage faulting. West of here, cumulative exhumation is irregular, varying by up to 5 km over large ( $\sim 75$  km) wavelength folds; however, maximum temperatures are consistently  $\sim 250\text{-}300^{\circ}\text{C}$  for carbonates above and west of the Lemhi arch, which is more than  $200^{\circ}\text{C}$  higher than comparable rocks in the adjacent foreland. The pre-thrusting, low-relief unconformity above the Lemhi arch, which served as the

early décollement to the fold-thrust belt, was everywhere buried to at least ~6.5 km depth, which is 1.5-4.0 km deeper than can be explained by the preserved stratigraphy. We hypothesize that a combination of Early Cretaceous deposition and/or folding and thrusting at higher structural levels buried the décollement of the Medicine Lodge-McKenzie thrust system to this depth, between ~145 and 80 Ma. These results suggest that the early orogenic wedge had a low taper angle above the Lemhi arch. We propose that this low taper was imposed by the thin stratigraphy over the low-relief Lemhi arch, which limited the geometry of potential décollements.

Subsequent growth of the orogenic wedge resulted in activation of a much deeper décollement, promoting an orogen-scale shift from burial to exhumation of the former décollement and the underlying Lemhi arch. This suggests that the growth of orogenic wedges may be fundamentally dependent on the thicknesses of the preexisting stratigraphy and the availability of potential décollements.

## **INTRODUCTION**

Continental fold-thrust belts develop at convergent plate boundaries within the upper continental crust and behave to a first order like critically tapered wedges (e.g., Davis et al., 1983). Critical taper theory has been consistently applied to thin-skinned continental fold-thrust belts that have a general wedge geometry with increasing exhumation toward their interiors; fold-thrust belts where critical taper theory has been successfully applied include those in the Sevier fold-thrust belt of Utah, Wyoming (e.g., DeCelles and Mitra, 1995), and Nevada (Long et al., 2014), the Canadian Rockies (e.g., Bally et al., 1966; Davis et al., 1983; Dahlen, 1990; Price, 2001; Fitz-Díaz et al., 2011), the modern Andes (e.g., Horton, 1999; Ghiglione and Ramos, 2005; McQuarrie et al., 2008; Carbonell et al., 2011; Anderson et al., 2018), and the Himalaya (Davis et al., 1983; Dahlen, 1990; Hilley and Strecker, 2004). Understanding how wedge

morphology and growth patterns are influenced by specific variables, like preexisting stratigraphy, is complicated because the self-destructive nature of orogenesis makes it difficult to reconstruct the early deformational history and geometry of orogenic wedges.

Information regarding the geometry of earlier phases of growing orogenic wedges may be obtained by documenting how much exhumation is recorded in regional unconformities.

Paleogeologic maps beneath post-orogenic unconformities highlight the cumulative exhumation achieved during orogenesis (e.g., Rodgers and Janecke, 1992; Long, 2012). This can yield very useful information, but only if the desired unconformities are preserved in the rock record and the preexisting stratigraphic thicknesses are known. When particular unconformities are not preserved or the thickness of eroded overburden is unknown, exhumation and its associated cooling of rocks are recorded as a thermal history (e.g., McQuarrie and Ehlers, 2017).

Fold-thrust belts experience not only exhumation and cooling of uplifted rocks in hanging walls of thrusts, but also burial and heating of rocks in footwalls, resulting in a particular thermal profile that mimics the eroded wedge geometry (Fig. 1). For instance, erosion of a simple critically tapered wedge produces rocks that experienced increasingly higher maximum temperatures toward the interior (Fig. 1a). More complicated wedge geometries may produce maximum temperature plateaus where the wedge is near its critical taper angle, and localized maximum temperatures reflect where exhumation has occurred over a footwall ramp (Fig. 1b). Simply put, burial and exhumation produce a thermal profile of an orogenic wedge that approximates the geometry of the surface slope.

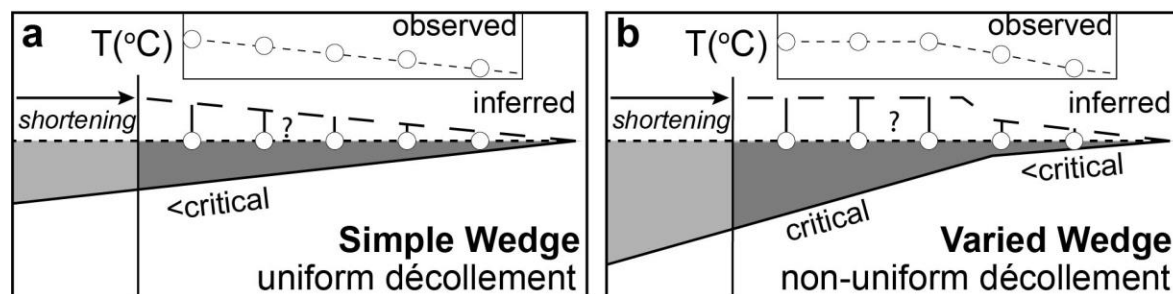


Figure 1. Hypothetical orogenic wedges illustrating how maximum burial depths, inferred from maximum temperatures, constrain the geometry of an orogenic wedge. Basal and surface slope shown in solid and dashed black line, with erosion level shown as dotted line. Predicted maximum temperature profiles for hypothetical samples along a transect are shown in the inset above. Note that the thermal profile mimics the wedge geometry.

Paleothermometers can independently constrain the maximum burial depths of rocks, thereby providing an empirical way to constrain the geometry of ancient orogenic wedges, even with incomplete knowledge of preexisting stratigraphic thicknesses (e.g., Bollinger et al., 2004; Chen et al., 2011; Labaume et al., 2016; McQuarrie and Ehlers, 2017; Nibourel et al., 2018, 2021; Muirhead et al., 2019; Anderson et al., 2021; Corrado et al., 2021). In particular, Raman Spectroscopy of Carbonaceous Material (RSCM) offers a simple way to investigate the thermal history of carbon-bearing carbonate and fine-grained siliciclastic rocks that are not easily analyzed by conventional low-temperature thermochronometers (e.g., Beyssac et al., 2002; Rahl et al., 2005; Muirhead et al., 2019). The temperature-dependent, one way reaction of organic carbon to graphite (Buseck and Beyssac, 2014) is utilized by RSCM to yield robust and reproducible maximum temperature constraints that capture thermal events on geologic timescales (Nakamura et al., 2017), and at low temperatures  $<100^{\circ}\text{C}$  (Schito et al., 2017; Muirhead et al., 2019). In addition, maximum temperature data obtained by RSCM is much simpler than for conventional low-temperature thermochronometers (e.g., zircon and apatite (U-

Th)/He)) because fewer variables are involved (e.g., radiation damage, partial retention, annealing, and grain-size; Farley, 2000; Flowers et al., 2009; Schuster and Farley, 2009; Guenther et al., 2013; Guenther, 2021). These attributes make the RSCM method useful for independently constraining the geometries of orogenic wedges by offering data regarding maximum burial depths.

The Idaho-Montana fold-thrust belt lies within the Sevier and Laramide belts of the North American Cordillera and records the effects of variable stratigraphy on structural style (e.g., Kulik and Schmidt, 1988; Perry et al., 1988; Skipp, 1988a; DeCelles, 2004; Yonkee and Weil, 2014). Using RSCM to constrain maximum temperatures along a >350 km long transect, and quantifying exhumation magnitude based on an updated paleogeologic map, we constrain burial and exhumation across the Idaho-Montana fold-thrust belt (Fig. 2, 3). A general lack of syn-orogenic wedge-top strata, and the fact that thrust faults generally involve carbonate rocks and have moderate throws of a few kilometers, has prevented previous workers from using standard geochronological and thermochronological methods to investigate the kinematics and timing of deformation in the Idaho-Montana fold-thrust belt. As a result, the timing and magnitude of thrust related burial and exhumation in the Idaho-Montana portion of the North American Cordillera (e.g., Skipp and Hait, 1977; Ruppel and Lopez, 1984; ; Perry et al., 1988; Skipp, 1988a) remains poorly constrained, especially when compared to the Canadian Rockies to the north (e.g., Bally et al., 1966; Price and Mountjoy, 1970; Price, 1981; Evenchick et al., 2007) and the Wyoming salient to the south (e.g., Royse et al., 1975; Royse, 1993; DeCelles and Mitra, 1995; Gentry et al., 2018; Yonkee et al., 2019). Available conodont alteration index (CAI) data along the Idaho-Montana fold-thrust belt suggest a steep maximum temperature gradient near the foreland, northeast of the Tendency Mountains (Perry et al., 1983), and consistently high

temperatures ( $\sim 300^{\circ}\text{C}$ ) in the hinterland, southwest of the Lost River Range (Harris et al., 1980). However, the non-systematic distribution of the collected samples makes the geometry of this thermal profile uncertain and these results have not been previously interpreted in a regional context (Fig. 1). Furthermore, a recent model predicts that early thin-skinned phases of the orogenic wedge have been overprinted by later thick-skinned phases (Parker and Pearson, 2021). With systematic sampling across the study area, we empirically constrain the pattern of maximum burial temperatures along the transect, and use the data to determine stratigraphic burial depths and a possible paleo surface slope of the orogenic wedge. The results highlight the thermal signature of the enigmatic early phase of deformation ( $\sim 145\text{-}90$  Ma) in the Idaho-Montana fold-thrust belt and document dismemberment and reorganization of the orogenic wedge during a transition to thick-skinned thrusting in Late Cretaceous to Eocene time ( $\sim 90\text{-}53$  Ma). Using RSCM helps to elucidate the geometry of the early orogenic wedge that was later overprinted during progressive deformation, suggesting that the geometry of the preexisting stratigraphy may set limits on the wedge geometry, resulting in activation of a deeper mid-crustal décollement once a threshold amount of shortening is surpassed.

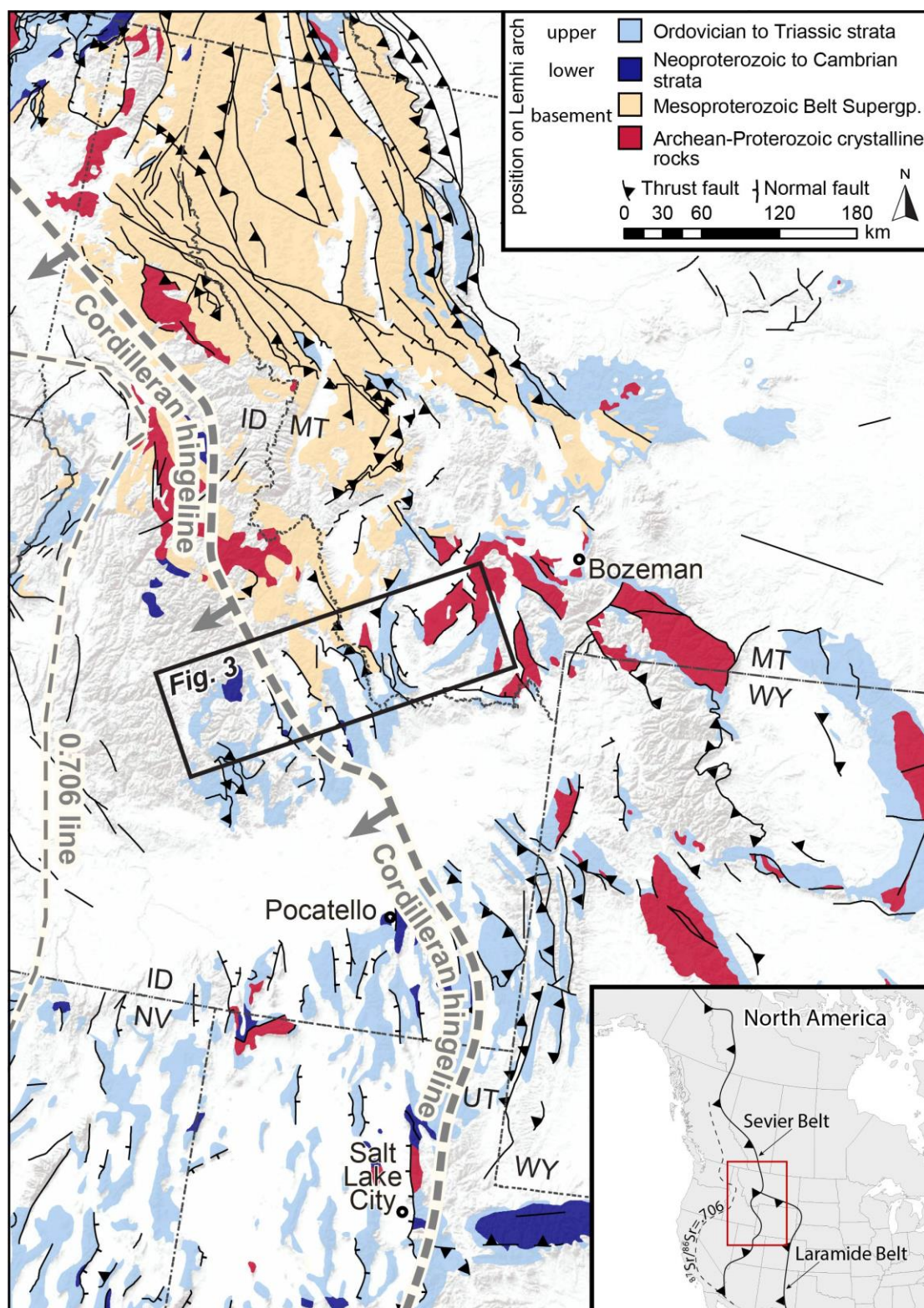


Figure 2. Simplified geologic map of the northern part of the U.S. Cordillera, highlighting the stratigraphy related to the Lemhi arch. Inset map in the lower right shows the Sevier and Laramide Belts

*of the North American Cordillera. Cordilleran hingeline denotes the approximate cratonic margin, locally coincident with the edge of the Lemhi arch, signified by a rapid increase in the thickness of passive margin strata to the west and pinching out of lower Cambrian strata to the east.*

## **GEOLOGIC BACKGROUND**

### **Lemhi arch stratigraphy**

The retroarc continental fold-thrust belt of the Late Jurassic to early Eocene North American Cordillera spans much of western North America (Fig. 2; e.g., Armstrong, 1968; Burchfiel and Davis, 1975; Dickinson and Snyder, 1978; Oldow et al., 1989; Miller et al., 1992; DeCelles, 2004; Dickinson, 2004; Yonkee and Weil, 2015). Like elsewhere in the Cordillera, the Idaho-Montana fold-thrust belt developed mostly within rift and passive margin strata flanking the western edge of the Laurentian continent (e.g., Skipp and Hall, 1980; Peterson, 1981). However, weak Neoproterozoic to Cambrian strata that host the décollement in much of the Sevier fold-thrust belt (e.g., O'Brien, 1960; Armstrong, 1968; Dahlstrom, 1970; Coogan, 1992; McMechan, 2001; DeCelles and Coogan, 2006; Yonkee et al., 2019) are largely absent along much of the Idaho-Montana fold thrust belt, where the lower part of the rift-passive margin stratigraphy pinches out against a major basement high termed the Lemhi arch (Fig. 2; Sloss, 1954). The Lemhi arch consists of tilted fault blocks of Mesoproterozoic quartzites of the Lemhi sub basin of the Belt Supergroup in central Idaho and Paleoproterozoic and Archean crystalline basement and metasedimentary rocks within the Dillon block of the Wyoming craton in southwestern Montana (Scholten, 1957; Ruppel, 1986; Link et al., 2017; Brennan et al., 2020). The unconformities and condensed sections within the Neoproterozoic to Cambrian rift-to-drift strata in the vicinity of the Lemhi arch (e.g., Scholten, 1957; Lund et al., 2010; Yonkee et al., 2014; Grader et al., 2017; Brennan et al., 2020; Milton, 2020) make the Idaho-Montana fold-

thrust belt a suitable place to test how inherited rift architecture and stratigraphy may influence the geometry and kinematics of the fold-thrust belt.

In east-central Idaho, an intra-Devonian unconformity marks the lowest regionally continuous passive margin strata on top of the Lemhi arch (Grader et al., 2017). Above this unconformity, uppermost Devonian to Pennsylvanian mixed siliciclastic and carbonate rocks are regionally extensive, defining a west-facing shelf to slope transition that drapes the Lemhi arch (e.g., Rose, 1976; Grader et al., 2017; Hofmann, 2020). These middle Paleozoic strata host a décollement to many thrusts of the upper, thin-skinned, Idaho-Montana fold-thrust belt (e.g., Skipp, 1988a; Perry et al., 1988; Parker and Pearson, 2021), with a hingeline that mimics both the geometry of the former rift margin and the later Sevier fold-thrust belt (e.g., Armstrong, 1968; Burchfiel and Davis, 1975; Rose, 1976; Picha and Gibson, 1985; Mitra, 1997). The lack of preservation of Permian to Cretaceous strata throughout much of the central portion of the Idaho-Montana fold-thrust belt, and the presence of localized latest Devonian-Mississippian (Antler orogeny) to Pennsylvanian-Permian (Ancestral Rockies orogeny) transpressional and/or foreland basins and associated unconformities in the Pioneer, White Knob, and Boulder mountains (Mahoney et al., 1991; Link et al., 1996; Geslin, 1998; Beranek et al., 2016; Leary et al., 2017) make the pre-orogenic geometry of the uppermost strata unclear. Despite this uncertainty, it is clear that both the laterally discontinuous lower package of Neoproterozoic to Devonian rocks and the thin but laterally continuous upper stratigraphic package of Devonian and younger rocks surrounding the Lemhi arch severely limit the availability of weak detachment horizons in the later fold-thrust-belt (Skipp, 1988a; Parker and Pearson, 2021).

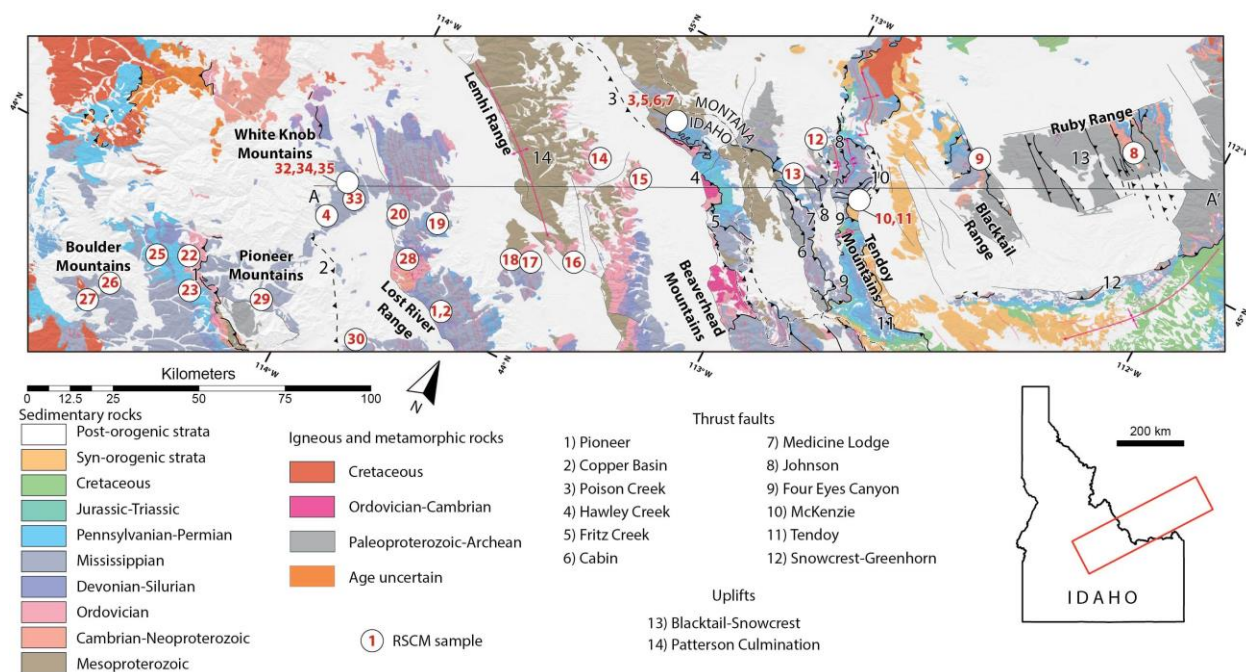


Figure 3. Simplified geologic map of the study area (redrafted from Parker and Pearson, in prep), with major thrusts numbered. Cross section line is referenced in subsequent figures. Geographic names referenced in the text are labeled. See Table 2 for more information on samples.

### Exhumation patterns

As a result of the stratigraphic complexities related to the Lemhi arch, the Idaho-Montana fold-thrust belt displays a wide range of structural styles and a variable amount of exhumation, making the wedge geometry unclear. The major thrust faults of the region are shown in Fig. 3. Structural style generally changes above and below the Lemhi arch unconformities (e.g., Hait, 1965; Beutner, 1968; Scholten and Ramspott, 1968). Immediately above the highest Lemhi arch unconformity, kilometer-wavelength detachment folds rooted in Mississippian and Devonian shales and siltstones are observed (Hait, 1965; Mapel, 1965; Beutner, 1968; Scholten and Ramspott, 1968; Messina, 1993; Fisher and Anastasio, 1994; Anastasio et al., 1997). Detachment folds are commonly upright in the Lost River Range (e.g., Messina, 1993), but overturned to recumbent in the Lemhi Range and Beaverhead Mountains (e.g., Hait, 1965; Beutner, 1968;

Scholten and Ramspott, 1968; M'Gonigle, 1982; Little and Clayton, 2017), signifying increasing shear strain toward the foreland along a décollement just above the Lemhi arch (Parker and Pearson, 2021). Major regional thrusts such as the Thompson Gulch and Medicine Lodge (Fig. 3) utilized this décollement (e.g., Skipp, 1988a; Lund, 2018), with a frontal ramp ultimately continuing to the surface in a localized foreland basin (e.g., Ryder and Scholten, 1973; Garber et al., 2020). This décollement was tilted and/or cross cut by younger, more deeply detached structures (Hait, 1965; Beutner, 1968; Scholten and Ramspott, 1968; Skipp, 1988a). For example, the Thompson Gulch and correlative thrusts are tilted and crosscut by the Baby Joe Gulch-Hawley Creek thrust (Lucchitta, 1966; Lund, 2018; Parker and Pearson, 2021). Adjacent to this structural low a regional-scale plunging anticlinorium, the Patterson culmination, exhumed a portion of the Lemhi arch and tilted the overlying detachment folds in the Lemhi Range (Hait, 1965; Beutner, 1968).

The Lemhi arch was exhumed by thrusts that are characterized by a thick-skinned structural style such as the Poison Creek-Baby Joe Gulch-Hawley Creek thrust system (Fig. 3; Lucchitta, 1966; Hansen and Pearson, 2016; Parker and Pearson, 2021). While there is a recognizable mechanical stratigraphy across the region that relates to the Lemhi arch, younger deformation of the Lemhi arch resulted in a complex and irregular exhumation pattern that eroded or overprinted evidence of older deformation at higher structural levels.

Though the older phase of thin-skinned deformation above the Lemhi arch is scantily preserved, the magnitude of exhumation related to shortening was documented by Rodgers and Janecke's (1992) paleogeologic map of the regional, post-orogenic unconformity marked by the base of the Eocene Challis Volcanic Group. The paleogeologic map highlights large wavelength

(~75 km) folds that plunge toward the southeast, exhuming Mesoproterozoic to Permian rocks in and adjacent to the Lemhi arch.

### **USING BURIAL ESTIMATES TO CONSTRAIN WEDGE GEOMETRY**

Retro-arc fold-thrust belts are often successfully modeled in the context of critical taper theory (e.g., Davis et al., 1983). This simple and predictive model views active mountain belts as growing wedges of deforming material, using the analogy of an advancing snowplow that piles a forward-tapering wedge of snow by scraping along a fixed base. Horizontal shortening and vertical thickening accommodated by folding and/or thrust faulting on the crustal-scale results in a wedge-shaped geometry of the fold-thrust belt; the upper surface of the orogenic wedge is defined by the surface slope of the growing wedge and a basal slope is governed by the dip of the basal fold-thrust belt detachment. The wedge taper angle is the sum of these two angles. As horizontal shortening and vertical thickening occur, the surface slope and taper angle increase until they surpass a critical value set by the compressive strength of the material within the wedge and the frictional resistance to sliding at the base. Once this threshold is surpassed, a new “in-sequence” thrust fault (or fold) propagates forward, thereby reducing the surface slope and decreasing the taper angle as deformation advances toward undeformed crust. The cycle continues as “out-of-sequence” thrusts thicken the interior of the wedge, once again increasing the taper angle toward failure. In sandbox models, this alternating process of internal thickening and forward advance of the wedge of deformed material is governed purely by changes in surface slope because the décollement is usually fixed at the base of the model.

In nature, however, because wedge growth is facilitated by successive formation of new décollements (basal slope) which involve progressively deeper rocks, the stratigraphy itself may limit the ability of the wedge to grow. The freedom to activate a new décollement at relatively

deeper stratigraphic levels means that the stress state of the wedge may be balanced not only by changing the surface slope, but also by changing the basal slope. It has long been observed that thrust faults cut across stratigraphic layers of varying strength in a stair step fashion as they follow the path of least resistance (Rich, 1934). Therefore, pre-thrusting stratal geometries and the distribution of weak rocks like shales and silty carbonates may determine the basal slope, which in turn impacts the surface slope (e.g., Lawton et al., 1994; Boyer, 1995; Mitra, 1997). In other words the mechanical stratigraphy of the crust determines the path of least resistance, thereby limiting the angle and position of the basal slope to the growing wedge.

In order to employ critical taper theory in the study of ancient orogenic belts and to investigate the potential role of stratigraphy in regulating wedge geometry and growth, it is therefore crucial to constrain both the surface and basal slope through time. Basal slope may be inferred from surface mapping and through creation of balanced and restored cross sections. Inferring the surface slope requires additional constraints, such as the thermal history of sedimentary rocks. Where magmatic activity is absent, the maximum temperature recorded in a sedimentary rock gives a maximum burial depth, assuming a geothermal gradient and surface temperature. Whatever the burial mechanism, by calculating maximum burial depths along a transect, a slope can be generated relative to the sampled datum (Fig. 1). The rate of change of the maximum temperature trend should scale with the time-averaged surface slope of the wedge. Constructing a maximum temperature profile across the Idaho-Montana fold-thrust belt allows for estimations of burial depths and of the former wedge geometry.

## METHODS

### *Raman spectroscopy of carbonaceous material*

In this study, we infer the wedge geometry for the Idaho-Montana fold-thrust belt by using RSCM to obtain maximum temperatures along a regional transect (Fig. 1, 3). A balanced and restored regional cross section provides context and constrains the geometry of the pre-orogenic stratigraphy and décollement (Parker and Pearson, in prep). Forty-two samples of dark, fine-grained carbonate and siliciclastic rocks were collected for RSCM along a ~350 km long transect across the study area (Fig. 3). Samples with known stratigraphic separations in the Lost River and Beaverhead ranges constrain a reasonable maximum paleogeothermal gradient, which is presented in the discussion section. With these geothermal gradient estimates, we use calculated maximum temperatures as a proxy for maximum burial depths. When possible, samples were collected from near the intra-Devonian Lemhi arch unconformity (Lemhi arch unconformity of Grader et al., 2017), and near the top of the regionally extensive Mississippian part of the stratigraphy. By targeting these two stratigraphic datums, we can use the regional stratigraphic thickness to make first-order inferences about the original basin geometry and/or the dimensions of the critically tapered orogenic wedge.

Standard 30  $\mu$ m-thick, microprobe-polished thin sections were analyzed at the University of Colorado Boulder using a LabRAM HR Evolution Raman microscope. For each sample, 18 spots of carbonaceous material were analyzed using a 532 nm (green) laser. For each spot, two analyses with 5 second acquisition times each were collected at 25% power and averaged. A 10 second acquisition time at 50% power was used for samples that had significant noise in the spectra due to high fluorescence.

Iterative curve fitting was performed using IFORS software (Lünsdorf and Lünsdorf, 2016), downloaded with the author's permission from <http://www.sediment.uni-goettingen.de/download/>. This method is preferred because its automated and iterative modelling approach removes user bias (Lünsdorf et al., 2014), and does not assume a set number or position of defect peaks (ex. D1-4; Lünsdorf et al., 2017), which themselves vary with maximum temperature (Schito et al., 2017). The method quantifies temperature-dependent changes to shape of the peaks of the D- and G-bands (Fig. 4a): D-band peaks get narrower and relatively taller, and G-band peaks get narrower and relatively smaller with increasing maximum temperature from ~50-400°C (e.g., Lünsdorf et al., 2017; Schito et al., 2017). Rather than using the heights and widths of the graphite (G) and D1-4 peaks to calculate temperature (e.g., Rahl et al., 2005), this method uses the scaled total area of the G and D bands to calculate temperature (Lünsdorf et al., 2017). Simply put, this method sums all intensity values in the respective D and G bands, for Raman shift values between 1000 and 1800  $\text{cm}^{-1}$ , and divides them by the maximum intensity value in the respective band ( $D_{\text{max}}$  or  $G_{\text{max}}$ ). Examples of the curve fitting process are illustrated in Fig. 4b and 3c, with shaded areas under the respective curves highlighting the areas used in the calculations. Using a calibration curve (Lünsdorf and Lünsdorf, 2016), scaled total area values were then converted to maximum temperatures (°C).

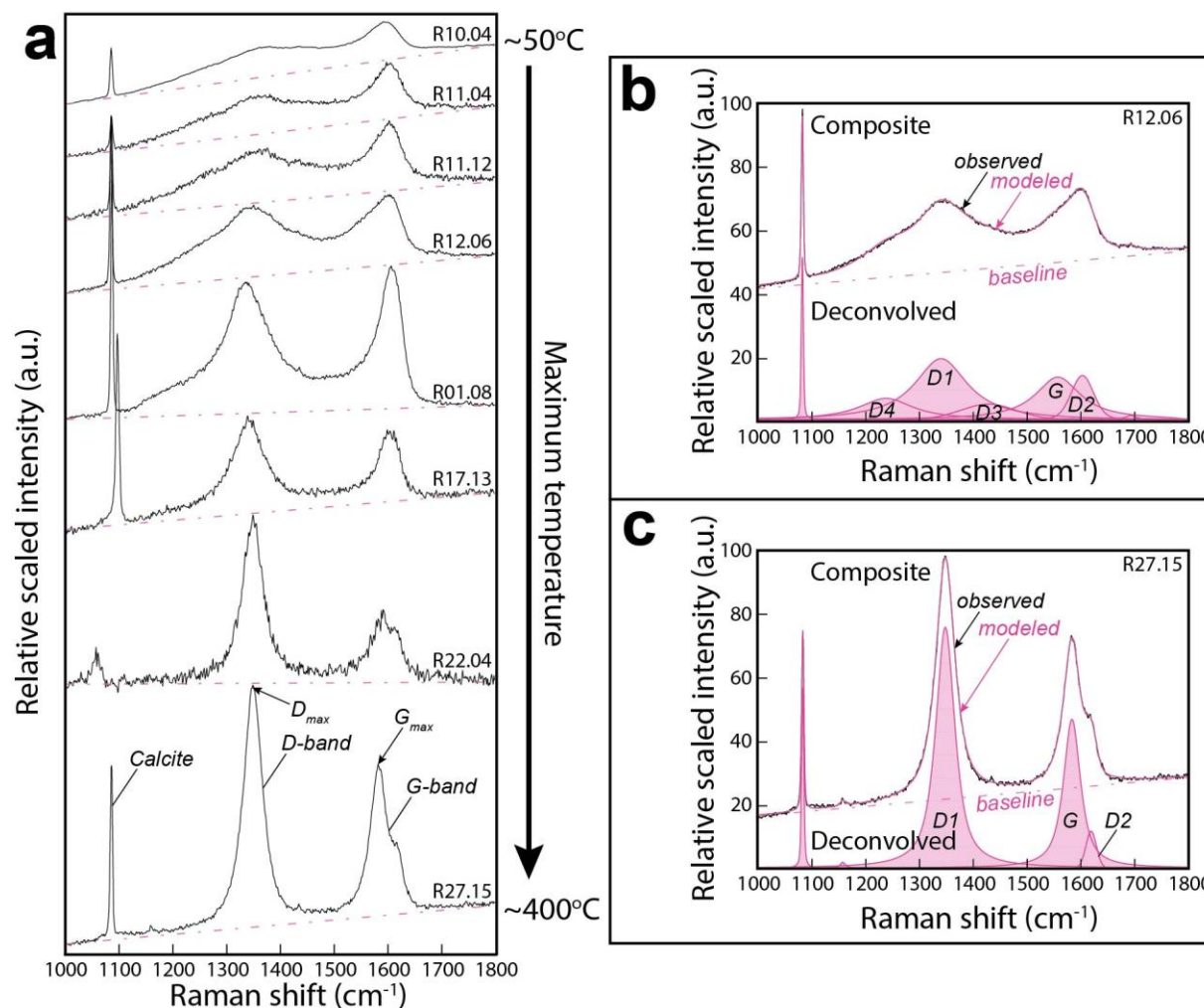


Figure 4. Representative examples of RSCM spectra from samples with calculated maximum temperatures ranging from  $\sim 50$  to  $400^\circ\text{C}$ . **a)** Changes in the overall shape of the spectra, above a baseline, as a function of temperature. Spectra represent  $\sim 50^\circ\text{C}$  increments. Note that the D-band gets narrower and taller and the G-band gets narrower and shorter with increasing maximum temperature. Sharp calcite peak is labeled. Sample and spot analysis numbers are shown on right. See supplementary material for raw and processed data. Composite and deconvoluted spectra with corresponding D and G peaks labeled are shown in **b)** and **c)**. Note that the position, size, and number of G and D(1-4) peaks vary between the two samples, not as a function of temperature. Shaded regions denote the corresponding areas of each peak, between the modeled curve and the baseline, that are used to calculate the temperature dependent scaled-total area.

To calculate the scaled total area, narrow window of 1000-1800  $\text{cm}^{-1}$ , and a simple linear regression function was used as the baseline (personal communication, N.K. Lünsdorf, 2021) by taking the difference between measured and modeled intensity values and interpolating between them (Fig. 4). This simplified approach avoids erroneous over interpretation of noisy spectra, and yields comparable results to the default settings (Lünsdorf and Lünsdorf, 2016; Lünsdorf et al., 2017) for spectra with a high signal to noise ratio. While selecting a baseline, the spectra is deconvolved into its principal G and D peaks (Fig. 4b,c). This is done iteratively using pseudo-Voigt functions to model the G and D peaks and adding the baseline function, until the composite spectra can be recreated with residuals  $\leq 1\%$ . This iterative curve-fitting process is performed three times for each spot.

Using an empirically-derived calibration curve from Lünsdorf and Lünsdorf (2016), the averaged scaled total area values were used to calculate maximum temperature. Uncertainties typically range from  $\sim 36\text{-}40^\circ\text{C}$  for temperatures calculated for individual spots (Lünsdorf et al., 2017). It is important to note that the particular calibration curve used is not constrained below  $\sim 140^\circ\text{C}$  and instead relies on a linear projection for values in this range. Spectra were accepted if: (1) at least two peaks are visible; (2) all peaks occur entirely within the window (1000-1800  $\text{cm}^{-1}$ ); and (3) no unimodal peaks overprint the D band. Individual calculated temperatures were only accepted if they were  $>0^\circ\text{C}$  and not an outlier by  $>100^\circ\text{C}$ .

### ***Map of maximum temperature and stratigraphic burial depth***

Two contour maps were created showing exhumation magnitude (Fig. 5) and maximum temperature (Fig. 8). To create the exhumation map, the lithology below the sub-Eocene unconformity was identified at 298 locations, including all locations of Rodgers and Janecke (1992) and additional locations on published maps. Minimum exhumation magnitude (km) was

estimated at each point using stratigraphic thicknesses reported on geologic maps and regional stratigraphic columns of pre-Cretaceous strata. A complete list of all locations, exhumation values, and references can be found in the supplementary materials.

The maximum temperature contour map uses results of this study and 149 compiled maximum temperature values, inferred from CAI, Rock-Eval pyrolysis, vitrinite reflectance, and deformation mechanisms that constrain deformation temperatures (Table 1). Compiled data was projected onto the cross section line (Fig. 6) for samples that have the same structural position as RSCM samples of this study (see Table 1). Reported CAI values were converted to maximum temperature and associated uncertainty following the key of Epstein et al. (1977, Fig. 5), which is calibrated by field and laboratory data. Maximum temperatures were calculated from vitrinite reflectance ( $R_o$ ) values using the calibration curve for burial heating of Barker and Pawlewicz (1994, Fig. 1). Maximum temperatures were calculated from Rock-Eval pyrolysis values using the calibration curve of Zdanaviciute and Lazauskiene (2009, Fig. 5). Both contour maps were created in ArcMap 10.6, using the inverse distance weighted toolbox, and trimmed to the area of interest.

## **RESULTS**

Figure 5 shows a map of cumulative exhumation magnitude, modified and updated from Rodgers and Janecke (1992). This exhumation map shows that exhumation along the transect is highly irregular, with large wavelength (~75 km) highs and lows. High exhumation magnitudes (>4-5 km) reflect erosion (inferred to be Cretaceous in age) of the Lemhi arch and its thick outboard rift succession that constitutes the largest wavelength folds of the Idaho-Montana fold thrust belt. Importantly, the areas with the highest exhumation magnitudes do not correspond with mapped thrusts at the surface as expected for a simple, wedge-shaped orogenic belt.

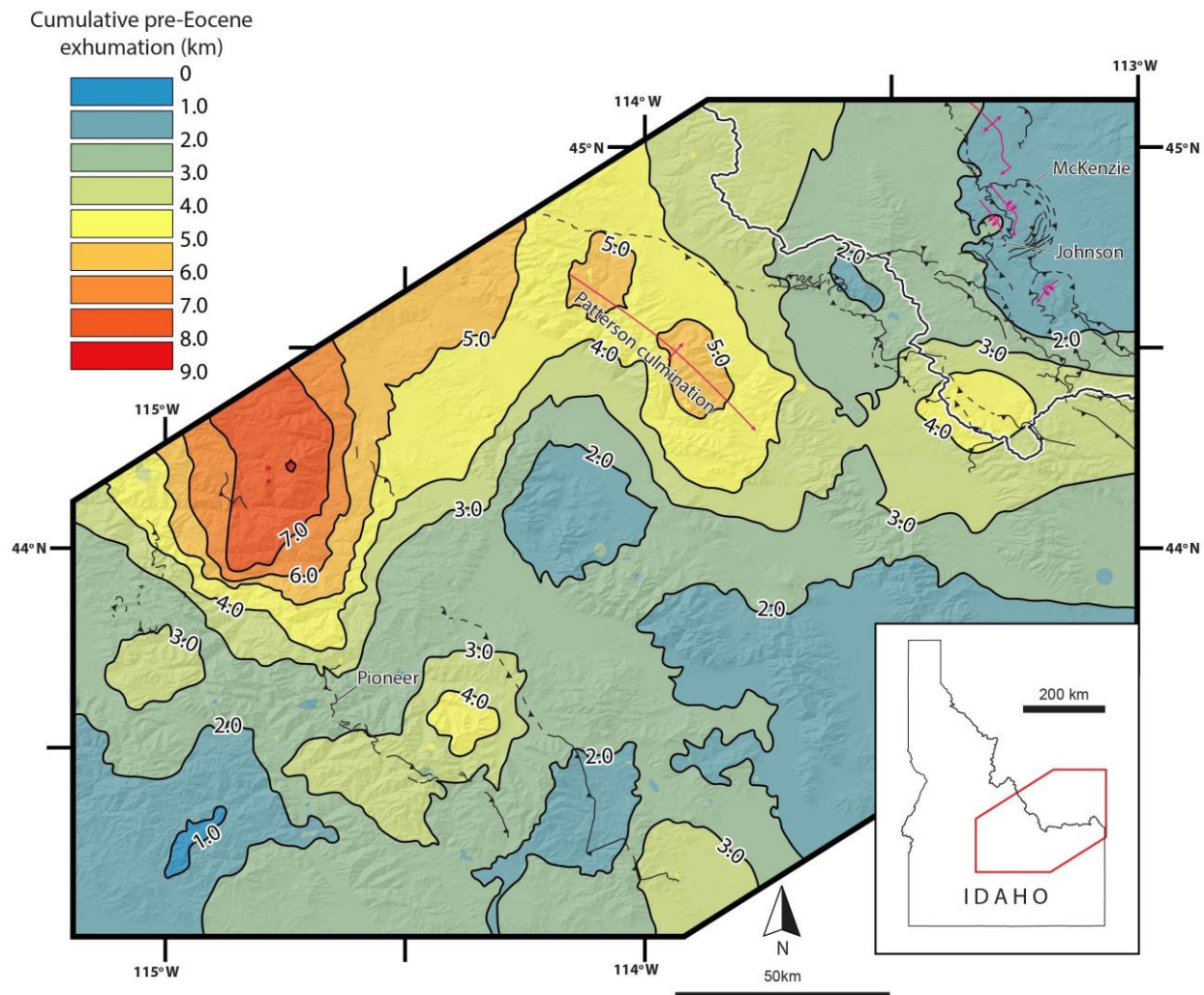


Figure 5. Contour map of cumulative exhumation magnitude below the Eocene Challis Volcanic Group unconformity, modified from paleogeologic map of Rodgers and Janecke (1992). Major thrusts and folds from Fig. 3 are overlain.

Thirty-two of the forty-two RSCM samples yielded acceptable maximum temperatures (Table 2; Fig. 3). Fig. 6 shows the results projected on a line extending beyond the regional cross section, restored for Cenozoic normal faulting, shown in Fig. 7 (Parker and Pearson, in prep). The inset in Fig. 7 shows the results in their approximate stratigraphic position. The maximum temperature reported for each sample is a weighted mean of all accepted spot values (n), not including their individual 36-40°C (mean of 36.8°C) uncertainties. Propagated 2 $\sigma$  uncertainty

values (internal and external) are reported for maximum temperature values of individual samples. Calculated maximum temperatures and uncertainties, as well as measured Raman shift ( $\text{cm}^{-1}$ ) and associated intensity values and curve-fitting model results, for individual spots are reported in the supplementary material ( ).

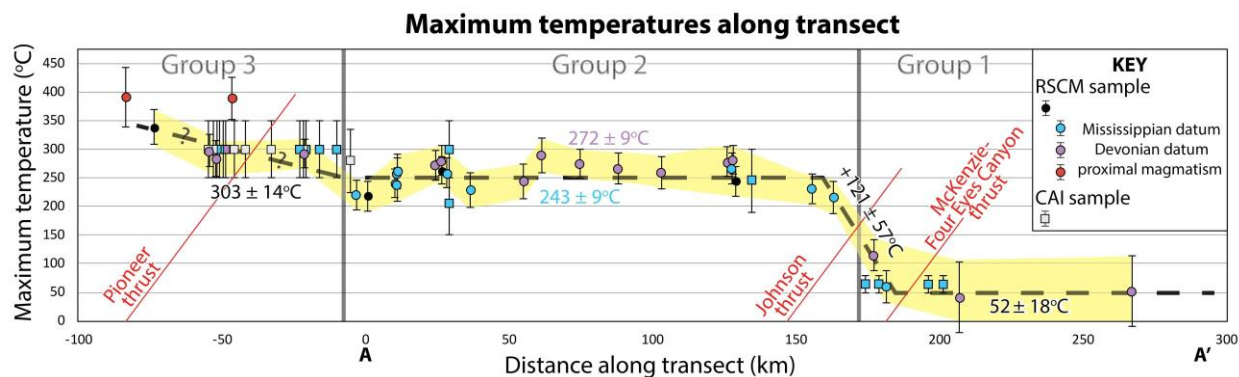


Figure 6. Maximum temperature results and  $2\sigma$  uncertainties from RSCM and compiled CAI data (Table 1; Harris et al., 1980; Perry et al., 1983; Anastasio et al., 2004), projected along cross section (see Fig. 3). Key thrusts that cross the transect are shown in red and discussed in the text. The yellow field denotes the uncertainty envelope of the RSCM samples. The black dashed line approximates the best fit of the data. The data is split into three groups, discussed in the text. Labeled values report the calculated mean of each group and are color coded to the key.

The temperature results (Fig. 6) delineate three internally consistent groups, which we describe from the foreland (northeast) to the hinterland (southwest). The first group contains the lowest temperature samples, from the Ruby Range and Blacktail and Tendoy Mountains of Montana, which give a weighted mean maximum temperature of  $52 \pm 18^\circ\text{C}$ . Though this value is below the sensitivity of our calibration curve ( $\sim 140^\circ\text{C}$ ), it is within the range measurable by RSCM (e.g., Rahl, et al., 2005; Schito et al., 2017; Muirhead et al., 2019). Available CAI values of 1 suggest a comparable maximum temperature of  $\sim 65 \pm 15^\circ\text{C}$  nearest to the Mississippian datum (Perry et al., 1983). Samples 8-10 have weighted mean temperatures of  $52 \pm 61^\circ\text{C}$  ( $n=6$ ),

$42 \pm 62^\circ\text{C}$  (n=3), and  $60 \pm 29^\circ\text{C}$  (n=16). Sample 11 gives a higher result of  $115 \pm 27^\circ\text{C}$  (n=18).

The samples nearest to the Devonian datum (8, 9, 11) overlap within uncertainty with the sample nearest to the Mississippian datum (10) (Fig. 6), demonstrating that rocks of group 1 were all heated to comparably low temperatures.

Group 2 samples show a uniform maximum temperature across a >160 km region, giving a weighted mean of  $243 \pm 9^\circ\text{C}$  for the Mississippian datum and  $272 \pm 9^\circ\text{C}$  for the Devonian datum. A sharp increase in maximum temperatures occurs in the Tendoy Mountains (Fig. 6), defining the boundary between sample groups 1 and 2. Between samples 10/11 and 12 (Fig. 3), maximum temperatures increase by at least  $\sim 60^\circ\text{C}$  and perhaps as much as  $\sim 180^\circ\text{C}$  over a distance of <15 km at the same stratigraphic horizon but across the Johnson thrust (Fig. 7). Two Mississippian samples from the Tendoy Mountains (12, and 13) have weighted mean maximum temperatures of  $231 \pm 26^\circ\text{C}$  (n=17), and  $216 \pm 29^\circ\text{C}$  (n=18) respectively. Four samples from the central Beaverhead Mountains near the Idaho-Montana border were collected in the context of recently published mapping at the 1:24,000 scale (Parker and Pearson, 2020). These samples (7, 3, 5, and 6) have weighted mean maximum temperatures of  $281 \pm 25^\circ\text{C}$  (n=17),  $278 \pm 26^\circ\text{C}$  (n=18),  $267 \pm 27^\circ\text{C}$  (n=18), and  $244 \pm 25^\circ\text{C}$  (n=18) respectively. These samples span from precisely at the Devonian datum to hundreds of meters above the Mississippian datum, suggesting a general upsection decrease in temperature, although the calculated temperatures overlap within uncertainty, giving a weighted mean of  $267 \pm 13^\circ\text{C}$ . This interpretation is consistent with a local CAI value of 4 (Perry et al., 1983) that suggests a maximum temperature of  $\sim 245 \pm 55^\circ\text{C}$  nearest to the Mississippian datum.

Five samples from the Lemhi Range and Donkey Hills of east-central Idaho (Fig. 3) follow the Devonian datum >30 km across the regional-scale anticlinorium of the Patterson

culmination (Fig. 7). These samples (15, 14, 16, 17, and 18) have weighted mean maximum temperatures of  $260 \pm 28^\circ\text{C}$  (n=17),  $267 \pm 27^\circ\text{C}$  (n=15),  $275 \pm 25^\circ\text{C}$  (n=18),  $290 \pm 30^\circ\text{C}$  (n=16), and  $244 \pm 30^\circ\text{C}$  (n=18) respectively. All of these values overlap within uncertainty, giving a weighted mean of  $267 \pm 12^\circ\text{C}$ . The final eleven samples from group 2 come from the folded Devonian and Mississippian sections in the Lost River Range and White Knob Mountains of Idaho. These samples (19, 1, 2, 28, 20, 35, 34, 32, 33, 4, and 30) have weighted mean maximum temperatures of  $229 \pm 31^\circ\text{C}$  (n=19),  $259 \pm 26^\circ\text{C}$  (n=16),  $280 \pm 26^\circ\text{C}$  (n=17),  $273 \pm 26^\circ\text{C}$  (n=17),  $263 \pm 24^\circ\text{C}$  (n=18),  $263 \pm 28^\circ\text{C}$  (n=18),  $239 \pm 29^\circ\text{C}$  (n=18),  $258 \pm 27^\circ\text{C}$  (n=18),  $241 \pm 25^\circ\text{C}$  (n=18),  $218 \pm 26^\circ\text{C}$  (n=18), and  $221 \pm 26^\circ\text{C}$  (n=18) respectively. Of the samples with stratigraphic control, 2 samples near the Devonian datum overlap and give a weighted mean of  $277 \pm 18^\circ\text{C}$ , whereas seven samples near the Mississippian datum overlap and give a weighted mean of  $244 \pm 10^\circ\text{C}$ . These values agree with a local CAI of 5 (Harris et al., 1980) that suggests maximum temperatures of  $\sim 300 \pm 50^\circ\text{C}$ . Temperatures calculated from illite crystallinity and deformation lamellae in calcite also suggest temperatures ranging from  $\sim 200\text{-}300^\circ\text{C}$  (Anastasio et al., 2004).

The third group contains six samples from the Pioneer and Boulder Mountains of central Idaho (not shown on Fig. 7) that give a weighted mean of  $303 \pm 14^\circ\text{C}$ , when two outliers are excluded. This value is consistent with fifteen CAI samples with values of 5 that suggest maximum temperatures of  $\sim 300 \pm 50^\circ\text{C}$  (Harris et al., 1980). Stratigraphic context is not as robust for most of these samples, which may explain some of the differences from groups 2 and 3. Four samples from group 3 (29, 23, 25, and 26) have weighted mean maximum temperatures of  $292 \pm 25^\circ\text{C}$  (n=18),  $284 \pm 31^\circ\text{C}$  (n=14),  $298 \pm 29^\circ\text{C}$  (n=18), and  $339 \pm 31^\circ\text{C}$  (n=17) respectively. These samples come from Devonian, and Pennsylvanian-Permian formations,

respectively. Two additional outliers (22 and 27) are mostly distinct from this sub-population with weighted mean maximum temperatures of  $390 \pm 37^\circ\text{C}$  (n=18), and  $392 \pm 52^\circ\text{C}$  (n=4). Both of these outliers are within  $\sim 500$  m of mapped intrusive bodies.

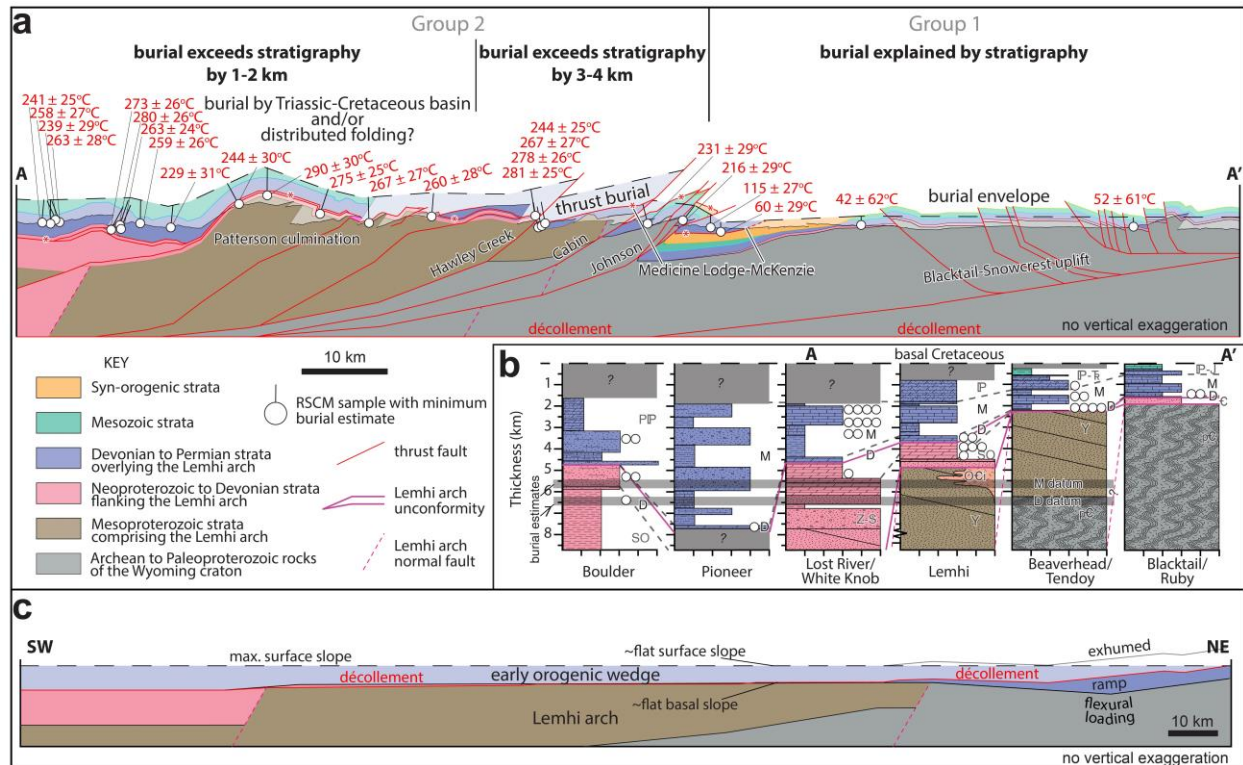


Figure 7. Structural and stratigraphic interpretations of the temperature data. **a**) Simplified cross section of (Parker and Pearson, in prep), restored to remove Cenozoic normal faulting (omitted), with projected samples and interpreted minimum burial estimates shown for Groups 1 and 2 (Fig. 6). Dashed line above cross section shows the hypothesized maximum burial envelope. Red asterisks show correlative regional décollement of Parker and Pearson (2021). **b**) Stratigraphic context of samples for various ranges, shown in Fig. 3, with preserved thicknesses of strata below the basal Cretaceous. Solid pink lines show positions of the intra-Devonian and sub-Ordovician Lemhi arch unconformities. Burial estimates and uncertainty are shown for the Mississippian and Devonian datum. **c**) Hypothesized wedge geometry at ca. 90 Ma. Basal detachment is shown in red.

## DISCUSSION

### Geothermal gradient and burial estimates across the region

Using data from multiple independent paleothermometers (RSCM, CAI, and  $R_o$ ), we document an abrupt increase in maximum temperature across the Johnson thrust (thrust D of Dubois, 1982) and uniform maximum temperatures within much of the Idaho-Montana fold-thrust belt (Fig. 6, 8); this suggests that significant and approximately uniform burial occurred across much of the Idaho-Montana fold thrust belt, with an abrupt front occurring across the Johnson thrust in the Tendoy Mountains. The RSCM results replicate results from CAI and  $R_o$  data, suggesting that the recorded temperatures are reasonable. Available low-temperature thermochronologic data (zircon (U-Th)/He, closure temperatures  $\sim 180^\circ\text{C}$ ; Guenther et al., 2013) are generally reset for samples southwest of the Tendoy Mountains (e.g., Hansen and Pearson, 2016; Fayon et al., 2017; Kaempfer et al., 2019), but not for samples within the Montana foreland to the northeast (e.g., Carrapa et al., 2019; Kaempfer et al., in review; Ronemus, 2021). This and the internal consistency of the RSCM and CAI data suggests that the calculated maximum temperatures are accurate. Fluid flow and deformation likely had a negligible impact on our results because our sampling strategy avoided highly veined or deformed units. It is likely that the two highest temperature samples, (22 and 27) which are outliers at  $\sim 390^\circ\text{C}$ , were heated by local magmatism. Magmatic heating has been shown to affect RSCM samples over fairly short distances of  $\sim 0.5$  km (e.g., Süssenberger et al., 2020). Finally, two spectra (samples 1 and 2) were analyzed using a more widely adopted method (Rahl et al., 2005) but yielded the same result, suggesting that the automated IFORs methodology yields accurate and reproducible results (Lünsdorf et al., 2017). For these reasons, we argue that the regional trend of elevated temperatures between  $\sim 250^\circ\text{C}$  and  $300^\circ\text{C}$  for carbonates above the Lemhi arch is robust.

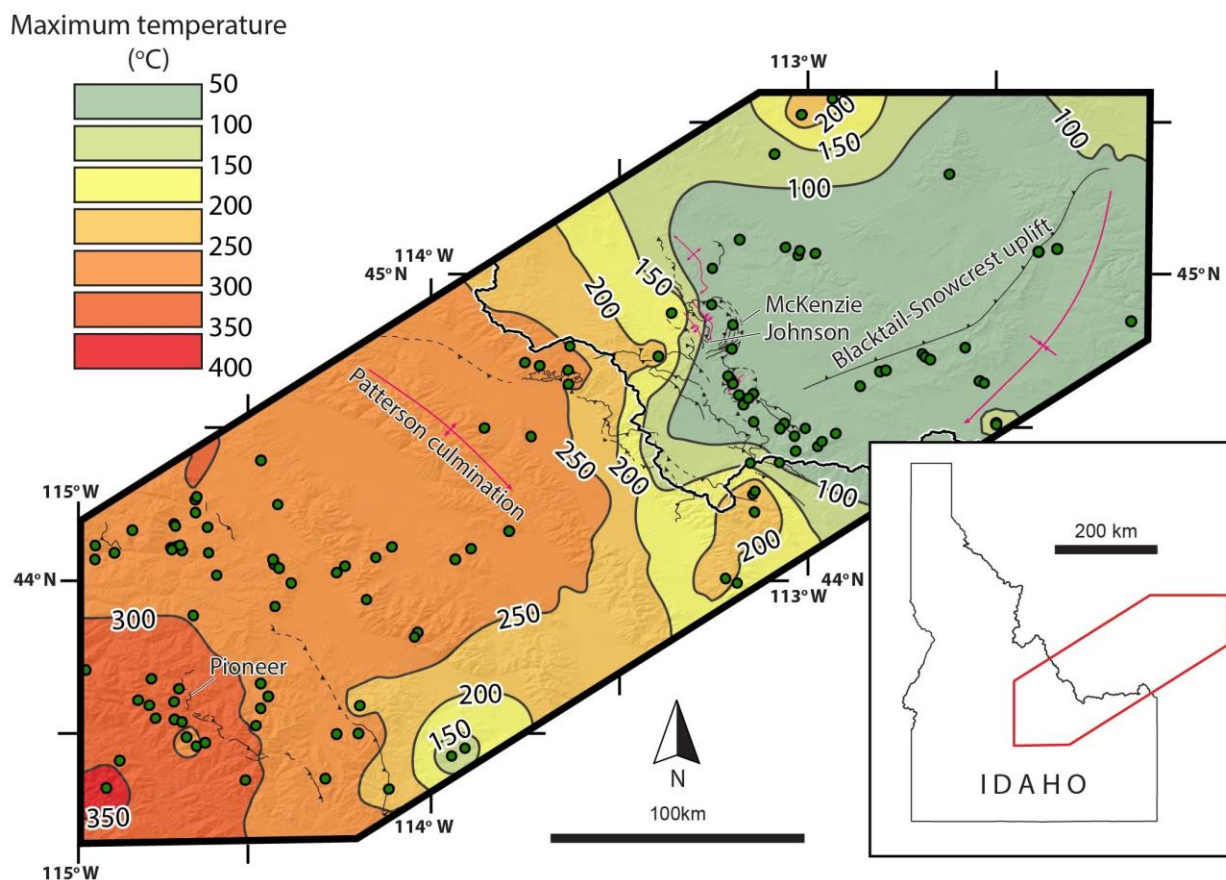


Figure 8. Contour map of maximum temperatures in strata above the Lemhi arch, from RSCM results of this study and CAI data compiled from the literature (green dots show data points). Major thrusts and folds from Fig. 3 are overlaid, with key thrusts of Fig. 6 labeled.

In order to infer burial depth from calculated maximum temperatures, the associated geothermal gradient must be known. Foreland basins typically have low geothermal gradients ( $\sim 22^{\circ}\text{C}/\text{km}$ ; Allen and Allen, 1990). However, rather than assume a geothermal gradient to calculate burial depth, there are several localities along our transect where we can independently constrain maximum geothermal gradients by comparing maximum temperatures over a known vertical distance. Samples from the central Beaverhead Mountains and Lost River Range cover  $\geq 1$  km of section over short map distances (Fig. 7), thereby offering some constraints regarding the maximum permissible geothermal gradient. In the central Beaverhead Mountains,

temperatures range from 244°C ( $\pm 25$ ) to 281°C ( $\pm 27$ ) over a stratigraphic distance of  $\sim 1$  km, suggesting a maximum geothermal gradient of  $\sim 35$ -40°C/km. Two samples from a vertical transect on Lost River Peak have temperatures of 259°C and 280°C ( $\pm 26$ ) over a stratigraphic distance of  $\sim 750$  m, suggesting a geothermal gradient of  $\sim 30$ °C/km. Most Mississippian and Devonian samples overlap within uncertainty (Fig. 6), suggesting that a geothermal gradient of  $\sim 30$ -40°C/km is reasonable.

In order to make conservative maximum burial estimates, we assume a high but reasonable geothermal gradient of  $\sim 40$ °C/km and a mean surface temperature of  $\sim 10$ °C (e.g., Wilf et al., 2003). The mean maximum temperatures are regionally consistent for all the Mississippian (243°C  $\pm 9$ ) and Devonian (272°C  $\pm 9$ ) samples respectively, giving burial estimates of 5.6 km ( $\pm 0.2$ ) and 6.4 km ( $\pm 0.2$ ). Burial estimates for group 2 samples range from 4.5 km ( $\pm 0.7$ ) to 6.3 km ( $\pm 0.8$ ), much more than the preserved stratigraphic thicknesses on top of the Lemhi arch which range from  $\sim 2.5$  - 4.5 km (Fig. 7; Parker and Pearson, 2021). The discrepancy between estimated burial depths and observed maximum temperatures is most pronounced in the central Beaverhead Mountains (Fig. 7), where burial estimates of at least 5.3 km ( $\pm 0.6$ ) for Pennsylvanian strata and 6.1 km ( $\pm 0.7$ ) for Devonian strata exceed the observed stratigraphic thickness by at least  $\sim 2$ -3.5 km. Even in the thicker section outboard of the Lemhi arch, burial estimates exceed stratigraphic thickness by at least 1 or 2 kilometers (Fig. 7). Only a few samples in the Pioneer and Boulder Mountains have calculated temperatures that may be explained by stratigraphic burial alone, due to thick localized basin development and exhumation during the Antler and Ancestral Rocky Mountain orogenies (Mahoney et al., 1991; Link et al., 1996, 2014; Geslin, 1998; Beranek et al., 2016). Thus, the Lemhi arch was apparently buried 1.5-4.0 km

deeper than the accounted for stratigraphic depths, meaning that the samples must have been buried by strata or thrusts that are now eroded.

### **Regional burial during early (pre-90 Ma) thrusting**

In order to investigate potential causes of burial of the Lemhi arch, relative timing must be constrained by comparing observed maximum temperatures in rocks with younger deformation features. While the maximum temperatures observed across the region are consistent (Fig. 8), they do not correlate with the pattern of cumulative pre-Eocene exhumation (Fig. 5; Rodgers and Janecke, 1992), suggesting that burial preceded much of the pre-Eocene exhumation and is not related to late-stage folding or faulting. The presence of carbonate mylonite in the thin-skinned Thompson Gulch thrust, which is crosscut by the thick-skinned Baby Joe Gulch thrust, requires that the host rocks were hotter than the threshold for carbonate plasticity ( $> \sim 250^{\circ}\text{C}$ ) during slip on the Thompson Gulch thrust and before slip along the Baby Joe Gulch thrust (Parker and Pearson, 2021). Like for the Baby Joe Gulch thrust, maximum temperatures are shifted across the Johnson thrust, demonstrating that maximum burial predates this thrust as well (Fig. 6, 7). Similarly, Devonian samples above the Patterson culmination give overlapping temperature estimates with a mean of  $267^{\circ}\text{C} \pm 15$ , despite over 3 km of structural relief (Fig. 7), demonstrating they were achieved before uplift of the Lemhi arch. The regionally consistent maximum temperatures, in all but the samples from the hanging wall of the McKenzie and Four Eyes Canyon thrusts, require consistent burial and subsequent exhumation of the Lemhi arch (Fig. 7). Therefore maximum temperatures must have occurred during the early phase of shortening and before late stage folding, faulting, uplift, and exhumation of the Lemhi arch.

The absolute age of burial heating during the early phase of shortening can be constrained using available maximum depositional ages in the adjacent foreland basin and low-temperature

thermochronologic data from the hanging walls of regional thrusts. Crustal thickening in the arc and fore arc from ca. 140 to 90 Ma (McKay et al., 2017; Braudy et al., 2017; Montz and Kruckenberg, 2017) and detrital zircons in the foreland matching Cambrian to Mississippian sources from west of the Lemhi arch (Rosenblume et al., 2021; Gardner et al., in prep; Rosenblume et al., in prep.), demonstrate that the Idaho-Montana fold-thrust belt was already well developed by mid-Early Cretaceous time. Specifically, maximum depositional ages and provenance studies for the Kootenai Formation, the oldest definitive foredeep deposit in the study area, demonstrate that shortening and exhumation down to lower Paleozoic levels occurred in the adjacent fold-thrust belt by ca. 145 Ma (Finzel and Rosenblume, 2021; Rosenblume et al., 2021). However, age constraints on regional-scale thrusts of the Idaho-Montana fold-thrust belt are nearly entirely < 90 Ma, more than 45 m.y. younger than the Kootenai Formation (Finzel and Rosenblume, 2021; Rosenblume et al. 2021). Zircon (U-Th)/He thermochronologic data suggest that the Lemhi arch was cooled below  $\sim 180^{\circ}\text{C}$  at  $\sim 87$  Ma for the Patterson culmination (Fayon et al., 2017) and  $\sim 68$  Ma for the Poison Creek (Hansen and Pearson, 2016) and Hawley Creek thrusts (Kaempfer et al., in prep), bracketing the youngest possible age of burial heating. This age range agrees with provenance studies that suggest that strata of the Lemhi sub basin, which make up the Lemhi arch, were not a sediment source to the foreland basin until during deposition of the Frontier Formation at  $\sim 90$ -85 Ma (Rosenblume et al., in prep). Further, 500 Ma zircons that are unique to the Beaverhead plutonic belt that is exposed in the hanging wall of the Baby Joe Gulch-Hawley Creek thrust system first appeared in the Beaverhead Group at  $\sim 67$  Ma (Garber et al., 2020). Maximum burial must have occurred prior to these exhumation ages. It is possible that burial was progressive over as much as 65 m.y., from  $\sim 145$  to 70 Ma. Therefore, maximum burial of the Lemhi arch occurred after  $\sim 145$  and prior to  $\sim 90$ -70 Ma.

Restoring the late-stage faults and folds that disrupt the observed maximum temperature pattern allows us to describe the geometry of the early-stage burial envelope and make reasonable hypotheses regarding the geometry of the eroded orogenic wedge. Restoring the Johnson thrust (Thrust D of DuBois, 1982) so that the Lemhi arch unconformity is continuous results in >4 km of burial difference between the samples, enough to account for the observed ~160°C temperature difference between groups 1 and 2, assuming a reasonable geothermal gradient of ~40°C/km. In other words, the sharp maximum temperature increase of 121°C ( $\pm 57$ ) over a distance of < 15 km is likely a product of late-stage faulting on the Johnson thrust that juxtaposed different structural levels. The geometry during early deformation can be visualized by following the stars on Fig. 5, shown along the Medicine Lodge-McKenzie thrust system, which form a continuous décollement when faults and folds of the Lemhi arch are restored. The initially continuous wedge of the Medicine Lodge-McKenzie thrust system was folded, faulted, uplifted, and exhumed by more deeply detached thick-skinned thrusts, such as the Hawley Creek and Johnson thrusts. This interpretation is consistent with correlative hanging wall and footwall stratigraphy in the Medicine Lodge and McKenzie (and Four Eyes Canyon) thrusts (e.g., Perry et al., 1988; Skipp, 1988a). Samples in the central Beaverhead Mountains come from the same structural position, within the footwall of the Thompson Gulch thrust, which links the flat décollement near the intra-Devonian unconformity in the Lemhi Range to the footwall ramp of the Medicine Lodge thrust (Parker and Pearson, in prep.). Samples farther to the southwest, from the Lemhi and Lost River ranges, come from just above and below this flat regional décollement (White Knob fold belt of Hait, 1965; Beutner, 1968). Laying flat isotherms and a 40°C/km geothermal gradient on this geometry recreates the observed temperatures (Fig. 7c). In summary, restoration of late-stage thrust faults and folds highlights the décollement geometry of the

Medicine Lodge-McKenzie thrust system, with a regional flat near the intra-Devonian unconformity of the Lemhi arch at ~ 6.5 km depth and a frontal ramp between the Beaverhead and Tendoy Mountains.

Consistent burial of the Lemhi arch across the region during the early phase of deformation (prior to ~90-70 Ma) may be explained by several mechanisms. A now completely eroded (“phantom;” Royse, 1993) Early Cretaceous basin is one possible hypothesis because rocks of this age are not preserved, and therefore have an unknown thickness. However, the observed temperatures and thicknesses require that the hypothesized basin must thicken from ~1.5 to 4.0 km deep between the Lost River Range and Beaverhead Mountains. This apparent basin geometry is inconsistent with predictions of a “phantom foredeep” (Royse, 1993) because accommodation in foredeep basins is expected to increase toward the hinterland, due to flexure adjacent to thrust loading (e.g., DeCelles, 2012). A hinterland (or wedge-top) basin is a more permissible hypothesis due to the wide and nearly uniform shape of the burial envelope, as is expected above a weak décollement (e.g., Simpson, 2010). This hypothesis predicts exhumation and recycling into adjacent foreland basin deposits prior to ~90-70 Ma. Potential evidence of this may be recorded in the upper Blackleaf Formation, which was flooded with detritus from recycled Permian and Triassic strata and Cretaceous arc detritus at ca. 105-100 Ma (Gardner, 2021). A “phantom” hinterland basin is one permissible hypothesis for the cause of burial heating in the study area that may be testable with ongoing provenance studies in the foreland basin system.

Distributed folding and faulting at high structural levels (Pennsylvanian or younger) is a simpler and more testable hypothesis for the cause of burial because independent evidence exists for this. Evidence of crustal thickening and erosion at high structural levels is found in the

provenance of the upper Blackleaf Formation, which suggests upper Paleozoic and Triassic sources from central Idaho at ca. 110-100 Ma (Gardner, 2021; Rosenblume et al., in prep.). Doubling the thickness of the section by thrust burial simply explains the observed maximum temperatures of samples in the footwalls of the Thompson Gulch and Medicine Lodge thrusts, which we hypothesize represent the décollement of the early fold-thrust belt (Parker and Pearson, 2021). Therefore, another permissible hypothesis is that thrusting/folding above a flat décollement overlying the Lemhi arch and thrusting above the leading footwall ramp buried the samples to their observed maximum temperatures sometime between ~ 145 and 70 Ma. Both hypotheses interpret early thrusting as the indirect or direct cause of burial and heating.

### **Thin stratigraphy promotes reorganization of the orogenic wedge**

A combination of burial by folding, thrusting, and/or deposition is a simple explanation for the observed temperature anomaly. Relative timing constraints suggest that this burial predated Late Cretaceous thick-skinned thrusting. Thus, burial is thought to have occurred during earlier thin-skinned thrusting above the Lemhi arch unconformity, which had a shallow basal décollement; this implies an initial low-angle wedge geometry above the low-relief Lemhi arch basement high. Because the thickness of the wedge apparently mimicked the low-relief unconformity that draped the Lemhi arch and acted as the décollement (Fig. 7c), this suggests a causal relationship between pre-thrusting stratigraphy and the resulting low-taper fold-thrust belt. In order to thicken the wedge and increase the taper angle toward its critical taper value required for further growth of the orogenic wedge, a step-down of the basal décollement into the Lemhi arch provided an alternative way to increase wedge taper. In other words, deformation above the flat décollement following the top of the Lemhi arch apparently was not capable of increasing the taper angle for self-similar propagation of the wedge.

Our results suggest there was a consistent limit to the thickness of the wedge that could be constructed above the flat-lying Lemhi arch, adding independent support for the double-decker model of Parker and Pearson (2021). In other words, the switch from early thin-skinned thrusting and burial of the Lemhi arch to exhumation by thick-skinned thrusts within it must have everywhere occurred once the Lemhi arch unconformity was at a depth of ~6.5 km. This model is appealing from a regional standpoint because it identifies the structure that accommodated the undocumented Early Cretaceous shortening in the Idaho-Montana fold-thrust belt: a décollement that followed the intra-Devonian Lemhi arch unconformity (i.e., Medicine Lodge-McKenzie thrust system). This model also suggests that thin stratigraphy overlying a basement high limited the dimensions of the wedge by not only determining the path of the basal décollement, but also by setting the threshold at which the stress state of the wedge could no longer be balanced without establishing a new décollement in the mechanical basement. In other words, thin-skinned thrusting in the thin passive margin stratigraphy accommodated its maximum amount of shortening, before the décollement stepped down and began accommodating shortening in a more thick-skinned style.

An implication of this study is that the availability of potential décollements, in the form of weak sedimentary cover rocks, may fundamentally limit the ability of an orogenic wedge to grow in two related ways: (1) by determining the maximum allowable surface slope that can be built above a particular décollement, and (2) by determining when and where the basal décollement must migrate in order to increase the taper angle by increasing the basal slope. The transition we describe from a low-relief wedge detached in the upper crust that buries a basement high, to a higher-relief wedge detached in the middle crust that exhumes the basement high and former orogenic wedge is similar to recent models proposed by Lacombe and Bellahsen (2016)

and Tavani et al. (2021). This study demonstrates not only that RSCM and other paleothermometers are useful tools for documenting and investigating switches from early burial to late exhumation phases in orogenic wedges, but also that the thicknesses of sedimentary cover rocks may be a more important factor than is presently recognized (Lacombe and Bellahsen, 2016; Lescoutre and Manatschal, 2020; Tavani et al., 2021). Thin preexisting stratigraphy may control the growth of an orogenic wedge by essentially dampening the ability of the surface slope to increase, thereby prompting a deeper basal décollement to activate in order to balance the stress. Continued investigations using palaeothermometry in the shallow crust may be an effective way to investigate how the mere presence or absence of sedimentary cover rocks may set this threshold, setting the stage for behavior of future growing orogenic wedges.

## CONCLUSIONS

Raman spectroscopy of carbonaceous material (RSCM) of samples collected over a more than 350 km wide transect of the Idaho-Montana fold-thrust belt yields a low-relief maximum temperature profile (at ca. 145-70 Ma) averaging  $\sim 254^{\circ}\text{C}$  ( $\pm 22$ ), over the  $\sim 160$  km wide Lemhi arch basement high. Elevated temperatures are higher than can be explained by stratigraphic burial alone. Observed temperatures constrain a maximum geothermal gradient of  $\sim 30\text{-}40^{\circ}\text{C}/\text{km}$ , suggesting at least an additional 1.5-4.0 kilometers of burial must have occurred between  $\sim 145$  and 90-70 Ma. Burial was most likely caused by a combination of distributed folding, thrust faulting, and possibly deposition, with a décollement just above the uppermost Lemhi arch unconformity. This early orogenic wedge is inferred to have had a low taper angle, mimicking the geometry of the Lemhi arch basement high that hosted the décollement. After being buried to  $\sim 6.5$  km, the décollement was abandoned for a deeper one, resulting in the observed cumulative exhumation patterns. Folding, faulting, and exhumation of the early low-relief wedge and the

underlying Lemhi arch led to the disparity between the variable cumulative exhumation magnitudes inferred from the sub-Eocene unconformity and the consistent maximum temperatures recorded in the rocks above the Lemhi arch.

Our results suggest that orogenic wedges formed in thin stratigraphic cover rocks may be subject to dynamic reorganization as décollements are forced to migrate beneath the former wedge in order to achieve a critical taper angle. The thickness of the preexisting strata may limit the maximum possible thickness and surface slope of the wedge, requiring activation of a new décollement in order to increase the taper angle of the system. Thermal profiles of fold-thrust belts may be particularly useful for documenting such self-organized wedge reorganizations and investigating how the distribution of weak stratigraphic layers in the upper crust may set thresholds that govern the growth of orogenic wedges.

#### **DATA AVAILABILITY**

Data supporting the results of this study can be found in the manuscript text, the supplemental materials file, and publications referenced in the text.

#### **CONFLICTS OF INTEREST**

The authors declare that they have no conflicts of interest.

#### **ACKNOWLEDGEMENTS**

This study represents a portion of SP's PhD dissertation. We thank Chase Porter for collecting some samples in the western part of the transect as well as Eric Elliston, Alexis Ault, Kelly Bradbury, Tyler Paladino, and Keno Lünsdorf for their assistance during data collection and processing. Funding for this research was provided by Geological Society of America graduate student research grant, Tobacco Root Geological Society field scholarship, an Idaho

State University Center for Ecological Research and Education grant to SP, and NSF-Tectonics EAR-1728563 to DP.

### **SUPPLEMENTARY MATERIAL**

<sup>1</sup>GSA Data Repository item 201Xxxx, which includes raw Raman data, deconvolved spectra models, and calculated maximum temperatures for each spot, is available online at [www.geosociety.org/pubs/ft20XX.htm](http://www.geosociety.org/pubs/ft20XX.htm), or on request from [editing@geosociety.org](mailto:editing@geosociety.org).

### **REFERENCES CITED**

- Allen, P.A., and Allen, J.R., 1990, Basin Analysis, Principles and Applications: Oxford, Blackwell Scientific Publications.
- Allmendinger, R.W., and Gubbels, T., 1996, Pure and simple shear plateau uplift, Altiplano-Puna, Argentina and Bolivia: Tectonophysics, vol. 259, no. 1-3, p. 1-13, doi:10.1016/0040-1951(96)00024-8.
- Anastasio, D. J., Fisher, D. M., Messina, T. A., and Holl, J. E., 1997, Kinematics of décollement folding in the Lost River Range, Idaho: Journal of Structural Geology, v. 19, no. 3–4, p. 355–368, doi:10.1016/S0191-8141(97)83028-3.
- Anastasio, D.J., Bebout, G.E. and Holl, J.E., 2004, Extra-basinal fluid infiltration, mass transfer, and volume strain during folding: Insights from the Idaho-Montana thrust belt: American Journal of Science, v. 304, no. 4, p. 333-369, doi:10.2475/ajs.304.4.333.
- Anderson, R.B., Long, S.P., Horton, B.K., Thomson, S.N., Calle, A.Z. and Stockli, D.F., 2018, Orogenic wedge evolution of the central Andes, Bolivia (21 S): Implications for Cordilleran cyclicity: Tectonics, v. 37, no. 10, p. 3577-3609, doi:10.1029/2018TC005132.
- Anderson, R.B., Long, S.P., Horton, B.K., Calle, A.Z. and Soignard, E., 2021, Late Paleozoic

- Gondwanide deformation in the Central Andes: Insights from RSCM thermometry and thermal modeling, southern Bolivia: *Gondwana Research*, vol. 94, p. 222-242, doi:10.1016/j.gr.2021.03.002.
- Armstrong, R. L., 1968, Sevier orogenic belt in Nevada and Utah: *Geological Society of America Bulletin*, v. 79, no. 4, p. 429-458, doi:10.1130/0016-7606(1968)79[429:SOBINA]2.0.CO;2.
- Bally, A. W., Gordy, P. L., and Stewart, G. A., 1966, Structure, seismic data, and orogenic evolution of southern Canadian Rocky Mountains: *Bulletin of Canadian Petroleum Geology*, vol. 14, no. 3, p. 337-381, doi:10.35767/gscpgbull.14.3.337.
- Barker, C.E., and Pawlewicz, M.J., 1994, Calculation of Vitrinite Reflectance from Thermal Histories and Peak Temperatures: A comparison of methods, *in* Mukhopadhyay, P.K., and Dow, W.G., eds., *Vitrinite Reflectance as a Maturity Parameter: Applications and Limitations*, American Chemical Society, Symposium Series, vol. 570, p. 216–229.
- Beranek, L.P., Link, P.K. and Fanning, C.M., 2016, Detrital zircon record of mid-Paleozoic convergent margin activity in the northern US Rocky Mountains: Implications for the Antler orogeny and early evolution of the North American Cordillera: *Lithosphere*, vol. 8, no. 5, p. 533-550, doi:10.1130/L557.1.
- Best, M.G., Barr, D.L., Christiansen, E.H., Gromme, S., Deino, A.L. and Tingey, D.G., 2009, The Great Basin Altiplano during the middle Cenozoic ignimbrite flareup: Insights from volcanic rocks: *International Geology Review*, vol. 51, no. 7-8, p. 589-633, doi:10.1080/00206810902867690.
- Beutner, E. C., 1968, Structure and tectonics of the southern Lemhi Range, Idaho [doctoral dissertation]: State College, Pennsylvania State University, 106 p.

- Beysac, O., Goffé, B., Chopin, C. and Rouzaud, J.N., 2002, Raman spectra of carbonaceous material in metasediments: a new geothermometer: *Journal of Metamorphic Geology*, vol. 20, no. 9, p. 859-871, doi:10.1046/j.1525-1314.2002.00408.x.
- Bollinger, L., Avouac, J.P., Beysac, O., Catlos, E.J., Harrison, T.M., Grove, M., Goffé, B. and Sapkota, S., 2004, Thermal structure and exhumation history of the Lesser Himalaya in central Nepal: *Tectonics*, vol. 23, no. 5, doi:10.1029/2003TC001564.
- Boyer, S.E., 1995, Sedimentary basin taper as a factor controlling the geometry and advance of thrust belts: *American Journal of Science*, vol. 295, no. 10, p. 1220-1254, doi:10.2475/ajs.295.10.1220.
- Braudy, N., Gaschnig, R.M., Wilford, D., Vervoort, J.D., Nelson, C.L., Davidson, C., Kahn, M.J. and Tikoff, B., 2017, Timing and deformation conditions of the western Idaho shear zone, West Mountain, west-central Idaho: *Lithosphere*, vol. 9, no. 2, p. 157-183, doi:10.1130/L519.1.
- Brennan, D.T., M. Pearson, D.M., Link, P.K., and Chamberlain K.R., 2020, Neoproterozoic Windermere Supergroup near Bayhorse, Idaho: late-stage Rodinian rifting was deflected west around the Belt basin: *Tectonics*, vol. 39, no. 8, p. 1-27, doi:10.1029/2020TC006145.
- Burchfiel, B.C., and Davis, G.A., 1975, Nature and controls of Cordilleran orogenesis, western United States: Extensions of an earlier synthesis: *American Journal of Science*, vol. 275, no. A, p. 363-396.
- Buseck, P.R. and Beysac, O., 2014, From organic matter to graphite: Graphitization: *Elements*, Vol. 10, no. 6, p. 421-426, doi:10.2113/gselements.10.6.421.
- Carbonell, P.J.T., Dimieri, L.V. and Olivero, E.B., 2011, Progressive deformation of a Coulomb

- thrust wedge: the eastern Fuegian Andes Thrust-Fold Belt: Geological Society, London, Special Publications, vol. 349, no. 1, p. 123-147, doi:10.1144/SP349.7.
- Carrapa, B., DeCelles, P.G. and Romero, M., 2019, Early inception of the Laramide orogeny in southwestern Montana and northern Wyoming: Implications for models of flat-slab subduction: *Journal of Geophysical Research: Solid Earth*, vol. 124, no. 2, p. 2102-2123, doi:10.1029/2018JB016888.
- Chen, S., Moore, A.L., Cai, W., Suk, J.W., An, J., Mishra, C., Amos, C., Magnuson, C.W., Kang, J., Shi, L. and Ruoff, R.S., 2011, Raman measurements of thermal transport in suspended monolayer graphene of variable sizes in vacuum and gaseous environments: *ACS Nano*, vol. 5, no. 1, p. 321-328, doi:10.1021/nn102915x.
- Coney, P.J. and Harms, T.A., 1984, Cordilleran metamorphic core complexes: Cenozoic extensional relics of Mesozoic compression: *Geology*, vol. 12, no. 9, p. 550-554, doi:10.1130/0091-7613(1984)12<550:CMCCCE>2.0.CO;2.
- Coogan, J. C., 1992, Structural evolution of piggyback basins in the Wyoming-Idaho-Utah thrust belt, *in* Link, P.K., Kuntz, M. A., and Platt, L. B., eds., *Regional geology of eastern Idaho and western Wyoming*: Boulder, Colorado, Geological Society of America Memoir, v. 179, p. 55–81, doi:10.1130/MEM179-p55.
- Corrado, S., Gusmeo, T., Schito, A., Alania, V., Enukidze, O., Conventi, E. and Cavazza, W., 2021, Validating far-field deformation styles from the Adjara-Trialeti fold-and-thrust belt to the Greater Caucasus (Georgia) through multi-proxy thermal maturity datasets: *Marine and Petroleum Geology*, p.105141, doi:10.1016/j.marpetgeo.2021.105141.
- Dahlen, F.A., 1990, Critical taper model of fold-and-thrust belts and accretionary wedges:

- Annual Review of Earth and Planetary Sciences, vol. 18, no. 1, p. 55-99.
- Dahlstrom, C. D., 1970, Structural geology in the eastern margin of the Canadian Rocky Mountains: Bulletin of Canadian Petroleum Geology, vol. 18, no. 3, p. 332-406, doi:10.35767/gscpgbull.18.3.332.
- Davis, D., Suppe, J., and Dahlen, F. A., 1983, Mechanics of fold-and-thrust belts and accretionary wedges: Journal of Geophysical Research: Solid Earth, vol. 88, no. B2, p. 1153-1172, doi:10.1029/JB088iB02p01153.
- DeCelles, P.G., 2004, Late Jurassic to Eocene evolution of the Cordilleran thrust belt and foreland basin system, western USA: American Journal of Science, vol. 304, no. 2, p. 105-168, doi:10.2475/ajs.304.2.105.
- DeCelles, P.G., 2012, Foreland basin systems revisited: Variations in response to tectonic settings, *in* Busby, C., and Azor, A., eds., Tectonics of sedimentary basins: Recent advances: Hoboken, New Jersey, Wiley-Blackwell, p. 405-426, doi: 10.1002/9781444347166.
- DeCelles, P.G. and Mitra, G., 1995, History of the Sevier orogenic wedge in terms of critical taper models, northeast Utah and southwest Wyoming: Geological Society of America Bulletin, vol. 107, no. 4, p. 454-462, doi:10.1130/0016-7606(1995)107<0454:HOTSOW>2.3.CO;2.
- DeCelles, P.G., and Coogan, J. C., 2006, Regional structure and kinematic history of the Sevier fold-and-thrust belt, central Utah: Geological Society of America Bulletin, vol. 118, no. 7-8, p. 841-864, doi:10.1130/B25759.1.
- Dickinson, W.R., and Snyder, W. S., 1978, Plate tectonics of the Laramide orogeny, *in* Matthews, V., ed., Laramide folding associated with basement block faulting in the

- western United States: Boulder, Colorado, Geological Society of America Memoir 151, p. 355-366, doi:10.1130/MEM151-p355.
- Dickinson, W.R., 2004, Evolution of the North American cordillera: Annual Review of Earth and Planetary Sciences, vol. 32, p.13-45.
- Dilek, Y. and Moores, E.M., 1999, A Tibetan model for the early Tertiary western United States: Journal of the Geological Society, vol. 156, no. 5, p. 929-941, doi:10.1144/gsjgs.156.5.0929.
- DuBois, D.P., 1982, Tectonic framework of basement thrust terrane, northern Tendency range, southwest Montana, *in* Powers, R.B., ed., Geologic Studies of the Cordilleran Thrust Belt: Denver, Colorado, Rocky Mountain Association of Geologists v. 1, p. 145-156.
- Dyman, T.S., Palacas, J.G., Tysdal, R.G., Perry Jr, W.J. and Pawlewicz, M.J., 1996, Source rock potential of middle cretaceous rocks in southwestern Montana: American Association of Petroleum Geologist bulletin, vol. 80, no. 8, p. 1177-1183, doi:10.1306/64ED8CD2-1724-11D7-8645000102C1865D.
- Epstein, A.G., Epstein, J. B., and Harris, L.D., 1977, Conodont Color Alteration: An index to Organic metamorphism: U.S Geological Survey Professional Paper, vol. 995, 27 p., doi:10.3133/pp995.
- Evenchick, C.A., McMechan, M.E., McNicoll, V.J. and Carr, S.D., 2007, A synthesis of the Jurassic–Cretaceous tectonic evolution of the central and southeastern Canadian Cordillera: Exploring links across the orogeny, *in* Sears, J.W., Harms, T.A, Evenchick, C.A., eds., Whence the Mountains? Inquiries into the Evolution of Orogenic Systems: A Volume in Honor of Raymond A. Price: Boulder, Colorado, Geological Society of America Special Paper 433, p. 117-145, doi:10.1130/2007.2433(06).

- Farley, K.A., 2000, Helium diffusion from apatite: General behavior as illustrated by Durango Fluorapatite: *Journal of Geophysical Research: Solid Earth*, vol. 105, no. B2, p. 2903-2914, doi:10.1029/1999JB900348.
- Fayon, A.K., Tikoff, B., Kahn, M. and Gaschnig, R.M., 2017, Cooling and exhumation of the southern Idaho batholith: *Lithosphere*, vol. 9, no. 2, p. 299-314, doi:10.1130/L565.1.
- Finzel, E.S. and Rosenblume, J.A., 2021, Dating lacustrine carbonate strata with detrital zircon U-Pb geochronology: *Geology*, vol. 49, no. 3, p. 294-298, doi:10.1130/G48070.1.
- Fisher, D.M. and Anastasio, D.J., 1994, Kinematic analysis of a large-scale leading edge fold, Lost River Range, Idaho: *Journal of Structural Geology*, vol. 16, no. 3, p. 337-354, doi:10.1016/0191-8141(94)90039-6.
- Fitz-Diaz, E., Hudleston, P. and Tolson, G., 2011, Comparison of tectonic styles in the Mexican and Canadian Rocky Mountain fold-thrust belt, *in* Poblet, J., Lisle, R.J., eds., *Kinematic Evolution and Structural Styles of Fold-and-Thrust Belts*: London, UK, Geological Society, London, Special Publications 349, p. 149-167, doi:10.1144/SP349.8.
- Flowers, R.M., Ketcham, R.A., Shuster, D.L. and Farley, K.A., 2009, Apatite (U–Th)/He thermochronometry using a radiation damage accumulation and annealing model. *Geochimica et Cosmochimica Acta*, vol. 73, no. 8, p. 2347-2365, doi:10.1016/j.gca.2009.01.015.
- Garber, K. L., Finzel, E. S., and Pearson, D. M., 2020, Provenance of Synorogenic Foreland Basin Strata in Southwestern Montana Requires Revision of Existing Models for Laramide Tectonism: *North American Cordillera: Tectonics*, vol. 39, no. 2, p. 1-26,

doi:10.1029/2019TC005944.

Gentry, A., Yonkee, W.A., Wells, M.L., Balgord, E.A., 2018, Resolving the history of early fault slip and foreland basin evolution along the Wyoming salient of the Sevier fold-and-thrust belt: Integrating detrital zircon geochronology, provenance modeling, and subsidence analysis, *in* Ingersoll, R.V., Lawton, T.F., Graham, S.A., *Tectonics, Sedimentary Basins, and Provenance: A Celebration of the Career of William R. Dickinson*: Boulder, Colorado, Geological Society of America 540, p. 509-545, doi:10.1130/2018.2540(23).

Geslin, J.K., 1998, Distal Ancestral Rocky Mountains tectonism: Evolution of the Pennsylvanian-Permian Oquirrh–Wood River basin, southern Idaho: *Geological Society of America Bulletin*, vol. 110, no. 5, p. 644-663,  
doi:10.1130/0016-7606(1998)110<0644:DARMTE>2.3.CO;2.

Ghiglione, M.C. and Ramos, V.A., 2005, Progression of deformation and sedimentation in the southernmost Andes: *Tectonophysics*, vol. 405, no. 1-4, p. 25-46,  
doi:10.1016/j.tecto.2005.05.004.

Grader, G. W., Isaacson, P. E., Doughty, P. T., Pope, M. C., and Desantis, M. K., 2017, Idaho Lost River shelf to Montana craton: North American Late Devonian stratigraphy, surfaces, and intrashelf basin, *in* Playton, T.E., Kerans, C., and Weissenberger, A.W., eds., *New advances in Devonian Carbonates: Outcrop analogs, reservoirs, and chronostratigraphy*: Tulsa, Oklahoma, Society for Sedimentary Geology Special Publication 107, p. 347-379, doi: 10.2110/sepmsp.107.12.

Guenther, W.R., Reiners, P.W., Ketcham, R.A., Nasdala, L. and Giester, G., 2013, Helium diffusion in natural zircon: Radiation damage, anisotropy, and the interpretation of zircon (U-Th)/He thermochronology: *American Journal of Science*, vol. 313, no. 3, p. 145-198.

doi:10.2475/03.2013.01.

- Guenther, W.R., 2021, Implementation of an alpha damage annealing model for zircon (U Th)/He thermochronology with comparison to a zircon fission track annealing model: *Geochemistry, Geophysics, Geosystems*, vol. 22, no. 2, doi:10.1029/2019GC008757.
- Hait Jr, M. H., 1965, Structure of the Gilmore area, Lemhi Range, Idaho [doctoral dissertation]: State College, Pennsylvania State University, 134 p.
- Hansen, C. M., and Pearson, D. M., 2016, Geologic Map of the Poison Creek Thrust Fault and Vicinity near Poison Peak and Twin Peaks, Lemhi County, Idaho: Idaho Geological Survey Technical Report T-16-1, scale 1:24,000.
- Harris, A.G., Wardlaw, B.R., Rust, C.C., and Merrill, G.K., 1980, Maps for assessing thermal maturity (conodont color alteration index maps) in Ordovician through Triassic rocks in Nevada and Utah and adjacent parts of Idaho and California: U.S. Geological Survey Miscellaneous Investigations Series Map I-1249, scale 1:2,500,000, 2 sheets.
- Hilley, G.E. and Strecker, M.R., 2004, Steady state erosion of critical Coulomb wedges with applications to Taiwan and the Himalaya: *Journal of Geophysical Research: Solid Earth*, vol. 109, no. B01411, 17 p., doi:10.1029/2002JB002284.
- Hofmann, M.H., 2020, The Devonian sedimentary record of Montana, *in* Metesh, J., ed., *Geology of Montana: Butte, Montana, Montana Bureau of Mines and Geology*, v. 1, p. 1-51.
- Horton, B.K., 1999, Erosional control on the geometry and kinematics of thrust belt development in the central Andes: *Tectonics*, vol. 18, no. 6, p. 1292-1304, doi:10.1029/1999TC900051.

- Isacks, B.L., 1988, Uplift of the central Andean plateau and bending of the Bolivian orocline: *Journal of Geophysical Research: Solid Earth*, vol. 93, no. B4, p. 3211-3231, doi:10.1029/JB093iB04p03211.
- Kaempfer J.M., Guenther, W.R., Pearson, D.M., 2019, constraining the timing of deformation in southwestern Montana basement cored ranges using low temperature thermochronology: *Geological Society of America Abstracts with Programs*, v. 51, no. 5, doi: 10.1130/abs/2019AM-336173.
- Labaume, P., Meresse, F., Jolivet, M., Teixell, A. and Lahfid, A., 2016, Tectonothermal history of an exhumed thrust-sheet-top basin: An example from the south Pyrenean thrust belt: *Tectonics*, vol. 35, no. 5, p. 1280-1313, doi:10.1002/2016TC004192.
- Lacombe, O., and Bellahsen, N., 2016, Thick-skinned tectonics and basement-involved fold-thrust belts: insights from selected Cenozoic orogens: *Geological Magazine*, vol. 153, no. 5-6, p. 763-810, doi:10.1017/S0016756816000078.
- Lawton, T.F., Boyer, S.E. and Schmitt, J.G., 1994, Influence of inherited taper on structural variability and conglomerate distribution, Cordilleran fold and thrust belt, western United States: *Geology*, vol. 22, no. 4, p. 339-342, doi:10.1130/0091-7613(1994)022<0339:IOITOS>2.3.CO;2.
- Leary, R.J., Umhoefer, P., Smith, M.E. and Riggs, N., 2017, A three-sided orogen: A new tectonic model for Ancestral Rocky Mountain uplift and basin development: *Geology*, vol. 45, no. 8, p. 735-738, doi:10.1130/G39041.1.
- Lescoutre, R. and Manatschal, G., 2020, Role of rift-inheritance and segmentation for orogenic evolution: example from the Pyrenean-Cantabrian system: *Bulletin de la Société Géologique de France*, vol. 191, no. 1, doi:10.1051/bsgf/2020021.

- Link, P.K, Warren, I., Preacher, J.M., and Skipp, B., 1996, Stratigraphic analysis and interpretation of the Mississippian Copper Basin Group, McGowan Creek Formation, and White Knob Limestone, south-central Idaho, *in* Longman, M.W., and Sonnefeld, eds., Paleozoic of the Rocky Mountain Region: Denver, Colorado, Rocky Mountain Section, Society for Sedimentary Geology, p. 117-144.
- Link, P.K., Mahon, R.C., Beranek, L.P., Campbell-Stone, E.A. and Lynds, R., 2014, Detrital zircon provenance of Pennsylvanian to Permian sandstones from the Wyoming craton and Wood River Basin, Idaho, USA: *Rocky Mountain Geology*, vol. 49, no. 2, p. 115-136, doi:10.2113/gsrocky.49.2.115.
- Link, P.K., Todt, M.K., Pearson, D.M. and Thomas, R.C., 2017, 500–490 Ma detrital zircons in Upper Cambrian Worm Creek and correlative sandstones, Idaho, Montana, and Wyoming: Magmatism and tectonism within the passive margin: *Lithosphere*, vol. 9, no. 6, p. 910-926, doi:10.1130/L671.1.
- Little, W.W., and Clayton, R.W., 2017, Field guide to compressional structures along the western margin of the southern Beaverhead Mountain Range, Scott Butte 7.5' quadrangle, east-central Idaho: *Northwest Geology*, vol. 42, p. 133-142.
- Long, S.P., 2012, Magnitudes and spatial patterns of erosional exhumation in the Sevier hinterland, eastern Nevada and western Utah, USA: Insights from a Paleogene paleogeologic map: *Geosphere*, vol. 8, no. 4, p. 881-901, doi:10.1130/GES00783.1.
- Lucchitta, B. K., 1966, Structure of the Hawley Creek area, Idaho-Montana [P.h.D. dissertation]: University Park, Pennsylvania State University, 204 p.
- Lund, K., 2018, Geologic map of the central Beaverhead Mountains, Lemhi County, Idaho, and

- Beaverhead County, Montana: U.S. Geological Survey Scientific Investigations Map 3413, scale 1:50,000.
- Lund, K., Aleinikoff, J. N., Evans, K. V., DuBray, E. A., Dewitt, E. H., and Unruh, D. M., 2010, SHRIMP U-Pb dating of recurrent Cryogenian and Late Cambrian–Early Ordovician alkalic magmatism in central Idaho: Implications for Rodinian rift tectonics: Geological Society of America Bulletin, vol. 122, no. 3-4, 430-453, doi:10.1130/B26565.1.
- Lünsdorf, N.K., Dunkl, I., Schmidt, B.C., Rantitsch, G. and von Eynatten, H., 2014, Towards a higher comparability of geothermometric data obtained by Raman spectroscopy of carbonaceous material. Part I: evaluation of biasing factors: Geostandards and Geoanalytical Research, vol. 38, no. 1, p. 73-94, doi:10.1111/j.1751-908X.2013.12011.x.
- Lünsdorf, N.K. and Lünsdorf, J.O., 2016, Evaluating Raman spectra of carbonaceous matter by automated, iterative curve-fitting: International Journal of Coal Geology, vol. 160, p. 51-62, doi:10.1016/j.coal.2016.04.008.
- Lünsdorf, N.K., Dunkl, I., Schmidt, B.C., Rantitsch, G. and von Eynatten, H., 2017, Towards a higher comparability of geothermometric data obtained by Raman spectroscopy of carbonaceous material. Part 2: A revised geothermometer: Geostandards and Geoanalytical Research, vol. 41, no. 4, p. 593-612, doi:10.1111/ggr.12178.
- Mahoney, J.B., Link, P.K., Burton, B.R., Geslin, J.K. and O'Brien, J.P., 1991, Pennsylvanian and Permian Sun Valley Group, Wood River basin, south-central Idaho, *in* Cooper, J.D., and Stevens, C.H., eds., Paleozoic Paleogeography of the Western United States-II: Tujunga, California, Pacific Section. Society for Sedimentary Geology v. 67, p. 551-579.

- Mapel, W.J., Read, W.H., and Smith, R.K., 1965, Geologic map and sections of the Doublespring quadrangle, Custer and Lemhi Counties, Idaho: U.S. Geological Survey, Geologic Quadrangle Map GQ-464, scale 1:62,500.
- McKay, M.P., Bollen, E.M., Gray, K.D., Stowell, H.H. and Schwartz, J.J., 2017, Prolonged metamorphism during long-lived terrane accretion: Sm-Nd garnet and U-Pb zircon geochronology and pressure-temperature paths from the Salmon River suture zone, west central Idaho, USA: *Lithosphere*, vol. 9, no. 5, p. 683-701, doi:10.1130/L642.1.
- McMechan, M.E., 2001, Large-scale duplex structures in the McConnell thrust sheet, Rocky Mountains, Southwest Alberta: *Bulletin of Canadian Petroleum Geology*, vol. 49, no. 3, p. 408-425, doi:10.2113/49.3.408.
- McQuarrie, N., Barnes, J.B. and Ehlers, T.A., 2008, Geometric, kinematic, and erosional history of the central Andean Plateau, Bolivia (15–17 S): *Tectonics*, vol. 27, no. 3, doi:10.1029/2006TC002054.
- McQuarrie, N. and Ehlers, T.A., 2017, Techniques for understanding fold-thrust belt kinematics and thermal evolution, *in* Law, RD, Thigpen, JR, Merschat, AJ, and Stowell, HH, *Linkages and Feedbacks in Orogenic Systems: Boulder, Colorado*, Geological Society of America Memoirs 213, p. 25-54, doi:10.1130/2017.1213(02).
- Messina, T. A., 1993, The geometry and kinematics of intra-thrust sheet decollement folding: Lost River Range, Idaho [MS thesis]: Bethlehem, Lehigh University, 50 p.
- M'Gonigle, J.W., 1982, Devonian carbonate-breccia units in southwestern Montana and Idaho; a review of brecciating mechanisms, *in* Powers, R.B., ed., *Geologic Studies of the Cordilleran Thrust Belt: Denver, Colorado*, Rocky Mountain Association of Geologists v. 1, p. 677-689.

- Miller, E.L., Miller, M.M., Stevens, C.H., Wright, J.E., and Madrid, R., 1992, Late Paleozoic paleogeographic and tectonic evolution of the western U.S. Cordillera, *in* Burchfiel, B.C., Lipman, P.W., and Zoback, M.L., eds., *The Cordilleran orogen: Conterminous U.S.*: Boulder, Colorado, Geological Society of America, *The Geology of North America*, v. G-3, p. 57–106.
- Milton, J., 2020, Geologic mapping, stratigraphy, and detrital zircon geochronology of the southeastern Borah Peak horst, Custer County, Idaho: Age reassignment and correlation of Neoproterozoic to lower Paleozoic strata [MS thesis]: Pocatello, Idaho State University, 131 p.
- Mitra, G., 1997, Evolution of salients in a fold-and-thrust belt: The effects of sedimentary basin geometry, strain distribution and critical taper, *in* Sengupta, S., ed., *Evolution of geological structures in micro-to macro-scales*: London, UK, Chapman & Hall, pp. 59-90.
- Montz, W.J. and Kruckenberg, S.C., 2017, Cretaceous partial melting, deformation, and exhumation of the Potters Pond migmatite domain, west-central Idaho: *Lithosphere*, vol. 9, no. 2, p. 205-222, doi:10.1130/L555.1.
- Morley, C.K., von Hagke, C., Hansberry, R., Collins, A., Kanitpanyacharoen, W. and King, R., 2018, Review of major shale-dominated detachment and thrust characteristics in the diagenetic zone: Part II, rock mechanics and microscopic scale: *Earth-Science Reviews*, vol. 176, p. 19-50, doi:10.1016/j.earscirev.2017.09.015.
- Muirhead, D.K., Bond, C.E., Watkins, H., Butler, R.W.H., Schito, A., Crawford, Z. and Marpino, A., 2020, Raman spectroscopy: an effective thermal marker in low temperature carbonaceous fold–thrust belts: Geological Society, London, *Special Publications*, vol. 490, no. 1, p. 135-151, doi:10.1144/SP490-2019-27.

- Nibourel, L., Berger, A., Egli, D., Luensdorf, N.K. and Herwegh, M., 2018, Large vertical displacements of a crystalline massif recorded by Raman thermometry: *Geology*, vol. 46, no. 10, p. 879-882, doi:10.1130/G45121.1.
- Nibourel, L., Berger, A., Egli, D., Heuberger, S. and Herwegh, M., 2021, Structural and thermal evolution of the eastern Aar Massif: insights from structural field work and Raman thermometry: *Swiss Journal of Geosciences*, vol. 114, no. 1, p. 1-43, doi:10.1186/s00015-020-00381-3.
- O'Brien, C.A.E., 1960, The structural geology of the Boule and Bosche Ranges in the Canadian Rocky Mountains: *Quarterly Journal of the Geological Society*, vol. 116, no. 1-4, p. 409-431, doi:10.1144/gsjgs.116.1.0409.
- Oldow, J.S., Bally, A.W., Ave Lallemand, H.G., Leeman, W., 1989, Phanerozoic evolution of the North American Cordillera, United States and Canada, *in* Bally, A.W., and Palmer, A.R., eds., *The Geology of North America — An overview: Boulder, Colorado, Geological Society of America, The Geology of North America*, vol. A, p. 139-232, doi:10.1130/DNAG-GNA-A.139.
- Parker, S.D, and Pearson, D.M., 2020, Geologic map of the northern part of the Leadore quadrangle, Lemhi County, Idaho: Idaho Geological Survey Technical Report T-20-03, scale 1:24,000.
- Parker, S.D. and Pearson, D.M., 2021, Pre-thrusting stratigraphic control on the transition from a thin to thick-skinned structural style: An example from the double-decker Idaho-Montana fold-thrust belt: *Tectonics*, vol. 40, no. 5, p.e2020TC006429, doi:10.1029/2020TC006429.
- Perry Jr, W.J., Wardlaw, B.R., Bostick, N.H., and Maughan, E.K., 1983, Structure, burial

- history, and petroleum potential of frontal thrust belt and adjacent foreland, southwest Montana: *The American Association of Petroleum Geologists Bulletin*, vol. 67, no. 5, p. 725-743, doi:10.1306/03B5B6A0-16D1-11D7-8645000102C1865D.
- Perry Jr, W.J., Haley, J.C., Nichols, D.J., Hammons, P.M., and Ponton, J.D., 1988, Interactions of Rocky Mountain foreland and Cordilleran thrust belt in Lima region, southwest Montana, *in* Schmidt, J., and Perry, W.J., eds., *Interaction of the Rocky Mountain Foreland and the Cordilleran Thrust Belt*: Boulder, Colorado, Geological Society of America Memoir, v. 171, p 267-290, doi:10.1130/MEM171-p267.
- Peterson, J.A., 1981, General stratigraphy and regional paleostructure of the western Montana overthrust belt, *in* Tucker, T.E., Aram, R.B., Brinker, W.F., and Grabb, R.F., *Montana Geological Society field conference & symposium guidebook to southwest Montana: Billings, Montana, Montana Geological Society*, p. 5-35.
- Picha, F. and Gibson, R.I., 1985, Cordilleran hingeline: Late Precambrian rifted margin of the North American craton and its impact on the depositional and structural history, Utah and Nevada: *Geology*, vol. 13, no. 7, p. 465-468, doi:10.1130/00917613(1985)13<465:CHLPRM>2.0.CO;2.
- Price, R.A., and Mountjoy, E.W., 1970, Geologic structure of the Canadian Rocky Mountains between Bow and Athabasca Rivers—a progress report, *in* Wheeler, J.O., *Structure of the southern Canadian Cordillera*: St. John's, Newfoundland, Geological Association of Canada Special Paper, v. 6, p. 7-25.
- Price, R., 1981, The Cordilleran foreland thrust and fold belt in the southern Canadian Rocky Mountains: Geological Society, London, Special Publications, vol. 9, no. 1, p. 427-448. doi:10.1144/GSL.SP.1981.009.01.39.

- Price, R.A., 2001, An evaluation of models for the kinematic evolution of thrust and fold belts: structural analysis of a transverse fault zone in the Front Ranges of the Canadian Rockies north of Banff, Alberta: *Journal of Structural Geology*, v. 23, no. 6-7, p. 1079-1088, doi:10.1016/S0191-8141(00)00177-2.
- Rahl, J.M., Anderson, K.M., Brandon, M.T. and Fassoulas, C., 2005, Raman spectroscopic carbonaceous material thermometry of low-grade metamorphic rocks: Calibration and application to tectonic exhumation in Crete, Greece: *Earth and Planetary Science Letters*, vol. 240, no. 2, p. 339-354, doi:10.1016/j.epsl.2005.09.055.
- Rich, J. L., 1934, Mechanics of Low-Angle Overthrust Faulting as Illustrated by Cumberland Thrust Block, Virginia, Kentucky, and Tennessee: *The American Association of Petroleum Geologists Bulletin* vol. 18, no.12, p. 1584–1596, doi:10.1306/3D932C94-16B1-11D7-8645000102C1865D.
- Rodgers, D. W., and Janecke, S. U., 1992, Tertiary paleogeologic maps of the western Idaho Wyoming-Montana thrust belt, *in* Link, P.K., Kuntz, M.A., and Piatt, L.B., eds., *Regional Geology of Eastern Idaho and Western Wyoming*: Boulder, Colorado, Geological Society of America Memoir, v. 179, p 83-94), doi:10.1130/MEM179-p83.
- Rose, P.R., 1976, Mississippian carbonate shelf margins, western United States: *Journal of Research, U.S. Geological Survey*, vol. 4, no. 4, p. 449-466.
- Rosenblume, J.A., Finzel, E.S., and Pearson, D.M., 2021, Early Cretaceous provenance, sediment dispersal, and foreland basin development in southwestern Montana, North American Cordillera: *Tectonics*, vol. 40, p. 1–31, doi:10.1029/2020TC006561.
- Royse F., 1993, An overview of the geologic structure of the thrust belt in Wyoming, northern Utah, and eastern Idaho, *in* Snoke, A.W., Steidtmann, J.R., Roberts, S.M., eds., *Geology*

- of Wyoming: Laramie, Wyoming, Geological Survey of Wyoming Memoir vol. 5, pp. 272-311.
- Royse Jr, F., Warner, M.T., and Reese, D.L., 1975, Thrust Belt Structural Geometry and Related Stratigraphic Problems Wyoming-Idaho-Northern Utah, *in* Bolyard, D.W., (ed.), Symposium on deep drilling frontiers in the central Rocky Mountains: Denver, Colorado, Rocky Mountain Association of Geologists, p. 41-45.
- Ruppel, E.T., 1986, The Lemhi Arch: A Late Proterozoic and Early Paleozoic Landmass in Central Idaho., *in* Peterson, J.A., ed., Paleotectonics and sedimentation in the Rocky Mountain Region, United States: Denver, Colorado, American Association of Petroleum Geologists Memoir, vol. 41, p. 119-130, doi:10.1306/M41456C6.
- Ruppel, E.T., and Lopez, D.A., 1984, The thrust belt in Southwest Montana and east-central Idaho: U.S Geological Survey Professional Paper, vol. 1278, 45 p., doi:10.3133/pp1278.
- Ryder, R. T., and Scholten, R., 1973, Syntectonic conglomerates in southwestern Montana: Their nature, origin, and tectonic significance: Geological Society of America Bulletin, vol. 84, no. 3, p. 773-796, doi:10.1130/0016-7606(1973)84<773:SCISMT>2.0.CO;2.
- Schito, A., Romano, C., Corrado, S., Grigo, D. and Poe, B., 2017, Diagenetic thermal evolution of organic matter by Raman spectroscopy: Organic Geochemistry, vol. 106, p. 57-67, doi:10.1016/j.orggeochem.2016.12.006.
- Scholten, R., 1957, Paleozoic evolution of the geosynclinal margin north of the Snake River Plain, Idaho-Montana: Geological Society of America Bulletin, vol. 68, no. 2, p. 151-170, doi:10.1130/0016-7606(1957)68[151:PEOTGM]2.0.CO;2.
- Scholten, R., and Ramspott, L. D., 1968, Tectonic Mechanisms Indicated by Structural

- Framework of Central Beaverhead Range, Idaho Montana: Boulder, Colorado, Geological Society of America Special Paper 105, 59 p., doi:10.1130/SPE104-p1.
- Shuster, D.L. and Farley, K.A., 2009, The influence of artificial radiation damage and thermal annealing on helium diffusion kinetics in apatite: *Geochimica et cosmochimica acta*, vol. 73, no. 1, p. 183-196, doi:10.1016/j.gca.2008.10.013.
- Simpson, G.D., 2010, Influence of the mechanical behaviour of brittle–ductile fold–thrust belts on the development of foreland basins: *Basin Research*, vol. 22, no. 2, p. 139-156. doi:10.1111/j.1365-2117.2009.00406.x.
- Skipp, B., 1988a, Cordilleran thrust belt and faulted foreland in the Beaverhead Mountains, Idaho and Montana, *in* Schmidt, J., and Perry, W.J., eds., *Interaction of the Rocky Mountain Foreland and the Cordilleran Thrust Belt*: Boulder, Colorado, Geological Society of America Memoir, vol. 171, p 237-266, doi:10.1130/MEM171-p237.
- Skipp, B., 1988b, Geologic map of Mackay 4 (Grouse) NE Quadrangle, Butte and Custer counties, Idaho: U.S Geological Survey Open-File Report 88-423, scale 1:24,000, doi:10.3133/ofr88423.
- Skipp, B., and Hait, M.H., 1977, Allochthons along the northeast margin of the Snake River Plain, Idaho, *in* Heisey, E.L., Lawson, D.E., Norwood, E.R., Wach, P.G., and Hale, L.A. eds., *Robky Mountain thrust belt geology and resources; 29<sup>th</sup> annual field conference guidebook*: Casper, Wyoming, Wyoming Geological Association, p. 499-515.
- Skipp, B. and Hall, W.E., 1980, Upper Paleozoic paleotectonics and paleogeography of Idaho, *in* Fouch, T.D., and Magatham, eds., *Paleozoic paleogeography of west-central United*

- States symposium 1: Denver, Colorado, Rocky Mountain Section, Society for Sedimentary Geology, p. 387-422.
- Skipp, B., Kuntz, M.A., and Morgan, L.A., 1989, Geologic map of Mackay 4 (Grouse) SE Quadrangle, Butte County, Idaho: U.S Geological Survey Open-File Report 89-431, scale 1:24,000, doi:10.3133/ofr89431.
- Skipp, B., and Bollmann, D.D., 1992, Geologic map of Blizzard Mountain North quadrangle, Blaine and Butte counties, Idaho: U.S Geological Survey Open-File Report 92-280, scale 1:24,000, doi:10.3133/ofr92280.
- Sloss, L.L., 1954, Lemhi Arch, a mid-Paleozoic positive element in south-central Idaho: Geological Society of America Bulletin, vol. 65, no. 4, p.365-368.  
doi:10.1130/0016-7606(1954)65[365:LAAMPE]2.0.CO;2.
- Süssenberger, A., Schmidt, S.T., Schmidt, F.H., and Weinkauf, M.F., 2020, Reaction progress of clay minerals and carbonaceous matter in a contact metamorphic aureole (Torres del Paine intrusion, Chile): European Journal of Mineralogy, vol. 32, no. 6, p.653-671, doi:10.5194/ejm-32-653-2020.
- Tavani, S., Granado, P., Corradetti, A., Camanni, G., Vignaroli, G., Manatschal, G., Mazzoli, S., Muñoz, J. A., and Parente, M., 2021, Rift inheritance controls the switch from thin-to thick-skinned thrusting and basal décollement re-localization at the subduction-to collision transition: Geological Society of America Bulletin, p. 1-14.  
doi:10.1130/B35800.1
- Wilf, P., Johnson, K.R. and Huber, B.T., 2003, Correlated terrestrial and marine evidence for global climate changes before mass extinction at the Cretaceous–Paleogene boundary: Proceedings of the National Academy of Sciences, vol. 100, no. 2, p. 599-604,

doi:10.1073/pnas.0234701100.

Yonkee, W.A., and Weil, A.B., 2015, Tectonic evolution of the Sevier and Laramide belts within the North American Cordillera orogenic system: *Earth-Science Reviews*, vol. 150, p. 531-593, doi:10.1016/j.earscirev.2015.08.001.

Yonkee, W.A., Dehler, C.D., Link, P.K., Balgord, E.A., Keeley, J.A., Hayes, D.S., Wells, M.L., Fanning, C.M. and Johnston, S.M., 2014, Tectono-stratigraphic framework of Neoproterozoic to Cambrian strata, west-central US: Protracted rifting, glaciation, and evolution of the North American Cordilleran margin: *Earth-Science Reviews*, vol. 136, p. 59-95, doi:10.1016/j.earscirev.2014.05.004.

Yonkee, W.A., Eleogram, B., Wells, M.L., Stockli, D.F., Kelley, S. and Barber, D.E., 2019, Fault slip and exhumation history of the Willard thrust sheet, Sevier fold-thrust belt, Utah: Relations to wedge propagation, hinterland uplift, and foreland basin Sedimentation: *Tectonics*, vol. 38, no. 8, p. 2850-2893, doi:10.1029/2018TC005444.

Zdanavičiūtė, O. and Lazauskienė, J., 2009, Organic matter of Early Silurian succession—the potential source of unconventional gas in the Baltic Basin (Lithuania): *Baltica*, vol. 22, no. 2, p. 89-98.

TABLE 1. COMPILED MAXIMUM TEMPERATURE ESTIMATES

Source	Latitude (°N)	Longitude (°W)	Method	Calculated maximum temperature (°C)	2 $\sigma$ uncertainty (°C)	Age of sample
Harris et al., 1980	43.743586	114.242310	CAI	300*	50	Pennsylvanian
Harris et al., 1980	43.752172	114.219154	CAI	300*	50	Permian
Anastasio et al., 2004	44.226800	113.830000	IC	220*†	N.D.#	Mississippian
Anastasio et al., 2004	44.226800	113.830000	DL	300 *§	N.D.#	Mississippian
Perry et al., 1983	45.049248	112.635985	CAI	65*	15	Mississippian
Perry et al., 1983	45.035727	112.640244	CAI	65*	15	Permian
Perry et al., 1983	45.057798	112.673885	CAI	65*	15	Mississippian
Perry et al., 1983	45.078857	112.795662	CAI	65*	15	Permian
Perry et al., 1983	45.003803	112.867536	CAI	65*	15	Mississippian
Perry et al., 1983	44.906584	112.869582	CAI	65*	15	Mississippian
Perry et al., 1983	44.798313	113.245847	CAI	245*	55	Mississippian
Harris et al., 1980	44.267680	113.722263	CAI	300*	50	Mississippian
Harris et al., 1980	43.775189	113.812798	CAI	300*	50	Mississippian
Harris et al., 1980	43.773732	113.870773	CAI	300*	50	Mississippian
Harris et al., 1980	43.873818	114.051995	CAI	300*	50	Mississippian
Harris et al., 1980	43.907033	114.071576	CAI	300*	50	Mississippian
Harris et al., 1980	43.796034	114.084436	CAI	300*	50	Ordovician
Harris et al., 1980	44.195200	114.186006	CAI	280*	55	Ordovician
Harris et al., 1980	44.088911	114.248239	CAI	300*	50	Devonian
Harris et al., 1980	43.807356	114.280323	CAI	300*	50	Devonian
Harris et al., 1980	43.894375	114.289352	CAI	300*	50	Ordovician
Harris et al., 1980	43.813164	114.301430	CAI	300*	50	Permian
Harris et al., 1980	43.921507	114.361212	CAI	300*	50	Pennsylvanian
Harris et al., 1980	43.850455	114.367098	CAI	300*	50	Pennsylvanian
Harris et al., 1980	43.863891	114.396026	CAI	300*	50	Permian
Harris et al., 1980	43.498869	113.667295	CAI	280	55	Mississippian
Harris et al., 1980	43.528462	113.769188	CAI	300	50	Devonian
Harris et al., 1980	43.628433	113.186401	CAI	300	50	Mississippian
Harris et al., 1980	43.652199	114.112596	CAI	300	50	Pennsylvanian
Harris et al., 1980	43.655111	113.900452	CAI	300	50	Mississippian
Harris et al., 1980	43.945350	114.535100	CAI	300	50	Pennsylvanian
Harris et al., 1980	44.115428	112.738733	CAI	120	40	Pennsylvanian
Harris et al., 1980	44.168525	112.804815	CAI	155	45	Mississippian
Harris et al., 1980	44.182081	112.836945	CAI	260	50	Devonian
Harris et al., 1980	44.239188	114.509949	CAI	300	50	Mississippian
Harris et al., 1980	44.255154	114.207318	CAI	300	50	Silurian
Harris et al., 1980	44.255312	114.458509	CAI	280	55	Silurian
Harris et al., 1980	44.260683	114.277957	CAI	300	50	Devonian
Harris et al., 1980	44.262497	114.305275	CAI	300	50	Devonian
Harris et al., 1980	44.268588	114.308394	CAI	300	50	Neoproterozoic
Harris et al., 1980	44.271456	114.291459	CAI	300	50	Silurian
Harris et al., 1980	44.273794	114.284044	CAI	300	50	Devonian
Harris et al., 1980	44.275261	114.507767	CAI	300	50	Ordovician
Harris et al., 1980	44.315794	114.410449	CAI	300	50	Neoproterozoic
Harris et al., 1980	44.322006	114.210449	CAI	300	50	Silurian
Harris et al., 1980	44.326512	114.296044	CAI	300	50	Devonian

Harris et al., 1980	44.332324	114.298233	CAI	300	50	Neoproterozoic
Harris et al., 1980	44.357393	112.758147	CAI	300	50	Mississippian
Harris et al., 1980	44.362415	114.242627	CAI	300	50	Silurian
Harris et al., 1980	44.382296	114.023137	CAI	300	50	Devonian
Harris et al., 1980	44.396321	114.243581	CAI	300	50	Silurian
Harris et al., 1980	44.403587	114.238037	CAI	300	50	Devonian
Harris et al., 1980	44.411919	112.755994	CAI	245	55	Mississippian
Harris et al., 1980	44.499178	114.068719	CAI	300	50	Devonian
Dyman et al., 1996	44.858333	111.758333	REP	103	N.D.#	Cretaceous
Dyman et al., 1996	44.858333	111.758333	REP	103	N.D.#	Cretaceous
Dyman et al., 1996	44.858333	111.758333	VR	83	N.D.#	Cretaceous
Dyman et al., 1996	44.543719	112.116796	REP	92	N.D.#	Cretaceous
Dyman et al., 1996	44.543719	112.116796	REP	99	N.D.#	Cretaceous
Dyman et al., 1996	44.543719	112.116796	REP	109	N.D.#	Cretaceous
Dyman et al., 1996	44.543719	112.116796	REP	99	N.D.#	Cretaceous
Dyman et al., 1996	44.543719	112.116796	VR	142	N.D.#	Cretaceous
Dyman et al., 1996	44.543719	112.116796	VR	93	N.D.#	Cretaceous
Dyman et al., 1996	44.543719	112.116796	VR	103	N.D.#	Cretaceous
Dyman et al., 1996	44.543719	112.116796	VR	67	N.D.#	Cretaceous
Dyman et al., 1996	44.587229	112.116915	VR	87	N.D.#	Cretaceous
Dyman et al., 1996	44.587229	112.116915	VR	83	N.D.#	Cretaceous
Dyman et al., 1996	44.696288	112.146737	VR	80	N.D.#	Cretaceous
Dyman et al., 1996	44.790566	112.197477	REP	113	N.D.#	Cretaceous
Dyman et al., 1996	44.790566	112.197477	REP	115	N.D.#	Cretaceous
Dyman et al., 1996	44.790566	112.197477	REP	115	N.D.#	Cretaceous
Dyman et al., 1996	44.790566	112.197477	VR	87	N.D.#	Cretaceous
Dyman et al., 1996	44.790566	112.197477	VR	73	N.D.#	Cretaceous
Dyman et al., 1996	45.044127	112.003849	REP	109	N.D.#	Cretaceous
Dyman et al., 1996	45.044127	112.003849	REP	121	N.D.#	Cretaceous
Dyman et al., 1996	45.044127	112.003849	REP	103	N.D.#	Cretaceous
Dyman et al., 1996	45.044127	112.003849	VR	98	N.D.#	Cretaceous
Dyman et al., 1996	45.044127	112.003849	VR	94	N.D.#	Cretaceous
Dyman et al., 1996	45.044127	112.003849	VR	89	N.D.#	Cretaceous
Dyman et al., 1996	45.044127	112.003849	VR	84	N.D.#	Cretaceous
Dyman et al., 1996	45.044127	112.003849	VR	113	N.D.#	Cretaceous
Dyman et al., 1996	45.044127	112.003849	VR	106	N.D.#	Cretaceous
Dyman et al., 1996	45.051423	111.952687	REP	105	N.D.#	Cretaceous
Dyman et al., 1996	45.051423	111.952687	REP	99	N.D.#	Cretaceous
Dyman et al., 1996	45.051423	111.952687	REP	105	N.D.#	Cretaceous
Dyman et al., 1996	45.051423	111.952687	VR	106	N.D.#	Cretaceous
Dyman et al., 1996	45.072077	111.270637	REP	111	N.D.#	Cretaceous
Dyman et al., 1996	45.072077	111.270637	REP	94	N.D.#	Cretaceous
Dyman et al., 1996	45.072077	111.270637	REP	81	N.D.#	Cretaceous
Dyman et al., 1996	45.072077	111.270637	VR	146	N.D.#	Cretaceous
Dyman et al., 1996	45.072077	111.270637	VR	55	N.D.#	Cretaceous
Dyman et al., 1996	45.072077	111.270637	VR	76	N.D.#	Cretaceous
Dyman et al., 1996	45.27544	111.230246	REP	103	N.D.#	Cretaceous
Dyman et al., 1996	45.27544	111.230246	REP	174	N.D.#	Cretaceous
Dyman et al., 1996	45.27544	111.230246	VR	135	N.D.#	Cretaceous
Dyman et al., 1996	45.27544	111.230246	VR	229	N.D.#	Cretaceous
Dyman et al., 1996	45.27544	111.230246	VR	234	N.D.#	Cretaceous
Dyman et al., 1996	45.305395	112.702688	VR	117	N.D.#	Cretaceous
Dyman et al., 1996	45.305395	112.702688	VR	122	N.D.#	Cretaceous
Dyman et al., 1996	45.408507	112.629948	VR	239	N.D.#	Cretaceous
Dyman et al., 1996	45.408507	112.629948	VR	235	N.D.#	Cretaceous
Dyman et al., 1996	45.408507	112.629948	VR	232	N.D.#	Cretaceous

Dyman et al., 1996	45.408507	112.629948	VR	203	N.D.#	Cretaceous
Dyman et al., 1996	45.451930	112.546732	VR	203	N.D.#	Cretaceous
Dyman et al., 1996	45.451930	112.546732	VR	203	N.D.#	Cretaceous
Dyman et al., 1996	45.451930	112.546732	VR	232	N.D.#	Cretaceous
Perry et al., 1983	44.403178	112.763104	CAI	245	55	Mississippian
Perry et al., 1983	44.487415	112.768680	CAI	155	45	Mississippian
Perry et al., 1983	44.488203	112.691250	CAI	85	15	Mississippian
Perry et al., 1983	44.517606	112.648296	CAI	65	15	Triassic
Perry et al., 1983	44.529285	112.590356	CAI	65	15	Triassic
Perry et al., 1983	44.542547	112.580047	CAI	65	15	Triassic
Perry et al., 1983	44.557547	112.650852	VR	96	N.D.#	Mississippian
Perry et al., 1983	44.557547	112.650852	VR	80	N.D.#	Mississippian
Perry et al., 1983	44.563114	112.542414	CAI	65	15	Permian
Perry et al., 1983	44.577761	112.623007	CAI	65	15	Mississippian
Perry et al., 1983	44.578479	112.689780	VR	10	N.D.#	Mississippian
Perry et al., 1983	44.578479	112.689780	VR	33	N.D.#	Mississippian
Perry et al., 1983	44.590154	112.116141	VR	87	N.D.#	Cretaceous
Perry et al., 1983	44.590154	112.116141	VR	83	N.D.#	Cretaceous
Perry et al., 1983	44.590154	112.116141	VR	153	N.D.#	Permian
Perry et al., 1983	44.590154	112.116141	VR	171	N.D.#	Devonian
Perry et al., 1983	44.591458	112.677356	CAI	65	15	Mississippian
Perry et al., 1983	44.596552	112.759940	CAI	70	20	Mississippian
Perry et al., 1983	44.641822	112.787251	CAI	65	15	Permian
Perry et al., 1983	44.657928	112.773417	VR	30	N.D.#	Mississippian
Perry et al., 1983	44.657928	112.773417	VR	51	N.D.#	Mississippian
Perry et al., 1983	44.658391	112.774828	CAI	65	15	Mississippian
Perry et al., 1983	44.666501	112.798758	CAI	65	15	Triassic
Perry et al., 1983	44.670510	112.760982	CAI	65	15	Mississippian
Perry et al., 1983	44.689679	112.476041	CAI	70	20	Mississippian
Perry et al., 1983	44.696627	112.815680	VR	65	N.D.#	Mississippian
Perry et al., 1983	44.696627	112.815680	VR	65	N.D.#	Mississippian
Perry et al., 1983	44.700825	112.159972	VR	80	N.D.#	Cretaceous
Perry et al., 1983	44.700825	112.159972	VR	139	N.D.#	Mississippian
Perry et al., 1983	44.707106	112.819505	CAI	65	15	Triassic
Perry et al., 1983	44.717603	112.826993	CAI	65	15	Triassic
Perry et al., 1983	44.728259	112.424491	CAI	65	15	Mississippian
Perry et al., 1983	44.730411	112.409159	CAI	65	15	Mississippian
Perry et al., 1983	44.759495	112.290632	CAI	65	15	Triassic
Perry et al., 1983	44.766021	112.303276	CAI	65	15	Permian
Perry et al., 1983	44.774672	112.310897	CAI	65	15	Mississippian
Skipp and Bollmann, 1992	43.514654	113.683260	CAI	280	55	Mississippian
Skipp et al., 1989	43.596111	113.525982	CAI	180	45	Devonian
Skipp et al., 1989	43.601142	113.524593	CAI	245	55	Mississippian
Skipp, 1988b	43.627184	113.524601	CAI	110	40	Mississippian
Skipp, 1988b	43.712880	113.564716	CAI	100	40	Mississippian
Skipp, 1988b	43.734321	113.529245	CAI	140	40	Mississippian
Skipp, 1988b	43.625992	113.732590	CAI	180	45	Mississippian

\*Projected onto cross section line, see Fig. 6.

†Temperature calculated using illite crystallinity method. Kübler indices average  $0.20^\circ 2\Theta$ .

§Temperature estimated from deformation lamellae with sub grains in calcite.

#N.D. = not determined.

*Table 1. Compiled maximum temperature data from CAI, vitrinite reflectance (VR), Rock-Eval pyrolysis (REP), illite crystallinity (IC), and deformation lamellar in calcite (DL).*

TABLE 2. RAMAN SPECTROSCOPY OF CARBONACEOUS MATERIAL SAMPLES

Sample number	Latitude (°N)	Longitude (°W)	Formation	Lithology	n	Calculated maximum temperature (°C)	2 $\sigma$ uncertainty (°C)
1	44.04209	113.6546	Surrett	lime wackestone	16	259	26
2	44.02847	113.6614	Middle Canyon	silty lime mudstone	17	280	26
3	44.75583	113.3666	Middle Canyon	silty dolo mudstone	17	278	26
4	44.11175	114.0319	White Knob	lime wackestone	18	218	26
5	44.74677	113.3285	Scott Peak	lime wackestone	17	267	27
6	44.69739	113.2514	Snaky Canyon	dolo mudstone	18	244	25
7	44.73430	113.2524	Jefferson	dolo wackestone	18	281	25
8	45.24952	112.2385	Hasmark	dolo mudstone	6	52	61
9	45.04086	112.5953	Lodgepole	lime mudstone	3	42	62
10	44.79045	112.8179	Lombard	lime wackestone	16	60	29
11	44.85440	112.8147	Paine	lime wackestone	18	115	27
12	44.88496	112.9770	M undivided	lime wackestone	17	216	29
13	44.77135	113.0131	Tendoy Group	lime wackestone	18	231	26
14	44.58260	113.4751	Jefferson	dolo mudstone	15	267	27
15	44.55995	113.3511	Jefferson	dolo wackestone	17	260	28
16	44.30846	113.4111	Jefferson	dolo mudstone	18	275	25
17	44.26286	113.5116	Jefferson	dolo wackestone	16	290	30
18	44.23499	113.5542	Jefferson	dolo mudstone	18	244	30
19	44.23986	113.7644	Brazier	lime wackestone	19	229	31
20	44.19984	113.8681	McGowan	mudstone	18	263	24
22	43.85988	114.3009	Phi Kappa	siltstone	18	390	37
23	43.76615	114.2694	Milligan	siltstone	14	284	31
25	43.81614	114.3500	Milligan	lime mudstone	18	298	29
26	43.70930	114.4256	Wood River	siltstone	17	339	31
27	43.63229	114.4826	Wood River	calcareous siltstone	4	392	52
28	44.12883	113.7880	Jefferson	dolo wackestone	17	273	26
29	43.84278	114.0713	Drummond Mine	lime mudstone	18	292	25
30	43.84845	113.8084	White Knob	lime wackestone	18	221	26
32	44.22449	114.0341	South Creek	lime wackestone	18	258	27
33	44.17358	113.9894	White Knob	lime mudstone	18	241	25
34	44.21380	114.0219	White Knob	lime mudstone	18	239	29
35	44.23553	114.0375	Scott Peak	lime wackestone	18	263	28

*Table 2. Sample information and RSCM results of this study.*

### Chapter III:

A balanced and restored kinematic model integrating the Sevier and Laramide belts of the Idaho-Montana fold-thrust belt, U.S. Cordillera

# A balanced and restored kinematic model integrating the Sevier and Laramide belts of the Idaho-Montana fold-thrust belt, U.S. Cordillera

*Manuscript for submission to Geosphere*

**Stuart D. Parker<sup>1</sup> and David M. Pearson<sup>1</sup>**

*<sup>1</sup>Department of Geosciences, Idaho State University, Pocatello, Idaho 83209, USA*

## **ABSTRACT**

The Sevier and Laramide belts of the North American Cordillera are differentiated based on their contrasting thin and thick-skinned styles and are often inferred to have formed under different plate boundary conditions. However, spatial and temporal overlap in the Idaho-Montana fold-thrust belt suggests that these thin- to thick-skinned thrusts are kinematically linked. We present the first balanced and restored cross section that integrates the Sevier and Laramide belts, recording a minimum of 170 km of horizontal crustal shortening in the Idaho-Montana segment. From this, we propose a viable kinematic model that links thin- to thick-skinned thrusts, predicting that thin stratigraphy overlying the Lemhi arch basement high determined the geometry and relative timing of the later thrusts. Early shortening (pre ~90 Ma) was thin-skinned, with the flat-lying décollement of the Medicine Lodge-McKenzie thrust system following shales of the flooding-surface unconformity on top of the Lemhi arch. An overlap in activity between upper thin- and lower thick-skinned thrusting occurred ~90-70 Ma, as a mid-crustal décollement was activated and strain was efficiently transmitted through the

Lemhi arch to the Blacktail-Snowcrest uplift in the foreland. Progressive in-sequence linking of the lower and upper décollement increased the basal slope of the stratigraphically-controlled upper décollement, forming a regional-scale duplex of the Patterson culmination and internally thickening the wedge from the rear. Eventually the upper décollement was completely abandoned and exhumed by thick-skinned thrusts (Hawley Creek, Cabin, and Johnson) that continued to thicken the wedge. During the final stage of shortening (~70-55 Ma), the thick-skinned wedge advanced forward into the foreland. This model predicts that thin- to thick-skinned thrusts are linked by a mid-crustal décollement, with the geometry and tempo of the transition between styles determined by the thicknesses of the sedimentary cover rocks and availability of décollement horizons.

## **INTRODUCTION**

The North American Cordillera is a classic example of an ancient ocean-continent subduction system with a Jurassic to Paleogene retroarc fold-thrust belt that records interactions between variable preexisting stratigraphy and structural style, ranging from thin-skinned to thick-skinned (Armstrong, 1968; Burchfiel and Davis, 1975; Dickinson and Snyder, 1978; Oldow et al., 1989; Miller, 1992; DeCelles, 2004; Dickinson, 2004; Yonkee and Weil, 2015). Primarily focused on the sector of the North American Cordillera within the conterminous U.S. near the modern latitudes of Nevada, Utah, and Wyoming, many modern workers follow Armstrong's (1968) distinction between the Sevier and Laramide orogenic belts based upon the contrast in structural style and apparent age: the Sevier orogenic belt is often characterized by "décollement thrusts with displacements of tens of miles" whereas the Laramide orogenic belt is distinctly younger and consists of uplifts of "great blocks of crystalline basement along...steep thrust faults". This "fundamental distinction" between the Sevier and Laramide belts was based on the

interpretation that the two orogenic domains are distinct in age, style, and tectonic cause (Armstrong, 1968). Though this nomenclature continues to be used and many workers consider the “Sevier orogeny” and “Laramide orogeny” to represent disparate geologic events, more recent work has emphasized the overlap in timing and interconnected processes (e.g., Yonkee and Weil, 2015; Fitz-Díaz et al., 2018), as well as the continuum of structural styles (e.g., Parker and Pearson, 2021) that resulted in formation of the composite North American Cordilleran retroarc.

North of the classic Sevier-Laramide orogenic belts described by Armstrong (1968), the Idaho-Montana fold-thrust belt is an along-strike continuation but has received far less attention than elsewhere along the North American Cordillera (Fig. 1). Though the foreland of southwestern Montana is characterized by prominent basement-involved structures that are commonly lumped with Laramide-style structures of the Wyoming and Colorado foreland, the two structural domains overlapped in space (e.g., Coryell and Spang, 1988; Johnson and Sears, 1988; Kulik and Perry, 1988; Kulik and Schmidt, 1988; Perry et al., 1988; Schmidt et al., 1988; Skipp, 1988; Tysdal, 1988; Williams and Bartley, 1988; McDowell, 1997) to form a double-decker fold-thrust belt (Parker and Pearson, 2021): thin-skinned thrusts of the Sevier belt shortened Phanerozoic strata at shallower structural levels in an overlapping region where structurally underlying, basement-involved thrusts deformed mechanical basement that consist of crystalline rocks and Mesoproterozoic quartzites. Mutually crosscutting relationships between thin- to thick-skinned thrusts assigned to the “overlapping” Sevier and Laramide belts demonstrate continued orogenesis rather than discrete orogenic events (e.g., Kulik and Perry, 1988; Kulik and Schmidt, 1988; Lopez and Schmidt, 1988; Perry et al., 1988; Tysdal, 1988; McDowell, 1997; Parker and Pearson, 2021). Available age constraints indicate that exhumation

above structures of the Laramide belt in Montana began as early as ~120-80 Ma (Carrapa et al., 2019; Garber et al., 2020; Orme, 2020), considerably earlier than the deformation of the classic Laramide province (<75 Ma; Armstrong, 1968; Dickinson, 1988; Heller and Liu, 2016; Copeland et al., 2017; Lawton, 2019) and contemporaneous with deformation in the adjacent Sevier belt (e.g., Wiltschko and Dorr, 1983; Burtner and Nigrini, 1994; Kalakay et al., 2001; Hansen and Pearson, 2016; Garber et al., 2020; Rosenblume et al., 2021). Therefore, unlike the Nevada-Utah-Wyoming segment of the North American Cordillera, distinct structural domains cannot be assigned in map view for the Montana-Idaho fold-thrust belt on the basis of either structural style, relative age, or absolute age and thus distinguishing between the “Sevier” and “Laramide” orogenies has little utility in this region (Kulik and Schmidt, 1988; Parker and Pearson, 2021). Further, these lines of evidence suggest that the range of structural styles observed in the Idaho-Montana segment of the Sevier-Laramide fold-thrust belt—similar to other global orogenic belts (e.g., Lacombe and Bellahsen, 2016)—formed during progressive deformation, with kinematic linkages between thin- and thick-skinned structures (Kulik and Schmidt, 1988; Lacombe and Bellahsen, 2016; Lescoutre and Manatschal, 2020; Parker and Pearson, 2021; Tavani et al., 2021).

Overlapping and kinematically linked thin- and thick-skinned structures have been described for many global orogenic belts, with structural style best described along a continuum between thin- and thick-skinned endmembers (Lacombe and Bellahsen, 2016; Pfiffner, 2017; Butler et al., 2018). Thin-skinned thrusts generally have a low-angle décollement that follows weak sedimentary rocks of the upper crust (e.g., Bally et al., 1966; Dahlstrom, 1970; Boyer and Elliott, 1982). Thick-skinned thrusts cut across primary lithologic contacts (i.e., mechanical basement) at moderate to high angles, with décollements in the middle crust or deeper (e.g.,

Blackstone, 1940; Smithson et al., 1979; Allmendinger et al., 1987; Kulik and Schmidt, 1988; Erslev, 1993; Lacombe and Bellahsen, 2016; Pfiffner, 2017; Groshong and Porter, 2019). Like thin-skinned thrusts, thick-skinned thrusts and related folds can be balanced and restored using kinematic models to remove translation and rotation of fault blocks (e.g., Coward, 1983; Erslev, 1986, 1991, 1993; Stone, 1993; Groshong and Porter, 2019). Therefore, balanced and restored cross sections may employ both thin- and thick-skinned geometries in order to present viable kinematic models that link a wide range of structural styles with an integrated shortening history (e.g., Cristallini and Ramos, 2000; Molinaro et al., 2005; Scisciani and Montefalcone, 2006; Mouthereau et al., 2007; Lacombe and Bellahsen, 2016; Le Garzic et al., 2019; Smeraglia et al., 2021).

In the U.S. Cordillera, thin-skinned thrusts of the Sevier belt are recognized to have accommodated high-magnitude horizontal shortening of the North American crust during subduction of the steeply-dipping Farallon oceanic plate from Late Jurassic to Late Cretaceous time (e.g., DeCelles, 2004). In contrast, many workers have considered thick-skinned thrusts of the classic Laramide belt to have formed following a transition to flat-slab subduction (e.g., Coney and Reynolds, 1977; Dickinson and Snyder, 1978; Jordan and Allmendinger, 1986). The apparent coincidence in time between the inception of shallow subduction beneath the southwestern U.S. Cordillera and initiation of thick-skinned thrusts of the Laramide belt has prompted workers to hypothesize that Laramide tectonism also involved a change in the mechanism of stress transfer from the downgoing to the upper plate (e.g., Bird, 1984). A host of geodynamic models involving end-loading, basal traction, and/or weakening of the overlying plate during flat slab subduction are often invoked to explain the transition from thin- to thick-skinned deformation (e.g., Bird, 1984; Erslev, 1993; Jones et al., 2011). However, the spatial and

temporal overlap, as well as the observed continuum in structural style of thin- and thick-skinned thrusts in several localities along the North American Cordillera—including in the Idaho-Montana fold-thrust belt (Kulik and Schmidt, 1988; Parker and Pearson, 2021) and the Mexican fold-thrust belt (Fitz-Díaz et al., 2018; Williams et al., 2020)—obviate the need for a change in plate boundary geodynamics alone to explain the transition in structural style and instead suggest that the transition in structural style resulted from propagation of the fold-thrust belt into a heterogeneous stack of pre-thrusting strata. Further, only a few workers (Kulik and Schmidt, 1988; McClelland and Oldow, 2004) have attempted to integrate the Sevier and Laramide thrust systems into a kinematically linked fold-thrust belt. Integrating the Idaho-Montana fold-thrust belt into one fold-thrust system with varying structural styles is not only warranted by field observations (Parker and Pearson, 2021), but is also a promising approach for providing a descriptive and predictive kinematic model of how strain is accommodated within and transferred between the upper and middle crust in the absence of major changes in plate boundary geodynamics.

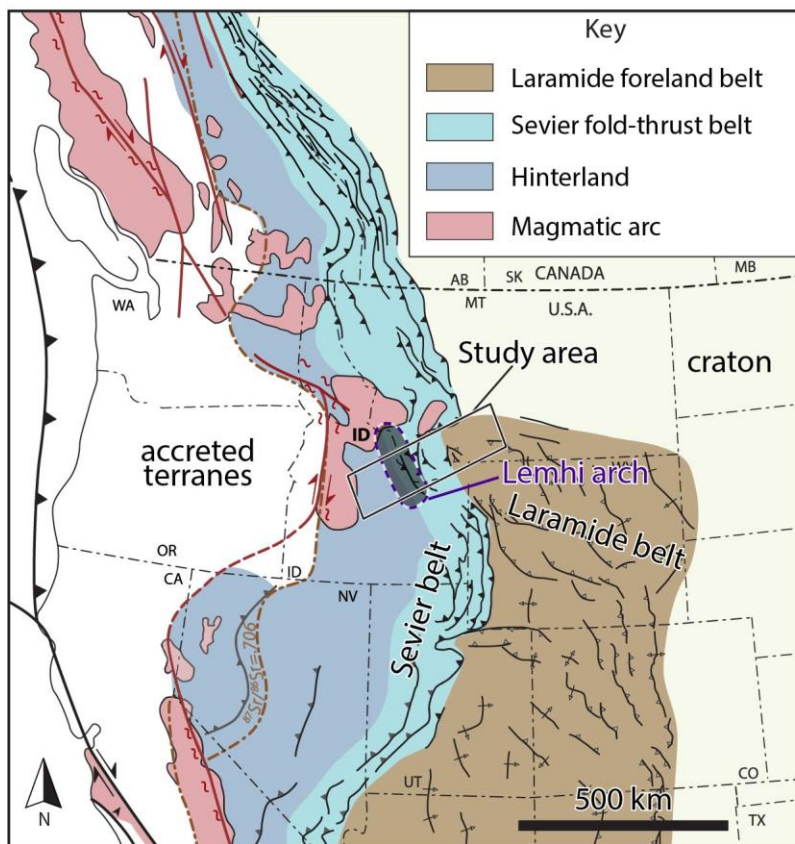


**Figure 1.** Overview map of the study area and structural domains of the North American Cordillera (modified from Yonkee and Weil, 2015).

Observations from the study area (Kulik and Schmidt, 1988; McClelland and Oldow, 2004; Parker and Pearson, 2021) and many continental fold thrust belts around the world (e.g., Allmendinger and Gubbels, 1996; Kley et al., 1999; Pearson et al., 2013; McGroder et al., 2015; Yonkee and Weil, 2015; Fitz-Díaz et al., 2018; Martínez et al., 2020; Williams et al., 2020) suggest that variations in fold-thrust belt structural style largely reflect deformation of variable crustal rheologies (Lacombe and Bellahsen, 2016; Pfiffner, 2017; Butler et al., 2018). In this

contribution, we present the first balanced and restored cross section that spans the interior, thin-skinned fold belt of the hinterland to the end-member thick-skinned uplifts of the foreland, encompassing the full range of structural domains in the North American Cordillera (Fig. 1). In doing so, we present an internally consistent kinematic model that suggests that variations in structural style are largely controlled by the prior distribution of sedimentary cover rocks which limit the availability of detachment horizons in the upper crust. From this model, we offer hypotheses regarding the relative timing of activity and shortening magnitudes of particular thrusts and the Idaho-Montana fold-thrust belt as a whole. Not only do our results fill a significant gap in the history of the North American Cordillera, but they also test recent models (e.g., Lacombe and Bellahsen, 2016; Parker and Pearson, 2021; Tavani et al., 2021) that describe the process by which strain is transferred from the upper to the middle crust during shortening of former rift margins, thereby producing self-organized changes in structural style and irregular space-time patterns. Adding to the growing body of observations that constitute the empirical basis for these models (e.g., Tavani et al., 2021), our results suggest that strain was first accommodated within brittle sedimentary cover rocks in the upper crust of the Laurentian passive margin, followed by a downward step in the basal décollement to the middle crust of the underlying and adjacent continental crust as deformation progressed past the rifted margin and toward the continent interior. Our simple model builds upon decades of work in the Sevier and Laramide belts by linking them together as a kinematically balanced section, allowing for a discussion regarding the role that rheology plays in determining not only the style but also the spatio-temporal patterns of orogenic wedges, without requiring particular events at the plate margin.

## **GEOLOGIC BACKGROUND**

### **Structural style and stratigraphic control**

The study area lies within the North American Cordillera, an Andean-style orogenic belt that records major horizontal shortening during Late Jurassic to Eocene ocean-continent subduction (e.g., Armstrong, 1968; Burchfiel and Davis, 1972, 1975; DeCelles, 2004; Dickinson, 2004; Yonkee and Weil, 2015). The structural style of the Sevier fold-thrust belt is widely described as thin-skinned because in general décollements follow stratigraphic contacts within rift and passive margin strata (Armstrong, 1968; Royse et al., 1975; Royse, 1993; Yonkee and Weil, 2015). Micaceous and fine-grained rocks of the Neoproterozoic to Cambrian Laurentian rift margin are particularly important detachment horizons throughout much of the Sevier fold-thrust belt (e.g., O'Brien, 1960; Armstrong and Oriel, 1965; Armstrong, 1968; Dahlstrom, 1970; Royse et al., 1975; Coogan, 1992; McMechan, 2001; DeCelles and Coogan, 2006; Yonkee et al., 2019). Though correlative Neoproterozoic to Cambrian rocks are present in the southwestern part of our study area in central Idaho, they are thinner along our transect and are completely missing across a significant unconformity farther to the northeast in east-central Idaho and southwestern Montana (e.g., Sloss, 1954; Scholten, 1957; Ruppel, 1986; Lund et al., 2003; Brennan et al., 2020). This distribution of strata highlights a prominent “basement” high within the retroarc fold-thrust belt, termed the Lemhi arch (Sloss, 1954), that was inherited from the Neoproterozoic to Ordovician rift margin and is overlain by thin passive margin strata (Fig. 2; Scholten, 1957; Ruppel, 1986; Lund et al., 2010; Grader et al., 2017; Link et al., 2017a; Brennan et al., 2020). This abrupt transition across variably extended continental crust of the craton had an impact not only on the thickness, facies, and stratigraphy of the rift to passive margin

succession (Lund et al., 2010; Yonkee et al., 2014; Brennan et al., 2020), but also on the structural style of the younger Idaho-Montana fold-thrust belt (Parker and Pearson, 2021).

The influence of the Lemhi arch on later fold-thrust geometry is best inferred from classifying the geometry of thrusts, from thin- to thick-skinned, and comparing their distribution to the stratigraphy (Parker and Pearson, 2021). Cross-cutting relationships between thin- and thick-skinned thrusts are well documented throughout the Idaho-Montana fold-thrust belt (e.g., Lopez and Schmidt, 1985; Skipp, 1988; Perry et al., 1988; Schmidt et al., 1988; Tysdal, 1988; McDowell, 1997; Parker and Pearson, 2021). Archean and Paleoproterozoic gneisses and schists of the Dillon block of the Wyoming craton (e.g., Condie, 1976), as well as Mesoproterozoic quartzites of the Lemhi sub basin (Ruppel, 1975) behave as mechanical basement, resulting in a more thick-skinned structural style that coincides with the basement-high of the Lemhi arch (Parker and Pearson, 2021). End-member thin- and thick-skinned thrusts do not delineate distinct domains in map view, but instead constitute a double-decker system with thin-skinned thrusts above the Lemhi arch and thick-skinned thrusts within it (Parker and Pearson, 2021). Similar geometries have been documented in many other fold-thrust belts globally (Lacombe and Bellahsen, 2016; Pfiffner, 2017; Tavani et al., 2021), including places like Taiwan and the Zagros that were original type localities for developing critical taper theory (e.g., Davis et al., 1983), but are now interpreted as having structurally underlying, thick-skinned components (Hung et al., 1999; Yang et al., 2001; Molinaro et al., 2005; Lacombe and Mouthereau, 2002; Mouthereau et al., 2006; Sherkati et al., 2006; Mouthereau et al., 2007; Mouthereau et al., 2012; Allen et al., 2013; Lacombe and Bellahsen, 2016; Le Garzic et al., 2019; Tavani et al., 2021). This double-decker geometry suggests kinematic compatibility between a range of structural styles and a model of progressive deformation that is controlled by the availability of weak

sedimentary cover rocks (Parker and Pearson, 2021) and/or the rheology of the crust inherited from its earlier development as a rifted continental margin (Lacombe and Bellahsen, 2016; Lescoutre and Manatschal, 2020; Tavani et al., 2021).

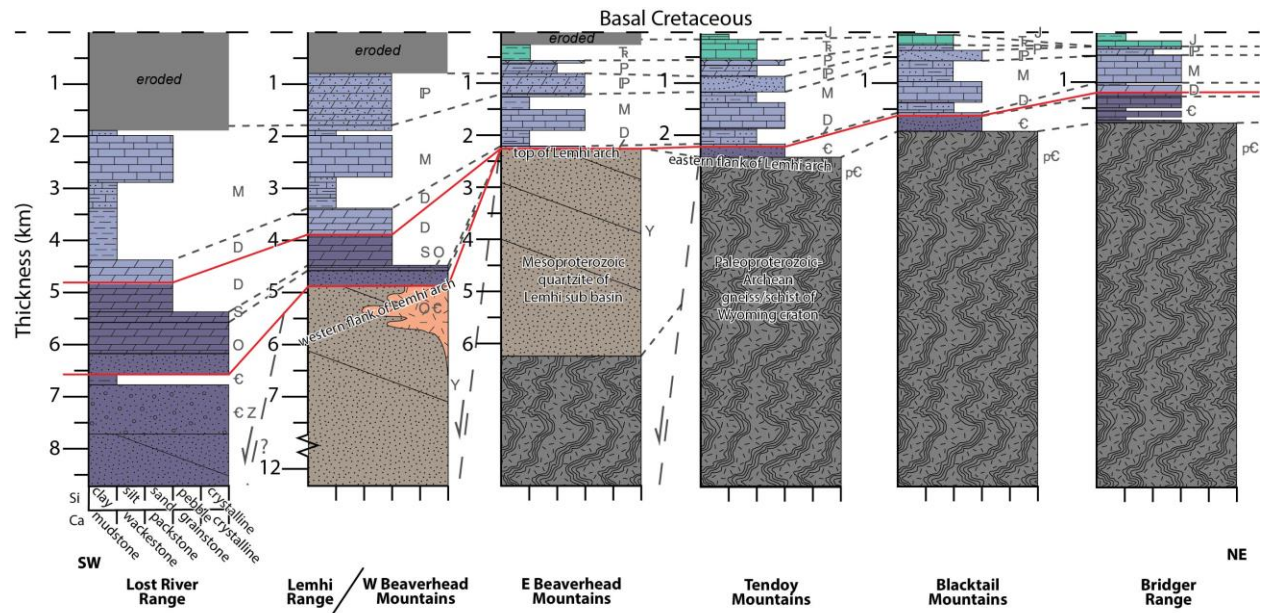


**Figure 2.** Generalized lithostratigraphic columns across the Idaho-Montana fold-thrust belt (see Plate 1 for locations). Red lines show sub-Ordovician and intra-Devonian Lemhi arch unconformities (Grader et al., 2017), with angular unconformities shown where appropriate. Lithologies and grain sizes for siliciclastic (Si) and carbonate (Ca) units are shown on x-axis. Green represents Mesozoic units; blue represents passive margin strata that are continuous above the Lemhi arch; pink represents rift and passive margin strata that pinch out against the Lemhi arch; tan represents quartzite-dominated western flank of the Lemhi arch; gray represents crystalline basement of the Wyoming craton. Approximate thicknesses are shown below a datum at the base of Cretaceous strata (or younger rocks, depending on erosion level). Generalized correlations of time periods and inferred normal faults are shown as dashed lines.

### **Existing constraints on the timing of thrusting**

Potential kinematic models must satisfy the independently-constrained, relative and absolute timing of thrusting in the study area. From the available age constraints along-strike elsewhere in the North American Cordillera (e.g., Wiltschko and Dorr, 1983; Harlan et al., 1988; Burtner and Nigrini, 1994) and the theoretical framework of critical taper theory (Davis et al., 1983; Dahlen et al., 1984; Dahlen, 1984, 1990; DeCelles and Mitra, 1995; Price, 2001), prior workers hypothesized that the Idaho-Montana fold-thrust belt generally progressed toward the foreland as a simple in-sequence system (Fig. 3, DeCelles, 2004). Limited existing evidence of out-of-sequence deformation comes from ~85 Ma initial activity within the thick-skinned Blacktail-Snowcrest uplift (Perry et al., 1983; Nichols et al., 1985) and cross-cutting relationships within the basement-involved Cabin thrust (Skipp, 1988), followed by cessation of thrusting by Eocene time (Harlan et al., 1988). More recent work—particularly from foreland basin strata in southwestern Montana—has further refined timing constraints for the Idaho-Montana fold-thrust belt and suggests that orogenesis had already resulted in exhumation down to lower Paleozoic levels by 145 Ma (Rosenblume et al., 2021) and continued to after ca. 66 Ma (Garber et al., 2020).

The oldest definitive foredeep deposit in the Idaho-Montana fold-thrust belt, the ca. 145-110 Ma Kootenai Formation, contains detritus interpreted to be shed from uplifted and exhumed Ordovician to Mississippian rocks carried by active thrusts west of the Lemhi arch in central Idaho (Rosenblume et al., 2021). The provenance of the overlying ca. 110-105 Ma Blackleaf Formation suggests continued shortening and unroofing down to Cambrian stratigraphic levels (Rosenblume et al., in prep.), with an episode of thrusting that exhumed Triassic to Permian sources likely in east-central Idaho above the Lemhi arch (Gardner, 2021). Independent

constraints on activity along the Pioneer thrust, which occurs west of the Lemhi arch in central Idaho (Plate 1), suggest that it is clearly older than a ~97 Ma pluton that cuts it (Montoya, 2019). Up to 2 km of volcanoclastic mudstones to sandstones and conglomerate of the ca. 95-85 Ma Frontier Formation (Dyman et al., 2008) record advancement of the thrust system and increased sedimentation (Rosenblume et al., in prep). The Frontier Formation is interpreted to have been sourced from western sources in the Idaho batholith, but also records exhumation of ca. 1.38 Ga intrusions and Belt basin quartzites of the Lemhi arch, eastern sources in Pennsylvanian/Permian strata, and proximal strata above the basement-involved Blacktail-Snowcrest uplift (Rosenblume et al., in prep); this signifies exhumation of deeper rocks within a broad region of the Idaho-Montana fold-thrust belt and is interpreted to reflect a downward shift in the basal décollement horizon. The overlying Beaverhead Group records additional unroofing of the Blacktail-Snowcrest uplift from ~83-81 Ma, but also contains >3 km of limestone and quartzite conglomerates sourced from proximal thrust sheets between ca. 83 and 66 Ma (Ryder and Scholten, 1973; Nichols et al., 1985; Perry et al., 1988; Garber et al., 2020). Available low-temperature thermochronological data from the Poison Creek and Hawley Creek thrusts, which are often interpreted as the western trailing edge of the Sevier belt (e.g., DeCelles, 2004; Yonkee and Weil, 2015), yield surprisingly young dates with calculated mean ages of ~68 and 85 Ma respectively (Hansen and Pearson, 2016; Kaempfer et al., 2019). The Tendoy thrust deforms ~83 Ma Beaverhead Group in its hanging wall and ~70 Ma Beaverhead Group in its footwall (Perry et al., 1988; Garber et al., 2020). These observations suggest similar ages for thrusts on the trailing and leading edge of the Sevier belt in Idaho-Montana. Documented crosscutting relationships give additional evidence of out-of-sequence thrusting (Skipp, 1988; Perry et al., 1988; Tysdal, 1988; McDowell, 1997; Parker and Pearson, 2021). While it remains unclear

whether or not foreland basin deposition near the Tendoy Range continued into Paleocene time (Perry et al., 1988; Haley et al., 1991; Garber et al., 2020), foreland uplifts of the Laramide belt were clearly active until 56 Ma in the Madison Range (DeCelles et al., 1987) and 53 Ma in the Bridger Range (Lageson, 1989). These observations are compatible with a general in-sequence progression of the Idaho-Montana fold-thrust belt from Early Cretaceous to early Late Cretaceous time, followed by apparently overlapping ages between thrust activity in the hinterland to the foreland, which suggests significant out-of-sequence fold-thrust belt behavior during Late Cretaceous time (Perry et al., 1988; Garber et al., 2020). Ongoing work will further constrain the timing of exhumation above individual thrusts (e.g., Kaempfer et al., 2019).

### **Prior shortening estimates within the study area**

The magnitude of horizontal shortening in the Idaho-Montana fold-thrust belt is poorly constrained. The most complete available (unbalanced) cross section (Skipp, 1988) interpreted a narrow (~50 km wide) Sevier belt, with several mapped thrusts between the hinterland and the foreland. These thrusts include (from west to east): the Poison Creek-Baby Joe Gulch-Hawley Creek, Fritz Creek, Cabin, Medicine Lodge-Four Eyes Canyon, and Tendoy thrusts (Lucchitta, 1966; Perry and Sando, 1982; Skipp, 1988, 1988; Perry et al., 1988; 1989; M'Gonigle, 1993, 1994; Schmitt et al., 1995; Lund, 2018; Parker and Pearson, 2021). Skipp (1988) interpreted these thrusts as a system of imbricated, basement-involved thrusts that accommodated <10 km of shortening on individual thrusts; the Medicine Lodge thrust is the only regional-scale thrust that was described as a simple thin-skinned thrust lacking basement involvement and was hypothesized to have accommodated nearly all (~40 km) of the shortening along the transect (Skipp, 1988). Altogether, Skipp (1988) estimated >50 km overall shortening in this region. Truncation of shallower thrusts by the deeper Cabin thrust (Skipp, 1988), as well as similar

cross-cutting relationships documented between the deeper Baby Joe Gulch and overlying Thompson Gulch thrusts (Parker and Pearson, 2020, 2021), requires at least two detachment horizons were activate at different times. West of these mapped thrusts, in the southern Beaverhead Mountains and Lemhi Range, km-scale recumbent folds (White Knob fold belt of Hait, 1965; Beutner, 1968) suggest that considerable amounts of shortening may have been accommodated by large-wavelength (>15 km) folding in the hinterland.

Whereas only ~50 km of shortening was hypothesized for the Idaho-Montana fold-thrust belt (Skipp, 1988), documented minimum shortening magnitudes are >200 km in the foreland fold-thrust belt of northwestern Montana and Alberta (Bally et. al., 1966; Price and Mountjoy, 1970; Price, 1981; Fermor and Moffat, 1992; McMechan and Thomas, 1993), >160 km in the Sevier belt of southeastern Idaho (Royse et al., 1975; Royse, 1993; Camilleri et al., 1997), >105 km in the Charleston-Nebo salient of north-central Utah (Constenius et al., 2003), and >240 km in the Sevier belt of central Nevada and Utah (DeCelles et al., 1995; Currie, 2002; DeCelles and Coogan, 2006; Long, 2015). These shortening estimates only consider the “Sevier fold-thrust belt” portion of the Cordillera, which appears to be balanced by folding in adjacent regions closer to the plate margin (e.g., Long, 2015), often referred to as the “metamorphic belt” (e.g., DeCelles, 2004) or “hinterland” (e.g., Yonkee et al., 2019). When considering the entire retroarc, the Sevier fold-thrust belt is thought to have accommodated at least ~350 km where it is well-studied (DeCelles and Coogan, 2006; DeCelles, 2012; Evenchick et al., 2007). Folded hinterland domains, like the study area between the Pioneer and Hawley Creek thrusts (Plate 1), generally lack surface exposures of large thrust faults, have very low relief, and often consist of fold trains in thicker and partly metamorphosed sedimentary rocks of the shelf-slope transition (e.g., Taylor et al., 2000; Long et al., 2014; Long, 2015). From these observations elsewhere in the Cordillera,

it is likely that ~100-300 km of undocumented shortening may have been accommodated in the study area by integrating the hinterland, Sevier, and Laramide belts.

### **Double-decker model for the Idaho-Montana fold-thrust belt**

Within the Idaho-Montana fold-thrust belt, a thin-skinned fold-thrust belt structurally overlies a deeper, thick-skinned fold-thrust belt, which is the basis for the double-decker model proposed by Parker and Pearson (2021). In this model, an irregular distribution of pre-thrusting stratigraphy across the Lemhi arch “basement” high was shortened by an early (pre ~90 Ma), upper thin-skinned system and was later overprinted by a lower thick-skinned system that shortened the entire package, including the underlying basement high. According to this model, thin- and thick-skinned thrusts of the entire Idaho-Montana fold-thrust belt behaved similarly to a critically tapered wedge, which generally propagated toward the foreland, but with a frontal basal décollement that stepped structurally downward with progressive deformation. As the frontal décollement stepped down into quartzites and crystalline basement rocks below rift and passive margin strata of the western Laurentian margin, within and east of the Lemhi arch the structural style transitioned toward thick-skinned. While the model of Parker and Pearson (2021) focuses on the distribution of weak sedimentary rocks, other recent models attribute the progressive transition from thin- to thick-skinned thrusting to involvement of viscous weak layers in the middle and lower crust, which vary laterally along with the crustal thickness inherited from the former rift margin (Lacombe and Bellahsen, 2016; Tavani et al., 2021). The Idaho-Montana fold-thrust belt provides a suitable place to develop models that link a variety of structural styles to a single progressive kinematic history and investigate the role that rheological differences in the brittle upper crust and plastic middle crust play in modifying the geometry and

tempo of the growing wedge. In order to investigate these topics, specific testable hypotheses are needed, in the form of viable kinematic models.

## **Stratigraphy**

Pre-orogenic stratigraphy of the study area is mostly composed of Neoproterozoic and Paleozoic rift and passive margin strata that thin eastward onto the Lemhi arch and continental shelf of southwestern Montana. The Lemhi arch basement high (Scholten, 1957) consists of Mesoproterozoic quartzites of the Lemhi sub basin (Umpleby, 1917; Ruppel, 1975), crystalline basement rocks of the Wyoming craton (Condie, 1976), and felsic intrusions of Mesoproterozoic (ca. 1.38 Ga; Evans and Zartman, 1990), Neoproterozoic (ca. 650 Ma; Lund et al., 2010), and Cambro-Ordovician age (ca. 500 Ma; Lund et al., 2010; Link et al., 2017a). As a result of Mesoproterozoic to Ordovician extensional faulting, the upper crust of the Lemhi arch is composed mostly of crystalline basement on its inboard (northeastern) flank (M'Gonigle, 1993, 1994; Dubois, 1982), with a few kilometers of overlying quartzite near its apex (Tysdal, 2002), and predominantly quartzite on its western flank with crystalline basement rocks at depth (Link et al., 2017b) in the plastic middle to lower crust.

A sub-Ordovician unconformity marks the top of discontinuous Neoproterozoic to Cambrian rocks on the flanks of the Lemhi arch, the base of which likely acts as a décollement (Montoya, 2019). This ~2.5 km thick rift-to-drift succession can be correlated with thicker and more stratigraphically complete sections along-strike in central and southeastern Idaho (Trimble, 1976; Link et al., 1987; Brennan et al., 2020), where they lie on crystalline basement and serve as the décollement to the fold-thrust belt in the Wyoming salient (Royse et al., 1975). Above the sub-Ordovician unconformity, a mostly carbonate Ordovician to Devonian passive margin succession pinches out against the flanks of the Lemhi arch from both sides. The sub-Ordovician

unconformity rests on (middle?) Cambrian strata near the White Knob Mountains and Lost River Range (Montoya, 2019; Brennan et al., 2020; Milton, 2020) but is strongly angular and underlain by Mesoproterozoic quartzites in the Lemhi and Beaverhead Ranges (Scholten, 1957; Scholten and Ramspott, 1968; James and Oaks, 1977; Ruppel 1986; Hansen and Pearson, 2016; Pearson and Link, 2017; Link et al., 2017a; Parker and Pearson, 2020), implying a pre-Ordovician normal fault between the two. The thickness of Ordovician to Devonian strata varies laterally near the Lemhi arch, as they ultimately either pinch out against or are cut by another normal fault in the Beaverhead Mountains (Grader et al., 2017; Parker and Pearson, 2021). The lateral discontinuity of these Neoproterozoic to Devonian rocks against the Lemhi arch disrupts the décollement of the Cordillera.

A regionally extensive intra-Devonian unconformity marks the top of the Lemhi arch (Grader et al., 2017), with laterally continuous shales and silty carbonate rocks above acting as a décollement (Skipp, 1988; Parker and Pearson, 2021). Whereas the upper part of the Devonian section is very thin, the overlying Mississippian section is a much thicker carbonate sequence constructed on the edge of the craton (Rose, 1976), becoming very thick and dominated by fine-grained siliciclastic rocks in the lower part of the section in the Lost River Range, northeast of the active highlands of the Antler orogeny (e.g., Sandburg, 1975; Wilson et al., 1994; Link et al., 1996). Detachment and fault-propagation folds (Fig. 3) commonly exploited fine-grained shales and silty limestones at the base and near the top of the Mississippian section (e.g., McGowan Creek, Middle Canyon, Lodgepole, Big Snowy, Railroad Canyon, and Lombard formations; Messina, 1993; Fisher and Anastasio, 1994; Anastasio et al., 1997). As a result, mixed carbonate and siliciclastic Mississippian and Pennsylvanian strata are often observed in impressive fold trains and in the hanging walls of thrusts (Hait, 1965; Beutner, 1968; Little and Clayton, 2017).

Mesozoic and earliest Cenozoic rocks that pre-date and are contemporaneous with shortening in the Idaho-Montana fold-thrust belt are nearly absent from the Idaho segment, making their influence on structural style unclear. The overall thickness of Triassic and Jurassic strata is insignificant at the scale of the cross section (Fig. 2), but available drill logs in the foreland suggest that these were important décollements (Gorder, 1960; Perry et al., 1981, 1983). Early Cretaceous foreland basin strata of the Kootenai and Blackleaf formations are relatively thin units (up to ~ 900 m thick), but also acted as décollements in the foreland (e.g., Brumbaugh and Hendrix, 1981; McBride, 1988; McDowell, 1997; Skipp et al., 2017). Overlying Late Cretaceous units are considerably thicker, forming kilometers-thick foreland basins adjacent to uplifts throughout the foreland (e.g., Ryder and Scholten, 1973; Haley, 1986; DeCelles et al., 1987; Haley et al., 1991; Vuke, 2020). Unfortunately, widespread erosion of Mesozoic and earliest Cenozoic rocks throughout much of the Idaho-Montana fold-thrust belt precludes a detailed analysis of the structural significance of these rocks in all but the foreland.

## **METHODS**

To constrain the relative timing and magnitude of shortening in the Idaho-Montana fold-thrust belt and develop a viable kinematic model, we created a regional-scale, area-balanced and restored cross section that spans most of the orogenic wedge, from the hinterland to the foreland. To our knowledge, this is the first balanced and restored cross section to integrate the Sevier and Laramide belts of the North American Cordillera. Available maps were compiled at 1:250,000 scale (see Plate 1 for references). Attitudes, contacts, available wells, sub-surface data, and published cross sections were projected onto the cross section line using Petroleum Experts' kinematic modeling software MOVE (see Plates 1 and 2 and supplementary material). Depths of burial estimated from maximum temperature results using Raman spectroscopy of carbonaceous

material (RSCM) (Parker and Pearson, in prep.) were projected to the cross section line and used to construct an approximate burial envelope to further constrain the cross section. Stratigraphic thicknesses used for segments of the cross section are shown in Fig 2. The cross section was originally hand drawn at 1:250,000 scale using accepted principles for creation of balanced cross sections (Dahlstrom, 1969) and then digitized, area balanced in detail, and progressively restored in MOVE. The simple shear module was used for all normal faults and for thrust faults with interpreted fault-bend folds. The fault-parallel flow module was used for thrust faults when fault-bend folds were lacking. A combination of forward and reverse modeling using the tri-shear module (Erslev, 1991) was used to approximately restore fault propagation folds. Detachment folds were schematically restored by pinning and unfolding contacts back to their original thickness. Forward modeling of the cross section used simple shear and fault parallel flow modules, but did not model folds in detail where independent constraints on folding variables were unavailable.

Normal faults were restored first along the cross section. When available, wells constrained the minimum thickness of hanging wall fill, allowing for more accurate hanging wall bed geometries to be inferred. Normal fault geometries were modeled in MOVE from hanging wall contacts when appropriate. An inferred décollement at 15 km below sea level (bsl) was used for all Basin and Range (post-Eocene) normal faults. This is consistent with the observed lowest extent of seismicity in the region (e.g., Richins et al., 1987; Smith et al., 1985). Based on the lowest elevation of the basement/cover contact inferred from drill logs (Perry et al., 1981, 1983; Dyman and Nichols, 1988), seismic reflection data (Lopez and Schmidt, 1985; McDowell, 1997; Johnson et al., 2005), and gravity models (Kulik and Schmidt, 1988), a regional basement/cover

elevation of ~ 4.5 km bsl was used in our restorations. A detailed description of criteria for constraining the regional basement-cover contact is included in the supplementary materials.



## **RESULTS**

### **Structural domains**

To gain a more complete understanding of the series of deformation events, we present our balanced and restored cross section at the 1:500,000 scale (Plate 2). Following convention, structures are grouped into structural domains based on structural style (see Fig. 1). These domains will be described from west to east (Plate 1, 2), before later presenting our model of progressive deformation in the following discussion. Specific descriptions and justifications for our interpretations are listed in the notes (Plate 1).

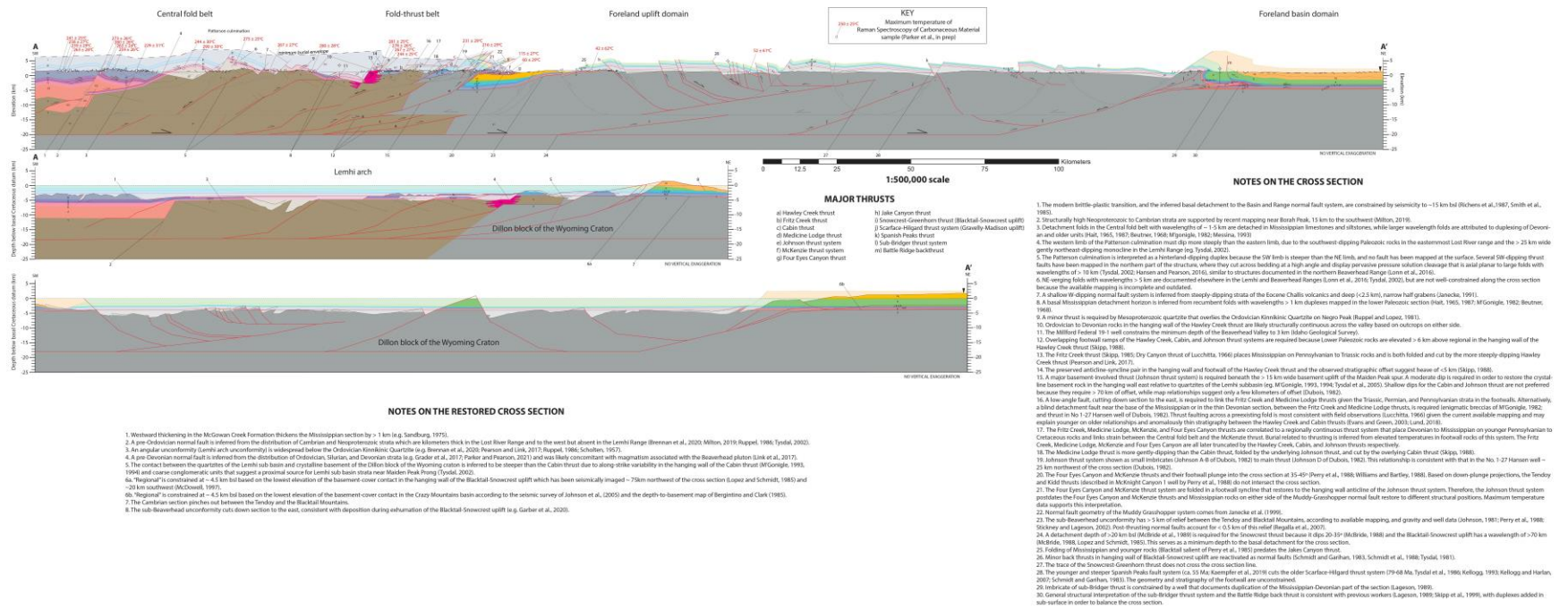


**Plate 2.** Area balanced and restored cross sections (see Plate 1 for accompanying map). Scale is 1:500,000. Note that the restored (undeformed) cross section is presented in two pieces. Maximum temperatures and burial estimates of Parker and Pearson (in prep) and approximate burial envelope are show

### *Central fold belt*

Between the Pioneer and Hawley Creek thrusts of east-central Idaho is a > 100 km wide zone consisting of folded Mesoproterozoic to Pennsylvanian strata that we will refer to as the central fold belt (hinterland on Fig. 1). While this region exhibits significant structural relief of up to ~10 km, it lacks surface exposures of thrust faults with significant (kilometers of) stratigraphic offset. The principal structures are the SE-plunging Patterson culmination (Janecke et al., 2000) that exposes Mesoproterozoic quartzites of the Lemhi arch in the Lemhi Range and a broad synclorium that exposes fold trains of primarily Mississippian and minor Pennsylvanian rocks in the Lost River Range. The wavelength of this 1<sup>st</sup>-order fold pair is at least ~70 km, suggesting a deep décollement/floor thrust in the middle crust. Smaller wavelength folds of a few kilometers to 5-10 km formed within overlying passive margin strata and suggest upper décollements (i.e., roof thrust) for the Patterson culmination near the intra-Devonian and sub-Ordovician unconformities (Fig. 3; Hait, 1965; Mapel, 1965; Beutner, 1968; Messina, 1993; Fisher and Anastasio, 1994; Anastasio et al., 1997). The Patterson culmination is interpreted as a hinterland-dipping duplex (Boyer and Elliott, 1982; Banks and Warburton, 1986), with the upper and lower décollement systems linked by a system of SW-dipping thrusts that cut across bedding of quartzites of the Lemhi sub-basin. Thus, we infer a linked upper and lower décollement, at the base of the overlying sedimentary cover rocks and within the middle crust of the Lemhi arch, for the central fold belt.

Both the upper and lower décollement appear to have been kinematically linked with the neighboring fold-thrust belt and foreland uplift domain. Detachment folds related to the upper décollement (Fig. 3) are upright to NE-verging in the Lost River Range, where they accommodated ~20% shortening (Anastasio et al., 1997; Messina, 1993); in the southern Lemhi

Range and Beaverhead Mountains, these folds are recumbent (Little and Clayton, 2017). Recumbent folds in the White Knob fold belt (Hait, 1965; Beutner, 1968; M'Gonigle, 1982), visible on the western side of the Beaverhead Valley, are apparently at the same structural and stratigraphic level as the Thompson Gulch-Fritz Creek thrust (Dry Canyon thrust of Lucchitta, 1966; Skipp, 1988, 1988; Parker and Pearson, 2021). This implies lateral continuity of the upper décollement that followed the intra-Devonian Lemhi arch unconformity. The lateral transition from open and upright folds to E- to NE-verging and recumbent folds suggests increasing components shear strain along the flat décollement, ultimately becoming a well-developed mylonite as the flat transitions to the ramp of the Thompson Gulch-Fritz Creek thrust (Parker and Pearson, 2021). Maximum temperatures along this datum constrain this décollement to a depth of at least ~6 km (Parker and Pearson, 2021, in prep). This demonstrates that shortening in the central fold belt was kinematically linked to the adjacent fold-thrust belt along the upper décollement, which is primarily at the base of the Mississippian, near the intra-Devonian unconformity, and marks the stratigraphically lowest laterally continuous strata above the Lemhi arch.

The lower décollement of the central fold belt fed slip to the upper décollement in the form of a duplex, and was contemporaneous with foreland uplifts that appear to have shared a mid-crustal décollement. The more steeply SW-dipping backlimb of the Patterson culmination suggests progressive rotation of hanging walls as deformation advanced in-sequence, with the spacing of the thrusts exceeding the magnitude of slip (e.g., McClay, 1992). In this interpretation, slip was fed from a deep mid-crustal décollement within the Lemhi arch to bedding-parallel detachment horizons above the Lemhi arch. Provenance studies in the Frontier Formation and Beaverhead Group infer a Mesoproterozoic source of detritus starting at ~ 90 Ma

(Garber et al., 2020; Rosenblume et al., 2021), suggesting that exhumation of the Patterson culmination was contemporaneous with exhumation and early uplift of the Blacktail-Snowcrest arch in the foreland uplift domain, >175 km away. Zircon helium (ZHe) data from quartzites within the Patterson culmination, ~ 15 km south of the cross section line, constrains cooling below ~180°C (Guenther et al., 2013) to  $87.7 \pm 5.4$  Ma (Fayon et al., 2017). Contemporaneous exhumation of the Patterson culmination and the Blacktail-Snowcrest uplift suggests that while most of the slip was fed from the lower to the upper décollement, a portion was transmitted a great distance through the middle crust of the Lemhi arch to the foreland uplift domain. In summary, while most of the shortening along the lower décollement was progressively linked to the upper décollement and ultimately the neighboring fold-thrust belt, a portion of the shortening on the lower décollement was kinematically linked to contemporaneous early uplift of the Blacktail-Snowcrest arch in the foreland uplift domain.

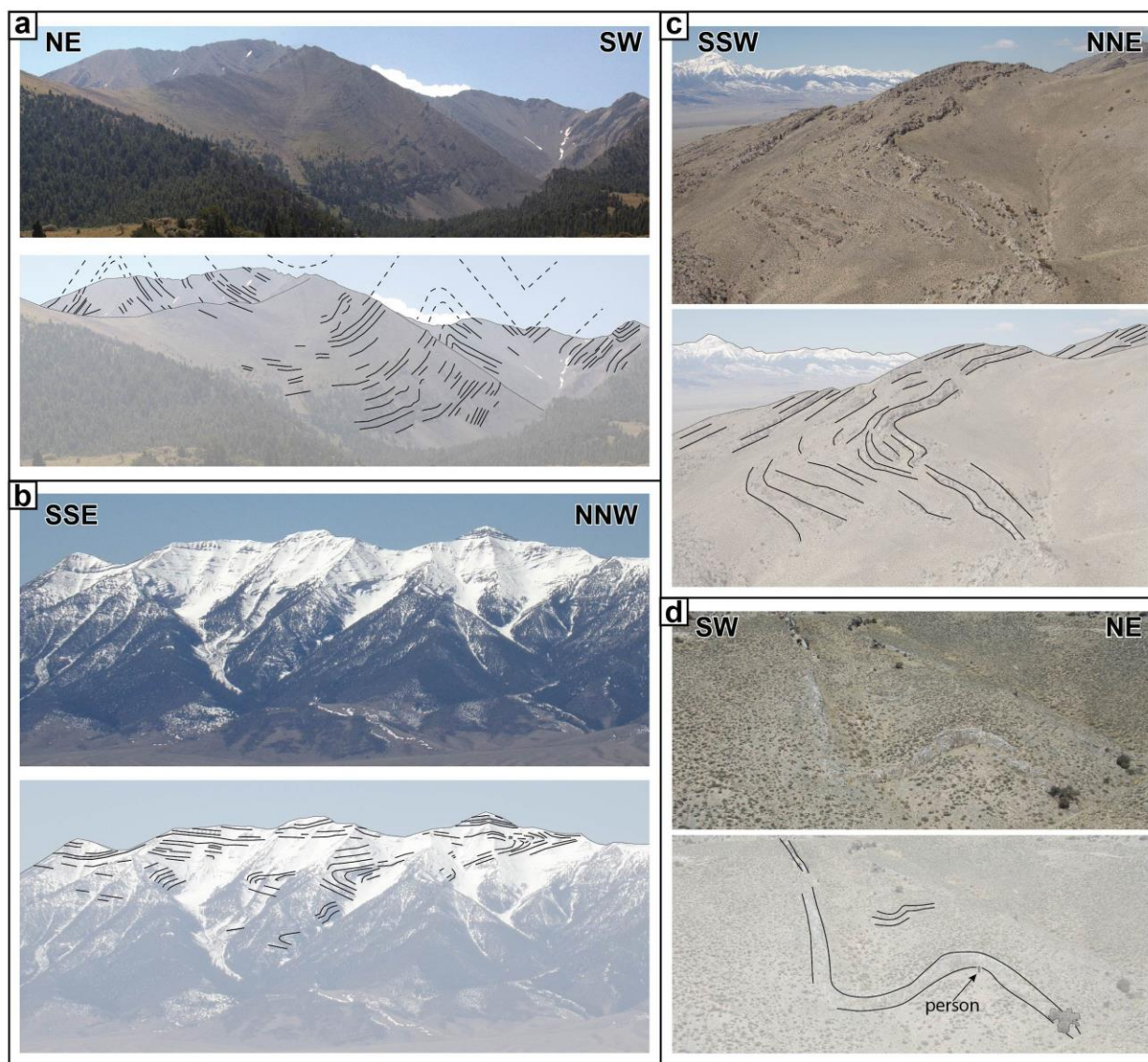


**Figure 3.** Outcrop photos and line drawings of folds within the Central fold belt (see Plate 1 for locations). **a)** Symmetrical, upright detachment folds in Mississippian carbonate rocks of the Lost River Range, viewed looking toward the southeast. Detachment horizon is in the McGowan Creek Formation. Approximately 1 km of topographic relief. **b)** Large recumbent folds in overturned Mississippian-Pennsylvanian carbonate rocks of the southern Lemhi Range, viewed obliquely looking toward the west-southwest. Flat-lying rocks on the summit are upside down. Approximately 1.3 km of topographic relief. **c)** NE-verging overturned syncline in

Mississippian carbonate rocks (Scott Peak and overlying Big Snowy formations) of the southern Beaverhead Mountains, viewed obliquely looking toward the west-northwest. Approximately 200 m of topographic relief in foreground. **d)** Folded basal contact of the Mississippian Big Snowy Formation, within hinge of overturned syncline in previous photo. The Big Snowy Formation acts as a regional detachment horizon. Person for scale in the hinge of the anticline.

### ***Fold-thrust belt***

In contrast to the central fold belt, numerous tightly-spaced thrust faults with significant stratigraphic offset occur in the Beaverhead and Tendoy mountains. Across the region, thrust faults (e.g., Thompson Gulch, Fritz Creek, Medicine Lodge, and McKenzie thrusts) shared a common décollement just above the intra-Devonian Lemhi arch unconformity, signifying strain compatibility with the central fold belt. Unlike the central fold belt, where deeper thrusts merge with this detachment horizon, mechanical basement-involved thrusts (Baby Joe Gulch, Hawley Creek, Cabin, and Johnson thrusts) in the fold-thrust belt domain truncated the overlying thrust system that is continuous above the intra-Devonian unconformity. The two classes of structures highlight upper and lower décollements that linked the adjacent central fold belt and foreland uplift domains.

***Upper décollement.*** The Thompson Gulch, Fritz Creek, Medicine Lodge, and McKenzie thrusts share an upper décollement that followed the intra-Devonian Lemhi arch unconformity with a frontal ramp exposed in the localized foreland basin of the Beaverhead Group between the Tendoy Mountains and Blacktail Mountains. Restoring slip on the later Hawley Creek, Cabin, and Johnson thrusts restores these thrusts to a continuous upper décollement, described previously. Field observations establish structural continuity between the Fritz Creek thrust (Dry Canyon thrust of Lucchitta, 1966) and the Thompson Gulch thrust, with both thrusts displaying

carbonate mylonite that cuts gently up section to the east in its footwall from the intra-Devonian unconformity to the Triassic (Parker and Pearson, 2020).

The Thompson Gulch, Fritz Creek, Medicine Lodge, and McKenzie thrusts have Devonian to Mississippian rocks in their hanging walls, but have a range of Pennsylvanian to Cretaceous rocks in their footwalls that constrain the approximate position of footwall ramps and flats. In the immediate footwall of the Thompson Gulch thrust, the basal Devonian contact is undeformed (Parker and Pearson, 2020), suggesting that the décollement has a footwall ramp between the correlative Fritz Creek thrust and the Medicine Lodge thrust. Whereas the footwall of the Fritz Creek thrust has Permian to Triassic rocks, the footwall of the Medicine Lodge thrust has Pennsylvanian rocks, suggesting the thrust cut down section in the direction of transport across a large fold in Mesoproterozoic quartzites (mapped by Ruppel, 1994). The alternative, that the Fritz Creek and Medicine Lodge thrusts represent two distinct ramps that branch off a shared décollement at the intra-Devonian unconformity, is not supported by field observations. A frontal footwall ramp from Pennsylvanian to uppermost Cretaceous strata is required between the Medicine Lodge and McKenzie thrusts, which both have the Four Eyes Canyon thrust in their footwall (Perry et al., 1988).

From these observations, we interpret the Thompson Gulch, Fritz Creek, Medicine Lodge, and McKenzie thrusts as a formerly integrated thrust system (referred to herein as the Medicine Lodge-McKenzie thrust system): The décollement of the Medicine Lodge-McKenzie thrust system was linked to the sub-horizontal upper décollement of the neighboring central fold belt, and likely cut across prior folds in the Beaverhead Mountains, and ultimately carried rocks above the intra-Devonian Lemhi arch unconformity to the surface along a frontal ramp in the Tendoy Mountains.

**Lower décollement.** Unlike the Central fold belt, where the lower décollement transferred slip to an upper décollement within a duplex, mechanical basement-involved thrusts rooted in the lower décollement (Baby Joe Gulch-Hawley Creek, Cabin, and Johnson) in the fold-thrust belt domain truncated the overlying upper décollement. Zircon helium dates of ~74 Ma and provenance matches after ~ 67 Ma suggest the Hawley Creek thrust was active at this time (Kaempfer et al., 2019; Garber et al., 2020). The Johnson thrust system crosscut the Medicine Lodge-McKenzie thrust system and deformed Beaverhead Group strata with maximum depositional ages of ca. 71 and 67 Ma (Garber et al., 2020), suggesting that it postdates all other deformation features. Therefore, these three thrusts likely deformed in-sequence and in quick succession.

The large wavelength of uplifted hanging walls, minimal shortening required for restoration, evidence of reactivation on the Hawley Creek thrust, moderate fault dips, and the piggy back relationship between the Cabin and Johnson thrusts, suggests that these thrusts are thick-skinned in style. Rocks in the hanging walls of the Baby Joe Gulch-Hawley Creek, Cabin, and Johnson thrusts are far above regional with structural lows in the Lost River Range, Beaverhead, and Tendoy Mountains, defining a wavelength of ~75 km. The hanging wall anticline of the Baby Joe-Hawley Creek thrust restores on the ~35° fault with ~3-4 km of heave (Parker and Pearson, 2021; Skipp, 1988), and changes in stratigraphy across the fault suggest reactivation of a normal fault (Parker and Pearson, 2021). The Johnson thrust must have a dip of  $\geq 10^\circ$ , based on map relationships, observed dips, and the fact that it is structurally beneath the Medicine Lodge-McKenzie and Cabin thrusts. These observations suggest a thick-skinned style, permissible with a mid-crustal décollement that is shared with the neighboring Patterson culmination and Blacktail-Snowcrest uplift (McBride et al., 1992). The alternative interpretation

of a thin-skinned fault geometry requires more than 70 km of slip on the Hawley Creek of Cabin thrust, and an entirely blind footwall flat that is not supported by any independent evidence. Our preferred interpretation of the Hawley Creek, Cabin, and Johnson thrusts as thick-skinned thrusts suggests that the Sevier and Laramide belts (Fig. 1) are not synonymous with thin- and thick-skinned styles but are kinematically linked by a décollement in the middle crust (O'Neill, 1990; McClelland and Oldow, 2004; Parker and Pearson, 2021).

### ***Foreland uplift domain***

The foreland uplift domain consists of widely spaced (>50 km) uplifts of variable orientation that exposed crystalline basement rocks of the Dillon block of the Wyoming craton. Our interpretations in this region are largely summaries of previous work (e.g., Schmidt and Garihan, 1983; Sheedlo, 1984; McBride, 1988; Schmidt et al., 1988; Lageson, 1989). The foreland basin domain basically consists of two overlapping thrust and back-thrust systems or “pop ups” (e.g., Erslev, 1993) that appear to have advanced in-sequence: the Blacktail-Snowcrest and Gravelly-Madison uplifts, and the Madison-Gallatin uplift (Fig. 3, Schmidt et al., 1988).

The cross section cuts obliquely through the Blacktail-Snowcrest and Gravelly-Madison uplifts, which likely had a more E-W transport direction according to available slickenside data (Schmidt and Garihan, 1983; Schmidt et al., 1988). For transport-parallel cross sections of the Blacktail-Snowcrest uplift, refer to McBride (1988) and Sheedlo (1984). A mid-crustal detachment depth of ~ 23-25 km bsl is suggested by the wavelength of the uplift, the observed dip of the thrust, and stratigraphic relationships that argue for and were used to constrain the geometry of a reactivated normal fault (McBride et al., 1992). The western backlimb of the Blacktail-Snowcrest uplift consists of a moderately dipping basement-cover contact with ~ 7 km of structural relief, which is cut by the sub-Beaverhead Group unconformity. Exhumation of the

Blacktail-Snowcrest uplift began between ca. 90-85 Ma and was well under way by 82 Ma (Nichols et al., 1985; Rosenblume et al., in prep; Garber et al., 2020), contemporaneous with shortening in the neighboring fold-thrust belt (e.g., Haley et al., 1991; McDowell, 1997; Perry et al., 1988; Schmidt et al., 1988). The Greenhorn-Snowcrest thrust system exhumed the Blacktail-Snowcrest uplift and transferred slip to numerous back thrusts (Schmidt and Garihan, 1983; Schmidt et al., 1988; Tysdal, 1981, 1988) and the underlying Scarface-Hilgard thrust system (Gravelly-Madison arch, Schmidt et al., 1993). Crosscutting igneous rocks and depositional ages of the Livingston Formation bracket the age of the Scarface-Hilgard thrust system between 79 and 69 Ma (Tysdal et al., 1986; DeCelles, 1987; Kellogg and Harlan, 2007). Contemporaneous deformation within the Patterson culmination, thick-skinned thrusts of the fold-thrust belt, and the Blacktail-Snowcrest and Gravelly-Madison arch at ~ 90-70 Ma supports the interpretation that all domains of the Idaho-Montana fold-thrust belt were kinematically linked by a mid-crustal (~25 km bsl) décollement at this time (Kulik and Schmidt, 1988; O'Neill et al., 1990; McClelland and Oldow, 2004).

The Madison-Gallatin uplift marks the front of the fold-thrust belt and is apparently younger than the Blacktail-Snowcrest and Gravelly-Madison uplifts because the back-verging Spanish Peaks fault (of the Madison-Gallatin uplift) truncates the Scarface-Hilgard thrust system (of the Gravelly-Madison arch, Schmidt and Garihan, 1983). Where best exposed, the Spanish Peaks thrust shows up to 5 km of stratigraphic offset (McMannis and Chadwick, 1964; Tysdal et al., 1986). The Cherry Creek thrust is smaller, with ~1.5 km of stratigraphic separation (McMannis and Chadwick, 1964) and a much smaller wavelength, suggesting that its detachment flattens at a few kilometers depth. The large wavelength of the Madison-Gallatin uplift, between the Spanish Peaks and sub-Bridger thrusts, is compatible with a mid-crustal décollement at ~25

km bsl. At the leading edge of the uplift, an east-verging overturned anticline/syncline pair with >7.5 km of relief is observed in the Bridger Range north of Bozeman, with no corresponding thrust mapped at the surface (e.g., Schmidt et al., 1988; Lageson, 1989). Only 10 km away, a drilled sub-surface thrust placed Devonian on Mississippian, ~2 km above regional, requiring at least two strands on the inferred sub-Bridger thrust (Lageson, 1989). The sub-Bridger thrust likely fed slip into the folded, syndeformational Crazy Mountains basin. The Battle Ridge back thrust accommodated tightening in the leading syncline and balanced bed-parallel thrusting of the sub-Bridger thrust, acting as a triangle zone (e.g., McClay, 1992; von Hagke and Malz, 2018) or tectonic wedge (Price, 1986). This interpretation follows that of previous workers (McMannis, 1955; Schmidt et al., 1988; Skipp et al., 1999; Lageson, 1989), who had slightly different subsurface interpretations. Zircon and apatite helium dates of ca. 55 Ma from the Spanish Peaks thrust (Kaempfer et al., 2019) and depositional ages of strata that pre- and post-date folding (Fort Union Formation and Absaroka-Gallatin volcanic field) in the Crazy Mountains basin (Harlan et al., 1988; Lageson, 1989; Vuke, 2020) brackets deformational ages to ca. 60-53 Ma. Therefore, out-of-sequence deformation at ca. 90-70 Ma was kinematically linked from the central fold belt to the pop-up trailing the Gravelly-Madison uplift by a mid-crustal décollement; deformation propagated in-sequence to the Madison-Gallatin pop-up, with a frontal ramp linking the décollement to the surface by a triangle zone in the deep Crazy Mountains foreland basin.

## DISCUSSION

### Shortening magnitudes

The presented balanced cross section restores along two principal detachment horizons, with an overall shortening magnitude of 244 km, or 36%. The upper décollement mostly followed the intra-Devonian unconformity atop the Lemhi arch and was fed slip from a ramp to the southwest. This upper décollement accommodated the bulk (~155 km or ~60%) of the total shortening. Incorporation of observed maximum temperatures and burial estimates (Parker and Pearson, in prep) suggests that a thicker (~ 6-8 km thick), southwestern section was thrust over a thin (~3-4 km) stratigraphic section overlying the Lemhi arch to the northeast. Our hypothesized linked Medicine Lodge-McKenzie thrust system, with a single thrust that acted as the décollement in the balanced restoration, requires a high magnitude of slip because the restored line length of the Mississippian strata observed in the hanging wall of the Four Eyes Canyon and McKenzie thrusts alone (~50 km) is greater than the distance between the nearest observed permissible footwall ramp (Thompson Gulch thrust, Parker and Pearson, 2021). The line length of Mississippian strata in the hanging wall of the Medicine Lodge-McKenzie thrust system requires it to restore west of the footwall ramp of the Fritz Creek thrust that marks the top of the Lemhi arch (correlative with Thompson Gulch thrust of Parker and Pearson, 2021; Skipp, 1988). Elsewhere in the Cordillera, individual, large-slip thrusts are observed linking folded hinterland regions to the foreland; for example the Willard (Yonkee et al., 2019), Canyon Range (DeCelles and Coogan, 2006), and Lewis thrusts (Sears, 2001; Fuentes et al., 2012) have shortening magnitudes of ~50, 100, and 150 km respectively. Our total shortening estimates of the upper system above the Lemhi arch (~155 km) and the system as a whole (244 km) are within the

range documented elsewhere within the North American Cordillera (e.g., DeCelles and Coogan, 2006; DeCelles, 2012; Evenchick et al., 2007).

### Forward kinematic model

The balanced and restored cross section, in conjunction with available age and depth constraints (Parker and Pearson, in prep) are the basis for a forward model that recreates the observed map patterns and interpreted subsurface geometries. The presented forward kinematic model (Fig. 4) will be described in four relative time steps, using the upper and lower décollements that have been described previously.

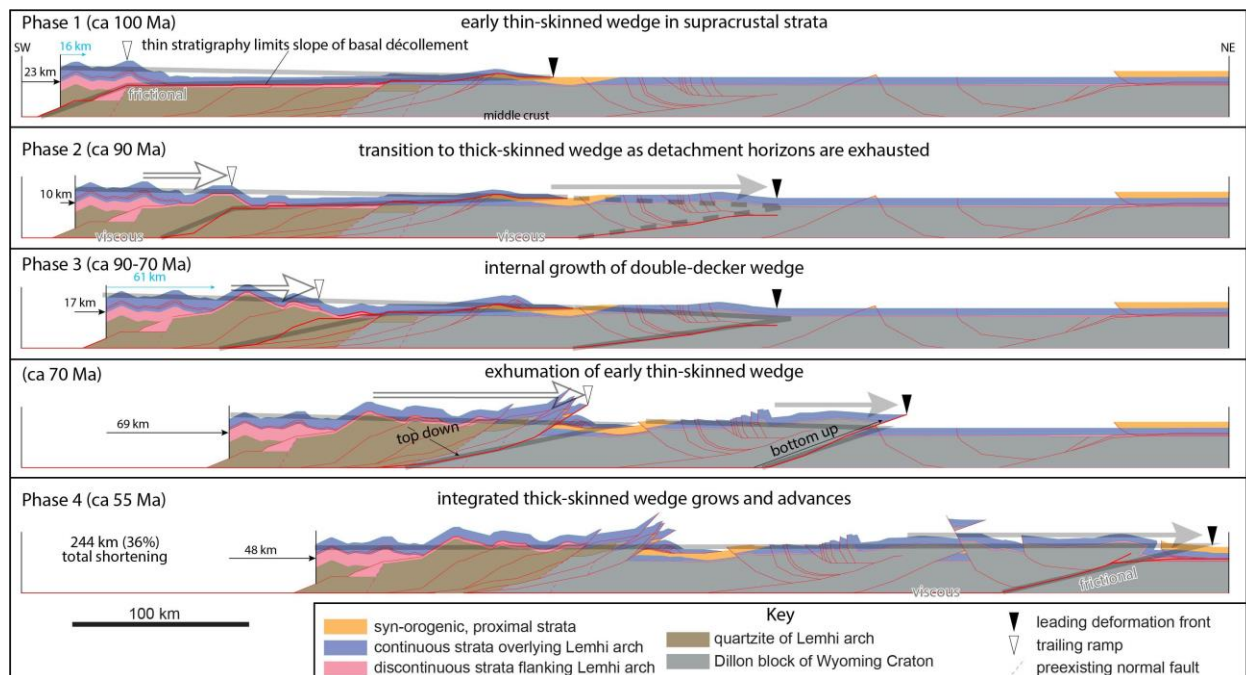


**Figure 4.** Forward kinematic model of the Idaho-Montana fold-thrust belt. Generalized wedge geometry is highlighted by gray line. Shortening magnitudes for each time step are shown for the upper and lower décollements and are labeled in blue and black, respectively. Arrows show advancement of the frontal and rear ramps.

### ***Phase 1***

Early deformation, which we call phase 1, accommodated a moderate amount of shortening (~40 km) on the upper décollement. A moderately dipping (~20°) ramp fed slip from detachments in the Mesoproterozoic and Neoproterozoic-Cambrian west of the Lemhi arch to the intra-Devonian unconformity that overlies the Lemhi arch. First-order folds were produced by fault-bend folding, whereas 2<sup>nd</sup>-order folds were formed by duplexes linking an intra-Devonian and sub-Mississippian detachment horizon. Smaller, 3<sup>rd</sup> order detachment folding along the sub-Mississippian detachment are not shown at this scale, but contribute to the overall thickness shown. Slip was transferred from these two detachment horizons to a single long thrust flat and then to a small ramp near the top of the Lemhi arch (Medicine Lodge-McKenzie thrust system), essentially doubling the thickness of the section above the thinnest part of the Lemhi arch (Parker and Pearson, in prep). A frontal ramp brought the hanging wall to the surface in the active foreland basin. The décollement geometry of the system avoided the Lemhi arch basement high by ramping through the thick package of Neoproterozoic to Cambrian strata west of the arch, then following the intra-Devonian unconformity along the western flank and over the top. As a result of the frictional décollement with this geometry, the wedge is very low-angle, which is consistent with the observed maximum temperature profile (Parker and Pearson, in prep). Unroofing and exhumation primarily occurred above the ramp west of the Lemhi arch, with sediment transported a long distance to the foreland during deposition of the Kootenai and Blackleaf formations between ~ 145-100 Ma (Rosenblume et al., 2021, in prep; Gardner, 2021).

### ***Phase 2***

A transitional phase began ca. 90 Ma as the basal décollement advanced by activating a deep décollement at ~25 km bsl. A ramp linked this deep décollement to the active upper

décollement above the Lemhi arch and fed slip to the front of the system in the form of a duplex. The first-order fold created above the blind ramp of the duplex represents the early Patterson culmination, which initiated before ~87-70 Ma (Fayon et al., 2017; Hansen and Pearson, 2016; Garber et al., 2020; Rosenblume et al., in prep). In effect, this accommodated internal thickening of the sub-critical wedge and increased taper angle as the décollement moved forward, cutting across bedding in quartzites within the western flank of the Lemhi arch. Internal thickening and increased basal slope angle resulted in a fold-thrust belt that resembled a super-critically tapered orogenic wedge, detached in the viscous middle crust. The viscous detachment efficiently transmitted the strain a great distance (consistent with modeling of Ruh et al., 2012; Borderie et al., 2018) through the Lemhi arch. As a result, exhumation of the Lemhi arch, above the Patterson culmination, coincided with early exhumation of the Blacktail-Snowcrest uplift in the foreland. In effect, the stratigraphy limited potential stratigraphic décollement geometries, making activation of a viscous mid-crustal décollement the most efficient way to advance the deformation wedge. The shift from a shallow frictional to a deep viscous décollement transferred strain through the Lemhi arch, giving the system an apparent bifurcation from one to two wedges as the scale of the structures increased drastically in response to the increased depth to detachment.

### ***Phase 3***

After the transitional phase, once strain was linked through the Lemhi arch by exploiting a weak layer in the viscous middle-crust, considerable (~85 km) shortening of the Lemhi arch itself occurred during phase 3 (~90-70 Ma), as well as continued shortening (~ 60 km) and exhumation of the overlying thin-skinned thrust system. After initiation of the Blacktail-Snowcrest uplift, the taper angle of the sub-critical wedge increased in the same way as before:

by advancing the upper décollement, thereby increasing the basal slope, and by internally shortening the wedge during out-of-sequence thrusting. As the Patterson culmination grew and the décollement migrated forward through the quartzite-dominated western flank of the Lemhi arch, hanging wall horses of formerly active thrusts were rotated toward the hinterland as slip was fed to the upper, thin-skinned décollement above the Lemhi arch. After the duplex propagated through the predominantly quartzitic western flank of the Lemhi arch, linking the upper and lower décollement, crystalline basement rock of the edge of the Dillon block was shortened by a series of tightly spaced in-sequence imbricate thrusts. Unlike the duplex of the Patterson culmination, these thrusts (Hawley Creek, Cabin, Johnson thrust) truncated the décollement of the upper thin-skinned system. It is important to note that slip continued to be fed to the active foreland basin in front of the Medicine Lodge-McKenzie system, which also had the effect of thickening the wedge and exhuming the overlying upper thin-skinned system. Meanwhile, active thrusts of the Blacktail-Snowcrest uplift also thickened the wedge. When super-critical conditions were achieved, the wedge propagated forward, sharing slip between the Blacktail-Snowcrest and Gravelly-Madison uplifts, which effectively acted as one pop-up. This sequence reproduced the two, mutually crosscutting and overlapping, hybrid thin- and thick-skinned systems that have been documented by previous workers (e.g., Kulik and Schmidt, 1988; Kulik and Perry, 1988; Perry et al., 1988; Schmidt et al., 1988; O'Neill et al., 1990; McDowell, 1997).

#### ***Phase 4***

The final phase of deformation ca. 55 Ma consisted of advancement of the wedge into the main foreland and into the Crazy Mountains basin. A considerable amount of shortening (~50 km) was accommodated mostly on the leading structure, the sub-Bridger thrust. This structure

has the geometry of a thick-skinned triangle-zone, and fed slip from the deep, mid-crustal viscous décollement at the base of the system to bedding-parallel blind thrusts in the thick foreland basin. Slip on formerly active structures ceased as those structures were completely abandoned and the newly active Spanish Peaks thrust crosscut the Scarface-Hilgard thrust system; basically, the pop-up of the Blacktail-Snowcrest/Gravelly-Madison uplift was abandoned in favor of the pop-up of the Madison-Gallatin uplift. Thickening of the Lemhi arch increased the overall wedge to a point that now the system could once again advance forward as a single, thick-skinned wedge. The Beaverhead Group records when deformation ceased between the Tendoy and Blacktail mountains; poorly constrained maximum depositional ages suggest this occurred between ~65-55 Ma (e.g., Perry et al., 1988; Haley et al., 1991; Garber et al., 2020). In summary, this forward kinematic model links the variety of structural styles that define the central fold belt, fold-thrust belt, foreland uplift, and foreland basin domains to a single progressive history of a forward and downward progressing wedge of deformation through a basement high.

### **Linking Sevier and Laramide belts in 3-D**

The two-dimensional forward kinematic model proposed above describes both the geometric relationship between end-member thin- and thick-skinned orogenic wedges and their kinematic continuity. Describing the geometry of these end-member thin- and thick-skinned wedges using other cross sections and map-view interpretations allows us to gain a more three-dimensional (3-D) understanding of the geometry, providing a solid foundation for testing and developing kinematic and dynamic models of strain partitioning in the crust. The cross section illustrates the double-decker geometry described by Parker and Pearson (2021) at a more regional scale, defining a single composite orogenic wedge with the “local” structural style

depending on the availability of sub-horizontal detachment horizons (Kulik and Schmidt, 1988), with the Lemhi arch and its related sedimentary cover rocks determining the structural style of particular thrusts as the early upper décollement was slowly replaced by a lower décollement.

Our forward model clarifies aspects of two particular models that aim to explain along-strike changes in structural style (O'Neill et al., 1990) and strain partitioning between the Sevier and Laramide belt (McClelland and Oldow, 2004) in the Idaho-Montana segment of the North American Cordillera. O'Neill et al. (1990) proposed a “thick-skinned displacement transfer zone that cuts basement rocks of the Lima [southwestern Montana] recess”, termed the “Dillon cut-off”. The transfer zone establishes along-strike continuity of the Sevier fold -thrust belt domain (Fig. 1) by linking the Disturbed belt and Helena salient of northwestern and central Montana to the southwestern Montana recess by a lateral ramp (Southwestern Montana Transfer Zone), and an oblique ramp (Dillon cut off) that cuts off the corner of the Dillon Block by reactivating a portion of the NW-dipping suture of the Paleoproterozoic Big Sky Orogeny (e.g., O'Neill and Lopez, 1985; Harms et al., 2004; Condit et al., 2015). Therefore, the generally thin-skinned Sevier belt contains local thick-skinned (defined as basement-involved) structures in southwestern Montana. Just south of where O'Neill et al., (1990) stopped their detailed description (the Armstead anticline), our cross section shows the imbricated Hawley Creek, Cabin, and Johnson thrusts chipping off the edge of the Dillon Block, signifying a continuation of the Dillon cut-off. In addition to reactivation of older structures (e.g., Schmidt et al., 1988; McBride et al., 1989; O'Neill et al., 1990; Parker and Pearson, 2021), variable crustal rheology caused by thickness changes in the rift-passive margin succession may explain the local occurrence of these thick-skinned structures in the largely thin-skinned belt.

Another oblique ramp system was hypothesized by McClelland and Oldow (2004) to link the major ramps in the décollements of the Sevier and Laramide belts. In this framework, the footwall ramp that exhumed the Belt basin (e.g., Sears, 1988) in the Sevier belt north of the study area must be linked to the frontal ramp of the Laramide belt. The trailing and leading ramp shown in our forward model (Fig. 4) are analogous to the ramps described for the Sevier and Laramide belts by McClelland and Oldow (2004), but in our model strain is transferred from one to another (phase 2) by activating a viscous mid-crustal décollement in the footwall of the former thin-skinned décollement. In other words, our forward model suggests that strain was progressively transferred from the trailing to the leading ramp, producing the décollement geometry highlighted by McClelland and Oldow (2004). Rather than being linked by a discrete oblique ramp, the Sevier and Laramide belts may have been linked by overlapping basement-involved ramps that migrated forward above a through-going mid-crustal décollement.

Our forward model suggests that the right-stepping mostly thin-skinned Sevier belt is linked by thick-skinned structures along strike as well as across strike. Initially, thin-skinned thrusts of a major recess linked the two salients by shortening above the basement high. Eventually the thick-skinned thrusts of the Dillon cut-off established the link through the intervening basement high, possibly with inherited weaknesses playing a role in determining not only the style of the local thrusts, but also their position. This is similar to a recently proposed model from the Pyrenees (Lescoutre and Manatschal, 2020) that explains along- and across-strike changes in structural style by three simple premises: (1) Thin (<~20 km) continental crust lacks a viscous mid-crust, and therefore deforms in a “coupled” (thin-skinned) fashion, whereas thick crust has a viscous mid-crust and therefore deforms in a “decoupled” (thick-skinned) fashion; (2) The thickness of the continental crust varies according to its history of rifting; and

(3) Rift margins are segmented, with thicker crust at accommodation zones, between step-overs of the fault trace. According to their model, a shift from thin- to thick-skinned thrusting is predicted everywhere the continental crust is thick enough to have a viscous middle crust (Fig. 5, Lescoutre and Manatschal, 2020); along-strike changes in structural style occur where the orogenic wedge crosses segment boundaries of the former rift margin, and across-strike changes in style occur where the orogenic wedge has advanced beyond the rift margin, into the adjacent thick continental crust.

From a descriptive standpoint, both the Belt basin and the western North American passive margin that make up the Sevier fold-thrust belt could be called “rifts” for the purposes of the model because they each consist of thick basins constructed on thinned crust (Picha and Gibson, 1985; Winston, 1986; Cressman, 1989; Sears et al., 1998; Lund et al., 2010; Yonkee et al., 2014; Brennan et al., 2020). Though the Lemhi sub basin contains thick strata, fine-grained intervals are uncommon, it is intruded by felsic plutons, and it has been tilted by pre-Ordovician normal faulting (e.g., Evans and Zartman, 1990; Doughty and Chamberlain, 1996; Lund et al., 2010; Link et al., 2017a; Brennan et al., 2020), and therefore may not behave like the Belt basin farther north. To the first-order, the Dillon cut-off model resembles the model of Lescoutre and Manatschal (2020), with the Lemhi arch acting as the thick-skinned segment boundary between the thin-skinned thrusts that exhume right-stepping “rifts” of the Belt basin to the north and the distal portions of the North American rift-passive margin to the south. Progressive transfer from thin- to thick-skinned thrusts outside of the “rift” margins explains the final décollement geometry (McClelland and Oldow, 2004). In other words, the Laramide belt marks where the orogenic wedge exceeded thin continental crust and thick sedimentary (and metasedimentary) cover rocks of former “rift” basins. This perspective may be worth pursuing for the North

American Cordillera and other continental fold-thrust belts that display a wide range of structural styles that seem to emerge generally at the same time but with out-of-sequence behavior.

### **Progressive changes in style related to stratigraphic and mid-crustal architecture**

We now focus our discussion on progressive models of deformation that predict spatial and temporal changes in structural style once rheological boundaries of the continental crust are crossed (e.g., Mouthereau et al., 2013; Lacombe and Bellahsen, 2016; Pfiffner, 2017; Lescoutre and Manatschal, 2020; Parker and Pearson, 2021; Tavani et al., 2021). We emphasize that these models do not preclude or require additional changes in plate boundary conditions (Lacombe and Bellahsen, 2016). Using the variables constrained within the scope of this study, we aim to explain why deformation jumped from the Patterson culmination to the Blacktail-Snowcrest uplift at ca. 90 Ma, and why the younger thick-skinned system overprinted the older thin-skinned system.

The presence or absence of a viscous middle crust, which we hypothesize served as the décollement to the thick-skinned system, explains much of the final 3-D geometry of the system. However, the presence/absence of thick continental crust cannot fully explain the spatio-temporal patterns observed in the study area because the minimally-extended continental crust of the Lemhi arch and Wyoming craton were always thick enough to have a viscous middle crust, yet deformation in much of this area was initially thin-skinned and only later transitioned to thick-skinned. Why did the viscous middle crust only become an important décollement after ca 90 Ma, when thick-skinned uplifts simultaneously emerged on either side of the Lemhi arch?

A sudden shift from thin- to thick-skinned thrusting may be explained by progressive thickening of the crust in the growing hinterland, which is hypothesized to have resulted in the

creation of ductile layers within the highly attenuated crust of the distal rift domain due to an increase in geothermal gradient during thrusting and foreland basin sedimentation; this may have established a laterally continuous mid-crustal weak horizon between the hinterland and the formerly isolated foreland (Lacombe and Bellahsen, 2016; Fig. 7, Tavani et al., 2021). This may have a two-fold effect by (1) establishing a link between once-isolated viscous detachment horizons in the now thickened hinterland and the always thick foreland and (2) changing the rate at which strain is transferred through the system (by changing the strength of the décollement). Numerical and analog models demonstrate that—compared to frictional detachments—viscous detachments result in a lower critical taper angle and are much more effective at rapidly transmitting strain to the front of the system (Williams et al., 1994; Ruh et al., 2012; Borderie et al., 2018). The combination of established continuity of viscous weak layers in the middle crust and switching from a frictional to a viscous décollement may give the deformation front the ability to essentially jump in front of its former thin-skinned system.

In order for an orogenic wedge to advance forward through a passive margin constructed on oceanic or transitional crust and into the continent, the décollement of the system must step down from stratigraphic weak layers in the upper crust to viscous weak layers in the middle crust (Tavani et al., 2021). Our forward kinematic model suggests that this transition was facilitated by the downward and forward shift of the trailing ramp to the former thin-skinned (frictional) décollement as strain was progressively linked into a single thick-skinned wedge (Fig. 4). Sedimentary cover rocks that cover the Lemhi arch determined the initial geometry of the upper thin-skinned décollement, which consists of ramp and a low-relief flat (Parker and Pearson, in prep). It is likely that the geometry or endpoint of the thick-skinned décollement, mainly thrusts of the Dillon cut-off, was determined by preexisting weaknesses (Schmidt et al., 1988; McBride

et al., 1989; O'Neill et al., 1990; Parker and Pearson, 2021). The forward advancing duplex of the Patterson culmination and the stacked imbricates of the Dillon cut-off gradually accommodated the transition from thin- to thick-skinned thrusting by incrementally increasing and smoothing out the basal slope of the former wedge (phase 2-3, Fig. 4). This suggests that, in addition to the mid-crustal processes highlighted by previous workers (Lacombe and Bellahsen, 2016; Lescoutre and Manatschal, 2020; Tavani et al., 2021), the availability of preexisting weaknesses in the upper crust (i.e., stratigraphy and inherited faults; Hilley et al., 2005) may have controlled the tempo of and provide the mechanism for the transfer of strain from the distal “oceanic” domain into the “continental crust.” Specifically, the downward/forward migration of the former décollement may be the mechanism by which the upper frictional and lower viscous décollement link most efficiently.

Stratigraphic and structural weaknesses in the upper crust may provide the most efficient way to internally thicken the wedge and transmit strain from the viscous middle crust to the surface by advancing the former décollement of the trailing system. While the emergence of a laterally continuous mid-crustal (viscous) detachment may flip the switch from thin- to thick-skinned thrusting and transmitting strain from the hinterland into the continent, the new décollement may not be effective at building relief in its interior, above its regional flat. Additionally, while it is easy to transmit the strain through the weak viscous middle crust itself, it is difficult to propagate through the strong overlying brittle crust and to the surface. The rheology of the upper crust may facilitate out-of-sequence growth of the wedge and transmission of stress to the surface, filling it out from the top down. Meanwhile, the rheology of the middle crust may facilitate in-sequence growth of the wedge, advancing it into the continent from the bottom up. This combined top-down and bottom-up approach may explain the apparent

bifurcation and later convergence of the wedge within the context of critical taper theory. This model may be useful for not only understanding how self-organized changes in structural style may emerge with progressive shortening, but also how the changing rheology of the middle and upper crust may itself govern the dynamic behavior of the orogenic belt.

## CONCLUSIONS

A spectrum of structural styles, ranging from thin- to thick-skinned, is explained with a single balanced and restored cross section that spans nearly the entirety of the Idaho-Montana fold thrust belt, linking the folded Sevier hinterland to the thick-skinned Laramide province. Integrating these different structural domains suggests that early (pre ~90 Ma) shortening was accommodated above an upper décollement that followed the unconformable top of the Lemhi arch basement high and fed slip to the Medicine Lodge-McKenzie thrust system to the northeast. Thin stratigraphy over the Lemhi arch limited the depth, basal angle, and geometry of this frictional upper décollement. As a consequence, the wedge advanced by activating a lower décollement within the weak viscous middle crust of the Lemhi arch. Activation of the viscous lower décollement efficiently transmitted strain to the foreland, resulting in contemporaneous early uplift of both the Patterson culmination and Blacktail-Snowcrest uplift on either side of the Lemhi arch at ca. 90-70 Ma. The wedge thickened by advancing the basal slope of the upper décollement, progressively linking the upper and lower décollements at the front and uplifting the older overlying upper décollement at the rear of the growing duplex. Once the weaker, quartzite-dominated western flank of the Lemhi arch was shortened, the upper décollement was completely abandoned as imbricated thick-skinned thrusts of the Hawley Creek, Cabin, and Johnson thrust systems truncated the former upper décollement. At this time, the system advanced forward by activating the pop-up of the Madison-Gallatin uplift, ultimately feeding slip

into the Crazy Mountains foreland basin by a triangle zone. The gradual transition from thin- to thick-skinned thrusting was self-organized as the frictional décollement was exhausted in favor of a viscous décollement in the middle crust. Activation of the viscous lower décollement appears to have rapidly transmitted strain through the Lemhi arch, growing the wedge by lengthening it at the base. Progressive abandonment of the frictional upper décollement lagged behind, as the Lemhi arch progressively shortened, thereby growing the wedge by thickening it from the top down. In total, we estimate that ~244 km of shortening was accommodated during this prolonged transition from a frictional thin-skinned system within sedimentary cover rocks to a viscous thick-skinned system within continental crust. The results of this study are consistent with recent proposed models that explain the emergence of thick-skinned thrusts in progressively deforming systems with variable rheologies of the middle crust. However, this case study from the Idaho-Montana fold-thrust belt suggests that upper crustal rheology, specifically the availability of weak sedimentary rocks that serve as regional décollement horizons, may determine the tempo and kinematics of the transition from thin- to thick-skinned thrusting, thereby facilitating the transfer of strain from a frictional décollement in the sedimentary cover rocks to a viscous décollement in the underlying continental crust.

## **ACKNOWLEDGMENTS**

This project was completed as a component of a S. Parker's Ph.D. dissertation at Idaho State University. We gratefully acknowledge Petex for use of MOVE software, funding from NSF-EAR grant 1728563 to D.M. Pearson, and conversations with Jim Coogan, Paul Link, Emily Finzel, Justin Rosenblume, Leslie Montoya, Chase Porter, and Cole Gardner.

**REFERENCES CITED**

- Allen, B., Saville, C., Blanc, E., Talebian, M., and Nissen, E., 2013, Orogenic plateau growth: expansion of the Turkish–Iranian Plateau across the Zagros fold-and-thrust belt: *Tectonics*, vol. 32, p. 171–90, doi:10.1002/tect.20025.
- Allmendinger, R.W., and Gubbels, T., 1996, Pure and simple shear plateau uplift, Altiplano Puna, Argentina and Bolivia: *Tectonophysics*, vol. 259, no. 1-3, p. 1-13, doi:10.1016/0040-1951(96)00024-8.
- Allmendinger, R.W., Hauge, T.A., Hauser, E.C., Potter, C.J., Klemperer, S.L., Nelson, K.D., Knuepfer, P., and Oliver, J., 1987, Overview of the COCORP 40° N transect, western United States: The fabric of an orogenic belt: *Geological Society of America Bulletin*, vol. 98, no. 3, p. 308-319, doi:10.1130/0016-7606(1987)98<308:OOTCNT>2.0.CO;2.
- Anastasio, D.J., Fisher, D.M., Messina, T.A., and Holl, J.E., 1997, Kinematics of décollement folding in the Lost River Range, Idaho: *Journal of Structural Geology*, vol. 19, no. 3-4, p. 355-368, doi:10.1016/S0191-8141(97)83028-3.
- Armstrong, R.L., 1968, Sevier orogenic belt in Nevada and Utah: *Geological Society of America Bulletin*, vol. 79, no. 4, p. 429-458, doi:10.1130/0016-7606(1968)79[429:SOBINA]2.0.CO;2.
- Armstrong, F.C. and Oriol, S.S., 1965, Tectonic development of Idaho-Wyoming thrust belt: *American Association of Petroleum Geologist Bulletin*, vol. 49, no. 11, p. 1847-1866, doi:10.1306/A663386E-16C0-11D7-8645000102C1865D.
- Bally, A. W., Gordy, P. L., and Stewart, G. A., 1966, Structure, seismic data, and orogenic evolution of southern Canadian Rocky Mountains: *Bulletin of Canadian Petroleum*

- Geology, vol. 14, no. 3, p. 337-381, doi:10.35767/gscpgbull.14.3.337.
- Beranek, L.P., Link, P.K. and Fanning, C.M., 2016, Detrital zircon record of mid-Paleozoic convergent margin activity in the northern US Rocky Mountains: Implications for the Antler orogeny and early evolution of the North American Cordillera: *Lithosphere*, vol. 8, no. 5, p. 533-550, doi:10.1130/L557.1.
- Beutner, E. C., 1968, Structure and tectonics of the southern Lemhi Range, Idaho [doctoral dissertation]: State College, Pennsylvania State University, 106 p.
- Bird, P., 1984, Laramide crustal thickening event in the Rocky Mountain foreland and Great Plains: *Tectonics*, vol. 3, no. 7, p. 741-758, doi:10.1029/TC003i007p00741.
- Blackstone Jr, D.L., 1940, Structure of the Pryor Mountains Montana: *The Journal of Geology*, vol. 48, no. 6, p. 590-618, doi:10.1086/624917.
- Borderie, S., Graveleau, F., Witt, C., & Vendeville, B.C., 2018, Impact of an interbedded viscous décollement on the structural and kinematic coupling in fold-and-thrust belts: Insights from analogue modeling: *Tectonophysics*, vol. 722, p. 118-137, doi:10.1016/j.tecto.2017.10.019.
- Boyer, S.E., and Elliott, D., 1982, Thrust systems: *The American Association of Petroleum Geologists Bulletin*, vol. 66, no. 9, p. 1196-1230, doi:10.1306/03B5A77D-16D1-11D7-8645000102C1865D.
- Brennan, D.T., M. Pearson, D.M., Link, P.K., and Chamberlain K.R., 2020, Neoproterozoic Windermere Supergroup near Bayhorse, Idaho: late-stage Rodinian rifting was deflected west around the Belt basin: *Tectonics*, vol. 39, no. 8, p. 1-27, doi:10.1029/2020TC006145.
- Brumbaugh, D.S. and Hendrix, T.E., 1981, The McCarthy Mountain structural salient

- southwestern Montana, *in* Tucker, T.E., Aram, R.B., Brinker, W.F., and Grabb, R.F., Montana Geological Society field conference & symposium guidebook to southwest Montana: Billings, Montana, Montana Geological Society, p. 201-210.
- Burchfiel, B., and Davis, G.A., 1972, Structural framework and evolution of the southern part of the Cordilleran orogen, western United States: *American Journal of Science*, vol. 272, no. 2, p. 97-118, doi:10.2475/ajs.272.2.97.
- Burchfiel, B.C., and Davis, G.A., 1975, Nature and controls of Cordilleran orogenesis, western United States: Extensions of an earlier synthesis: *American Journal of Science*, vol. 275, no. A, p. 363-396.
- Burtner, R.L. and Nigrini, A., 1994, Thermochronology of the Idaho-Wyoming thrust belt during the Sevier orogeny: A new, calibrated, multiprocess thermal model: *American Association of Petroleum Geologists bulletin*, vol. 78, no. 10, p. 1586-1612, doi:10.1306/A25FF229-171B-11D7-8645000102C1865D.
- Butler, R.W., Bond, C.E., Cooper, M.A., and Watkins, H., 2018, Interpreting structural geometry in fold-thrust belts: Why style matters: *Journal of Structural Geology*, vol. 114, p. 251-273, doi:10.1016/j.jsg.2018.06.019.
- Camilleri, P., Adolph Yonkee, W., Coogan, J., DeCelles, P.G., McGrew, A. and Wells, M., 1997, Hinterland to foreland transect through the Sevier orogen, northeast Nevada to north central Utah: Structural style, metamorphism, and kinematic history of a large contractional orogenic wedge: *Brigham Young University Geology Studies*, vol. 42, p. 297-309.
- Carrapa, B., DeCelles, P.G. and Romero, M., 2019, Early inception of the Laramide orogeny in southwestern Montana and northern Wyoming: Implications for models of flat-slab

- subduction: *Journal of Geophysical Research: Solid Earth*, vol. 124, no. 2, p. 2102-2123, doi:10.1029/2018JB016888.
- Cloetingh, S.A.P.L., Mañenco, L., Bada, G., Dinu, C. and Mocanu, V., 2005, The evolution of the Carpathians–Pannonian system: interaction between neotectonics, deep structure, polyphase orogeny and sedimentary basins in a source to sink natural laboratory: *Tectonophysics*, vol. 410, no. 1-4, p. 1-14, doi:10.1016/j.tecto.2005.08.014.
- Condie, K.C., 1976, Trace-element geochemistry of Archean greenstone belts: *Earth-Science Reviews*, vol. 12, no.4, p. 393-417, doi:10.1016/0012-8252(76)90012-X.
- Condit, C.B., Mahan, K.H., Ault, A.K. and Flowers, R.M., 2015, Foreland-directed propagation of high-grade tectonism in the deep roots of a Paleoproterozoic collisional orogen, SW Montana, USA: *Lithosphere*, vol. 7, no. 6, p. 625-645, doi:10.1130/L460.1.
- Constenius, K.N., Esser, R.P. and Layer, P.W., 2003, Extensional collapse of the Charleston Nebo salient and its relationship to space-time variations in Cordilleran orogenic belt tectonism and continental stratigraphy, *in* Reynolds, R.G., and Flores, R.M., eds., *Cenozoic systems of the Rocky Mountain region: Denver, Colorado, Rocky Mountain Section, Society for Sedimentary Geology*, p. 303-353.
- Coogan, J. C., 1992, Structural evolution of piggyback basins in the Wyoming-Idaho-Utah thrust belt, *in* Link, P.K., Kuntz, M. A., & Piatt, L. B., eds., *Regional geology of eastern Idaho and western Wyoming: Boulder, Colorado*, v. 179, p. 55–81, doi:10.1130/MEM179-p55.
- Copeland, P., Currie, C.A., Lawton, T.F. and Murphy, M.A., 2017, Location, location, location: The variable lifespan of the Laramide orogeny: *Geology*, vol. 45, no. 3, p. 223-226, doi:10.1130/G38810.1.

- Coryell, J.J., and Spang J.H., 1988, Structural geology of the Armstead anticline area, Beaverhead County, Montana, *in* J. Schmidt, and W. J. Perry eds., Interaction of the Rocky Mountain Foreland and the Cordilleran Thrust Belt: Boulder, Colorado, Geological Society of America Memoir 171, p. 217-227, doi:10.1130/MEM171-p217.
- Coward, M.P., 1983, Thrust tectonics, thin skinned or thick skinned, and the continuation of thrusts to deep in the crust: *Journal of Structural Geology*, vol. 5, no. 2, p. 113-123, doi:10.1016/0191-8141(83)90037-8.
- Cressman, E.R., 1989, Reconnaissance stratigraphy of the Prichard Formation (Middle Proterozoic) and the early development of the Belt Basin, Washington, Idaho, and Montana, United States Geological Survey, Professional Paper, v. 1490, 80 p, doi:10.3133/991490.
- Cristallini, E.O. and Ramos, V.A., 2000, Thick-skinned and thin-skinned thrusting in the La Ramada fold and thrust belt: crustal evolution of the High Andes of San Juan, Argentina (32° SL): *Tectonophysics*, vol. 317, no. 3-4, p. 205-235, doi:10.1016/S00401951(99)00276-0.
- Currie, B.S., 2002, Structural configuration of the Early Cretaceous Cordilleran foreland-basin system and Sevier thrust belt, Utah and Colorado: *The Journal of Geology*, vol. 110, no. 6, p. 697-718, doi:10.1086/342626.
- Dahlen, F.A., 1984, Noncohesive critical Coulomb wedges: An exact solution: *Journal of Geophysical Research: Solid Earth*, vol. 89, no. B12, p. 10125-10133, doi:10.1029/JB089iB12p10125.
- Dahlen, F.A., 1990, Critical taper model of fold-and-thrust belts and accretionary wedges: *Annual Review of Earth and Planetary Sciences*, vol. 18, no. 1, p. 55-99.

- Dahlstrom, C.D.A., 1969, Balanced cross sections: *Canadian Journal of Earth Sciences*, vol. 6, no. 4, p. 743-757, doi:10.1139/e69-069.
- Dahlstrom, C. D., 1970, Structural geology in the eastern margin of the Canadian Rocky Mountains: *Bulletin of Canadian Petroleum Geology*, vol. 18, no. 3, p. 332-406, doi:10.35767/gscpgbull.18.3.332.
- Davis, D., Suppe, J., and Dahlen, F. A., 1983, Mechanics of fold-and-thrust belts and accretionary wedges: *Journal of Geophysical Research: Solid Earth*, vol. 88, no. B2, p. 1153-1172, doi:10.1029/JB088iB02p01153.
- DeCelles, P.G., 2004, Late Jurassic to Eocene evolution of the Cordilleran thrust belt and foreland basin system, western USA: *American Journal of Science*, vol. 304, no. 2, p. 105-168, doi:10.2475/ajs.304.2.105.
- DeCelles, P.G., 2012, Foreland basin systems revisited: Variations in response to tectonic settings, *in* Busby, C., and Azor, A., eds., *Tectonics of sedimentary basins: Recent advances*: Hoboken, New Jersey, Wiley-Blackwell, p. 405-426, doi: 10.1002/9781444347166.
- Decelles, P.G., Tolson, R.B., Graham, S.A., Smith, G.A., Ingersoll, R.V., White, J., Schmidt, C.J., Rice, R., Moxon, I., Lemke, L. and Handschy, J.W., 1987, Laramide thrust generated alluvial-fan sedimentation, Sphinx Conglomerate, southwestern Montana: *American Association of Petroleum Geologist Bulletin*, vol. 71, no. 2, p. 135-155.
- DeCelles, P.G. and Mitra, G., 1995, History of the Sevier orogenic wedge in terms of critical taper models, northeast Utah and southwest Wyoming: *Geological Society of America Bulletin*, vol. 107, no. 4, p. 454-462, doi:10.1130/0016-7606(1995)107<0454:HOTSOW>2.3.CO;2.

- DeCelles, P.G., Lawton, T.F., and Mitra, G., 1995, Thrust timing, growth of structural culminations, and synorogenic sedimentation in the type Sevier orogenic belt, western United States. *Geology*, vol. 23, no. 8, p. 699-702, doi:10.1130/0091-7613(1995)023<0699:TTGOSC>2.3.CO;2.
- DeCelles, P.G., and Coogan, J. C., 2006, Regional structure and kinematic history of the Sevier fold-and-thrust belt, central Utah: *Geological Society of America Bulletin*, vol. 118, no. 7-8, p. 841-864, doi:10.1130/B25759.1.
- Dickinson, W.R., and Snyder, W. S., 1978, Plate tectonics of the Laramide orogeny, *in* Matthews, V., ed., *Laramide folding associated with basement block faulting in the western United States: Boulder, Colorado, Geological Society of America Memoir 151*, p. 355-366, doi:10.1130/MEM151-p355.
- Dickinson, W.R., 1988, Provenance and sediment dispersal in relation to paleotectonics and paleogeography of sedimentary basins, *in* Kleinspehn, K.L., and Paola, C., eds., *New perspectives in basin analysis: New York, New York, Springer*, p. 3-25, DOI: 10.1007/978-1-4612-3788-4\_1.
- Dickinson, W.R., 2004, Evolution of the North American cordillera: *Annual Review of Earth and Planetary Sciences*, vol. 32, p.13-45, doi:10.1146/annurev.earth.32.101802.120257.
- Doughty, P.T. and Chamberlain, K.R., 1996, Salmon River Arch revisited: new evidence for 1370 Ma rifting near the end of deposition in the Middle Proterozoic Belt basin: *Canadian Journal of Earth Sciences*, vol. 33, no. 7, p. 1037-1052, doi:10.1139/e96-079.
- DuBois, D.P., 1982, Tectonic framework of basement thrust terrane, northern Tendoy range, southwest Montana, *in* Powers, R.B., ed., *Geologic Studies of the Cordilleran Thrust*

- Belt: Denver, Colorado, Rocky Mountain Association of Geologists v. 1, p. 145-156.
- Dyman, T.S. and Nichols, D.J., 1988, Stratigraphy of mid-Cretaceous Blackleaf and lower part of the Frontier Formations in parts of Beaverhead and Madison Counties, Montana: Denver, Colorado, U.S. Geological Survey Bulletin 1773, 31 p., doi: 10.3133/b1773.
- Dyman, T.S., Tysdal, R.G., Perry Jr, W.J., Nichols, D.J. and Obradovich, J.D., 2008, Stratigraphy and structural setting of Upper Cretaceous frontier formation, western Centennial Mountains, southwestern Montana and southeastern Idaho: *Cretaceous Research*, vol. 29, no. 2, p. 237-248, doi:10.1016/j.cretres.2007.05.001.
- Erslev, E.A., 1986, Basement balancing of Rocky Mountain foreland uplifts: *Geology*, vol. 14, no. 3, p. 259-262, doi:10.1130/0091-7613(1986)14<259:BBORMF>2.0.CO;2.
- Erslev, E.A., 1991, Trishear fault-propagation folding: *Geology*, vol. 19, no. 6, p. 617-620, doi:10.1130/0091-7613(1991)019<0617:TFFP>2.3.CO;2.
- Erslev, E.A., 1993, Thrusts, Back-Thrusts and Detachments of Rocky Mountain Foreland Arches, *in* C.J. Schmidt, R.B. Chase, E.A. Erslev eds., *Laramide basement deformation in the Rocky Mountain foreland of the western United States*: Boulder, Colorado, Geological Society of America Special Paper, vol. 280, p. 339-358, doi: 10.1130/SPE280-p339.
- Evenchick, C.A., McMechan, M.E., McNicoll, V.J. and Carr, S.D., 2007, A synthesis of the Jurassic–Cretaceous tectonic evolution of the central and southeastern Canadian Cordillera: Exploring links across the orogeny, *in* Sears, J.W., Harms, T.A, Evenchick,

- C.A., eds., *Whence the Mountains? Inquiries into the Evolution of Orogenic Systems: A Volume in Honor of Raymond A. Price*: Boulder, Colorado, Geological Society of America Special Papers 433, p. 117-145, doi:10.1130/2007.2433(06).
- Fayon, A.K., Tikoff, B., Kahn, M. and Gaschnig, R.M., 2017, Cooling and exhumation of the southern Idaho batholith: *Lithosphere*, vol. 9, no. 2, p. 299-314, doi:10.1130/L565.1.
- Fermor, P.R., and Moffat, I.W. (1992). The Cordilleran collage and the foreland fold and thrust Belt, *in* R.W., MacQueen, and D. A. Leckie eds., *Foreland basins and fold belts*: Denver, Colorado, American Association of Petroleum Geologists vol. 55, p. 81-105, doi:10.1306/M55563.
- Fisher, D.M. and Anastasio, D.J., 1994, Kinematic analysis of a large-scale leading edge fold, Lost River Range, Idaho: *Journal of Structural Geology*, vol. 16, no. 3, p. 337-354, doi:10.1016/0191-8141(94)90039-6.
- Fitz-Díaz, E., Lawton, T.F., Juárez-Arriaga, E., and Chávez-Cabello, G., 2018, The Cretaceous Paleogene Mexican orogen: Structure, basin development, magmatism and tectonics: *Earth-Science Reviews*, vol. 183, p. 56–84, doi:10.1016/j.earscirev.2017.03.002.
- Fuentes, F., DeCelles, P.G. and Constenius, K.N., 2012, Regional structure and kinematic history of the Cordilleran fold-thrust belt in northwestern Montana, USA: *Geosphere*, vol., 8, no. 5, p. 1104-1128, doi:10.1130/GES00773.1.
- Garber, K. L., Finzel, E. S., and Pearson, D. M., 2020, Provenance of Synorogenic Foreland Basin Strata in Southwestern Montana Requires Revision of Existing Models for Laramide Tectonism: *North American Cordillera: Tectonics*, vol. 39, no. 2, p. 1-26,

doi:10.1029/2019TC005944.

Gorder, J.D., 1960, The Lima anticline, *in* Campau, D.E., Anisgard, H.W., and Egbert, R.L., 11<sup>th</sup> Annual Field Conference: west Yellowstone-earthquake area: Billings, Montana, p. 265-267.

Grader, G. W., Isaacson, P. E., Doughty, P. T., Pope, M. C., and Desantis, M. K., 2017, Idaho Lost River shelf to Montana craton: North American Late Devonian stratigraphy, surfaces, and intrashelf basin, *in* Playton, T.E., Kerans, C., and Weissenberger, A.W., eds., *New advances in Devonian Carbonates: Outcrop analogs, reservoirs, and chronostratigraphy*: Tulsa, Oklahoma, Society for Sedimentary Geology Special Publication 107, p. 347-379, doi: 10.2110/sepmsp.107.12.

Groshong, R.H., and Porter, R., 2019, Predictive models for the deep geometry of a thick skinned thrust matched to crustal structure: Wind River Range, western USA: *Lithosphere*, vol. 11, no. 4, p. 448-464, doi:10.1130/L1031.1.

Guenther, W.R., Reiners, P.W., Ketcham, R.A., Nasdala, L. and Giester, G., 2013, Helium diffusion in natural zircon: Radiation damage, anisotropy, and the interpretation of zircon (U-Th)/He thermochronology: *American Journal of Science*, vol. 313, no. 3, p. 145-198. doi:10.2475/03.2013.01.

Hait Jr, M.H., 1965, *Structure of the Gilmore area, Lemhi Range, Idaho* [doctoral dissertation]: State College, Pennsylvania State University, 134 p.

Haley, J.C., Bonilla, M.G., Meyer, R.F., Yeend, W.E., Lienkaemper, J.J., and Perry, W.J., 1991, *The Red Butte Conglomerate: A Thrust-belt-derived Conglomerate of the Beaverhead Group, Southwestern Montana*: Denver, Colorado, U.S. Geological Survey Bulletin, v. 1945, p. 1-19, doi: 10.3133/b1945.

- Haley, C.J., 1986, Upper Cretaceous (Beaverhead) synorogenic sediments of the Montana-Idaho thrust belt and adjacent foreland: Relationships between sedimentation and tectonism [Ph.D. dissertation]: Baltimore, John Hopkins University, 542 p.
- Hansen, C. M., and Pearson, D. M., 2016, Geologic Map of the Poison Creek Thrust Fault and Vicinity near Poison Peak and Twin Peaks, Lemhi County, Idaho: Idaho Geological Survey Technical Report T-16-1, scale 1:24,000.
- Harlan, S.S., Geissman, J.W., Lageson, D.R. and Snee, L.W., 1988, Paleomagnetic and isotopic dating of thrust-belt deformation along the eastern edge of the Helena salient, northern Crazy Mountains Basin, Montana: Geological Society of America Bulletin, vol. 100, no. 4, p. 492-499, doi:10.1130/0016-7606(1988)100<0492:PAIDOT>2.3.CO;2.
- Harms, T.A., Brady, J.B., Burger, R.H., and Cheney, J.T., 2004, Advances in the geology of the Tobacco Root Mountains, Montana, and their implications for the history of the northern Wyoming province, in Brady, J.B., Burger, R.H., Cheney, J.T., and Harms, T.A., eds., Precambrian geology of the Tobacco Root Mountains, Montana: Boulder, Colorado, Geological Society of America special papers 377, p. 227-243, doi: 10.1130/0-8137-2377-9.227.
- Heller, P.L. and Liu, L., 2016, Dynamic topography and vertical motion of the US Rocky Mountain region prior to and during the Laramide orogeny: Bulletin, vol. 128, no. 5-6, p. 973-988, doi:10.1130/B31431.1.
- Hilley, G.E., Blisniuk, P.M. and Strecker, M.R., 2005, Mechanics and erosion of basement-cored uplift provinces: Journal of Geophysical Research: Solid Earth, vol. 110, no. B12409, doi:10.1029/2005JB003704.
- Hung, J.H., Wiltschko, D.V., Lin, H.C., Hickman, J.B., Fang, P., and Bock, Y., 1999, Structure

- and motion of the southwestern Taiwan fold and thrust belt: *Terrestrial, Atmospheric and Oceanic Sciences*, vol. 10, p. 543–68, doi:10.3319/TAO.1999.10.3.543(T).
- James, W.C., and Oaks, R.Q., 1977, Petrology of the Kinnikinic Quartzite (Middle Ordovician), east-central Idaho: *Journal of Sedimentary Research*, vol. 47, no. 4, p. 1491-1511, doi:10.1306/212F73A1-2B24-11D7-8648000102C1865D.
- Janecke, S., McIntosh, W. and Good, S., 1999, Testing models of rift basins: Structure and stratigraphy of an Eocene-Oligocene supradetachment basin, Muddy Creek half graben, southwest Montana: *Basin Research*, vol. 11, no. 2, p. 143-166, doi:10.1046/j.1365-2117.1999.00092.x.
- Johnson, L.M., and Sears, J.W., 1988, Cordillera thrust belt-Rocky Mountain foreland interaction near Bannack, Montana, *in* J. Schmidt, and W. J. Perry eds., *Interaction of the Rocky Mountain Foreland and the Cordilleran Thrust Belt: Boulder, Colorado*, Geological Society of America Memoir 171, p. 229-236, doi:10.1130/MEM171-p229.
- Johnson, R.C., Finn, T.M., Taylor, D.J., and Nuccio, V.F., 2005, Stratigraphic framework, structure, and thermal maturity of Cretaceous and lower Tertiary rocks in relation to hydrocarbon potential, Crazy Mountains Basin, Montana: Denver, Colorado, U.S. Geological Survey Scientific Investigations Report 2004–5091, 95 p.
- Jones, C.H., Farmer, G.L., Sageman, B. and Zhong, S., 2011, Hydrodynamic mechanism for the Laramide orogeny: *Geosphere*, vol. 7, no. 1, p. 183-201, doi:10.1130/GES00575.1.
- Kaempfer J.M., Guenther, W.R., Pearson, D.M., 2019, constraining the timing of deformation in southwestern Montana basement cored ranges using low temperature thermochronology: *Geological Society of America Abstracts with Programs*, v. 51, no. 5,

doi: 10.1130/abs/2019AM-336173.

- Kalakay, T.J., John, B.E. and Lageson, D.R., 2001, Fault-controlled pluton emplacement in the Sevier fold-and-thrust belt of southwest Montana, USA: *Journal of Structural Geology*, vol. 23, no. 6-7, p. 1151-1165, doi:10.1016/S0191-8141(00)00182-6.
- Kellogg, K.S. and Harlan, S.S., 2007, New <sup>40</sup>Ar/<sup>39</sup>Ar age determinations and paleomagnetic results bearing on the tectonic and magmatic history of the northern Madison Range and Madison Valley region, southwestern Montana, USA: *Rocky Mountain Geology*, vol. 42, no. 2, p. 157-174, doi:10.2113/gsrocky.42.2.157.
- Kley, J., Monaldi, C.R., and Salfity, J.A., 1999, Along-strike segmentation of the Andean foreland: causes and consequences: *Tectonophysics*, vol. 301, no. 1-2, p. 75-94, doi:10.1016/S0040-1951(98)90223-2.
- Kulik, D.M., and Perry, W.J., 1988, The Blacktail-Snowcrest foreland uplift and its influence on structure of the Cordilleran thrust belt-Geological and geophysical evidence for the overlap province in southwestern Montana, *in* J. Schmidt, and W. J. Perry eds., *Interaction of the Rocky Mountain Foreland and the Cordilleran Thrust Belt*: Boulder, Colorado, Geological Society of America Memoir 171, p. 291-306, doi:10.1130/MEM171-p291.
- Kulik, D.M., and Schmidt, C.J., 1988, Region of overlap and styles of interaction of Cordilleran thrust belt and Rocky Mountain foreland, *in* J. Schmidt, and W. J. Perry eds., *Interaction of the Rocky Mountain Foreland and the Cordilleran Thrust Belt*: Boulder, Colorado, Geological Society of America Memoir 171, p. 75-98, doi:10.1130/MEM171-p75.
- Lacombe, O., & Mouthereau, F., 2002, Basement-involved shortening and deep detachment tectonics in forelands of orogens: insights from recent collision belts (Taiwan, western

- Alps, Pyrenees): *Tectonics*, vol. 21, p. 10-30, doi:10.1029/2001TC901018.
- Lacombe, O., & Bellahsen, N., 2016, Thick-skinned tectonics and basement-involved fold–thrust belts: insights from selected Cenozoic orogens: *Geological Magazine*, vol. 153, no. 5-6, p. 763-810, doi:10.1017/S0016756816000078.
- Lageson, D.R., 1989, Reactivation of a Proterozoic continental margin, Bridger Range, southwestern Montana, *in* French, D.E., and Grabb, R.F. eds., 1989 Field conference guidebook: Montana centennial edition, *Geologic Resources of Montana*, volume 1: Billings, Montana, Montana Geological Society, p. 279-298.
- Lawton, T.F., 2019, Laramide sedimentary basins and sediment-dispersal systems, *in* Miall A.D. ed., *The sedimentary basins of the United States and Canada*: Cambridge, Massachusetts, Elsevier, p. 529-557, vol. 2, doi:10.1016/B978-0-444-63895-3.00013-9.
- Le Garzic, E., Vergés, J., Sapin, F., Saura, E., Meresse, F., and Ringenbach, J.C., 2019, Evolution of the NW Zagros Fold-and-Thrust Belt in Kurdistan Region of Iraq from balanced and restored crustal-scale sections and forward modeling: *Journal of Structural Geology*, vol. 124, p. 51-69, doi:10.1016/j.jsg.2019.04.006.
- Lescoutre, R. and Manatschal, G., 2020, Role of rift-inheritance and segmentation for orogenic evolution: example from the Pyrenean-Cantabrian system: *Bulletin de la Société Géologique de France*, vol. 191, no. 1, doi:10.1051/bsgf/2020021.
- Link, P.K., Jansen, S.T., Halimdihardja, P., Lande, A. and Zahn, P., 1987, Stratigraphy of the Brigham Group (Late Proterozoic-Cambrian), Bannock, Portneuf, and Bear River Ranges, southeastern Idaho, *in* *The thrust belt revisited: Casper, Wyoming*, Wyoming Geological Association, Thirty eighth field conference guidebook, p. 133-148.

- Link, P.K., Warren, I., Preacher, J., and Skipp, B., 1996, Stratigraphic analysis and interpretation of the Mississippian Copper Basin Group, McGowan Creek Formation, and White Knob Limestone, south-central Idaho, in M. W. Longman and M. D. Sonnenfeld, eds., *Paleozoic Systems of the Rocky Mountain Region: Society for Sedimentary Geology Special Publication*, p. 117–144.
- Link, P.K., Todt, M.K., Pearson, D.M. and Thomas, R.C., 2017a, 500–490 Ma detrital zircons in Upper Cambrian Worm Creek and correlative sandstones, Idaho, Montana, and Wyoming: Magmatism and tectonism within the passive margin: *Lithosphere*, vol. 9, no. 6, p. 910-926, doi:10.1130/L671.1.
- Link, P.K., Autenrieth-Durk, K.M., Cameron, A., Fanning, C.M., Vogl, J.J., and Foster, D.A., 2017b, U-Pb zircon ages of the Wildhorse gneiss, Pioneer Mountains, south-central Idaho, and tectonic implications: *Geosphere*, v. 13, no. 3, p. 681–698, doi: 10.1130/GES01418.1.
- Little, W.W., and Clayton, R.W., 2017, Field guide to compressional structures along the western margin of the southern Beaverhead Mountain Range, Scott Butte 7.5' quadrangle, east-central Idaho: *Northwest Geology*, vol. 42, p. 133-142.
- Long, S.P., Henry, C.D., Muntean, J.L., Edmondo, G.P. and Cassel, E.J., 2014, Early Cretaceous construction of a structural culmination, Eureka, Nevada, USA: Implications for out-of-sequence deformation in the Sevier hinterland: *Geosphere*, vol. 10, no. 3, p. 564 584, doi:10.1130/GES00997.1.
- Long, S.P., 2015, An upper-crustal fold province in the hinterland of the Sevier orogenic belt, eastern Nevada, USA: A Cordilleran Valley and Ridge in the Basin and Range: *Geosphere*, vol. 11, no. 2, p. 404-424, doi:10.1130/GES01102.1.

- Lonn, J.D., Burmester, R.F., Lewis, R.S., and McFaddan, M.D., 2016, Giant folds and complex faults in Mesoproterozoic Lemhi strata of the Belt Supergroup, northern Beaverhead Mountains, Montana and Idaho, *in* J. W. Sears, and J. S. MacLean, eds., Belt Basin: Window to Mesoproterozoic Earth: Boulder, Colorado, Geological Society of America Special Paper 522, p. 139-162, doi:10.1130/2016.2522(06).
- Lopez, D.A., and Schmidt, C., 1985, Seismic profile across the leading edge of the fold and thrust belt of southwest Montana. *in* R.R., Gries ed., Seismic exploration of the Rocky Mountain region: Denver, Colorado, Rocky Mountain Association of Geologists, v. 1, p. 45-50.
- Lucchitta, B. K., 1966, Structure of the Hawley Creek area, Idaho-Montana [PhD dissertation]: University Park, Pennsylvania State University, 204 p.
- Lund, K., Aleinikoff, J.N., Evans, K.V. and Fanning, C.M., 2003, SHRIMP U-Pb geochronology of Neoproterozoic Windermere Supergroup, central Idaho: Implications for rifting of western Laurentia and synchronicity of Sturtian glacial deposits: Geological Society of America Bulletin, vol. 115, no. 3, p. 349-372, doi:10.1130/0016-7606(2003)115<0349:SUPGON>2.0.CO;2.
- Lund, K., Aleinikoff, J. N., Evans, K. V., DuBray, E. A., Dewitt, E. H., and Unruh, D. M., 2010, SHRIMP U-Pb dating of recurrent Cryogenian and Late Cambrian–Early Ordovician alkalic magmatism in central Idaho: Implications for Rodinian rift tectonics: Geological Society of America Bulletin, vol. 122, no. 3-4, 430-453, doi:10.1130/B26565.1.
- Lund, K., 2018, Geologic map of the central Beaverhead Mountains, Lemhi County, Idaho, and Beaverhead County, Montana: U.S. Geological Survey Scientific Investigations Map

3413, scale 1:50,000.

- Ma, C., Foster, D.A., Mueller, P.A., Dutrow, B.L. and Marsh, J., 2021, Mesozoic crustal melting and metamorphism in the US Cordilleran hinterland: Insights from the Sawtooth metamorphic complex, central Idaho: *Geological Society of America Bulletin*, doi:10.1130/B35837.1.
- Mapel, W.J., Read, W.H., and Smith, R.K., 1965, Geologic map and sections of the Doublespring quadrangle, Custer and Lemhi Counties, Idaho: U.S. Geological Survey, Geologic Quadrangle Map GQ-464, scale 1:62,500.
- Martínez, F., Kania, J., Muñoz, B., Riquelme, R. and López, C., 2020, Geometry and development of a hybrid thrust belt in an inner forearc setting: Insights from the Potrerillos Belt in the Central Andes, northern Chile: *Journal of South American Earth Sciences*, vol. 98, p.102439, doi:10.1016/j.jsames.2019.102439.
- McBride, 1988, Geometry and kinematics of the central Snowcrest Range: A Rocky Mountain Foreland uplift in southwestern Montana [MS thesis]: Kalamazoo, Western Michigan University, 267 p.
- McBride, B.C., Schmidt, C.J., Guthrie, G.E., and Sheedlo, M.K., 1992, Multiple reactivation of a collisional boundary: An example from southwestern Montana, *in* Bartholomew, M.J., Hyndman, D.W., Mogk, D., and Mason, R., eds., *Basement Tectonics*: Dordrecht, NL, Springer, v. 8, p. 341-357.
- McClay, K.R., 1992, *Thrust tectonics*: Dordrecht, NL, Springer, p. 419-433.
- McClelland, W.C. and Oldow, J.S., 2004, Displacement transfer between thick-and thin-skinned décollement systems in the central North American Cordillera: *Geological Society, London, Special Publications*, vol. 227, no. 1, p. 177-195,

doi:10.1144/GSL.SP.2004.227.01.10.

McDowell, R.J., 1997, Evidence for synchronous thin-skinned and basement deformation in the Cordilleran fold-thrust belt: the Tendoy Mountains, southwestern Montana: *Journal of Structural Geology*, vol. 19, no. 1, p. 77-87, doi:10.1016/S0191-8141(96)00044-2.

McGroder, M.F., Lease, R.O., and Pearson, D.M., 2015, Along-strike variation in structural styles and hydrocarbon occurrences, Subandean fold-and-thrust belt and inner foreland, Colombia to Argentina, *in* DeCelles, P.G., Ducea, M.N., Carrapa, B., and Kapp, P.A., eds., *Geodynamics of a Cordilleran Orogenic System: The Central Andes of Argentina and Northern Chile*: Boulder, Colorado, Geological Society of America Memoir 212, p. 79–113, doi:10.1130/2015.1212(05).

McMannis, W., and Chadwick, R.A., 1964, *Geology of the Garnet Mountain quadrangle*: Montana Bureau of Mines and Geology Bulletin, vol. 43, 47 p.

McMannis, W.J., 1955, *Geology of the Bridger Range, Montana*: Geological Society of America Bulletin, vol. 66, no. 11, p. 1385-1430, doi:10.1130/0016-7606(1955)66[1385:GOTBRM]2.0.CO;2.

McMechan, M.E., Thompson, R.I., Caldwell, W.G.E., and Kauffman, E.G., 1993, The Canadian Cordilleran fold and thrust belt south of 66 N and its influence on the Western Interior Basin, *in* Caldwell, W.G.E., and Kauffman, E.G., eds., *Evolution of the Western Interior Basin*: St. John's, Newfoundland, Geological Association of Canada, v. 39, p. 73-90.

McMechan, M.E., 2001, Large-scale duplex structures in the McConnell thrust sheet, Rocky Mountains, Southwest Alberta: *Bulletin of Canadian Petroleum Geology*, vol. 49, no. 3, p. 408-425, doi:10.2113/49.3.408.

- Messina, T. A., 1993, The geometry and kinematics of intra-thrust sheet decollement folding: Lost River Range, Idaho [MS thesis]: Bethlehem, Lehigh University, 50 p.
- M'Gonigle, J.W., 1982, Devonian carbonate-breccia units in southwestern Montana and Idaho; a review of brecciating mechanisms, *in* Powers, R.B., ed., Geologic Studies of the Cordilleran Thrust Belt: Denver, Colorado, Rocky Mountain Association of Geologists v. 1, p. 677-689.
- M'Gonigle, J.W., 1993, Geologic map of the Medicine Lodge Peak quadrangle, Beaverhead County, southwest Montana: U.S. Geological Survey Geologic Quadrangle Map GQ 1724, scale 1:24,000.
- M'Gonigle, J.W., 1994, Geologic map of the Deadman Pass quadrangle, Beaverhead County, Montana, and Lemhi County, Idaho: U.S. Geological Survey Geologic Quadrangle Map GQ-1753, scale 1:24,000.
- Miller, E.L., Miller, M.M., Stevens, C.H., Wright, J.E., and Madrid, R., 1992, Late Paleozoic paleogeographic and tectonic evolution of the western U.S. Cordillera, *in* Burchfiel, B.C., Lipman, P.W., and Zoback, M.L., eds., The Cordilleran orogen: Conterminous U.S.: Boulder, Colorado, Geological Society of America, The Geology of North America, v. G-3, p. 57–106.
- Milton, J., 2020, Geologic mapping, stratigraphy, and detrital zircon geochronology of the southeastern Borah Peak horst, Custer County, Idaho: Age reassignment and correlation of Neoproterozoic to lower Paleozoic strata [MS thesis]: Pocatello, Idaho State University, 131 p.
- Molinaro, M., Leturmy, P., Guezou, J.C., Frizon de Lamotte, D., and Eshraghi, S.A., 2005, The structure and kinematics of the southeastern Zagros fold-thrust belt, Iran: From thin

- skinned to thick-skinned tectonics: *Tectonics*, vol. 24, no. 3,  
doi:10.1029/2004TC001633.
- Montoya, L.M., 2019, Investigation of structural style within the Sevier cold-thrust belt along the southwestern boundary of the Lemhi arch, central Idaho [MS thesis]: Pocatello, Idaho State University, 80 p.
- Mouthereau, F., Lacombe, O., and Meyer, B., 2006, The Zagros Folded Belt (Fars, Iran): constraints from topography and critical wedge modelling: *Geophysical Journal International*, vol. 165, p. 336–56, doi:10.1111/j.1365-246X.2006.02855.x.
- Mouthereau, F., Tensi, J., Bellahsen, N., Lacombe, O., De Boisgrollier, T., and Kargar, S., 2007, Tertiary sequence of deformation in a thin-skinned/thick-skinned collision belt: The Zagros Folded Belt (Fars, Iran): *Tectonics*, vol. 26, no. 5,  
doi:10.1029/2007TC002098.
- Mouthereau, F., Lacombe, O., and Verges, J., 2012, Building the Zagros collisional orogen: timing, strain distribution and the dynamics of Arabia/Eurasia plate convergence: *Tectonophysics*, vol. 532–535, p. 27–60, doi:10.1016/j.tecto.2012.01.022.
- Mouthereau, F., Watts, A.B., and Burov, E., 2013, Structure of orogenic belts controlled by lithosphere age: *Nature Geoscience*, vol. 6, no. 9, p. 785-789,  
doi:10.1038/ngeo1902.
- Nichols, D.J., Perry Jr, W.J. and Haley Johns, J.C., 1985, Reinterpretation of the palynology and age of Laramide syntectonic deposits, southwestern Montana, and revision of the Beaverhead Group: *Geology*, vol. 13, no. 2, p. 149-153,  
doi:10.1130/0091-7613(1985)13<149:ROTPAA>2.0.CO;2.

- O'Brien, C.A.E., 1960, The structural geology of the Boule and Bosche Ranges in the Canadian Rocky Mountains: *Quarterly Journal of the Geological Society*, vol. 116, no. 1-4, p. 409-431, doi:10.1144/gsjgs.116.1.0409.
- O'Neill, J.M. and Lopez, D.A., 1985, Character and regional significance of Great Falls tectonic zone, east-central Idaho and west-central Montana: *American Association of Petroleum Geologists Bulletin*, vol. 69, no. 3, p. 437-447, doi:10.1306/AD462506-16F7-11D7-8645000102C1865D.
- O'Neill, J.M., Schmidt, C.J., and Genovese, P.W., 1990, Dillon cutoff-Basement-involved tectonic link between the disturbed belt of west-central Montana and the overthrust belt of extreme southwestern Montana: *Geology*, vol. 18, no. 11, p. 1107-1110. doi:10.1130/0091-7613(1990)018<1107:DCBITL>2.3.CO;2.
- Oldow, J.S., Bally, A.W., Ave Lallemand, H.G., Leeman, W., 1989, Phanerozoic evolution of the North American Cordillera, United States and Canada, in Bally, A.W., and Palmer, A.R., eds., *The Geology of North America — An overview*: Boulder, Colorado, Geological Society of America, *The Geology of North America*, vol. A, p. 139-232, doi:10.1130/DNAG-GNA-A.139.
- Orme, D.A., 2020, New Timing Constraints for the Onset of Laramide Deformation in Southwest Montana Challenge our Understanding of the Development of a Thick Skinned Structural Style During Flat-Slab Subduction: *Tectonics*, vol. 39, no. 12, p.e2020TC006193, doi:10.1029/2020TC006193.
- Parker, S.D, and Pearson, D.M., 2020, Geologic map of the northern part of the Leadore quadrangle, Lemhi County, Idaho: Idaho Geological Survey Technical Report T-20-03, scale 1:24,000.

- Parker, S.D. and Pearson, D.M., Pre-thrusting stratigraphic control on the transition from a thin to thick-skinned structural style: An example from the double-decker Idaho-Montana fold-thrust belt: *Tectonics*, vol. 40, no. 5, p.e2020TC006429, doi:10.1029/2020TC006429.
- Pavlis, T.L., 2013, Kinematic model for out-of-sequence thrusting: Motion of two ramp-flat faults and the production of upper plate duplex systems: *Journal of Structural Geology*, vol. 51, p. 132-143, doi:10.1016/j.jsg.2013.02.003.
- Pearson, D.M., Kapp, P., DeCelles, P.G., Reiners, P.W., Gehrels, G.E., Ducea, M.N., and Pullen, A., 2013, Influence of pre-Andean crustal structure on Cenozoic thrust belt kinematics and shortening magnitude: Northwestern Argentina: *Geosphere*, vol. 9, no. 6, p. 1766-1782, doi:10.1130/GES00923.1.
- Pearson, D.M., and Link, P.K., 2017, Field guide to the Lemhi arch and Mesozoic-early Cenozoic faults and folds in east-central Idaho: Beaverhead Mountains: *Northwest Geology*, vol. 46, p. 101-112.
- Perry Jr, W.J., and Sando, W.J., 1982, Sequence of deformation of Cordilleran thrust belt in Lima, Montana region, *in* Powers, R.B., ed., *Geologic studies of the Cordilleran thrust belt: Denver, Colorado*, Rocky Mountain Association of Geologists, v. 1, p. 137-144.
- Perry Jr, W.J., Ryder, R.T. and Maughan, E.K., 1981, The southern part of the southwest Montana thrust belt: a preliminary re-evaluation of structure, thermal maturation and petroleum potential, *in* Tucker, T.E., Aram, R.B., Brinker, W.F., and Grabb, R.F., *Montana Geological Society field conference & symposium guidebook to southwest Montana: Billings, Montana*, Montana Geological Society, p. 261-273.
- Perry Jr, W.J., Wardlaw, B.R., Bostick, N.H., and Maughan, E.K., 1983, Structure, burial

- history, and petroleum potential of frontal thrust belt and adjacent foreland, southwest Montana: *The American Association of Petroleum Geologists Bulletin*, vol. 67, no. 5, p. 725-743, doi:10.1306/03B5B6A0-16D1-11D7-8645000102C1865D.
- Perry Jr, W.J., Haley, J.C., Nichols, D.J., Hammons, P.M., and Ponton, J.D., 1988, Interactions of Rocky Mountain foreland and Cordilleran thrust belt in Lima region, southwest Montana, *in* Schmidt, J., and Perry, W.J., eds., *Interaction of the Rocky Mountain Foreland and the Cordilleran Thrust Belt*: Boulder, Colorado, Geological Society of America Memoir, v. 171, p 267-290, doi:10.1130/MEM171-p267.
- Pfiffner, O. A., 2017, Thick-skinned and thin-skinned tectonics: a global perspective. *Geosciences*, vol. 7, no. 3, 71 p., doi:10.3390/geosciences7030071.
- Picha, F. and Gibson, R.I., 1985, Cordilleran hingeline: Late Precambrian rifted margin of the North American craton and its impact on the depositional and structural history, Utah and Nevada: *Geology*, vol. 13, no. 7, p. 465-468, doi:10.1130/00917613(1985)13<465:CHLPRM>2.0.CO;2.
- Price, R.A., and Mountjoy, E.W., 1970, Geologic structure of the Canadian Rocky Mountains between Bow and Athabasca Rivers—a progress report, *in* Wheeler, J.O., *Structure of the southern Canadian Cordillera*: St. John's, Newfoundland, Geological Association of Canada Special Paper, v. 6, p. 7-25.
- Price, R., 1981, The Cordilleran foreland thrust and fold belt in the southern Canadian Rocky Mountains: Geological Society, London, Special Publications, vol. 9, no. 1, p. 427-448. doi:10.1144/GSL.SP.1981.009.01.39.
- Price, R.A., 1986, The southeastern Canadian Cordillera: thrust faulting, tectonic wedging, and delamination of the lithosphere: *Journal of structural Geology*, vol. 8, no. 3-4, p. 239-254,

doi:10.1016/0191-8141(86)90046-5.

- Price, R.A., 2001, An evaluation of models for the kinematic evolution of thrust and fold belts: structural analysis of a transverse fault zone in the Front Ranges of the Canadian Rockies north of Banff, Alberta: *Journal of Structural Geology*, v. 23, no. 6-7, p. 1079-1088, doi:10.1016/S0191-8141(00)00177-2.
- Reston, T. and Manatschal, G., 2011, Rifted margins: Building blocks of later collision. In Arc continent collision, *in* Brown, D., and Ryan, P.D., *Arc-Continent Collision*: Springer, Berlin, Heidelberg, p. 3-21, doi: 10.1007/978-3-540-88558-0\_1.
- Richins, W.D., Pechmann, J.C., Smith, R.B., Langer, C.J., Goter, S.K., Zollweg, J.E. and King, J.J., 1987, The 1983 Borah Peak, Idaho, earthquake and its aftershocks: *Bulletin of the Seismological Society of America*, vol. 77, no. 3, p. 694-723.
- Rosenblume, J.A., Finzel, E.S., and Pearson, D.M., 2021, Early Cretaceous provenance, sediment dispersal, and foreland basin development in southwestern Montana, North American Cordillera: *Tectonics*, vol. 40, p. 1–31, doi:10.1029/2020TC006561.
- Royse F., 1993, An overview of the geologic structure of the thrust belt in Wyoming, northern Utah, and eastern Idaho, *in* Snoke, A.W., Steidtmann, J.R., Roberts, S.M., eds., *Geology of Wyoming: Laramie, Wyoming, Geological Survey of Wyoming Memoir vol. 5*, pp. 272-311.
- Royse Jr, F., Warner, M.T., and Reese, D.L., 1975, Thrust Belt Structural Geometry and Related Stratigraphic Problems Wyoming-Idaho-Northern Utah, *in* Bolyard, D.W., *Symposium on deep drilling frontiers in the central Rocky Mountains*: Denver, Colorado, Rocky Mountain Association of Geologists, p. 41-45.
- Ruh, J.B., Kaus, B.J., and Burg, J.P., 2012, Numerical investigation of deformation mechanics in

- fold-and-thrust belts: Influence of rheology of single and multiple décollements: *Tectonics*, vol. 31, no. 3, doi:10.1029/2011TC003047.
- Ruppel, E.T., 1975, Precambrian and Lower Ordovician rocks in east-central Idaho: Denver, Colorado, U.S. Geological Survey Professional Paper 889, p. 1-23.
- Ruppel, E.T., 1986, The Lemhi Arch: A Late Proterozoic and Early Paleozoic Landmass in Central Idaho., *in* Peterson, J.A., ed., Paleotectonics and sedimentation in the Rocky Mountain Region, United States: Denver, Colorado, American Association of Petroleum Geologists memoir, v. 41, p. 119-130, doi:10.1306/M41456C6.
- Ruppel, E.T., 1994, Preliminary geologic map of the Tepee Mountain 7.5-minute quadrangle, Beaverhead County, Montana and Lemhi County, Idaho: Montana Bureau of Mines and Geology Open-File Reports 317, 1:24,000 scale.
- Ryder, R. T., and Scholten, R., 1973, Syntectonic conglomerates in southwestern Montana: Their nature, origin, and tectonic significance: *Geological Society of America Bulletin*, vol. 84, no. 3, p. 773-796, doi:10.1130/0016-7606(1973)84<773:SCISMT>2.0.CO;2.
- Sandberg, C.A., 1975, McGowan Creek Formation, new name for Lower Mississippian flysch sequence in east-central Idaho: *U.S. Geological Survey Bulletin*, vol. 1405-E, 11 p., doi:10.3133/b1405E.
- Schmidt, C.J., and Garihan, J.M., 1983, Laramide tectonic development of the Rocky Mountain foreland of southwestern Montana, *in*, Lowell, J.D., ed., *Rocky Mountain foreland basins and uplifts*: Denver, Colorado, Rocky Mountain Association of Geologists, p. 271-294.
- Schmidt, C.J., O'Neill, J.M., and Brandon, W.C., 1988, Influence of Rocky Mountain foreland uplifts on the development of the frontal fold and thrust belt, southwestern Montana, *in* Schmidt, C.J., and Perry, W.J., (eds.), *Interaction of the Rocky Mountain Foreland and*

- the Cordilleran Thrust Belt: Boulder, Colorado, Geological Society of America Memoir 17, p. 171-201, doi:10.1130/MEM171.
- Scholten, R., 1957, Paleozoic evolution of the geosynclinal margin north of the Snake River Plain, Idaho-Montana: Geological Society of America Bulletin, vol. 68, no. 2, p. 151-170, doi:10.1130/0016-7606(1957)68[151:PEOTGM]2.0.CO;2.
- Scholten, R., and Ramspott, L. D., 1968, Tectonic Mechanisms Indicated by Structural Framework of Central Beaverhead Range, Idaho Montana: Boulder, Colorado, Geological Society of America Special Paper 105, 59 p., doi:10.1130/SPE104-p1.
- Scisciani, V., Montefalcone, R., Mazzoli, S. and Butler, R.W.H., 2006, Coexistence of thin-and thick-skinned tectonics: an example from the Central Apennines, Italy, *in* Mazzoli, S., and Butler, R.W.H, Styles of Continental Contraction: Boulder, Colorado, Geological Society of America Special Paper 414, p. 33-54, doi:10.1130/2006.2414(03).
- Sears, J.W., 1988, Two major thrust slabs in the west-central Montana Cordillera, *in* Schmidt, C.J., and Perry, W.J., (eds.), Interaction of the Rocky Mountain Foreland and The Cordilleran Thrust Belt: Boulder, Colorado, Geological Society of America Memoir 17, p. 165-170, doi:10.1130/MEM171-P165.
- Sears, J.W., Chamberlain, K.R. and Buckley, S.N., 1998, Structural and U-Pb geochronological evidence for 1.47 Ga rifting in the Belt basin, western Montana: Canadian Journal of Earth Sciences, v. 35, no. 4, p. 467-475, doi:10.1139/e97-121.
- Sears, J.W., 2001, Emplacement and denudation history of the Lewis-Eldorado-Hoadley thrust slab in the northern Montana Cordillera, USA: Implications for steady-state orogenic processes: American Journal of Science, vol. 301, no. 4-5, p. 359-373,

doi:10.2475/ajs.301.4-5.359.

- Sheedlo, M., 1984, Structural geology of the northern Snowcrest Range, Beaverhead and Madison counties, Montana [MS thesis]: Kalamazoo, Western Michigan University, 132 p.
- Sherkati, S., Letouzey, J., and Frizon De Lamotte, D., 2006, Central Zagros fold-thrust belt (Iran): new insights from seismic data, field observation, and sandbox modeling: *Tectonics*, vol. 25, doi:10.1029/2004TC001766.
- Skipp, B., 1988, Cordilleran thrust belt and faulted foreland in the Beaverhead Mountains, Idaho and Montana, *in* Schmidt, J., and Perry, W.J., eds., *Interaction of the Rocky Mountain Foreland and the Cordilleran Thrust Belt*: Boulder, Colorado, Geological Society of America Memoir, vol. 171, p 237-266, doi:10.1130/MEM171-p237.
- Skipp, B., Lageson, D.R., and McMannis, W.J., 1999, Geologic map of the Sedan quadrangle, Gallatin and Park Counties, Montana: U.S. Geological Survey Geologic Investigations Series I-2634, 1 plate, scale 1:48,000.
- Skipp, B.A., Perry, W.J. Jr., and Janecke, S.U., 2017, Geologic map of the Lima Peaks 7.5' quadrangle, Beaverhead county, Montana: Montana Bureau of Mines and Geology Open file reports 692, scale 1:24,000.
- Sloss, L.L., 1954, Lemhi Arch, a mid-Paleozoic positive element in south-central Idaho: *Geological Society of America Bulletin*, vol. 65, no. 4, p.365-368.  
doi:10.1130/0016-7606(1954)65[365:LAAMPE]2.0.CO;2.
- Smeraglia, L., Fabbri, O. and Choulet, F., 2021, Variation in structural styles within fold-and thrust belts: insights from field mapping, cross-sections balancing, and 2D-kinematic modelling in the Jura Mountains (Eastern France): *Journal of Structural Geology*, vol.

149, p.104381, doi:10.1016/j.jsg.2021.104381.

Smith, R.B., Richins, W.D. and Doser, D.I., 1985, The 1983 Borah Peak, Idaho, earthquake: Regional seismicity, kinematics of faulting, and tectonic mechanism, *in* Stein, R.S., and Bucknam, R.C., eds., Proceedings, Workshop XXVIII on the Borah Peak, Idaho, Earthquake, : Denver, Colorado, US Geological Survey Open-File Report, v. 85, no. 290, p. 236-263.

Smithson, S.B., Brewer, J.A., Kaufman, S., Oliver, J.E., and Hurich, C.A., 1979, Structure of the Laramide Wind River uplift, Wyoming, from COCORP deep reflection data and from gravity data: *Journal of Geophysical Research: Solid Earth*, vol. 84, no. B11, p. 5955-5972, doi:10.1029/JB084iB11p05955.

Stone, D.S., Schmidt, C.J., Chase, R.B. and Erslev, E.A., 1993, Basement-involved thrust generated folds as seismically imaged in the subsurface of the central Rocky Mountain foreland, *in* C.J. Schmidt, R.B. Chase, E.A. Erslev eds., Laramide basement deformation in the Rocky Mountain foreland of the western United States: Boulder, Colorado, Geological Society of America Special Paper, vol. 280, p. 271-318, doi:10.1130/SPE280-p271.

Tavani, S., Granado, P., Corradetti, A., Camanni, G., Vignaroli, G., Manatschal, G., Mazzoli, S., Muñoz, J. A., and Parente, M., 2021, Rift inheritance controls the switch from thin-to thick-skinned thrusting and basal décollement re-localization at the subduction-to collision transition: *Geological Society of America Bulletin*, p. 1-14. doi:10.1130/B35800.1.

Taylor, W.J., Bartley, J.M., Martin, M.W., Geissman, J.W., Walker, J.D., Armstrong, P.A. and Fryxell, J.E., 2000, Relations between hinterland and foreland shortening: *Sevier*

- orogeny, central North American Cordillera: *Tectonics*, vol. 19, no. 6, p. 1124-1143,  
doi:10.1029/1999TC001141.
- Trimble, D.E., 1976, *Geology of the Michaud and Pocatello quadrangles, Bannock and Power counties, Idaho*: U.S. Geological Survey Bulletin 1400, 88 p.,  
doi:10.3133/b1400.
- Tysdal, R.G., 1981, Foreland deformation in the northern part of the Ruby Range of southwestern Montana, *in* Tucker, T.E., Aram, R.B., Brinker, W.F., and Grabb, R.F., *Montana Geological Society field conference & symposium guidebook to southwest Montana*: Billings, Montana, Montana Geological Society, p. 215-24.
- Tysdal, R.G., Marvin, R.F. and Dewitt, E.D., 1986, Late Cretaceous stratigraphy, deformation, and intrusion in the Madison Range of southwestern Montana: *Geological Society of America Bulletin*, vol. 97, no. 7, p. 859-868,  
doi:10.1130/0016-7606(1986)97<859:LCSDAI>2.0.CO;2.
- Tysdal, R.G., 1988, Deformation along the northeast side of Blacktail Mountains, *in* Schmidt, J., and Perry, W.J., eds., *Interaction of the Rocky Mountain Foreland and the Cordilleran Thrust Belt*: Boulder, Colorado, Geological Society of America Memoir 171, p 203-215,  
doi:10.1130/MEM171-p203.
- Tysdal, R.G., 2002, *Structural geology of western part of Lemhi Range, east-central Idaho*: Denver, Colorado, U.S. Geological Survey Professional Paper, v. 1659, p. 1-33,  
doi:10.3133/pp1659.
- Umpleby, J.B., 1917, *Geology and ore deposits of Lemhi County, Idaho*: Washington, D.C., U.S. Geological Survey Bulletin 528, 182 p., doi:10.3133/b528.
- Von Hagke, C., and Malz, A., 2018, Triangle zones—Geometry, kinematics, mechanics, and the

- need for appreciation of uncertainties: *Earth-Science Reviews*, vol. 177, p. 24-42,  
doi:10.1016/j.earscirev.2017.11.003.
- Vuke, S.M., 2020, Synorogenic basin deposits and associated Laramide uplifts in the Montana part of the Cordilleran foreland basin system, *in* Metesh, J., ed., *Geology of Montana: Butte, Montana, Montana Bureau of Mines and Geology*, v. 1, p. 1-39.  
51.
- Williams, N.S., and Bartley, J.M., 1988, Geometry and sequence of thrusting, McKnight and Kelmbeck Canyons, Tendoy Range, southwestern Montana, *in* J. Schmidt, and W. J. Perry eds., *Interaction of the Rocky Mountain Foreland and the Cordilleran Thrust Belt: Boulder, Colorado, Geological Society of America Memoir 171*, p. 307-318,  
doi:10.1130/MEM171-p307.
- Williams, C.A., Connors, C., Dahlen, F.A., Price, E.J., and Suppe, J., 1994, Effect of the brittle-ductile transition on the topography of compressive mountain belts on Earth and Venus: *Journal of Geophysical Research: Solid Earth*, vol. 99, no. B10, p. 19947-19974,  
doi:10.1029/94JB01407.
- Williams, S.A., Singleton, J.S., Prior, M.G., Mavor, S.P., Cross, G.E., and Stockli, D.F, 2020, The early Palaeogene transition from thin-skinned to thick-skinned shortening in the Potosí uplift, Sierra Madre Oriental, northeastern Mexico: *International Geology Review*, p. 1-21, doi:10.1080/00206814.2020.1805802.
- Wilson, E., Preacher, J.M., and Link, P.K., 1994, New constraints on the nature of the early Mississippian Antler sedimentary basin in Idaho: *Canadian Society of Petroleum Geologists Memoir*, v. 17, p. 155–174.
- Wiltschko, D.V., and Dorr, J.A., 1983, Timing of deformation in overthrust belt and foreland of

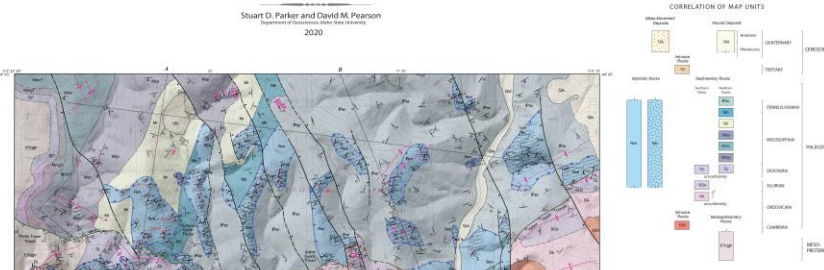
- Idaho, Wyoming, and Utah: American Association of Petroleum Geologists Bulletin, vol. 67, no. 8, p. 1304-1322, doi:10.1306/03B5B740-16D1-11D7-8645000102C1865D.
- Winston, D., 1986, Sedimentation and tectonics of the middle Proterozoic Belt basin, and their influence on Phanerozoic compression and extension in western Montana and northern Idaho, *in* Peterson, J.A., ed., Paleotectonics and Sedimentation in the Rocky Mountain Region, United States: American Association of Petroleum Geologists Memoir 41, p. 87-118.
- Yang, K.M., Huang, S.T., Wu, J.C., Lee, M., Ting, H.H. and Mei, W.W., 2001, The characteristics of sub-surface structure and evolution of the Tachianshan-Chukou thrust system: Annual Meeting of the Geological Society of China, pp. 82-4.
- Yonkee, W.A., and Weil, A.B., 2015, Tectonic evolution of the Sevier and Laramide belts within the North American Cordillera orogenic system: Earth-Science Reviews, vol. 150, p. 531-593, doi:10.1016/j.earscirev.2015.08.001.
- Yonkee, W.A., Dehler, C.D., Link, P.K., Balgord, E.A., Keeley, J.A., Hayes, D.S., Wells, M.L., Fanning, C.M. and Johnston, S.M., 2014, Tectono-stratigraphic framework of Neoproterozoic to Cambrian strata, west-central US: Protracted rifting, glaciation, and evolution of the North American Cordilleran margin: Earth-Science Reviews, vol. 136, p. 59-95, doi:10.1016/j.earscirev.2014.05.004.
- Yonkee, W.A., Eleogram, B., Wells, M.L., Stockli, D.F., Kelley, S. and Barber, D.E., 2019, Fault slip and exhumation history of the Willard thrust sheet, Sevier fold-thrust belt, Utah: Relations to wedge propagation, hinterland uplift, and foreland basin Sedimentation: Tectonics, vol. 38, no. 8, p. 2850-2893,

doi:10.1029/2018TC005444.

Appendix 1: Geologic map of the northern part of the Leadore Quadrangle

# GEOLOGIC MAP OF THE NORTHERN PART OF THE LEADORE QUADRANGLE, LEMHI COUNTY, IDAHO

Shaun D. Parker and David M. Pearson  
Department of Geology  
2020



## DESCRIPTION OF MAP UNITS

- 100 Thompson Gait (Thompson Gait)** - A thick, massive, light-colored sandstone and siltstone, locally shaly, with some thin beds of sandstone and siltstone. It is the dominant unit in the northern part of the quadrangle.
- 101 Leadore (Leadore)** - A thick, massive, light-colored sandstone and siltstone, locally shaly, with some thin beds of sandstone and siltstone. It is the dominant unit in the southern part of the quadrangle.
- 102 Thompson Gait (Thompson Gait)** - A thick, massive, light-colored sandstone and siltstone, locally shaly, with some thin beds of sandstone and siltstone. It is the dominant unit in the northern part of the quadrangle.
- 103 Leadore (Leadore)** - A thick, massive, light-colored sandstone and siltstone, locally shaly, with some thin beds of sandstone and siltstone. It is the dominant unit in the southern part of the quadrangle.

## INTRODUCTION

This map is a revision of the geologic map of the northern part of the Leadore Quadrangle, Lemhi County, Idaho, published by the U.S. Geological Survey in 1962. The map was revised to include new data and to update the geologic units and their relationships. The map shows the distribution of the Thompson Gait and Leadore units, and their relationships to other units in the area.

## SYMBOLS

- Symbol for Thompson Gait (Thompson Gait)
- Symbol for Leadore (Leadore)
- Symbol for Thompson Gait (Thompson Gait)
- Symbol for Leadore (Leadore)

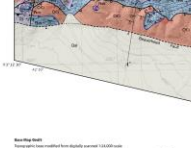


Figure 1. Geological cross-sections showing the relationship between the Thompson Gait and Leadore units.

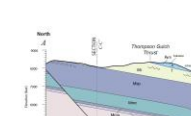


Figure 2. Geological cross-section showing the relationship between the Thompson Gait and Leadore units.

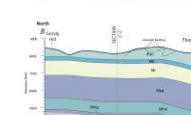


Figure 3. Geological cross-section showing the relationship between the Thompson Gait and Leadore units.



Figure 4. Geological cross-section showing the relationship between the Thompson Gait and Leadore units.



Figure 5. Photomicrograph of a thin section of a rock sample, showing the texture and mineralogy of the Thompson Gait.



Figure 6. Photomicrograph of a thin section of a rock sample, showing the texture and mineralogy of the Leadore.



Figure 7. Photomicrograph of a thin section of a rock sample, showing the texture and mineralogy of the Thompson Gait.

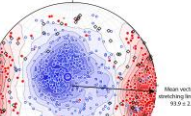


Figure 8. Photomicrograph of a thin section of a rock sample, showing the texture and mineralogy of the Leadore.



Figure 9. Photomicrograph of a thin section of a rock sample, showing the texture and mineralogy of the Thompson Gait.

## UNION PASS THRUST

The Union Pass Thrust is a major fault that separates the Thompson Gait from the Leadore. It is a normal fault that dips to the south. The fault is well exposed in the northern part of the quadrangle.

## LEADORE CANYON THRUST

The Leadore Canyon Thrust is a major fault that separates the Leadore from the Thompson Gait. It is a normal fault that dips to the north. The fault is well exposed in the southern part of the quadrangle.

## LEADORE PASS THRUST

The Leadore Pass Thrust is a major fault that separates the Leadore from the Thompson Gait. It is a normal fault that dips to the north. The fault is well exposed in the southern part of the quadrangle.

## UNION PASS FAULT

The Union Pass Fault is a major fault that separates the Thompson Gait from the Leadore. It is a normal fault that dips to the south. The fault is well exposed in the northern part of the quadrangle.

## LEADORE CANYON FAULT

The Leadore Canyon Fault is a major fault that separates the Leadore from the Thompson Gait. It is a normal fault that dips to the north. The fault is well exposed in the southern part of the quadrangle.

## LEADORE PASS FAULT

The Leadore Pass Fault is a major fault that separates the Leadore from the Thompson Gait. It is a normal fault that dips to the north. The fault is well exposed in the southern part of the quadrangle.

## THOMPSON GAIT THRUST

The Thompson Gait Thrust is a major fault that separates the Thompson Gait from the Leadore. It is a normal fault that dips to the south. The fault is well exposed in the northern part of the quadrangle.

## LEADORE CANYON THRUST

The Leadore Canyon Thrust is a major fault that separates the Leadore from the Thompson Gait. It is a normal fault that dips to the north. The fault is well exposed in the southern part of the quadrangle.

## LEADORE PASS THRUST

The Leadore Pass Thrust is a major fault that separates the Leadore from the Thompson Gait. It is a normal fault that dips to the north. The fault is well exposed in the southern part of the quadrangle.

## REFERENCES

Anderson, R.H., 1962. Geology of the Thompson Gait and Leadore, Lemhi County, Idaho. U.S. Geological Survey Bulletin 1110, 100 p.

Anderson, R.H., 1964. Geology of the Thompson Gait and Leadore, Lemhi County, Idaho. U.S. Geological Survey Bulletin 1110, 100 p.

Anderson, R.H., 1966. Geology of the Thompson Gait and Leadore, Lemhi County, Idaho. U.S. Geological Survey Bulletin 1110, 100 p.

Anderson, R.H., 1968. Geology of the Thompson Gait and Leadore, Lemhi County, Idaho. U.S. Geological Survey Bulletin 1110, 100 p.

Anderson, R.H., 1970. Geology of the Thompson Gait and Leadore, Lemhi County, Idaho. U.S. Geological Survey Bulletin 1110, 100 p.

Anderson, R.H., 1972. Geology of the Thompson Gait and Leadore, Lemhi County, Idaho. U.S. Geological Survey Bulletin 1110, 100 p.

Anderson, R.H., 1974. Geology of the Thompson Gait and Leadore, Lemhi County, Idaho. U.S. Geological Survey Bulletin 1110, 100 p.

Anderson, R.H., 1976. Geology of the Thompson Gait and Leadore, Lemhi County, Idaho. U.S. Geological Survey Bulletin 1110, 100 p.

Anderson, R.H., 1978. Geology of the Thompson Gait and Leadore, Lemhi County, Idaho. U.S. Geological Survey Bulletin 1110, 100 p.

Anderson, R.H., 1980. Geology of the Thompson Gait and Leadore, Lemhi County, Idaho. U.S. Geological Survey Bulletin 1110, 100 p.

Anderson, R.H., 1982. Geology of the Thompson Gait and Leadore, Lemhi County, Idaho. U.S. Geological Survey Bulletin 1110, 100 p.

Anderson, R.H., 1984. Geology of the Thompson Gait and Leadore, Lemhi County, Idaho. U.S. Geological Survey Bulletin 1110, 100 p.

Anderson, R.H., 1986. Geology of the Thompson Gait and Leadore, Lemhi County, Idaho. U.S. Geological Survey Bulletin 1110, 100 p.

Anderson, R.H., 1988. Geology of the Thompson Gait and Leadore, Lemhi County, Idaho. U.S. Geological Survey Bulletin 1110, 100 p.

Anderson, R.H., 1990. Geology of the Thompson Gait and Leadore, Lemhi County, Idaho. U.S. Geological Survey Bulletin 1110, 100 p.

Anderson, R.H., 1992. Geology of the Thompson Gait and Leadore, Lemhi County, Idaho. U.S. Geological Survey Bulletin 1110, 100 p.

Anderson, R.H., 1994. Geology of the Thompson Gait and Leadore, Lemhi County, Idaho. U.S. Geological Survey Bulletin 1110, 100 p.

Anderson, R.H., 1996. Geology of the Thompson Gait and Leadore, Lemhi County, Idaho. U.S. Geological Survey Bulletin 1110, 100 p.

Anderson, R.H., 1998. Geology of the Thompson Gait and Leadore, Lemhi County, Idaho. U.S. Geological Survey Bulletin 1110, 100 p.

Anderson, R.H., 2000. Geology of the Thompson Gait and Leadore, Lemhi County, Idaho. U.S. Geological Survey Bulletin 1110, 100 p.

Anderson, R.H., 2002. Geology of the Thompson Gait and Leadore, Lemhi County, Idaho. U.S. Geological Survey Bulletin 1110, 100 p.

Anderson, R.H., 2004. Geology of the Thompson Gait and Leadore, Lemhi County, Idaho. U.S. Geological Survey Bulletin 1110, 100 p.

Anderson, R.H., 2006. Geology of the Thompson Gait and Leadore, Lemhi County, Idaho. U.S. Geological Survey Bulletin 1110, 100 p.

Anderson, R.H., 2008. Geology of the Thompson Gait and Leadore, Lemhi County, Idaho. U.S. Geological Survey Bulletin 1110, 100 p.

Anderson, R.H., 2010. Geology of the Thompson Gait and Leadore, Lemhi County, Idaho. U.S. Geological Survey Bulletin 1110, 100 p.

Figure 10. Photomicrograph of a thin section of a rock sample, showing the texture and mineralogy of the Thompson Gait.

Figure 11. Photomicrograph of a thin section of a rock sample, showing the texture and mineralogy of the Leadore.

Figure 12. Photomicrograph of a thin section of a rock sample, showing the texture and mineralogy of the Thompson Gait.

Figure 13. Photomicrograph of a thin section of a rock sample, showing the texture and mineralogy of the Leadore.

Figure 14. Photomicrograph of a thin section of a rock sample, showing the texture and mineralogy of the Thompson Gait.

Figure 15. Photomicrograph of a thin section of a rock sample, showing the texture and mineralogy of the Leadore.

Figure 16. Photomicrograph of a thin section of a rock sample, showing the texture and mineralogy of the Thompson Gait.

Figure 17. Photomicrograph of a thin section of a rock sample, showing the texture and mineralogy of the Leadore.

Figure 18. Photomicrograph of a thin section of a rock sample, showing the texture and mineralogy of the Thompson Gait.